The role of src kinases in controlling neutrophil function in acute inflammation

James Gray Macfarlane

BM BCh (Oxon) MRCP (UK)

A thesis submitted in partial fulfilment of the requirements for the degree of Doctor of Philosophy

Institute of Cellular Medicine

Faculty of Medical Sciences

Newcastle University

October 2015

Declaration

I hereby declare that the material contained within this thesis is my own work unless otherwise stated within the text. The data contained within this thesis have not previously been submitted for the award of a higher degree at this or any other University.

James Macfarlane

October 2015

Abstract

The src family kinases are key cellular regulators of acute neutrophilic inflammation. When uncontrolled, this causes numerous inflammatory disorders, including the acute respiratory distress syndrome (ARDS). This is associated with an unacceptably high 90-day mortality and prolonged hospital admissions. ARDS currently has no effective pharmacological treatment.

The work contained in this thesis aimed to characterise the anti-inflammatory, pro-resolutionary effects of src kinase inhibition on various neutrophil functions, using novel in vitro and in vivo models of acute inflammation and resolution.

Results show that the src kinase inhibitors, PP1 and dasatinib, attenuate in vitro neutrophil extracellular degranulation in response to stimulation with formylated peptide, lipopolysaccharide and live bacteria. They also exert additional effects on integrin-dependent neutrophil functions, but have no effect on neutrophil fate or bacterial killing efficiency.

Src kinase inhibition of neutrophils also attenuates in vitro epithelial cell damage and promotes a pro-resolutionary environment, with improved macrophage efferocytosis of apoptotic neutrophils, by inhibiting the release of an unidentified soluble factor believed to be a product of neutrophil degranulation.

Extending these findings to in vivo murine models of bacteria- and acid-induced experimental lung inflammation, dasatinib exerts an inhibitory effect on markers of neutrophil degranulation in each model, at doses of 1mg/kg and 5mg/kg, respectively. At 10mg/kg, a detrimental effect is observed, as evidenced by reduced bacterial clearance, increased alveolar leak and extrapulmonary toxicity in the infection model and increased neutrophil influx, degranulation and alveolar haemorrhage in the acid model.

These findings highlight a possible therapeutic role of src kinase inhibition in inflammatory conditions driven by neutrophil influx and degranulation that is worthy of further study in other models of lung inflammation. Future work should focus on developing more specific inhibitors to offer selective control over neutrophil granule processing, and careful dosing to avoid undesired effects on bacterial killing mechanisms.

to Claudia, Iona and Sam

Acknowledgements

Firstly, I should like to express my sincere gratitude to my supervisor, Professor John Simpson, for his excellent guidance and relentless enthusiasm since I first worked with him as a respiratory trainee in Edinburgh in 2007. His patience, experience and immense knowledge have motivated me throughout my research and in writing this thesis.

Besides my supervisor, I should also like to acknowledge my funding body, the Wellcome Trust, my PhD assessors at Newcastle University: Professors Matt Collin and Jeff Pearson for their insightful comments and encouragement during annual reviews, as well as Dr Chris Ward, who offered me advice and reassurance whenever needed.

My sincere thanks also go to Professor Adriano Rossi, Dr David Dorward, Dr Chris Lucas and colleagues at Edinburgh University for offering me a fantastic opportunity to collaborate and join their team as a visiting researcher. Under Dr Dorward's guidance we carried out the in vivo experiments, without which it would have been impossible to test my hypotheses. Similarly, I thank the countless healthy volunteers from Newcastle University who kindly gave up their time and blood to provide us with healthy neutrophils, as well as the critically ill patients and their families, who participated in research studies to allow our group to test their innate immune function. I am also very grateful to Dr Anjam Khan at Newcastle University, who allowed me to carry out all the bacterial work in his microbiology laboratory.

I also thank all of the fellow members of our lab team for their support, intellectual discussions and hard work over the years. In particular, I should like to thank Dr Marie-Hélène Ruchaud-Sparagano and Mr Jonathan Scott for their excellent scientific teaching and advice that enabled me to learn, optimise and design challenging neutrophil assays.

Finally, I should like to thank Claudia, my wife, my children Iona and Sam, my parents John and Rosamund, and the rest of our family for their endless optimism, patience and motivation throughout my research and in writing this thesis.

Table of Contents

List of Figures

List of Tables

List of Abbreviations

ACCP	American College of Chest Physicians
ACK	Ammonium-Chloride-Potassium
AEBSF	4-(2-Aminoethyl) sulfonyl fluoride hydrochloride
AECC	American-European Consensus Conference
ALI	Acute lung injury
ALT	Alanine transaminase
ANOVA	Analysis of variance
APACHE	Acute Physiology and Chronic Health Evaluation
APC	Allophycocyanin
ARDS	Acute respiratory distress syndrome
ATCC	American Type Culture Collection
ATP	Adenosine triphosphate
BAL	Bronchoalveolar lavage
BALF	Bronchoalveolar lavage fluid
BCA assay	Bicinchoninic acid assay
BD	Becton Dickinson
BSA	Bovine serum albumin
CBA	Cytometric bead array
CCL	Chemokine ligand
CI	Confidence interval

CML	Chronic myeloid leukaemia
COX-2	Cyclooxygenase-2
Cyto B	Cytochalasin B
Cyto D	Cytochalasin D
GM-CSF	Granulocyte macrophage colony stimulating factor
DAPI	4',6-diamidino-2-phenylindole hydrochloride
DCS	Developmental Clinical Studies
DG	1,2-diradyl-*sn*-glycerol
DHR	Dihydrorhodamine 123
DMB	Dimethoxybenzidine
DMSO	Dimethyl sulfoxide
DNA	Deoxyribonucleic acid
DPI	Diphenyleneiodonium
EC	*Escherichia coli*
ECG	Electrocardiogram
ECL	Enhanced chemiluminescent
ECMO	Extracorporeal membrane oxygenation
EDTA	Ethylenediaminetetraacetic acid
ELISA	Enzyme linked immunoabsorbent assay
EVLP	Ex vivo lung perfusion
FACS	Fluorescence-activated cell sorting

FAK	Focal adhesion kinase
FCS	Foetal calf serum
FITC	Fluorescein isothiocyanate
FiO_2	Fraction of inspired oxygen
fMLP	N-Formylmethionyl-leucyl-phenylalanine
FPR1	Formylated peptide receptor 1
GFP	Green fluorescent protein
GPCR	G-protein coupled receptor
HAI	Hospital-acquired infection
HBSS	Hanks' balanced salt solution
HCl	Hydrochloric acid
HEPES	4-(2-hydroxyethyl)-1-piperazineethanesulfonic acid
HFOV	High frequency oscillatory ventilation
HIV	Human immunodeficiency virus
HNE	Human neutrophil elastase
HRP	Horseradish peroxidase
H_2SO_4	Sulphuric acid
H_2O_2	Hydrogen peroxide
ICAM	Intercellular adhesion molecule
ICU	Intensive care unit
IL	Interleukin

IMDM	Iscove's modified Dulbecco's medium
IP_3	Inositol-1,4,5-triphosphate
IQR	Interquartile range
JAK	Janus kinase
KC	Keratinocyte chemoattractant
KGF	Keratinocyte growth factor
LB	Luria Bertani
LBP	Lipopolysaccharide-binding protein
LDH	Lactate dehydrogenase
LH	Lithium heparin
LPS	Lipopolysaccharide
LTA	Lipotechoic acid
LTF	Lactoferrin
MAPK	Mitogen-activated protein kinase
MCP-1	Monocyte chemotactic protein 1
MDM	Monocyte-derived macrophages
MFI	Median fluorescence intensity
MMP	Matrix metalloproteinase
MOI	Multiplicity of infection
MPO	Myeloperoxidase
MRC	Medical Research Council

MS	Magnetic separation
MSC	Mesenchymal stem cell
NADPH oxidase	Nicotinamide adenine dinucleotide phosphate oxidase
NCTC	National Collection of Type Cultures
NETs	Neutrophil extracellular traps
NF-κB	Nuclear factor κB
NHLBI	National Heart, Lung and Blood Institute
NIH	National Institute of Health
NK	Natural killer
NLR	Nod-like receptor
NO	Nitric oxide
iNOS	Inducible nitric oxide synthase
OD	Optical density
PA	*Pseudomonas aeruginosa*
PAF	Platelet activating factor
PAI-1	Plasminogen activator inhibitor-1
PaO_2	Partial pressure of oxygen in arterial blood
PBMC	Peripheral blood mononuclear cell
PBN	Peripheral blood neutrophil
PBS	Phosphate buffered saline
PE	Phycoerythrin

PEEP	Positive end-expiratory pressure
PI	Propidium iodide
PI3K	Phosphoinosotide 3-kinase
PKC	Protein kinase C
PLC	Phospholipase C
PLD	Phospholipase D
PMA	Phorbol myristate acetate
PMN	Polymorphonuclear leukocytes
PMSF	Phenylmethanesulfonyl fluoride
Pyk-2	Proline-rich kinase 2
RA	Receptor antagonist
REC	Research Ethics Committee
RNS	Reactive nitrogen species
ROS	Reactive oxygen species
RPMI	Roswell Park Memorial Institute
SA	*Staphylococcus aureus*
SAP II	Simplified Acute Physiology II
SCCM	Society of Critical Care Medicine
SD	Standard deviation
SDS	Sodium Dodecyl Sulfate
SE	Standard error (of the mean)

SIK	Salt-inducible kinase
siRNA	Small interfering RNA
SIRS	Systemic Inflammatory Response Syndrome
SNARE	Soluble *N*-ethylmaleimide-sensitive factor Attachment Protein Receptor
SOD	Superoxide dismutase
SOFA	Sequential Organ Failure Assessment
STAT	Signal transducers and activators of transcription
TBS	Tris-buffered saline
TBS-T	Tris-buffered saline Tween
TEMED	Tetramethylethylenediamine
TLR	Toll-like receptor
TMB	3,3',5,5'-Tetramethylbenzidine
TNFα	Tumor necrosis factor α
TRALI	Transfusion-related acute lung injury
UK	United Kingdom
US	United States
VAP	Ventilator-associated pneumonia
VEGF	Vascular endothelial growth factor
V_T	Tidal volume
WCC	White cell count

Chapter 1. Introduction

1.1 Chapter Overview

This thesis addresses the acute inflammatory responses that are believed to cause acute lung injury (ALI) and its important clinical sequelae, namely the acute respiratory distress syndrome (ARDS). It describes my studies investigating cellular mechanisms involved in the pathogenesis of ARDS, a better understanding of which may unlock new avenues of research for novel therapeutic approaches for this condition, which is associated with a high mortality and considerable healthcare resource usage.

In this first chapter I shall summarise the current mechanistic and clinical understanding of ALI and ARDS, together with the hypotheses I set out to investigate. Subsequent chapters describe, detail and discuss the methods used and results obtained, followed by a general discussion.

1.2 Acute Lung Injury and Acute Respiratory Distress Syndrome

1.2.1 Definitions

The 1994 American-European Consensus Conference (AECC) defined ALI and ARDS as two distinct severe respiratory conditions differentiated by the severity of hypoxaemia, and requiring the following criteria to be met:

- **Acute** and persistent onset
- **Bilateral pulmonary infiltrates** on chest radiograph
- **Impaired oxygenation** independent of positive end-expiratory pressure (PEEP) delivered:
    - PaO_2:FiO_2 ratio ≤ 300 mmHg (40 kPa) **= ALI**
    - PaO_2:FiO_2 ratio ≤ 200 mmHg (26.7 kPa) **= ARDS**
- **Exclusion of cardiogenic pulmonary oedema** by clinical criteria (absence of left atrial hypertension) or by direct measurement of pulmonary capillary wedge pressure of < 18mmHg (2.4kPa)

PaO_2 = partial pressure of oxygen in arterial blood, FiO_2 = fraction of inspired oxygen. Adapted from AECC 1994 definition (Bernard et al. 1994).

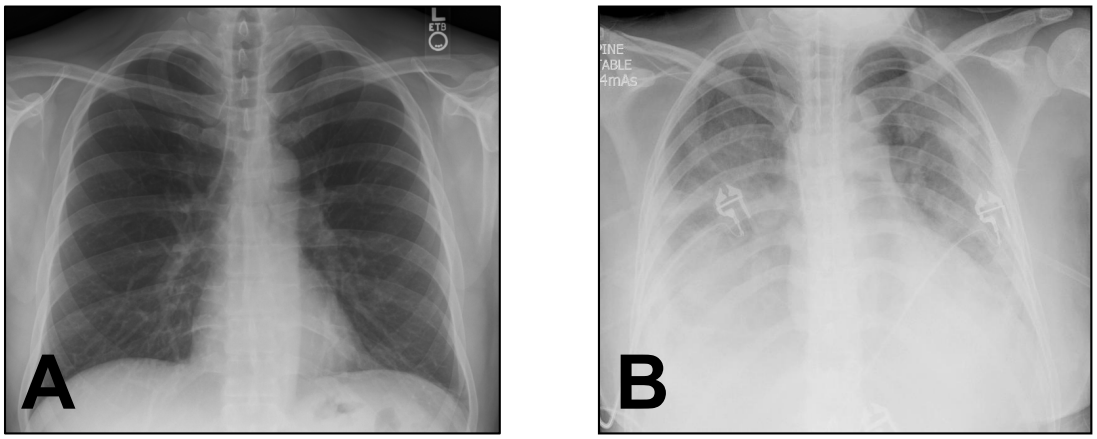

Figure 1-1 Chest radiographs of a healthy adult and a patient with ARDS
The chest radiograph of the patient with ARDS in B shows bilateral white (fluid-filled) pulmonary infiltrates compared to the black (air-filled) lung fields of a healthy adult in A.

A number of issues of reliability and validity with these definitions led a panel of international experts to meet in 2011 and revise the definition by consensus process. The “Berlin definition” removed the term “ALI” and incorporated it into three levels of ARDS severity graded by degree of hypoxaemia:

- **Impaired oxygenation** (with a minimum PEEP of 5 cm H_2O) with a reduced PaO_2:FiO_2 ratio
    - **Mild ARDS:** ratio is 201-300 mmHg (26.6-29.9 kPa)
    - **Moderate ARDS:** ratio is 101-200 mmHg (13.3-26.6 kPa)
    - **Severe ARDS:** ratio ≤ 100 mmHg (≤13.3 kPa)

  with:

- **Acute onset lung injury** (within 1 week of an apparent clinical insult with progressive respiratory symptoms)
- **Bilateral pulmonary infiltrates** on chest radiograph not explained by another respiratory pathology (e.g. pleural effusion, pneumothorax or pulmonary nodules)
- **Exclusion of heart failure or volume overload** as explanation of respiratory failure

Adapted from 2012 Berlin ARDS definition (Ranieri et al. 2012).

The term “Acute Lung Injury” or “ALI” is still nonetheless used clinically, but in the scientific literature it more commonly refers to experimentally induced lung injury in animal or human models.

1.2.2 Epidemiology and mortality

The largest prospective epidemiological study in 1999-2000 in the United States (US) estimated an age-adjusted incidence of 190,600 adult cases of ARDS in the US each year (Rubenfeld et al. 2005). There is some evidence to suggest the incidence has been decreasing over the last decade (Li et al. 2011). Inpatient mortality rates vary between 31 to 74% depending on the precise definition criteria used, with respiratory failure causing death in only 9 – 16% cases (Ware & Matthay 2000; Rubenfeld et al. 2005; Frutos-Vivar et al. 2004; Vincent et al. 2003). The Berlin definition was validated in 269 patients and predicts 90-day mortality according to the underlying severity: mild ARDS = 20% (11-31 95% Confidence interval - CI), moderate ARDS = 41% (33-49%) and severe ARDS = 52% (36-68%), overall ARDS mortality = 36% (Ranieri et al. 2012).

ARDS prolongs intensive care unit (ICU) admissions and leads to secondary hospital-acquired infections; per year in the US it was estimated to be associated with 3.6 million hospital days (Rubenfeld et al. 2005).

1.2.3 Aetiology and risk factors

The clinical conditions associated with the development of ARDS are divided into those originating within the lung itself (direct lung injury) and those distant from the lung (indirect lung injury), as shown in Table 1-1 below:

DIRECT LUNG INJURY	INDIRECT LUNG INJURY
Common causes	**Common causes**
• Pneumonia • Aspiration of gastric acid contents	• Severe sepsis • Severe trauma with shock
Less common causes	**Less common causes**
• Inhalational injury • Pulmonary contusions • Fat emboli • Near drowning episode • Reperfusion injury following lung transplantation or pulmonary embolectomy	• Cardiopulmonary bypass • Drug overdose • Acute pancreatitis • Transfusion-related acute lung injury (TRALI) • Disseminated intravascular coagulation • Head injury • Burns

Table 1-1 Clinical conditions associated with the development of ARDS
Table adapted from Ware and Matthay, 2000

In a series of 1113 patients, the commonest condition was severe sepsis (79% of all cases) from a suspected pulmonary (46%) or extrapulmonary source (33%). Less commonly associated was aspiration (11%), severe trauma (7%), blood transfusion (3%), drug overdose (3%) and acute pancreatitis (3%) (Rubenfeld et al. 2005). When 2 or more associated conditions are present, the risk of developing ARDS is significantly higher (Pepe et al. 1982).

The main independent risk factors for a poor outcome include disease severity as assessed by the Acute Physiology and Chronic Health Evaluation III (APACHE III) or the Simplified Acute Physiology II (SAP II) scores (Cooke et al. 2008), age >60, minute ventilation >13.9L/min, respiratory rate > 21, renal failure, liver failure and shock (Brown et al. 2011). Additional environmental risk factors of particular research interest are chronic alcohol abuse (Moss et al. 1996) and passive or active exposure to cigarette smoke, demonstrated in patients undergoing elective oesophagectomy (Tandon et al. 2001; Zingg et al. 2011), or following blunt chest trauma (Calfee et al. 2011). The mechanisms of cigarette smoke are not fully understood but may include activation of type II alveolar epithelial cells with consequent neutrophil influx in response to mechanical ventilation (Hirsch et al. 2014).

Research into genetic polymorphisms predisposing to the development of ARDS using genetic association studies has identified well over 20 candidate genes, whose functions in lung injury and repair give important clues about the pathogenesis of the condition (Gao & Barnes 2009). More recently, genome-wide association studies have identified single nucleotide polymorphisms (SNPs) in the *FARP2* gene (encoding a guanine nucleotide exchange factor that activates Rac-1, crucial in actin polymerisation, cell movement, adhesion and integrin signalling) and the *PPFIA1* gene (encoding liprin α, also involved in cell adhesion, integrin function and cell-matrix interactions) as major risk variants for ARDS (Wurfel et al. 2014; Christie et al. 2012).

1.2.4 Pathogenesis of ARDS

The following processes are central to the pathophysiology of ARDS within the lung and occur simultaneously. Our understanding is largely inferred from pathohistological appearances at post mortem.

1. Dysregulated lung inflammation with recruitment and influx of innate immune cells, particularly neutrophils, macrophages and dendritic cells.
2. Exaggeration and perpetuation of the inflammatory response through excessive neutrophil degranulation and synthesis of inflammatory mediators, including proteases, reactive oxygen species and cytokines.

3. Damage to and death of endothelial and epithelial cells, leading to increased permeability and leakage of leukocytes, erythrocytes, platelets and protein-rich exudative fluid into the alveolar space, impaired synthesis and release of pulmonary surfactant with subsequent formation of hyaline membranes on the basement membrane, causing impaired gas exchange and hypoxaemia.
4. Uncontrolled activation of the clotting cascade causing capillary microthromboses and impaired fibrinolysis within the alveoli.
   (Ware & Matthay 2000; Han & Mallampalli 2015)

Ware and Matthay's schematic diagram summarises these processes well (see Figure 1-2 below)

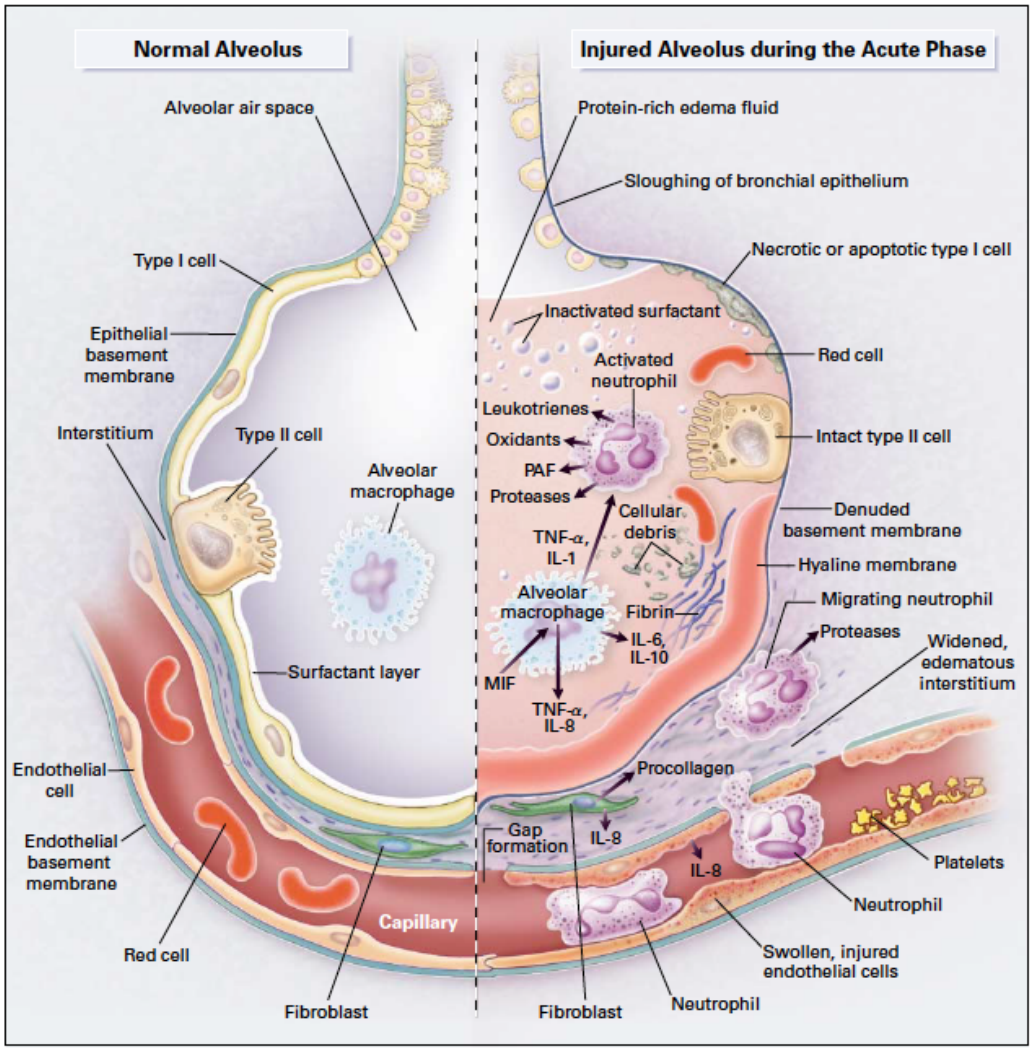

Figure 1-2 Cellular processes within the alveolus during the acute phase of ARDS
Image taken directly from Ware and Matthay, 2000

1.2.5 ARDS as a systemic disease

Although most typically manifested in the lung, ARDS should be considered as a systemic inflammatory disease (Han & Mallampalli 2015). Both alveolar and serum levels of key pro-inflammatory cytokines such as Tumor necrosis factor α (TNFα), Interleukin-1β (IL-1β), IL-6 and IL-8 are raised and persist in unresolving cases of ARDS (Meduri et al. 2009). There is also evidence of systemic immunosuppression with C5a anaphylatoxin-mediated peripheral blood neutrophil dysfunction (Solomkin et al. 1981; Huber-Lang et al. 2002) and endotoxin tolerance in peripheral blood mononuclear cells (Buttenschoen et al. 2008) that are likely to predispose ARDS patients to developing secondary hospital-acquired infections (HAIs). A breakdown in immune tolerance is also seen in over half of ARDS patients with rapid production of autoantibodies (Burbelo et al. 2010).

1.2.6 Resolution of ARDS

Effective resolution of ARDS requires re-establishment of intact epithelial and endothelial barrier function through proliferation and differentiation of resident type II alveolar epithelial cells (Adamson & Bowden 1974) or possibly from progenitor cells (McQualter et al. 2010), clearance of apoptotic neutrophils and cell debris by M2 (alternatively activated) alveolar macrophages in a process known as “efferocytosis” and reabsorption of alveolar fluid (Matthay et al. 2012).

1.2.7 Animal and human models of ARDS

Although rodent models have proven extremely useful in the study of certain mechanisms involved in ARDS, it should be stressed early on in this thesis that no single model has been able to replicate the three key features seen in ARDS patients: severe neutrophilic infiltration, hyaline membrane deposition and microthrombi formation. In essence these models allow scientists to test hypotheses in reproducible models of acute alveolar inflammation. Furthermore, myeloid cell development and distribution, pulmonary anatomy and physiology are markedly different between rodents and humans, meaning that translation of findings into human disease is challenging.

On the other hand, human models of ARDS such as one-lung ventilation, cardiopulmonary bypass, inhaled lipopolysaccharide (LPS) and ex vivo lung perfusion (EVLP) more closely replicate the biological mechanisms of ARDS, but are themselves limited by the low level of the inflammatory response as well as organ availability (Proudfoot et al. 2011).

1.2.8 Existing treatments for ARDS

The formation of the US ARDS Network (ARDSNet) by the National Heart, Lung and Blood Institute (NHLBI) and National Institute of Health (NIH) in 1994 has contributed significantly to a number of multicentre randomised clinical trials in ARDS. Clinical trials have tested a range of anti-inflammatory strategies with disappointingly little success.

9 small randomised trials of methylprednisolone in ARDS were reviewed in a recent meta-analysis; although there was a trend towards a positive mortality benefit when administered after the onset of ARDS, no statistically significant effect was evident (Peter et al. 2008). Sivelestat is a potent neutrophil elastase inhibitor that is used widely in clinical practice in the treatment of ARDS in Japan. A meta-analysis of 8 clinical trials of sivelestat showed no 30-day mortality benefit or increase in ventilator-free days (Iwata et al. 2010), despite promising data from trials of experimental lung inflammation in rats (Wang et al. 2014). Statins can influence inflammatory responses and are thought to have a role in predisposition to sepsis. A large ARDSNet trial of rosuvastatin in sepsis-associated ARDS was stopped early due to futility (Truwit et al. 2014), and a further large multicentre double-blinded clinical trial of 540 ARDS patients given either 80 mg simvastatin or placebo daily showed no difference in terms of ventilator-free days, days free from non-pulmonary organ failure, or mortality at 28 days (Boyle et al. 2015).

Inhaled nitric oxide (NO) is a potent pulmonary vasodilator and inhibitor of neutrophil adhesion. Although a preliminary phase II trial in ARDS showed impressive physiological effects with improved mean PaO_2 levels (Dellinger et al. 1998), these findings did not translate to any reversal of ARDS or mortality benefit (Lundin et al. 1999).

Exogenous surfactant therapy is of benefit in the respiratory distress syndrome in children, but showed no mortality benefit in a randomised, double-blind trial of 448 adult patients with ARDS, when delivered intratracheally for 24 hours only. There was however a significant improvement in oxygenation compared to patients receiving standard therapy (Spragg et al. 2004).

Other large randomised-controlled clinical studies showing no difference in mortality have tested liposomal prostaglandin E_1 (Abraham et al. 1999), ketoconazole (ARDSNet 2000a), lisofylline (a synthetic anti-inflammatory molecule) (ARDSNet 2002), aerosolised β_2 agonist (Matthay et al. 2011), intravenous β_2 agonist (Gates et al. 2013) and Omega-3 fatty acid supplementation (Rice et al. 2011).

The only randomised-controlled trial in ARDS to show unequivocal improved mortality was non-pharmacological, using “lung-protective ventilation” to limit ventilator-induced alveolar overdistension, or “volutrauma”. This trial compared the outcome of 861 ALI or ARDS patients randomised to ventilation with either a traditional tidal volume (V_T) of 12 ml/kg of predicted body weight and higher airway pressures or a V_T of 6 ml/kg and lower airway pressures (ARDSNet 2000). The trial was prematurely stopped because the mortality was significantly lower in the 6 ml/kg group (31% vs 39.8%; p=0.007). The lower V_T group spent significantly fewer days on a ventilator and suffered less extrapulmonary organ failure. Interestingly the 6 ml/kg group were numerically ‘sicker’ despite the improved mortality, with lower PaO_2, increased $PaCO_2$ and lower pH values. This led to the term “permissive hypercapnia” being adopted in ARDS clinical management.

A number of studies have tried to investigate the optimum level of PEEP to maximise oxygenation through alveolar recruitment and prevention of cycles of recruitment and derecruitment (“atelectrauma”), without causing circulatory depression and further lung injury from alveolar stretch. Another big ARDSNet trial in 2004 tested whether higher PEEP in ALI/ARDS patients (of less than 36 hours) receiving mechanical ventilation with a V_T of 6ml/kg improves clinical outcomes (Brower et al. 2004). The study was stopped early at the second interim analysis due to futility. Higher PEEP levels were actually associated with increased airway pressure, dead space and decreased venous return. A further

study in 2008 compared the “open-lung” strategy of a V_T of 6 ml/kg, plateau airway pressures of ≤ 40cm H_2O, recruitment manoeuvres and higher levels of PEEP with the control established strategy of a V_T of 6 ml/kg, plateau airway pressures of ≤ 30cm H_2O and lower levels of PEEP in 983 patients with ARDS (Meade et al. 2008). The open-lung strategy resulted in no difference in hospital mortality or barotrauma. A similar study tested whether increasing alveolar recruitment while limiting hyperinflation by setting a level of PEEP to achieve a plateau airway pressure of 28-30 cm H_2O reduced mortality (Mercat et al. 2008). Although there was no effect on mortality, the strategy improved lung function and decreased duration of mechanical ventilation and organ failure.

Prone position ventilation is known to improve oxygenation in severe ARDS by a number of mechanisms. A recent non-blinded, randomised-controlled trial in severe ARDS compared early prone positioning for at least 16 consecutive hours per day with supine positioning and found a 50% relative reduction in 28-day mortality in the prone group (16% prone vs 32.8% supine; $p<0.001$) and a significant reduction in unadjusted 90-day mortality (23.6% prone vs 41% supine; $p<0.001$) (Guérin et al. 2013). The control (supine) group were however more severely ill with higher Sequential Organ Failure Assessment (SOFA) scores and increased vasopressor requirements, whereas the prone group received more neuromuscular blockers, making the results more difficult to interpret.

Early administration of short-term neuromuscular blockers in severe ARDS may be of benefit (Papazian et al. 2010). Although the authors report a significant adjusted in-hospital 90-day mortality benefit (31.6% vs 40.7%; $p=0.08$), the trial’s original primary outcome was crude 90-day mortality (i.e. mortality rate at 90 days irrespective of location), affecting the validity of the results. The study needs to be repeated.

Further key clinical studies in ARDS have aimed to assess whether patients should be managed with fluid restriction or diuresis. Theoretically this should reduce pulmonary microvascular pressure and resultant alveolar oedema, which contributes to the marked hypoxaemia in ARDS. In 1000 ALI/ARDS patients, haemodynamic management guided by pulmonary artery catheter insertion offered no improvement in survival or organ function over central

venous catheter insertion, and was actually associated with more complications (Wheeler et al. 2006). In the same patients, liberal fluid management was compared with conservative fluid management (using fluid restriction or diuresis) according to explicit protocols and although 60-day mortality was unchanged, lung function and duration on a ventilator or in intensive care were reduced in the conservative fluid group, with no increased need for cardiovascular or renal support (Wiedemann et al. 2006).

There are no published guidelines in ARDS, but the current principles of best practice are summarised below:

1. Treat underlying cause (e.g. antibiotics for pneumonia or sepsis)
2. Protective lung ventilation with low tidal volumes and plateau-pressure limitation
3. Titration of FiO_2 and PEEP to achieve O_2 saturations of > 88%
4. Conservative fluid management once shock is treated
5. Consider neuromuscular paralysis, prone positioning, extracorporeal membrane oxygenation (ECMO) or high frequency oscillatory ventilation (HFOV) in severe ARDS with refractory hypoxaemia
6. Standard supportive care of critically ill patients with thromboprophylaxis to prevent deep vein thrombosis, optimum blood glucose control, prophylaxis against stress-induced gastrointestinal bleeding, haemodynamic support to maintain a mean arterial pressure >60mmHg, enteral nutrition and blood transfusions in patients with haemoglobin <7g/dL.

Adapted from BMJ Best Practice Online (Ware 2014)

1.2.9 Emerging treatments for ARDS

A myriad of studies have tested treatment strategies for ALI and ARDS in a variety of in vitro, ex vivo and in vivo human and animal models. These have all furthered our understanding of the pathogenesis of the condition. I have focussed on a few potential therapeutic targets below:

1. Cellular therapy with allogeneic human mesenchymal stem cells

Mesenchymal stem cells (MSCs) represent a promising new potential therapy in ARDS. They are simple to culture from adipose tissue or bone marrow and do not raise the same ethical issues as embryonic stem cells. The cells can differentiate into alveolar epithelial or pulmonary endothelial cells to repair cellular injury in ARDS. In mice subjected to intratracheal delivery of *E. coli*, intravenous murine non-autologous MSCs reduced markers of oxidative stress within bronchoalveolar fluid (BALF) but markers of bacterial survival and replication were not measured (Shalaby et al. 2014). These findings were recently replicated in a similar *E. coli* model in rats, in which MSC treatment actually enhanced antimicrobial activity in the lung through antimicrobial peptide (LL37) release. The capacity of ex vivo peripheral blood monocytes to phagocytose live bacteria was also increased in mice receiving MSC treatment. MSCs also increased the in vitro phagocytic capacity of the murine macrophage U937 cell line (Devaney et al. 2015). The mechanism of action of MSCs is fascinating. Using vital imaging with confocal and 2-photon microscopy, Islam et al. convincingly showed that bone-marrow derived stromal cells delivered intranasally appear to transfer mitochondria to pulmonary alveolar epithelial cells through connexin 43-containing gap junctional channels to increase alveolar adenosine triphosphate (ATP) levels and attenuate LPS-induced murine lung inflammation (Islam et al. 2012). Intratracheal therapy is also effective in an ex vivo perfused human lung model of *E. coli* endotoxin-induced injury and the mechanism is mediated by secretion of keratinocyte growth factor (KGF) (Lee et al. 2009). This finding led to a study testing whether recombinant KGF (palifermin) reduces alveolar injury in a human model of ARDS, in which healthy volunteers inhale LPS. Intravenous KGF was safe and although it did not affect levels of alveolar neutrophil recruitment or protein leak, KGF promoted surfactant protein D release and induced a pro-resolutionary environment in the lung (Shyamsundar et al. 2014). A multicentre randomised placebo-controlled trial of KGF is now underway to test whether KGF itself can improve oxygenation in patients with ARDS (Cross et al. 2013).

Furthermore, a Phase 1 study of intravenous adipose tissue-derived MSC therapy in 12 ARDS patients demonstrated safety (Zheng et al. 2014) and a further Phase 1/2 trial of intravenous bone-marrow derived MSCs in 69

moderate/severe ARDS patients in the US is currently recruiting (Liu et al. 2014), with a United Kingdom (UK) study also in preparation.

2. Aspirin

Neutrophil-platelet interactions contribute to inflammation in ARDS (Bozza et al. 2009). In a prospective study of 202 ARDS patients, aspirin therapy (either pre-hospital, in intensive care, or both) was associated with reduced mortality after multivariate analysis (Boyle et al. 2015). Aspirin was effective in attenuating lung injury in transfusion-related and acid-induced murine lung inflammation (Looney et al. 2009) and a clinical trial to test whether aspirin therapy is preventative in patients at high risk of developing ALI is recruiting at present (Kor et al. 2012).

3. Ubiquitin-proteasome system

Ubiquitin is a small molecule widely expressed across most mammalian cells. It marks proteins for degradation in the proteasome in a process known as “ubiquitination”. The final step of this process involves the action of one of hundreds of different ubiquitin ligases (E3 ligases) and offers a mechanism for selective therapeutic intervention (Bonifacino & Weissman 1998; Han & Mallampalli 2015). In ARDS the ubiquitin-proteasome system is activated (Vadász et al. 2012). One example of its action is the regulation of the Na, K-ATPase pump on alveolar epithelial cells that drives lung fluid clearance. In hypoxic conditions, the ion pump is degraded by ubiquitination, reducing alveolar fluid clearance (Dada et al. 2007). Proteasome inhibitors are in development as cancer therapies and evidence suggests that they may induce anti-inflammatory effects (Mallampalli et al. 2013).

1.2.10 Neutrophils and ARDS

Neutrophils are key cellular mediators involved in rapidly responding to and clearing bacterial and fungal infection. They are recruited early to the alveoli of patients with ARDS and their levels correlate with degree of hypoxia and protein leak and clinical outcome (Parsons et al. 1985; Weiland et al. 1986; Steinberg et al. 1994). When neutrophils are depleted in mice with cyclophosphamide or anti-neutrophil antibodies, LPS or haemorrhage-induced lung inflammation is

significantly reduced in mice, indicating a causative role (Abraham et al. 2000). Similarly, IL-8-mediated neutrophil recruitment is blocked when rabbits exposed to acid-induced lung inflammation are pre-treated with an anti-IL-8 monoclonal antibody (Folkesson et al. 1995).

Acute alveolar inflammation induces release of inflammatory mediators from platelets (Bozza et al. 2009), alveolar macrophages and epithelial cells, including the cytokines IL-1, IL-6, IL-8 and TNFα (Donnelly et al. 1993; Pugin et al. 1996; Chollet-Martin et al. 1996). The lung is unique in that primed circulating neutrophils become trapped or 'sequestered' in both postcapillary venules of the systemic circulation and alveolar capillaries of the pulmonary circulation through selectin and integrin-dependent mechanisms of tethering, rolling, activation and adhesion (Zemans et al. 2009; Gane & Stockley 2012). The activated neutrophils can then migrate through the inflamed endothelium along chemotactic gradients into the lung alveoli or interstitium (Maniatis et al. 2008). Interestingly, it has been put forward that the lung has the capability of regulating this process by 'deactivating' neutrophils, since only about 60% of peripheral blood neutrophils are activated in an acute inflammatory response, when 100% of the cardiac output passes through the lung vasculature (Summers et al. 2010).

Appropriately activated neutrophils transmigrate the endothelium and release their granule contents extracellularly through a process known as degranulation. Neutrophil apoptosis is delayed by macrophages to maximise pathogen recognition, phagocytosis and killing (Chopra et al. 2009).

Phagocytosis and killing of invading pathogenic microorganisms by neutrophils is a complex mechanism involving ingestion of opsonised organisms, fusion of the resulting phagosome with intracellular granules to form a phagolysosome and simultaneous assembly of the enzyme nicotinamide adenine dinucleotide phosphate (NADPH) oxidase to generate reactive oxygen and reactive nitrogen species. The microorganism is rapidly degraded by the combined action of proteases, reactive species and pH changes of the phagolysosomal environment just minutes after being phagocytosed (Segal 2005; Nauseef 2007).

Predicting the precise fate of the neutrophil after phagocytosis and bacterial killing is not fully understood. We know that activated neutrophils can lyse, necrose, apoptose or undergo an alternative programmed cell death sometimes known as 'NETosis' involving neutrophil extracellular trap (NET) formation. NETs are composed of chromatin and selected granule and cytoplasmic proteins. They are potently microbicidal and are thought to contribute to further extracellular bacterial killing in vivo (Brinkmann et al. 2004).

Overexuberant neutrophil activation causes direct and indirect tissue injury by release of proteases, cytokines and reactive oxygen species (ROS) (Grommes & Soehnlein 2011). Extracellular release of granule products is potently anti-microbial, pro-inflammatory and can therefore be considered as a physiological response when regulated, but dependent on the size of the inflammatory stimulus and the intensity of the neutrophil response, excessive neutrophil granule release may become pathological by causing damage to the alveolar epithelium, increased permeability and protein-rich fluid leak into the alveolar space (Hogg 1994). Human neutrophil elastase (HNE) degrades pulmonary surfactant, further contributing to alveolar collapse and injury (Liau et al. 1996).

Neutrophil-dependent processes have therefore been the therapeutic targets of numerous previous animal models of acute lung inflammation. More than 50 inhibition or knockout studies have targeted cytokines (TNFα, IL-1β), chemokines (IL-8 and its neutrophil receptor CXCR2), cell adhesion molecules (selectins and β_2 integrins), granule proteins (HNE, matrix metalloproteinases = MMP-8 and 9, cathepsin-G) or free radical release (through inhibition or gene deletion of NADPH oxidase and nitric oxide synthase) (Grommes & Soehnlein 2011). The majority of these studies demonstrated a protective effect, but it is important to consider publication bias in favour of positive studies. Translation of neutrophil therapies into clinical trials has proven difficult due to the heterogeneous nature of ARDS patients and redundancy of the molecules involved.

This thesis sought to tackle the challenge of inhibiting the mechanisms of degranulation in neutrophils, while maintaining sufficient neutrophil recruitment and function to achieve effective bacterial phagocytosis and killing.

1.3 Regulation of Degranulation in Neutrophils

1.3.1 Granule sorting

Neutrophils comprise 60-70% of circulating white blood cells in humans, but only 10-20% in mice (Doeing et al. 2003). They possess a short lifespan but their numbers in peripheral blood can increase several-fold when mobilised from bone marrow in response to infection. When fully mature, they have limited ability to synthesise proteins *de novo*, but their cytoplasm is packed with pre-formed granules capable of being released in large quantities into phagosomes or extracellularly by degranulation.

In the literature, the term ‘degranulation’ is commonly confused with the term ‘exocytosis’. For clarification, ‘exocytosis’ refers to the energy-dependent fusion of an intracellular vesicle with the plasma membrane, whereas ‘degranulation’ refers to the process by which granules containing anti-microbial cytotoxic molecules are released extracellularly from the plasma membrane **or** into intracellular membrane-bound phagosomes (or both).

During the stages of neutrophil differentiation, groups of granule proteins are sequentially generated and packaged into specific granule subsets: first primary, or “azurophilic” granules, containing potent enzymes such as myeloperoxidase (MPO), proteinase-3, cathepsins, defensins and HNE; then secondary or “specific” granules, predominantly containing the antimicrobial protein lactoferrin (LTF), lysozyme and alkaline phosphatase and then finally the tertiary granules, containing mainly MMP-8 and MMP-9 (Gullberg et al. 1997). A separate, fourth granule containing L-ficolin-1, an opsonin capable of activating the lectin complement pathway, has also been identified (Rorvig et al. 2009). “Secretory vesicles” are also present and contain albumin and *de novo* synthesised cytokines. The precise mechanisms of granule sorting are not fully understood. Most granule enzymes are synthesised in an inactive form and require conversion into their active form through proteolytic cleavage, a process dependent on the charged acidic environment generated within lysosomes (Sheshachalam et al. 2014).

1.3.2 Granule release

Upon stimulation, granule subsets have variable propensities for release by degranulation. Granules formed later in neutrophil differentiation are released more readily. When stimulated with N-Formylmethionyl-leucyl-phenylalanine (fMLP), human neutrophils release 100% secretory vesicles, 38% tertiary granules, 22% of secondary granules and 7% of primary granules; their release appears dependent on relative sensitivity to increasing intracellular Ca^{2+} concentrations (Sengeløv et al. 1993; Sengeløv et al. 1995).

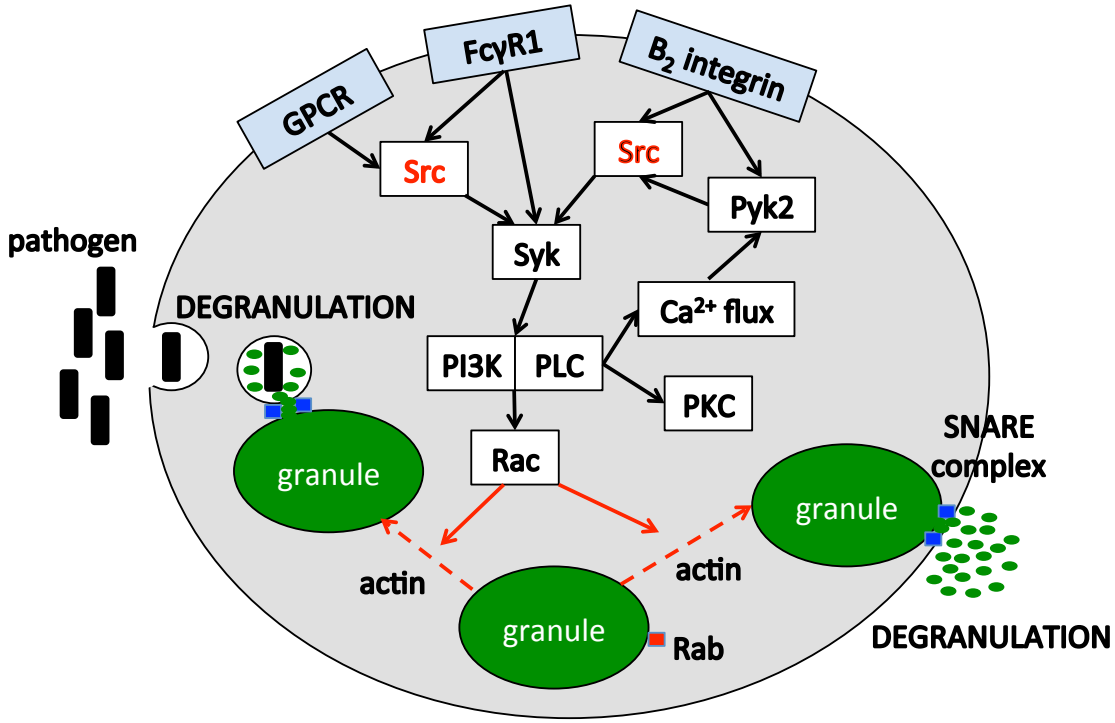

Figure 1-3 Schematic diagram of the main neutrophil signalling pathways regulating degranulation
GPCR=G-protein coupled receptor, Src=src kinase, Syk=syk kinase, PI3K=phosphoinosotide 3-kinase, PLC=phospholipase C, PKC=protein kinase C, Pyk2=proline rich kinase 2. Adapted from Sheshachalam et al, 2014

The mechanisms that regulate granule mobilisation and degranulation are highly complex and of central importance to this thesis. Figure 1-3 summarises the main identified pathways. Granules are mobilised by translocation along actin and tubulin networks, a process regulated by Rab, a small GTPase in the Ras superfamily. Membrane fusion is mediated by the formation of **S**oluble ***N***-ethylmaleimide-sensitive factor **A**ttachment Protein **Re**ceptor (SNARE) complexes between vesicle SNARE proteins (v-SNAREs) and target SNARE proteins (t-SNAREs) (Toonen & Verhage 2003; Lacy & Eitzen 2008).

1.3.3 Granule mobilisation is controlled by src kinases

Upstream of the fusion machinery, it is believed that degranulation is controlled by two binary signals, both of which signal via the src family of non-receptor tyrosine kinases (Sheshachalam et al. 2014). Tyrosine kinases are phosphorylated by receptor stimulation and are differentiated by their association to either the intracellular component of receptors (receptor tyrosine kinases) or cytoplasmic enzymes (non-receptor tyrosine kinases).

The first of these two binary signals is adhesion-dependent, involving β_2 integrins (Sengeløv et al. 1995) in vivo or by contact with biological surfaces in vitro (Nathan 1987). Complement receptor 3 (CR3)-mediated phagocytosis is itself mediated through β_2 integrin, inducing conformational changes through Rho G-protein activation (Caron & Hall 1998). Mocsai et al. identified a central role of the src family kinases Hck and Fgr in adhesion-dependent degranulation (Mócsai et al. 1999). Neutrophils adherent to fibrinogen or tissue culture plastic exhibit impaired degranulation when treated with the pan-src kinase inhibitor PP1. Similarly, neutrophils from $Hck^{-/-}$ $Fgr^{-/-}$ double knock-out mice adhere normally but cannot degranulate. This observation was not replicated in single knock-out $Hck^{-/-}$ or $Fgr^{-/-}$ mice.

A role for the highly expressed cytosolic non-receptor tyrosine kinase, proline-rich kinase 2 (pyk2), in transducing integrin-dependent signals to granule mobilisation has been discovered in $pyk2^{-/-}$ deficient mice (Kamen et al. 2011). The mechanism was shown to be dependent on phosphorylation of Vav (a Rac activator) and paxillin (microtubule assembly).

The second binary signal is dependent on receptor-mediated activation, leading to phosphorylation of src kinases and initiation of a kinase cascade. For example, the formylated peptide receptor 1 (FPR1) is a G-protein coupled receptor (GPCR) activated by formylated peptides formed by bacteria degradation and tissue injury. Neutrophils from $Hck^{-/-}$ $Fgr^{-/-}$ and $Hck^{-/-}$ $Fgr^{-/-}$ $Lyn^{-/-}$ knock-out mice do not degranulate or release extracellular superoxide in response to fMLP, but can increase Ca^{2+} influx (Fumagalli et al. 2007). The precise mechanisms linking GPCR activation with src kinase phosphorylation are not fully understood, but they are likely to occur in parallel to GPCR

activation of the phosphoinosotide 3-kinase γ (PI3Kγ) and phospholipase Cβ (PLCβ) pathways (Futosi et al. 2013).

Fcγ receptors on neutrophils, particularly FcγR1 (CD64), recognise immunoglobulin (Ig)G-opsonised microbes and initiate phagocytosis via Cdc42 and Rac (Caron & Hall 1998). The mechanism of degranulation was previously thought to be independent of src kinases, through activation of another important non-receptor tyrosine kinase Syk kinase, also downstream of src kinases in the kinase cascade (Kiefer et al. 1998; Mócsai et al. 2002). However, recently published data by Mocsai's group showed that $Hck^{-/-}$ $Fgr^{-/-}$ $Lyn^{-/-}$ triple knock-out mice were unable to generate an in vivo pro-inflammatory environment in a model of autoantibody (FcR)-mediated skin inflammation, suggesting that src kinases are also integral to FcR-mediated degranulation (Kovács et al. 2014). Although no myeloid cells accumulated at the site of inflammation (resembling the phenotype of β_2 integrin deficient mice), there was not a true impairment in migration, confirmed when they produced chimeras with ½ wild-type myeloid cells and ½ $Hck^{-/-}$ $Fgr^{-/-}$ $Lyn^{-/-}$ deficient cells.

Although both the binary signals described above are mediated through src kinase phosphorylation, each signal requires an activation threshold to initiate degranulation, preventing the adverse effects of degranulation with lesser stimuli (Sheshachalam et al. 2014). However, this tight regulation is lost in a number of inflammatory conditions, including ARDS, severe asthma, rheumatoid arthritis, septic shock and ischaemia/reperfusion injury. Further understanding the mechanisms of degranulation, particularly those regulating individual granule subset translocation and fusion with specific membranes, may offer a number of exciting new therapeutic targets in these conditions.

1.4 Src Kinases

1.4.1 Biology of src kinases

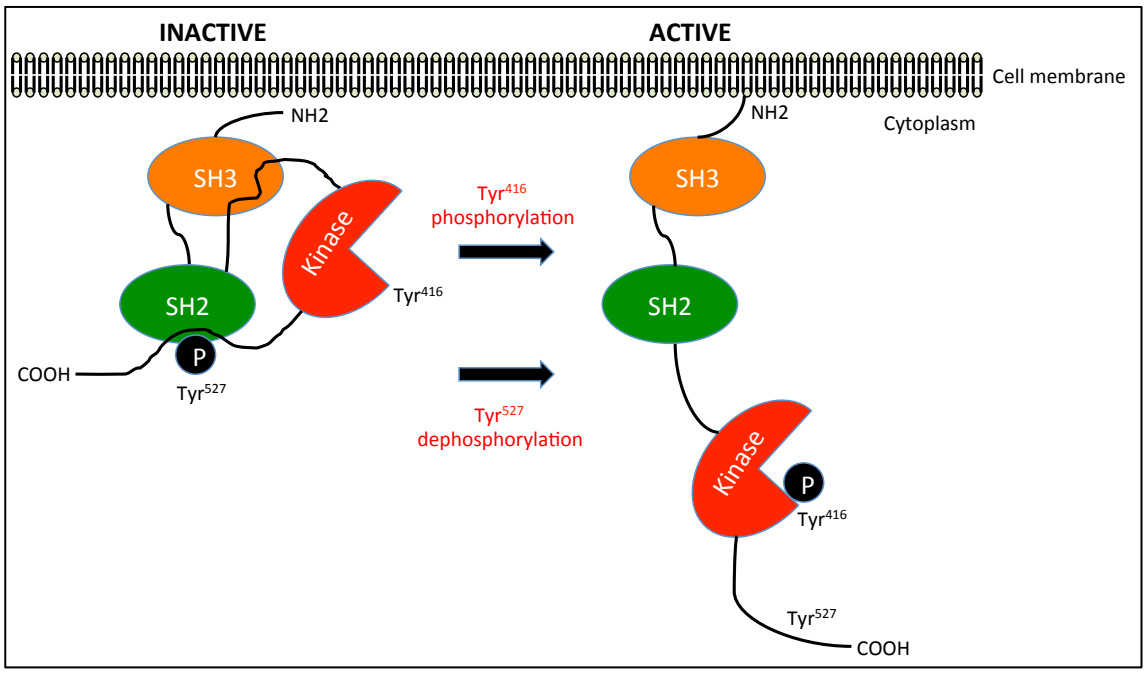

Figure 1-4 Regulation of src kinase activation
SH3 = Src Homology 3 Domain, SH2 = Src Homology 2 Domain. Adapted from Frame 2002

The Src family of tyrosine kinases includes 8 identified members in human cells: c-src, Fyn and Yes are ubiquitously expressed in all cell types; Fgr, Hck and Lyn are predominantly expressed in granulocytes, monocytes and macrophages; whereas Blk and Lck are also found in lymphocytes (Thomas & Brugge 1997). All src kinases share a common regulatory mechanism, shown in Figure 1-4 above. Activity is regulated at two sites: phosphorylation of Tyr^{416} in the catalytic domain switches on enzyme activity, while phosphorylation of Tyr^{527} in the carboxy-terminal tail switches off enzyme activity (Hunter 1987). Src kinases are activated by interaction with a variety of cell-surface receptors and they can activate enzymes at the plasma membrane, the actin cytoskeleton and at cell-cell adhesions. As a result, they have a pivotal role in regulating numerous key cellular functions, including proliferation, differentiation, survival, motility and acute inflammatory responses (Okutani et al. 2006). Indeed c-src (short for sarcoma) was the first discovered oncogene and led to a Nobel Prize for its discovery (Oppermann et al. 1979). C-src overexpression is observed in about 50% of colon, liver, lung, breast and pancreas tumours (Dehm & Bonham

2004). Most of the research into src kinases over the last 35 years has therefore been in the field of oncology, but many researchers have also studied their role in immune cell signalling.

1.4.2 Src kinases and ARDS

Much of our current understanding has come from in vivo studies of LPS-induced lung inflammation in animals, using either pharmacological inhibition of src kinases or knock-out models. A number of small chemical src kinase inhibitors have been developed for cancer treatment, including the pyrrolopyrimidines PP1 and PP2. As discussed in section 1.2.7 above, when interpreting data from rodent models, a note of caution should be observed before applying it to ARDS in humans.

A handful of key studies have implicated src kinase activation in the pathogenesis of ARDS. In rats subjected to oxidant stress induced by haemorrhagic shock/resuscitation followed by intratracheal LPS, alveolar macrophages showed increased Hck activation by Western blotting compared to sham animals treated with LPS. Pre-treatment with PP2 reduced this augmented effect in vivo (Khadaroo et al. 2004). Severgnini et al. demonstrated that both intraperitoneal and intranasal LPS exposure in mice induces signal transducers and activators of transcription (STAT) transcription factors in whole lung samples, peaking at 1 h (all lung cells) and 6 h (neutrophils and monocytes). Both Janus kinase (JAK) and src kinases are known to activate STAT3. Western blot analysis showed activation of JAK and src kinases at 30 min with a peak at 2 h, correlating with the peak in STAT3. The same observation was seen in acid-induced lung inflammation (Severgnini et al. 2004). The authors went on to test PP2 and another selective src kinase inhibitor, SU-6656, in the same model. Both inhibitors attenuated lung inflammation, capillary permeability and LPS-induced cytokines levels, even when given up to 6 h after LPS. Both STAT3 phosphorylation and JAK activation were reduced, suggesting that JAK/STAT are downstream of src kinases, as PP2 does not inhibit JAK. PP2 also reduced mortality when mice were given a lethal dose of LPS (Severgnini et al. 2005). Lee et al. then demonstrated that PP1 pre-treatment of mice undergoing LPS challenge blocked nuclear factor κB (NF-κB) activation, with an associated reduction in

integrin signalling. Pre-treated mice had less lung inflammation, as measured by alveolar protein leak, neutrophil recruitment and alveolar TNFα and MMP-9 levels (Lee et al. 2007).

As discussed earlier, mechanical ventilation may contribute to the pathogenesis of ARDS. Mechanical strain induces c-src activation in fetal rat lung cells and the injury is accentuated by phosphotyrosine phosphatases (which prevent deactivation of tyrosine kinases) and attenuated by tyrosine kinase inhibition (Liu et al. 1996; Parker et al. 1998). A more recent study investigated the anti-inflammatory properties of the anaesthetic ropivacaine on a 'double-hit' murine model of ARDS, involving LPS exposure and volutrauma from high tidal volume ventilation (Piegeler et al. 2014). Ropivacaine reduced excess lung water parameters and MPO activity, and the effect appeared to be through inhibition of src activation and phosphorylation of intercellular adhesion molecule-1 (ICAM-1) and caveolin-1, which maintain pulmonary endothelial barrier function.

A major challenge to dissecting out the roles of individual src kinases is the lack of specificity of the available inhibitors. Specificity of expression in certain cell types and transgenic models give further clues about their individual roles, but like all tyrosine kinases they are likely to exhibit considerable redundancy in function. In an endotoxic shock model involving intraperitoneal injection of LPS, $Hck^{-/-}$ $Fgr^{-/-}$ double knock-out mice showed only 20% mortality at high dose LPS (30 mg/kg) and 0% mortality at lower doses (≤ 20 mg/kg), compared to wild type mice that showed 50% mortality at low dose LPS (5 mg/kg) and 100% mortality at doses ≥ 10 mg/kg (Lowell & Berton 1998). This effect was not observed in single knock-out mice. The double knock-out mice displayed clinical signs of endotoxaemia and had equally high levels of inflammatory cytokines. Unlike wild type mice, that became neutropenic in peripheral blood due to sequestration in the tissues with accompanying exponential end-organ injury until 48 h, $Hck^{-/-}$ $Fgr^{-/-}$ mice showed a dramatic rise in peripheral blood neutrophils after an initial 2-4 h dip, with markers of end-organ injury peaking at 6 h and remaining stable until 48 h. It therefore seems that Hck and Fgr, in combination, are responsible for amplifying and perpetuating the inflammation induced by LPS. However, when Hck alone was rendered constitutively active in $Hck^{F/F}$ "knock-in" mice, spontaneous lung inflammation occurs with extensive eosinophilic and mononuclear cell infiltration into the alveoli and lung

interstitium. Unsurprisingly these mice are exquisitely sensitive to LPS (Ernst et al. 2002).

A role in mediating lung inflammation in ARDS has been attributed to other src kinases also expressed in non-myeloid cells, such as endothelial cells. In bovine pulmonary endothelial cells exposed to both LPS and TNFα, PP1 and PP2 inhibited inducible nitric oxide synthase (iNOS) expression and NO production (Chang et al. 2008). NO overproduction has been implicated in the pathogenesis of ARDS. The authors then used short interfering ribonucleic acid (siRNA) techniques on cultured human pulmonary microvascular endothelial cells to identify the specific src kinases involved. Fyn, Yes, c-src, Lyn, but not Blk, could all be inhibited by siRNA, but only Fyn inhibition prevented NO production in this model. Interestingly, Lyn has recently been shown to have an opposing role, compared to other endothelial src kinases, Yes and c-src (Han et al. 2013). $Lyn^{-/-}$ single knock-out mice showed increased mortality and vascular permeability in response to LPS or vascular endothelial growth factor (VEGF) challenge compared to wild type. The effect is mediated via focal adhesion kinase (FAK) co-localisation and phosphorylation by Lyn, leading to stabilisation of endothelial adherens junctions.

1.5 Summary

Putting these findings together, the published literature suggest that src kinases have a central role in the acute inflammatory responses implicated in the pathogenesis of ARDS, through recruitment, activation and degranulation of leukocytes and dysregulation of vascular permeability. Src inhibition therefore holds great promise as a therapeutic strategy in ARDS, as well as other conditions characterised by an acute inflammatory response. Some of the side effects of long-term treatment with src kinase inhibitors are likely to be avoided with short-term use, but dosing and timing in relation to the inflammatory response remain a significant challenge.

1.6 Unanswered Questions

Until now, in vivo studies have mainly been carried out using LPS to induce lung inflammation. Although this model utilises a reliable stimulus and permits identification of some underlying mechanisms, it is extremely difficult to draw direct parallels with the wide clinical spectrum of ARDS. More clinically relevant in vivo animal models should therefore test pathogen-induced lung inflammation. Until now these models have not been used to test src kinase inhibition. There is an obvious concern that, in the presence of infection, inhibition of acute inflammation may lead to detrimental effects by impairment of phagocytosis and bacterial killing by neutrophils and macrophages. For example, in mice exposed to intratracheal *Pseudomonas aeruginosa,* neutralising antibodies to CXCR2 (IL-8β receptor) markedly attenuated neutrophil recruitment, bacterial clearance and increased mortality (Tsai et al. 2000). Conversely, when the anti-inflammatory cytokine IL-10 is neutralised in mice exposed to intratracheal *Klebsiella pneumoniae*, pre-treated mice had significantly less bacteria in lung homogenates with improved survival, suggesting that adequate clearance of bacteria requires a rapid and vigorous innate immune response (Greenberger et al. 1995).

How src kinases control other key functions of neutrophils, such as CR3-mediated and FcR-mediated phagocytosis, intracellular bacterial killing, apoptosis and oxidative burst, has not been fully characterised. While carrying out my in vitro studies described in Chapter 3, Mocsai's group published an investigation into the effects of a clinically licensed oral src/Abl kinase inhibitor, dasatinib, on pro-inflammatory functions of human neutrophils (Futosi et al. 2012). Interestingly there was little effect on phagocytosis and bacterial killing, raising further hope for a safe therapeutic role of src kinase inhibition in ARDS.

When infection is not the initial trigger mechanism, such as in acid-induced lung inflammation, src kinase inhibition may prove effective in blocking excessive neutrophil degranulation. Although the mechanisms of lung inflammation differ from those already studied in LPS-induced injury, neutrophils remain key cellular mediators of injury. Acid aspiration is the third commonest cause of ARDS, accounting for 1 out of every 10 cases and therefore represents a valid and novel model in which to study src kinase inhibition.

The resolution phase of ARDS is equally as important as the initiation phase, though it is often overlooked in clinical research, where the focus is understandably on improving short-term mortality. It is also very challenging to research at an in vitro level, where the complex interplay of pro- and anti-inflammatory signals are impossible to recreate. However, the secondary effects of inhibiting src kinases in neutrophils on subsequent apoptotic cell clearance has not been studied and would be of great interest. An anti-inflammatory strategy such as this may actually promote effective resolution.

Having identified these important areas of study, I will now present my thesis aims and hypotheses, based on my analysis of the published clinical and scientific literature to date.

1.7 Aims and Hypotheses

In this thesis I will address 3 main bodies of work to test my 3 main hypotheses. They will comprise the three results chapters 3, 4 and 5.

1.7.1 An investigation into the effects of src kinase inhibitors on neutrophil function in vitro

In Chapter 3, I will test my first hypothesis:

1. *"In vitro* src *kinase inhibition in human neutrophils reduces extracellular degranulation in response to both chemical and live bacterial stimuli, without impairing efficient neutrophil phagocytosis and intracellular killing of bacteria"*

As part of this work, I will also aim to design and optimise assays for use in future in vivo and in vitro experiments. I will further describe the effect of src kinase inhibition on other key neutrophil functions, determine optimum concentrations of inhibitors for use in future experiments and select an inhibitor for use in in vivo models of bacteria and acid-induced lung inflammation.

1.7.2 An investigation into the effect of src kinase inhibition on in vivo models of bacteria and acid-induced acute lung inflammation

In Chapter 4, I will test my second hypothesis:

2. *"Inhibition of the* src *kinase pathway attenuates neutrophil recruitment to the alveolar and interstitial spaces, neutrophil degranulation and endothelial cell injury and leak in in vivo models of bacteria and acid-induced acute lung inflammation"*

This novel in vivo work will also test whether src kinase inhibitors, when administered systemically, may induce a detrimental outcome by inhibiting innate immune cell clearance of bacteria.

1.7.3 An investigation into the effect of src kinase inhibitors on the processes of neutrophil-mediated epithelial cell damage and macrophage efferocytosis of apoptotic cells

The in vitro work in Chapter 5 is novel, but based on my interpretation of previously published data, I would hypothesise that:

3. *"In vitro* src *kinase inhibition of human neutrophils attenuates neutrophil-mediated epithelial cell damage whilst promoting a pro-resolutionary environment, allowing efficient apoptotic cell clearance"*

I will also design in vitro and ex vivo models, with the common stimulus of live bacteria, to test my hypothesis and investigate underlying mechanisms.

Chapter 2. Materials and Methods

2.1 Chapter Overview

This chapter details the experimental techniques I used to test my hypotheses. Materials, reagents and their suppliers are listed, followed by a detailed explanation of the methods, referencing the subsequent results chapter(s) in which each individual method is utilised. The precise experimental protocols for Chapter 5 are more complicated and I have therefore included these together with the results in Chapter 5 itself, to aid the reader in interpreting the data.

2.2 Materials, Reagents, Animals, Bacteria and Cell Lines

This section details all the materials, reagents, animals, bacterial strains and cell lines used in the experiments, together with their suppliers. The details of individual laboratory machine equipment is included within the methods section.

2.2.1 Materials

Scientific Laboratory Supplies Ltd. (Nottingham, UK)

- 40 µm cell strainer
- Corning 75 cm^2 tissue culture flasks
- Corning tissue culture-treated 24-well sterile plates
- NUNC Maxisorp flat bottom 96 well enzyme linked immunoabsorbent assay (ELISA) microplates

Greiner Bio-One Ltd (Stonehouse, UK)

- 15 ml and 50 ml Falcon tubes
- 30 ml universal containers
- 7 ml Bijou tubes
- Polystyrene (96 well) flat bottom microplates

Life Technologies (Paisley, UK)

- 0.5, 1.5 and 2 ml eppendorf tubes
- 0.2 um syringe filters

Becton Dickinson (BD) Biosciences (Oxford, UK)

- Fluorescence-activated cell sorting (FACS) tubes
- Vacutainer® heparin tubes

Appleton Woods Ltd. (Birmingham, UK)

- Corning 24 well Transwell filters, clear polyester membrane, 6.5 mm, 3.0 um pore size
- Corning 24 well Transwell filters, clear polyester membrane, 6.5 mm, 0.4 um pore size

Merck Millipore (UK) Ltd. (Feltham, UK)

- Millicell Hanging Cell Culture Insert, polyethylene terephthalate, 1.0 µm pore size

VWR International Ltd. (Leicester, UK)

- 13 mm cover slips

Miltenyi Biotec Ltd. (Surrey, UK)

- CD14 microbeads
- Human MACS Magnetic separation (MS) columns

Bertin Technologies (France)

- 2 ml homogeniser tubes (Precellys Ceramic Kit 1.4 mm)

Sigma Aldrich Ltd. (Gillingham, UK)

- 3MM Whatman blotting paper (10 cm x 100 m)
- Corning microscope slides, frosted one end, one side

GE Healthcare Life Science (Little Chalfont, UK)

- Amersham Hyperfilm (18 x 24 cm)

Beckman Coulter (UK) Ltd. (High Wycombe, UK)

- Flow-Check Fluorospheres

2.2.2 Reagents

Sigma Aldrich Ltd. (Gillingham, UK)

- 2% Gelatin solution
- 4-(2-Aminoethyl) sulfonyl fluoride hydrochloride (AEBSF)
- 4-(2-hydroxyethyl)-1-piperazineethanesulfonic acid (HEPES)
- 4′,6-diamidino-2-phenylindole dihydrochloride (DAPI)
- Acetone
- Bovine serum albumin (BSA)
- Antipain
- Aprotinin
- Avertin
- Benzamidine
- Beta-mercaptoethanol
- Calcium chloride
- Chymostatin
- Cytochalasin B
- Cytochalasin D
- Cytochrome c

- Dimethoxybenzidine (DMB)
- Dimethyl sulfoxide (DMSO)
- DPX
- Dulbecco's phosphate buffered saline (PBS) 10X (no Ca^{2+}, no Mg^{2+}) and Dulbecco's PBS 1X (no Ca^{2+}, no Mg^{2+})
- Ethylenediaminetetraacetic acid (EDTA)
- Foetal calf serum (FCS)
- Giemsa stain
- Glycerine
- Glycine
- Hanks' balanced salt solution (HBSS) with and without Ca^{2+} and Mg^{2+}
- High resolution agarose
- Hydrochloric acid (HCl)
- IgG1 isotype control from murine myeloma
- Leupeptin
- Lipopolysaccharide (LPS) from *E. Coli* 026:B6
- Luria Bertani (LB) broth and agar
- Methanol
- N-Acetyl-L-cysteine
- N-formyl methinyl leucyl phenylalanine (fMLP)
- Nonidet P-40
- O-Dianisidine dihydrochloride
- Platelet activating factor (PAF)
- Paraformaldehyde
- Pepstatin A
- Phenylmethanesulfonyl fluoride (PMSF)
- Phorbol myristate acetate (PMA)
- Potassium Chloride
- Potassium Phosphate monobasic
- PP1
- Sivelestat sodium salt hydrate
- Sodium bicarbonate
- Sodium carbonate
- Sodium chloride
- Sodium citrate 3.8% solution
- Sodium Dodecyl Sulfate (SDS)
- Sodium fluoride
- Sodium orthovanadate
- Sodium Phosphate dibasic
- Streptavidin Peroxidase from *S. avidnii*
- Sulphuric acid (H_2SO_4)
- Superoxide dismutase (SOD)
- Tetramethylethylenediamine (TEMED)
- Triton X-100 solution
- Trizma base
- Trypan blue
- Trypsin
- Tween 20
- Zymosan A from *Saccharomyces cerevisiae*

Life Technologies (Paisley, UK)

- Ammonium-Chloride-Potassium (ACK) lysis buffer
- Anti-human IL-1β, IL-6, IL-8, IL-1RA, IL-10, TNFα, Monocyte chemotactic protein (MCP)-1 antibody pairs for ELISA
- Dihydrorhodamine 123 (DHR)
- Fetal Bovine Serum
- Iscove's modified Dulbecco's medium (IMDM) with and without phenol red
- Molecular Probes CountBright™ Absolute Counting Beads
- Penicillin/Streptomycin 100X solution
- pHrodo red *E. coli* and green *S. aureus* bioparticles
- Pierce bicinchoninic acid (BCA) Protein Assay kit
- Pierce HALT protease & phosphatase inhibitor cocktail (100X)
- Roswell Park Memorial Institute (RPMI)-1640

Biolegend UK Ltd. (London, UK)

- Allophycocyanin (APC)-conjugated mouse anti-human CD62L monoclonal antibody (IgG, κ)
- APC-conjugated mouse anti-human CD63 monoclonal antibody (IgG1, κ)
- Fluorescein isothiocyanate (FITC)-conjugated rat anti-mouse CD11b monoclonal antibody (IgG2b, κ)
- Pacific Blue- conjugated rat anti-mouse Ly6G monoclonal antibody (IgG2a, κ)
- Phycoerythrin (PE)-conjugated mouse anti-human CD66b monoclonal antibody (IgM, κ)
- PE-conjugated rat anti-mouse CD63 monoclonal antibody (IgG2a, κ)
- PE/Cy7-conjugated mouse anti-human CD16 monoclonal antibody (IgG1, κ)
- PerCP/Cy5.5-conjugated mouse anti-human CD11b monoclonal antibody (IgG1, κ)
- Rat anti-mouse CD16/32 Fc blocking monoclonal antibody (IgG2a, λ)

Cell Signalling Technology (Danvers, MA, US)

- Mouse anti-human total src IgG1 antibody
- Rabbit anti-human phospho-p38 Mitogen-activated protein kinase (MAPK) antibody
- Rabbit anti-human phospho-src Tyr^{416} antibody
- Rabbit anti-human total p38 MAPK antibody

Abcam (Cambridge, UK)

- Biotin-conjugated rabbit anti-human LTF polyclonal antibody (IgG)
- Human LTF protein
- Mouse anti-human LTF monoclonal antibody (IgG1, κ)

Stratech Scientific Ltd. (Suffolk, UK)

- Horseradish peroxidase (HRP)-conjugated goat anti-rabbit IgG secondary antibody
- HRP-conjugated goat anti-mouse IgG secondary antibody

R&D Systems Inc. (Abingdon, UK)

- Anti-mouse keratinocyte chemoattractant (KC), IL-6, IL-10, TNFα, MPO, Chemokine ligand-2 (CCL-2) antibody pairs for ELISA

eBioscience Ltd. (Hatfield, UK)

- Mouse soluble IgM ELISA kit

Novatein Biosciences (Woburn, MA, US)

- Mouse LTF ELISA kit

BD Biosciences (Oxford, UK)

- FACS Lysing Solution
- OptEIA 3,3',5,5'-Tetramethylbenzidine (TMB)/Hydrogen peroxide (H_2O_2) Substrate reagent set
- Pharmlyse Lysing buffer (10X concentrate)

Pharmacosmos (Holbaek, Denmark)

- Dextran T500

GE Healthcare Life Science (Little Chalfont, UK)

- Amersham Hybond enhanced chemiluminescent (ECL)
- Percoll Plus

Cambridge Bioscience Ltd. (Cambridge, UK)

- 10x Annexin binding buffer
- Annexin V APC
- Bosutinib
- Dasatinib
- Propidium iodide solution

Bio-Rad Laboratories Ltd. (Hemel Hempstead, UK)

- 30% Acrylamide/Bis Solution (37.5:1)

- Precision Plus Protein Western C Standards

IBG Immunor Ltd. (Shoreham-by-Sea, UK)

- Reastain Diff-Quik stain

Roche Diagnostics Ltd. (W Sussex, UK)

- Collagenase D
- Cytotoxicity lactate dehydrogenase (LDH) detection kit

ChemoMetec A/S (Allerod, Denmark)

- ChemoMetec reagent A-100 and reagent B

Elanco Animal Health (Basingstoke, UK)

- Atipamezole (Antisedan)
- Medetomidine

Pfizer UK Ltd. (Walton Oaks, UK)

- Ketamine

Tesco PLC (Cheshunt, UK)

- Marvel original dried skimmed milk powder

All chemicals were reconstituted upon arrival from suppliers in the appropriate solvents, aliquoted and stored at the suggested temperature according to the product datasheets. All reagents prepared in DMSO were aliquoted at an appropriate molar concentration to ensure that the final DMSO concentration in all assays did not exceed 0.02%.

2.2.3 Animals

8-10 week old female C57/BL6 mice were purchased from Harlan UK Ltd.

2.2.4 Bacteria

Pseudomonas aeruginosa strain PA01 was a kind donation from Professor Kenn Geddes' group, Institute for Cell and Molecular Biosciences, Newcastle University, UK.

Staphylococcus aureus (SA) strain National Collection of Type Cultures (NCTC) 8325 was a kind donation from Dr Elizabeth Veal's group, Institute for Cell and Molecular Biosciences, Newcastle University, UK.

Escherichia coli strain K-12 was a kind donation from Dr Anjam Khan's group, Institute for Cell and Molecular Biosciences, Newcastle University, UK.

Escherichia coli strain American Type Culture Collection (ATCC) 25922 was kindly provided by Professor Adriano Rossi's group, Centre for Inflammation Research, University of Edinburgh, UK.

2.2.5 Cell lines

The A549 cell line (Chapter 5), or *'adenocarcinomic human alveolar basal epithelial cell line'* was a kind donation from Professor John Kirby's group, Institute of Cellular Medicine, Newcastle University, UK. The A549 cell line was originally derived from culturing explanted lung cancer tissue (Giard et al. 1973).

2.3 Recruitment of Volunteers and Patients

2.3.1 Healthy volunteers

(chapters 3 and 5)

Staff and students from Newcastle University were recruited into the study named **"Role of Inflammation in Human Immunity"** (Research Ethics Committee number 12/NE/0121) and gave informed, written consent to donate blood. Up to 160 ml of fresh blood was taken from each volunteer via a 21 gauge hypodermic needle or a 21 gauge butterfly infusion set and decanted immediately into 15 ml or 50 ml Falcon tubes containing sodium citrate at a final concentration of 0.38%. Blood was stored at room temperature and subsequent isolation of blood cell components was commenced within 30 min. For whole blood flow cytometry experiments, blood was collected into BD Vacutainer® heparin tubes and stored at room temperature.

2.3.2 Patients

(chapter 5)

By December 2013, members of our research group began recruiting patients to a Medical Research Council (MRC) – Developmental Clinical Studies (DCS)-funded randomised trial **"Does Granulocyte Macrophage Colony Stimulating Factor (GM-CSF) restore effective neutrophil function in critically ill patients?"** (Research Ethics Committee number 12/YH/0083, EudraCT number 2011-005815-10).

Critically ill patients, defined as those admitted to ICU within the previous 48 h and meeting the criteria for the Systemic Inflammatory Response Syndrome (SIRS); namely at least two of: temperature of < 36^{o}C or > 38^{o}C; pulse > 90 beats per minute; respiratory rate > 20 breaths per minute or a partial pressure of CO_2 < 4.3 kPa; and a white cell count (WCC) < 4 x 10^9/L or > 12 x 10^9/L (American College of Chest Physicians - ACCP/Society of Critical Care Medicine - SCCM Consensus 1992). In addition all patients required support of at least one organ system (eg inotropic/vasopressor support, invasive ventilation or renal replacement therapy) and were expected to survive beyond 48 h. Patients were recruited from four general ICUs situated in two teaching

hospitals in Newcastle upon Tyne (Freeman Hospital and Royal Victoria Infirmary), a district general hospital in Gateshead (Queen Elizabeth Hospital) and a teaching hospital in Sunderland (Sunderland Royal Hospital). Exclusion criteria are listed in Table 2-1 below.

1) Absence/refusal of informed consent	13) Solid organ or bone marrow transplantation
2) Current prescription of a colony stimulating factor	14) Use of maintenance immunosuppressive drugs other than maintenance corticosteroids (allowed up to 10 mg prednisolone/day or equivalent)
3) Any history of allergy/adverse reaction to GM-CSF	15) Known human immunodeficiency virus (HIV) infection
4) Total white cell count > 30 x 10^9/L at the time of screening	16) Active connective tissue disease (eg. rheumatoid disease, systemic lupus erythematosus requiring active pharmacological treatment)
5) Haemoglobin < 7.5 g/dL at the time of screening	17) ST segment elevation myocardial infarction, acute pericarditis (by electrocardiogram - ECG criteria) or pulmonary embolism (radiographically confirmed) in previous week
6) Age < 18 years	18) Involvement in any study involving an investigational medicinal product in the previous 30 days
7) Pregnancy or lactation	
8) Known in-born errors of neutrophil metabolism	
9) Known haematological malignancy and/or known to have >10% peripheral blood cell blasts	
10) Known aplastic anaemia or pancytopaenia	
11) Platelet count < 50 x 10^9/L	
12) Chemotherapy or radiotherapy within the last 24 h	

Table 2-1: Exclusion criteria used for recruitment of critically ill patients

In eligible patients with capacity, informed consent was taken. In patients without capacity, consent was taken from a personal legal representative (e.g. next of kin) or if no family member was present or available, it was provided by a professional legal representative (i.e. an independent ICU consultant physician not directly responsible for the patient's care). A 15 ml blood sample was taken into sodium citrate (end concentration 0.38%) on day 0 prior to

randomisation and an array of study-specific immunological assays were carried out by the study team. Isolated neutrophils surplus to the number required to complete the study were used in the A549 epithelial cell damage model, as outlined in the study protocol and approved by the Research Ethics Committee (REC) (see Chapter 5).

2.4 Isolation of Neutrophils

(Chapters 3 and 5)

Neutrophils were isolated from citrated whole blood by dextran sedimentation and fractionation through isotonic discontinuous Percoll gradients (Haslett et al. 1985). Briefly, citrated blood was centrifuged for 20 min at 300g. The upper layer of platelet rich plasma was removed (Figure 2-1A), placed in a glass serum tube and 1M $CaCl_2$ solution was added (110 µl per 5 ml) before incubating at 37^{o}C to induce platelet aggregation (Figure 2-1E) and form autologous serum, used in subsequent experiments. Meanwhile 2.5 ml of warmed filter-sterilised 6% dextran solution was added per 10 ml of cell pellet, the volume made up to 50 ml with warmed 0.9% normal saline and allowed to sediment for 30 min (Figure 2-1B). The upper leucocyte layer was then transferred to a fresh 50 ml Falcon tube, additional saline added and centrifuged for 5 min at 200g. 2.5 ml of Percoll Plus in phosphate buffered saline without Ca^{2+} or Mg^{2+} ions (PBS-) was added to the cell pellet and layered onto 2.5 ml of 77% Percoll, layered above 2.5 ml of 81% Percoll in a 15 ml Falcon tube (Figure 2-1C), then centrifuged for 20 min at 700g. The upper peripheral blood mononuclear cell (PBMC) layer and lower granulocyte layers (Figure 2-1D) were harvested separately and transferred to fresh tubes before washing once in HBSS without Ca^{2+} or Mg^{2+} ions (HBSS-). A cell count was then performed using a haemacytometer before a second wash with HBSS-. At this point, cells were resuspended at assay-dependent concentrations in warmed Iscove's modified Dulbecco's medium (IMDM) with phenol red, IMDM (phenol red-free) or HBSS with Ca^{2+} and Mg^{2+} ions (HBSS+), depending on the specific assay.

Cell viability of each preparation was assessed using trypan blue exclusion and cell purity by morphology on cytocentrifuge preparations (cytospins). Cytospins were prepared throughout using a ThermoScientific Shandon Cytospin 3 centrifuge (Fisher Scientific UK Ltd., Paisley, UK); 12g for 3 min. Slides were air-dried, fixed in acetone for 10 min and stained in Giemsa for 10 min. Only preparations containing >95% neutrophil purity and with >95% viability were used in experiments (Figure 2-1F).

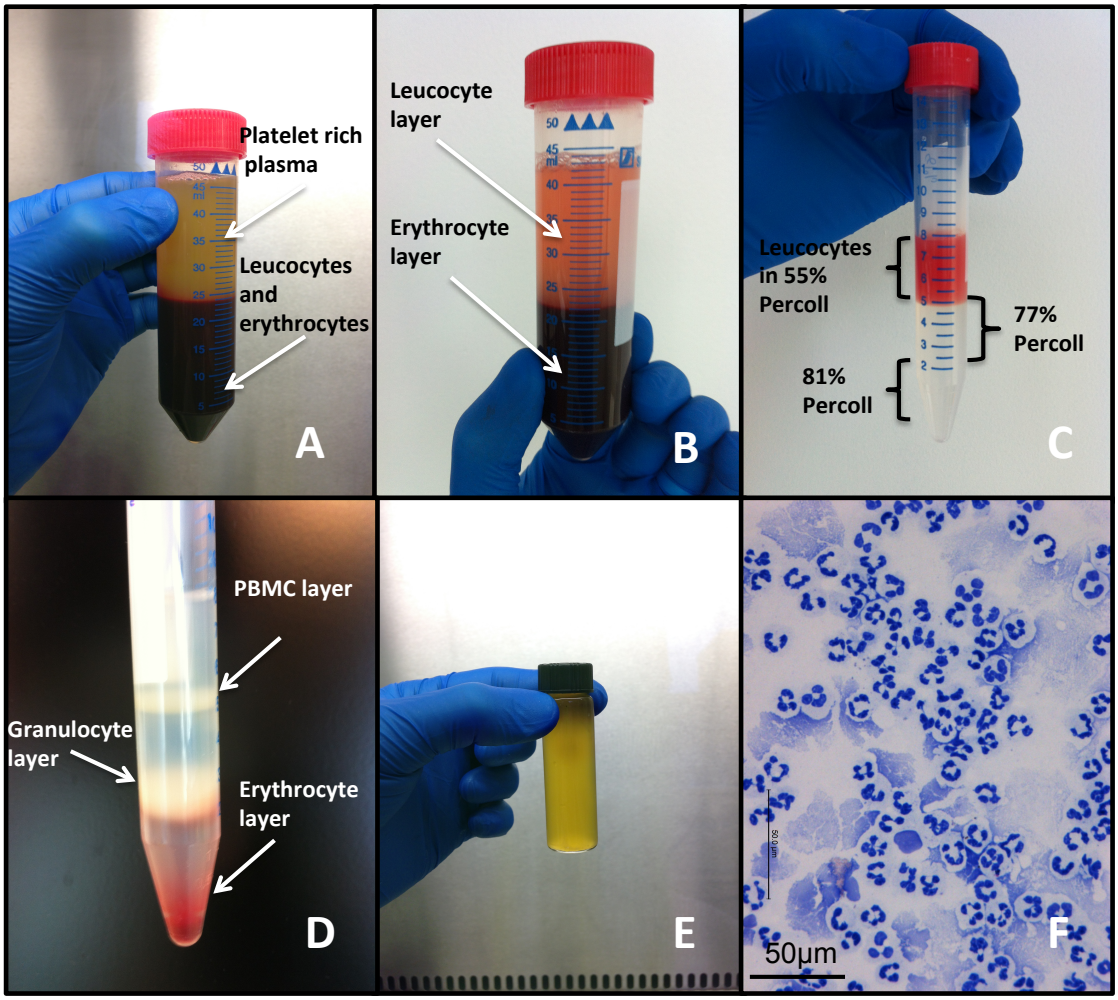

Figure 2-1 Isolation of neutrophils from human blood (Percoll method)
Centrifugation of citrated whole blood to form a platelet rich plasma (A), dextran sedimentation to form a leucocyte rich layer (B), fractionation through isotonic discontinuous Percoll gradients to form PBMC and granulocytes layers (C and D), generation of autologous platelet-free serum (E) and appearance of Giemsa-stained, purified neutrophils on cytocentrifuge preparation (F).

2.5 Isolation of Monocytes

(Chapter 5)

PBMCs were isolated from citrated whole blood by density gradient separation using Ficoll-Paque™ (density = 1.077g/ml) according to the manufacturer's instructions, with slight modifications. Briefly, 20 ml of citrated blood was diluted 1:2 with warmed PBS- and layered upon 10 ml of Ficoll solution in a 50 ml Falcon tube (Figure 2-2A) and centrifuged at 700g for 15 min. The PBMC layer was harvested and transferred to a fresh 50 ml tube (Figure 2-2B), washed twice in 50 ml of warmed PBS- for 10 min at 300g before performing a cell count with assessment of cell viability and purity as described in methods section 1.1 (Figure 2-2D). A typical yield was 2 x 10^7 PBMCs from 20 ml of blood. After a further wash the cell pellet was resuspended in 80 µl of ice-cold wash buffer (composed of PBS-, pH 7.2, 0.5% BSA and 2 mM EDTA) and 20 µl CD14 MACS microbeads per 10^7 total cells and incubated at 4^{o}C for 15 min. The cells were washed by adding 2 ml of ice-cold buffer per 10^7 cells, the pellet resuspended in 500 µl buffer and added to a pre-moistened MACS MS column fixed to a MACS column magnet (Figure 2-2C). The column was washed through three times with 500 µl wash buffer to remove CD14 negative cells. The column was then removed from the magnet and the CD14 positive cells were flushed into a fresh 50 ml tube using 1 ml of wash buffer. A further cell count with assessment of purity and viability was carried out (Figure 2-2E), before resuspending in pre-warmed assay medium at the desired cell concentration and plating onto 24-well tissue culture plates.

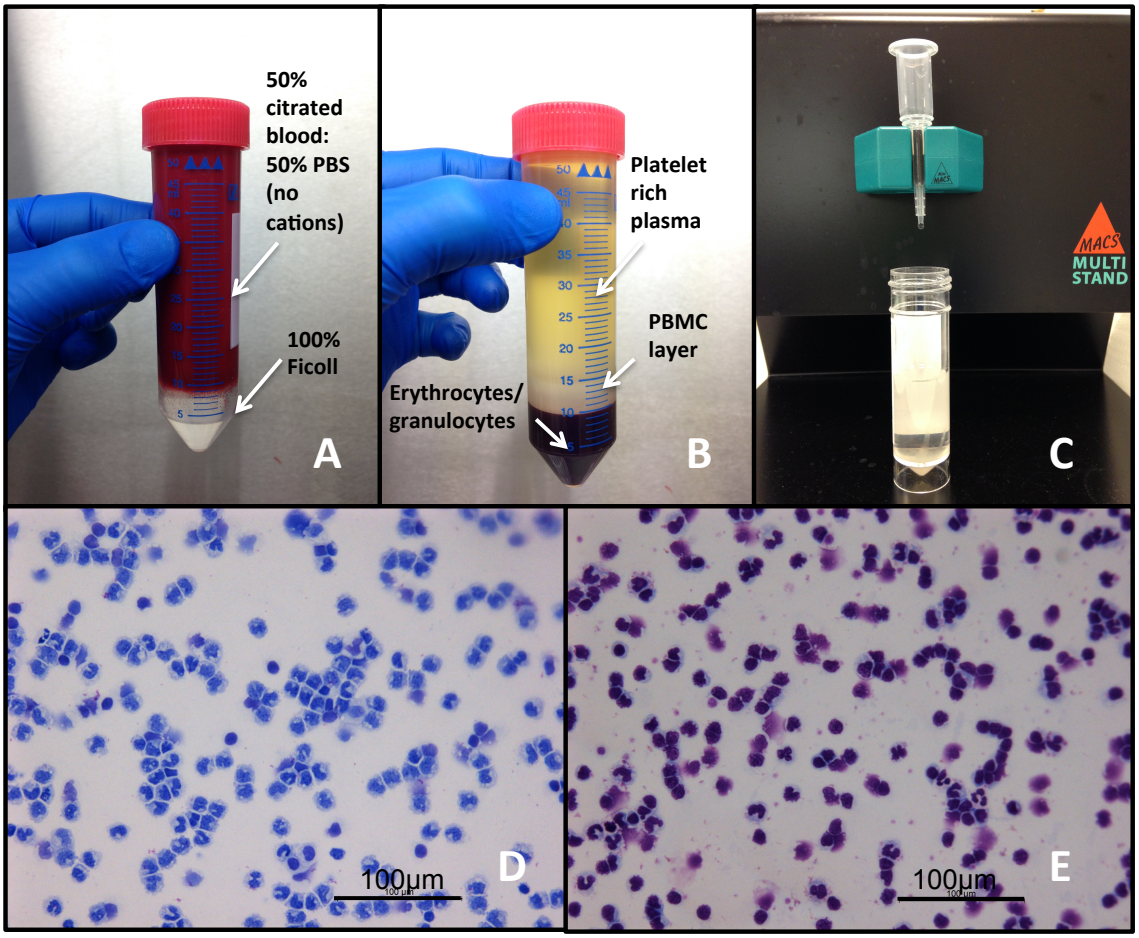

Figure 2-2 Isolation of CD14 positive monocytes from human blood
Centrifugation of diluted citrated blood over Ficoll solution (A) to form platelet rich plasma and a layer of PBMCs (B). CD14 MACS microbeads are incubated with PBMCs and passed through a MACS MS column surrounded by a MACS column magnet (C). Representative cytospin preparations of PBMCs before CD14 selection (D) and monocytes after CD14 selection (E)

2.6 Chemical Pre-treatment of Isolated Neutrophils and Blood

(Chapters 3 and 5)

Unless otherwise indicated, chemical pre-treatment of neutrophils was carried out in the final assay medium supplemented with 1% autologous serum in 2 ml round-bottomed eppendorf tubes, 15 or 50 ml Falcon tubes for 30 min at 37^{o}C in a shaking water bath. In experiments involving adherent neutrophils, chemicals were added for 30 min after a 30 min adherence step. In whole blood flow cytometry experiments, heparinised blood was pre-treated in 2 ml round-bottomed eppendorfs for 30 min in a 37^{o}C incubator.

2.7 Culture of Monocyte-derived Macrophages (MDMs) from Monocytes

(Chapter 5)

CD14 positive monocytes isolated from whole blood (see section 1.1) were resuspended at 2.5 x 10^5/ml in warmed IMDM (containing phenol red) and added to 24-well tissue culture plates at 2.5 x 10^5 per well. After 60 min incubation at 37^{o}C and 5% CO_2, the culture medium was supplemented with 10% autologous serum with penicillin and streptomycin (final concentrations 100 units/ml and 100 µg/ml respectively). The medium was then changed at days 3 and 5 and matured MDMs were used in experiments at day 7 or 8. Purity of MDMs was assessed by cell morphology on cytospin staining of detached cells and direct staining of well bottoms, as well as by CD11b/CD14 staining on flow cytometry.

2.8 Culture of A549 Cells

(Chapter 5)

A549 cells were grown to 90% confluence in RPMI-1640 medium supplemented with 10% heat-inactivated foetal calf serum (FCS) and penicillin/streptomycin in 7.5 cm^2 tissue culture flasks at 37^oC with 5% CO_2. To use or split cells, the flasks were rinsed once in PBS- to remove serum before adding 5 ml of Trypsin/EDTA solution and incubating at 37^oC for 5 to 10 min. Before use, cells were counted and washed twice in phenol red-free IMDM.

2.9 Western Blotting

(Chapter 3)

2.9.1 Sample preparation

5 x 10^6 healthy neutrophils in 1 ml IMDM/1% serum were used per condition. Cells were pre-treated with various concentrations of inhibitors/vehicle control for 30 min in round-bottomed eppendorf tubes in a shaking waterbath at 37^{o}C. Stimulation was initiated with 100 ng/ml LPS (pre-incubated for 60 min in serum) or control for 15 min at 37^{o}C. Tubes were placed on ice, washed twice in ice-cold PBS- containing 1 mM sodium orthovanadate and 1 mM phenylmethanesulfonylfluoride (PMSF). 100 µl of lysis buffer containing protease and phosphatase inhibitors (composed of 100 nM Tris-Hydrochloric acid - HCl pH 8.0, 100 mM Sodium Chloride - NaCl, 2 mM EDTA, 1% Nonidet-P40, 5 mM sodium orthovanadate, 50 mM sodium fluoride, 0.3 U/ml aprotinin, 2 mM PMSF, 50 µg/ml benzamidine and 5 µg/ml of antipain, leupeptin, chymostatin and pepstatin A) was added to each cell pellet and incubated on ice for 20 min with vigorous aspiration up and down through a P200 pipette tip to aid lysis. After 5 min of centrifugation at 12,000 g/4^{o}C, supernatants were transferred to fresh tubes and frozen immediately at -80^{o}C, after removing 20 µl for measurement of total protein using the BCA protein assay. Using this method of sample preparation, approximately 100 µg protein was retrieved per 5 x 10^6 neutrophils.

2.9.2 Polyacrylamide gel electrophoresis and transfer to nitrocellulose membrane

Samples were thawed and denatured by adding 5X reducing sample buffer (10% sodium dodecyl sulphate, 25% 2-mercaptoethanol, 50% glycerol, 0.001% bromophenol blue and 0.32 M Tris HCl) and the mixture boiled at 95^{o}C for 5 min. Each tube was vortexed briefly before centrifuging for 5 min at 12,000 g. 40 µg of each supernatant (appropriate volumes calculated using the BCA assay total protein measurements) was loaded onto a 10% polyacrylamide gel with a separate lane for molecular weight markers. The gel was submerged in running buffer (25 mM Tris base, 190 mM glycine, 0.1% SDS; pH 8.3) and run at 70 mA until the migration front reached the bottom of the gel. Proteins were

transferred onto a nitrocellulose membrane in transfer buffer (25 mM Tris base, 190 mM glycine, 0.1% SDS, 20% methanol; pH 8.3) at 100 V for 1 h.

2.9.3 Incubation with primary and secondary antibodies

Membranes were washed in Tris-buffered saline Tween (TBS-T; made by adding 0.1% Tween 20 to a 1:10 dilution of 10X TBS in ultrapure water (10X TBS = 24.23g Trizma HCl, 80.06g NaCl mixed in 1000 ml total volume ultrapure water; pH 7.6) and blocked in either 5% Marvel milk powder in TBS-T or 5% BSA in TBS-T (depending on the individual antibody) for 1 h under agitation. Primary antibodies were diluted in 5% BSA/TBS-T or 5% milk/TBS-T at the manufacturer's suggested dilution and incubated at 4^{o}C overnight.

The following morning, the membrane was washed three times for 10 min in TBS-T before adding either HRP-conjugated goat anti-rabbit IgG or HRP-conjugated goat anti-mouse IgG secondary antibodies, diluted 1:2000 in TBS-T and incubated under agitation for 2 h. The membranes were washed a final 3 times in TBS-T, before adding enhanced chemiluminescent (ECL) for 60 s, removing the excess and developing on X-ray film in a dark room.

The antibodies listed in table 2.2 opposite were used to test phosphorylation of src kinases and p38 MAPK by neutrophils in response to LPS.

Primary antibody	Dilution	Blocking buffer	Secondary antibody	Dilution
Mouse anti-human total src IgG1	1:1000	5% milk in TBS-T	HRP-conjugated goat anti-mouse IgG	1:2000
Rabbit anti-human phospho-src Tyr^{416}	1:1000	5% BSA in TBS-T	HRP-conjugated goat anti-rabbit IgG	1:2000
Rabbit anti-human total p38 MAPK	1:1000	5% milk in TBS-T	HRP-conjugated goat anti-rabbit IgG	1:2000
Rabbit anti-human phospho-p38 MAPK	1:2000	5% milk in TBS-T	HRP-conjugated goat anti-rabbit IgG	1:2000

Table 2-2 List of primary and secondary antibodies used in Western blotting

2.10 Enzyme-linked Immunoabsorbent Assay (ELISA)

(Chapter 3, 4 and 5)

Sandwich ELISA using paired antibodies was an experimental technique used throughout the project to measure the concentration of a variety of pro- and anti-inflammatory cytokines in cell supernatant or murine BALF. ELISA kits were purchased and the assay carried out according to the manufacturer's instructions, with some slight modifications. Briefly, 96-well NUNC Maxisorp plates were coated overnight at 4^{o}C with 50 µl of coating antibody dissolved in 0.1 M bicarbonate buffer; pH 9.4 (made by dissolving 4.3 g sodium bicarbonate, 5.3 g sodium carbonate in 1000 ml distilled water). The next day, plates were washed twice with 200 µl of PBS-/0.5% Tween before blocking for 1 h at room temperature with 200 µl assay buffer (0.5% BSA and 0.1% Tween 20 dissolved in PBS-).

Meanwhile, 7 standards (including assay buffer alone) were prepared by 1:2 serial dilutions in assay buffer on ice and samples were thawed and diluted in assay buffer if necessary, as directed by previous titration experiments. 50 µl of standards and samples (in duplicate) were pipetted into designated wells. 50 µl of detection antibody diluted in assay buffer were added to each well and the plate incubated for 2 h at room temperature with continual shaking (450 rpm). The plate was then washed 5 times with 200 µl of PBS Tween and 100 µl streptavidin-HRP solution diluted in assay buffer added to each well and incubated for 30 min at room temperature with continual shaking (450 rpm). The plate was washed a final 5 times with PBS Tween before adding 100 µl of a freshly prepared 1:1 mixture of 3,3',5,5'-Tetramethylbenzidine (TMB) solution and hydrogen peroxide (H_2O_2) solution. The plate was then incubated for 30 min at room temperature with continual shaking before stopping the reaction with the addition of 100 µl of 2N sulphuric acid. The absorbance of each well was measured at 450 nm within 30 min of adding the stop solution on a FLUOstar Omega spectrophotometer (BMG Labtech, Ortenberg, Germany). Results were calculated using a 4-parameter fit standard curve. Standard curve r^2 values were routinely above 0.95. Values falling outside of the standard curve values were excluded. In initial titration experiments, sample dilutions that

yielded optical density $(OD)_{450}$ values falling within the exponential part of the standard curve were used for all subsequent experiments.

The following ELISA antibody pair kits were used: human IL-6, IL-8, IL-1RA, IL-10, TNFα, MCP-1 (Fisher Scientific UK Ltd., Paisley, UK); mouse KC, IL-6, IL-10, TNFα, MPO, CCL-2 (R&D Systems Inc., Abingdon, UK), mouse soluble IgM (eBioscience Ltd., Hatfield, UK). A pre-coated ELISA kit was purchased to measure mouse LTF concentrations (Novatein Biosciences, Woburn, US).

2.11 Efferocytosis by Monocyte-derived Macrophages (MDMs)

(Chapter 5)

These assays were adapted and optimised for use from previously published protocols from Edinburgh (Hart et al. 2008; Dorward et al. 2014)

2.11.1 Preparation of apoptotic neutrophils

Freshly isolated neutrophils were incubated in suspension at 4 x 10^6/ml in IMDM (containing phenol red) supplemented with 0.5% BSA and penicillin/streptomycin for 24 h at 37^{o}C. Apoptosis rates were checked using cytospin staining and cell morphology and flow cytometric analysis with Annexin V APC/Propidium iodide (PI) staining (see section 0). Apoptotic neutrophils were recounted and washed three times with warm IMDM prior to use in MDM efferocytosis assays.

2.11.2 Phagocytosis of apoptotic neutrophils by MDMs

Mature MDMs (day 7 or 8) cultured at 2.5 x 10^5 per well in 24-well plates were rinsed with warm IMDM before adding 1 ml fresh IMDM containing 1 x 10^6 non-autologous apoptotic neutrophils (ratio ~ 1 MDM : 4 apoptotic neutrophils), 10% autologous serum and penicllin/streptomycin. They were incubated for 18 h at 37^{o}C/5% CO_2 to allow phagocytosis of the apoptotic neutrophils by the MDMs and adequate production of pro- and anti-inflammatory cytokines. At this point, supernatants were removed, aliquoted and stored at -80^{o}C prior to cytokine analysis. Remaining adherent cells were washed at least three times with PBS- to remove excess non-internalised apoptotic neutrophils, air dried, fixed in 4% paraformaldehyde for 15 min and stained for MPO with PBS- containing 0.03% (v/v) hydrogen peroxide and 0.1 mg/ml dimethoxybenzidine (DMB) for 30 min at 37^{o}C. Development of a brown colour indicated the presence of a neutrophil, which stain intensely for MPO. Cells were examined through a Nikon TMS Inverted microscope (Nikon UK Ltd., Kingston upon Thames, UK). The percentage of MDMs containing at least one MPO^+ apoptotic neutrophil was determined by counting four randomly selected fields containing at least 100 MDMs.

2.11.3 Cytokine measurement in MDM supernatant

Aliquoted supernatants were thawed at room temperature and analysed by ELISA (see ELISA method 1.1) for the presence of pro-inflammatory cytokines (IL-6, IL-8, TNFα, MCP-1, IL-1β) and anti-inflammatory cytokines (IL-1RA, IL-10). IL-1β, IL-6, IL-10 and TNFα were analysed on neat samples; IL-1RA and MCP-1 on 1:2 diluted samples and IL-8 on 1:50 diluted samples.

2.12 Phagocytosis Assays

(Chapters 3 and 4)

2.12.1 Opsonised zymosan

This in vitro phagocytosis assay has been validated in the literature (Morris et al. 2011; Conway Morris et al. 2009). Briefly, 5 x 10^5 freshly isolated neutrophils were left to adhere to tissue culture plastic in IMDM (containing phenol red) supplemented with 1% autologous serum for 30 min at 37°C/5% CO_2. Cells were then incubated for 30 min with 0.02 mg autologous serum-opsonised zymosan (50% autologous serum for 60 min at 37°C). Neutrophils were then washed 3 times with PBS-, air dried, fixed with methanol and stained with Giemsa. Using a Nikon TMS Inverted microscope (Nikon UK Ltd., Kingston upon Thames, UK), the percentage of neutrophils ingesting two or more zymosan particles was quantified by counting a minimum of 100 cells in four randomly selected fields (see Figure 2-3 below).

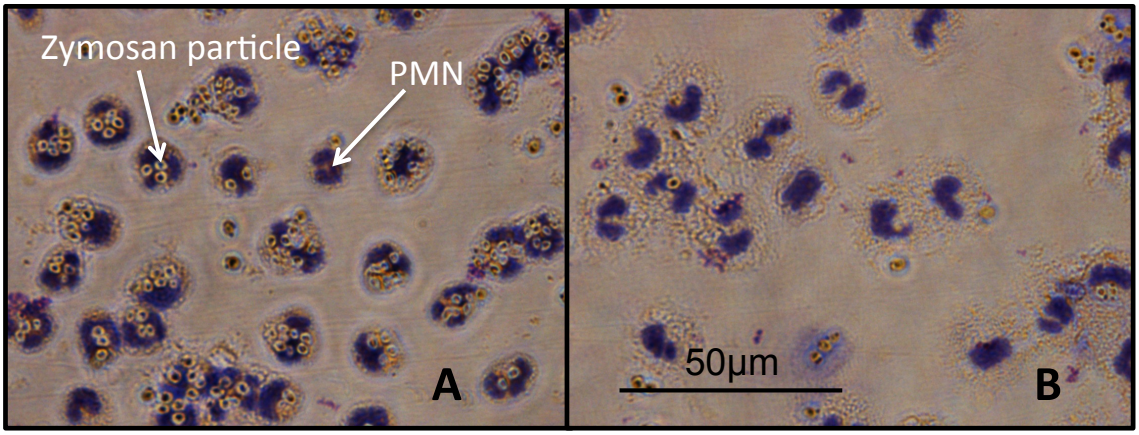

Figure 2-3 Phagocytosis of serum-opsonised zymosan particles
Representative x400 magnification images of healthy control neutrophils ingesting zymosan particles (A) compared with dysfunctional neutrophils from critically ill patients (B). Images from 4 experiments using samples from 4 independent volunteers.

2.12.2 pHrodo™ Bioparticles

These killed fluorescent *Staphylococcus aureus* (pHrodo SA) and *Escherichia coli* (pHrodo EC) bioparticles are conjugated to pH-sensitive phrodo Green and Red dyes, respectively. They are non-fluorescent outside a cell at a neutral pH,

but will fluoresce brightly at an acidic pH, such as in a neutrophil phagolysosome. This removes the need for wash or quenching steps. SA and EC were chosen as common, representative Gram positive and negative species, respectively.

In whole blood phagocytosis assays, the bioparticles were reconstituted in IMDM (no phenol red) at 2 mg/ml, vortexed for 30 s and placed in a sonicating waterbath for 30 s to achieve a monocellular suspension. To 100 µl of heparinised blood pre-treated with control or src kinase inhibitors in 2 ml round-bottomed eppendorf tubes, 20 µl of bioparticle suspension was added and incubated for 30 min in a shaking water bath at 37^{o}C. The presence of serum in blood removed the need for a separate opsonisation step. Tubes were placed on ice for 5 min to prevent further phagocytosis before adding 1.8 ml of Pharmlyse solution at room temperature for 15 min. Cells were washed using 2 cycles on a BD FACS Lyse Wash Assistant machine (BD Biosciences, Oxford, UK) and stored at 4^{o}C in the dark before analysis. Flow cytometric analysis (FACSCanto II, BD Biosciences, Oxford, UK) involved gating on neutrophils by forward/side scatter properties and measuring their median fluorescence intensity (MFI) at the appropriate laser wavelengths (Figure 2-4). Phrodo green SA particles have 509nm/533nm excitation/emission properties and were therefore analysed using a 488 530/30 laser. Phrodo red EC particles have 560nm/585nm excitation/emission properties and were analysed using a 488 585/42 laser.

To measure phagocytosis by adherent neutrophils, freshly isolated neutrophils were resuspended at 2 x 10^6/ml in IMDM (no phenol red) with 1% autologous serum and 100 µl (2 x 10^5 cells) was added to triplicate wells of a flat-bottomed 96-well tissue culture plate. Titration experiments demonstrated this to be the optimal cell density to achieve maximum phagocytosis (as estimated by mean fluorescence). After 30 min adherence at 37^{o}C/5% CO_2, neutrophils were pre-treated with appropriate chemicals/control medium for 30 min before adding 100 µl of a 1:15 dilution of a 1 mg/ml stock suspension of autologous-serum-opsonised phrodo SA or EC bioparticles, prepared as detailed above. This dilution factor was chosen in order to achieve a multiplicity of infection (MOI) of 10 bioparticles : 1 neutrophil, after estimating bioparticle concentrations using a haemacytometer and light microscope with a x100 oil immersion objective.

Plates were centrifuged for 5 min at 200g to bring the bioparticles in contact with the adherent neutrophils, before incubating for a further 30 min and then placing on ice. Plates were read immediately using a TECAN Infinite® 200 Pro spectrophotometer (Tecan UK Ltd., Reading, UK). The median fluorescence of triplicate wells (16 flashes per well) was corrected for IMDM/1% autologous serum values. Phrodo SA was excited at 500 nm (+/- 9 nm) and its emission recorded at 520 nm (+/-20 nm); phrodo EC was excited at 550 nm (+/-9 nm) and its emission recorded at 585 nm (+/-20 nm).

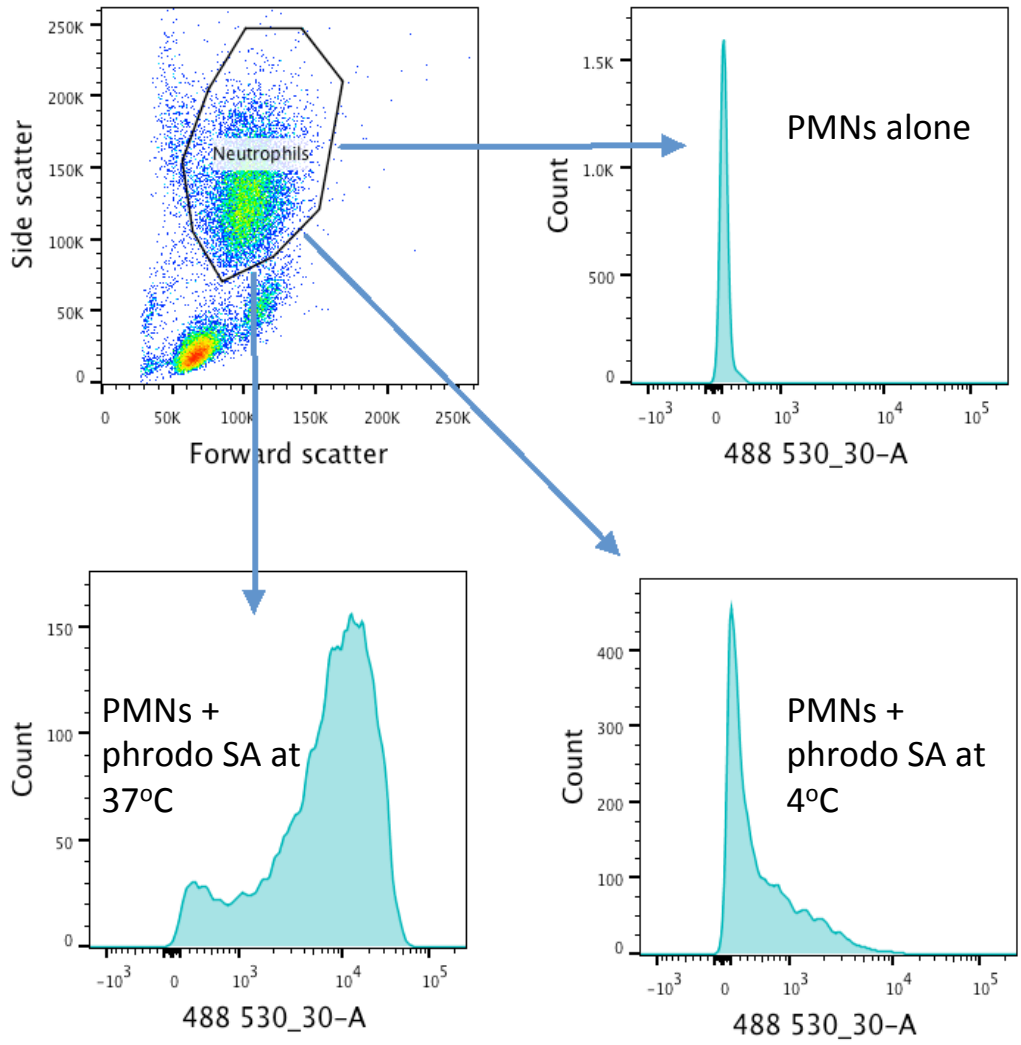

Figure 2-4 Gating strategy for analysis of phagocytosis of phrodo SA by neutrophils in whole blood
Neutrophils are identified and gated by their forward and side scatter properties and the 530nm fluorescence distribution of the gated population plotted (top left plot). Neutrophils alone have minimal autofluorescence (top right). The control condition at 4°C inhibits neutrophil phagocytosis (bottom right) but at 37°C the neutrophils phagocytose phrodo SA (bottom left). Representative plots from 3 control experiments.

2.13 Live Bacterial Killing Assay

(Chapters 3 and 5)

The ability of neutrophils to kill *Pseudomonas aeruginosa*, *S. aureus* and *E. coli* was tested in vitro by adapting previously described methods (Hampton et al. 1994; Hampton & Winterbourn 1999; Conway Morris et al. 2009). Briefly, *P. aeruginosa* strain PA01, *S. aureus* strain NCTC 8325 and *E. coli* strain K-12 W3110 were grown for 12 h in LB broth at 37^{o}C in a shaking incubator, before being sub-cultured into 20 ml of fresh LB Broth at 1:200 dilution in a 50 ml Falcon tube and grown for a further 150 min to enter early/mid logarithmic phase. Aliquots of this early log culture were taken and diluted to an optical density of 0.2 at 595 nm in IMDM.

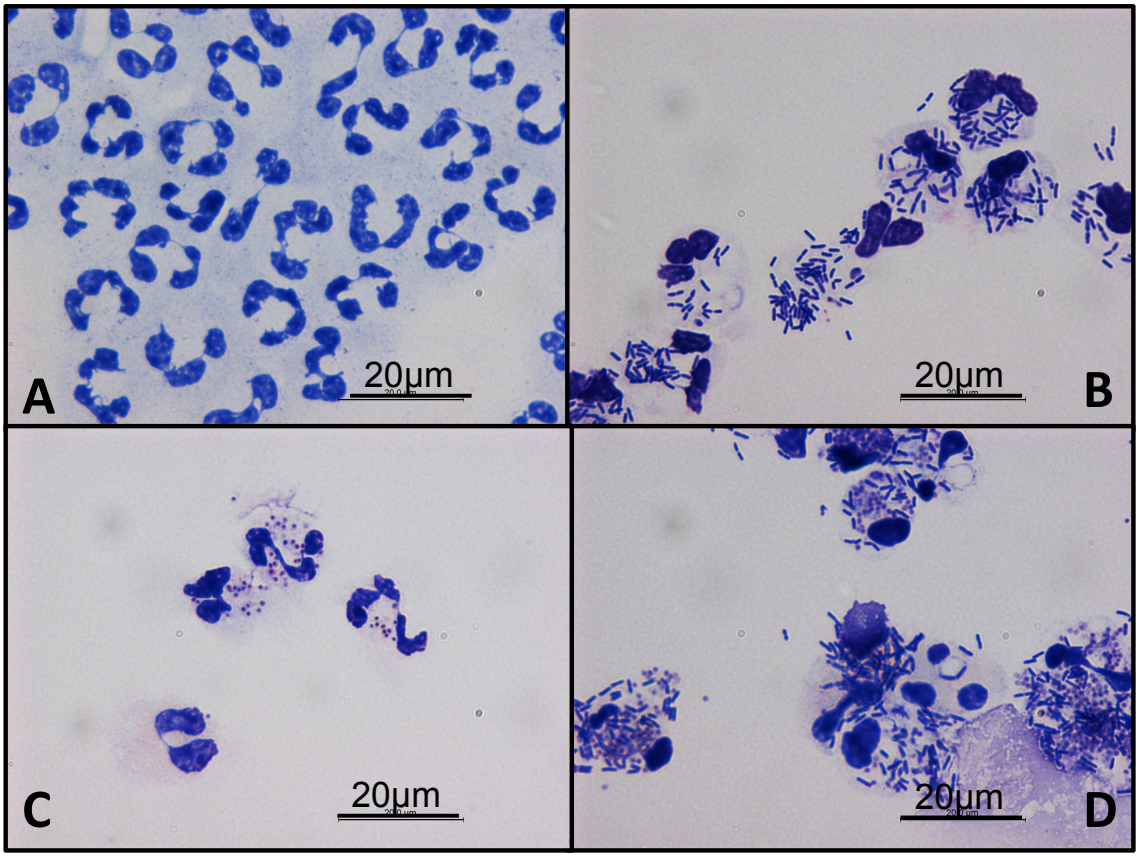

Figure 2-5 Cytospin preparations demonstrating healthy neutrophils ingesting *P.aeruginosa* and *S. aureus*
x1000 photographs of Giemsa-stained cytospin preparations of healthy neutrophils (A), and neutrophils ingesting live PA01 (B), live *S. aureus* (C) and both live PA01 and SA (D). Giemsa stains both Gram +ve and Gram –ve cocci and bacilli purple. Representative images from 3 control experiments.

Based on previously calculated growth curves for all 3 strains, the resulting suspensions were diluted 1:2 (SA), 1:6 (PA01) and 1:4 (EC) to achieve a bacterial concentration of 2 x 10^7 colony forming units (cfu)/ml. 50% autologous serum was added to promote opsonisation for 30 min at 37^{o}C, then washed twice with IMDM and resuspended at the original concentration. 500 µl of the bacterial suspension was added to 1 x 10^6 neutrophils suspended in 500 µL IMDM or control medium alone (corresponding to a live bacteria: neutrophil ratio of approximately 10:1) and the mixture incubated at 37^{0}C in a tube rotator (Bibby Scientific Ltd., Stone, UK), to keep the neutrophils in suspension (Figure 2-5). Duplicate samples were taken at 0 min (control only) and 30 min (control and neutrophil samples), treated with 0.1% Triton to lyse cells and release intracellular bacteria for 5 min at room temperature before diluting by a factor of 1:10,000 by serial dilution in PBS-. 100 µl of the resulting bacterial suspensions was plated out onto duplicate plates containing LB agar and incubated overnight at 37^{o}C to determine colony counts.

Neutrophils were exposed to an MOI of 10:1 for 30 min because initial experiments showed that at this ratio, healthy neutrophils were at least 'bacteriostatic' and often 'bactericidal' and their function could be significantly manipulated by inhibitors. Also neutrophil viability diminishes rapidly after 30 min exposure, particularly in response to *P. aeruginosa* but also *S. aureus* (data not shown). Efficiency of killing was expressed as the fold change in bacterial concentration of the final bacterial suspension compared to the original concentration:

$$\boldsymbol{Bacterial\ killing\ efficiency} = \frac{\text{cfu/ml at t} = 30\ \text{min}}{\text{cfu/ml at t} = 0\ \text{min}}$$

2.14 Under-agarose Chemotaxis Assay

(Chapter 3)

This assay was based on the original protocol described by Nelson et al. (Nelson et al. 1975). Two clean glass slides per condition were dipped in 0.5% gelatin solution and allowed to dry. Meanwhile agarose medium was prepared with IMDM (with phenol red) containing 1% BSA, 1% melted agarose and 0.25% gelatin and 5 ml poured onto each slide and allowed to set at 4^{o}C. Using a template and 3 mm diameter hollow cutting needle attached to a vacuum pump, two sets of 3 wells were prepared in each slide immediately before use (see Figure 2-6 opposite).

Freshly isolated neutrophils were resuspended at 2.5 x 10^7/ml in IMDM containing 1% autologous serum and 10 µl (250,000 cells) placed in each central well. 10 µl chemoattractant (fMLP in PBS-, final concentration 100 nM) was placed in one well and 10 µl control PBS- in the other well. The slides were then incubated at 37^{o}C/5% CO_2 for 2 h before fixation in 2.5% paraformaldehyde for at least 30 min. The slides were then rinsed, dried and stained with Giemsa solution.

Neutrophil migration patterns were photographed through a x4 objective using a Nikon Eclipse light microscope and camera (Nikon UK Ltd., Kingston upon Thames, UK). Results were expressed as a 'relative chemotactic index' in arbitrary units, defined as:

$$\boldsymbol{Relative\ chemotactic\ index} = 1000 \times \left(\frac{Distance\ migrated\ to\ fMLP / Distance\ migrated\ to\ control}{Distance\ migrated\ to\ control} \right)$$

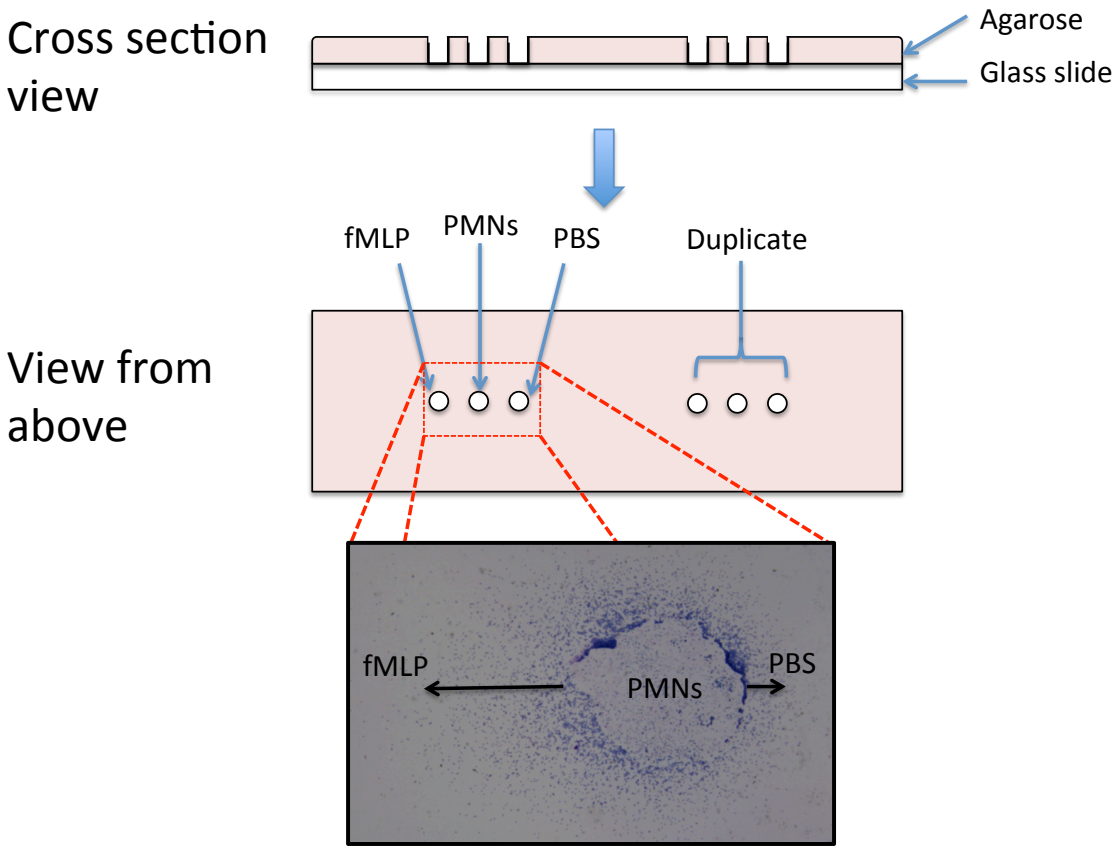

Figure 2-6 Under-agarose chemotaxis assay method

2.15 Adhesion Assay

(Chapter 3)

This flow cytometric assay of neutrophil adhesion to plastic was adapted from that described by Clark et al. (Clark et al. 1997). Briefly, fresh neutrophils were resuspended at 1 x 10^6/ml in IMDM (with phenol red) with 1% autologous serum and 500 µl cell suspension added to wells of a 24 well plate as well as a round-bottomed eppendorf tube to use for the total cell count. Chemicals and inhibitors were added in addition to fMLP (50 nM final concentration) to promote adhesion. After 60 min incubation at 37^{o}C/5% CO_2, the wells were washed twice with PBS- to remove non-adherent cells. 250 µl of IMDM and 250 µl of Trypsin/EDTA were added per well and aspirated up and down to detach all cells into suspension. 400 µl of each suspension (and the 'total cell count' tube) were transferred to FACS tubes and 20 µl of well-vortexed CountBright™ Absolute Counting Beads added (exact concentration of beads is lot-specific but approximately 20,000 in 20 µl) prior to analysing using flow cytometry. The number of neutrophils analysed per 2000 beads was counted and the results expressed as % adherence (see Figure 2-7 opposite).

$$\%\,\boldsymbol{Adherence} = 100\% \times \frac{Number\ of\ adherent\ neutrophils}{Initial\ total\ cell\ count}$$

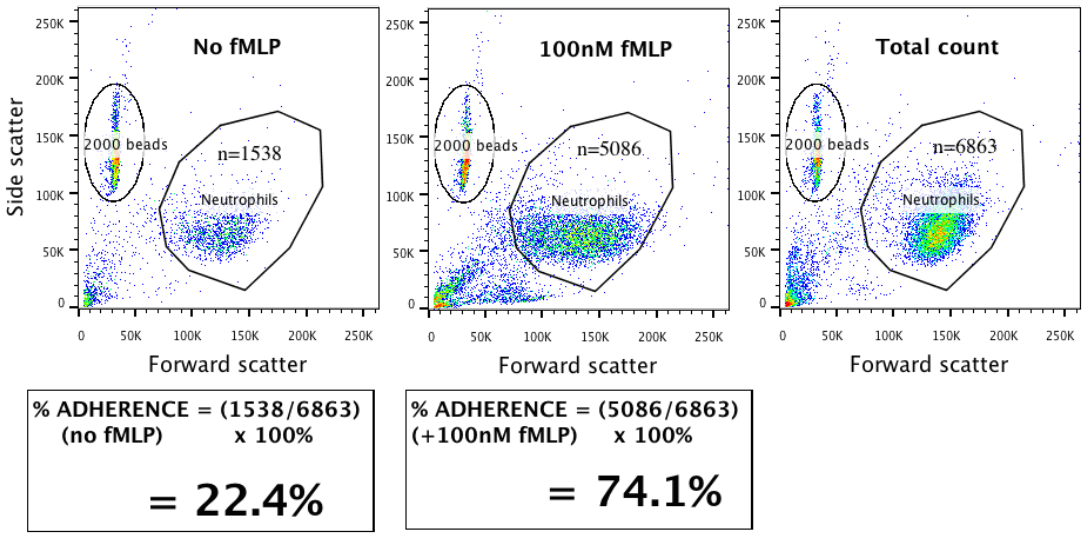

Figure 2-7 Measurement of neutrophil adhesion using CountBright Absolute counting beads

Representative control flow cytometry plots with % adherence calculations showing that only 22.4% of unstimulated neutrophils become firmly adherent to tissue culture plastic (left-hand plot) compared to 74.1% of neutrophils stimulated by 100 nM fMLP (middle plot). Plots from 4 experiments using samples from 4 independent volunteers.

2.16 Measurement of Neutrophil Apoptosis

(Chapter 3)

Isolated neutrophils were resuspended at 1 x 10^6/ml in IMDM with 1% autologous serum, treated with chemicals and inhibitors and incubated at 37^{o}C/5% CO_2. At 30 min, 6 h and 24 h, aliquots were removed and analysed for rates of apoptosis by performing a cytospin, counting the percentage of apoptotic cells (by morphological criteria at light microscopy) and also by staining with Annexin V APC and PI. Briefly, 500 µl cell suspension was washed twice with cold PBS- and resuspended in 1 x Annexin V Binding buffer at 1 x 10^6/ml. 100 µl of the suspension was transferred to a FACS tube and 5 µl Annexin V APC and 1 µl of 1 mg/ml PI added, mixed and the tube incubated in the dark at room temperature for 15 min. 400 µl of 1x binding buffer was added and the sample analysed by flow cytometry, gating on neutrophils and recording at least 5000 events. No compensation was required for APC and PI fluorescence. The gating strategy is shown opposite in Figure 2-8.

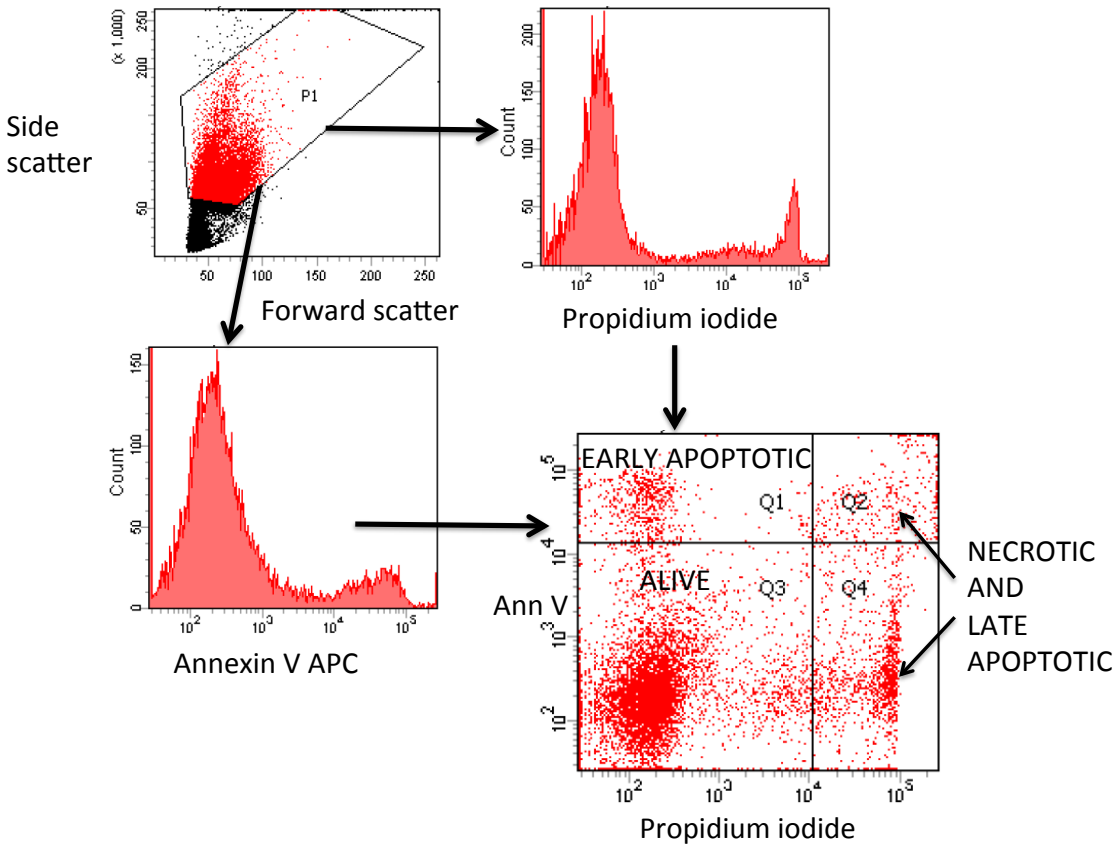

Figure 2-8 Gating strategy used to measure neutrophil apoptosis by Annexin V/PI binding

Neutrophils are distinguished from debris by their forward/side scatter properties and their relative binding to Annexin V APC and PI expressed (bottom right plot). Annexin $V^{-}PI^{-}$ cells are alive, Annexin $V^{+}PI^{-}$ cells are in the early stages of apoptosis whereas Annexin V^{+or-} PI^{+} cells are either necrotic or undergoing late apoptosis. Plots from 3 control experiments.

2.17 Assessment of Cytotoxicity by LDH Release

(Chapter 3)

Direct cytotoxicity induced by pre-treating healthy neutrophils with different chemicals was tested using a Roche lactate dehydrogenase (LDH) cytotoxicity kit according to the manufacturer's instructions. Briefly, 5 x 10^4 neutrophils in 100 µl of IMDM (no phenol red) were added to triplicate wells of a 96-well plate and chemicals to be tested were added in a further 100 µl of IMDM. In control samples, Triton X-100 (final concentration 1%, as positive control) or IMDM alone (as negative control) were added. The plate was incubated for 60 min at 37^{o}C/5% CO_2 before being placed on ice and centrifuged for 5 min at 200g. 100 µl of each supernatant was transferred to a fresh plate and 100 µl of freshly prepared LDH reaction mixture added, before incubating for 30 min at room temperature in the dark. IMDM-corrected absorbance values at 490 nm were measured using a TECAN Infinite® 200 Pro spectrophotometer. Results were expressed as % LDH release, where:

$$\%\ \boldsymbol{LDH\ release} = \frac{OD\ value\ of\ pretreated\ 5 \times 10^4\ cells}{OD\ value\ of\ Tritonised\ 5 \times 10^4\ cells}$$

Initial titration experiments established that the optimum cell density to avoid over-crowding of cells (by direct microscopic visualisation) and a sufficient OD difference between an equivalent number of untreated and fully lysed cells was 5 x 10^4 per well (Figure 2-9 opposite).

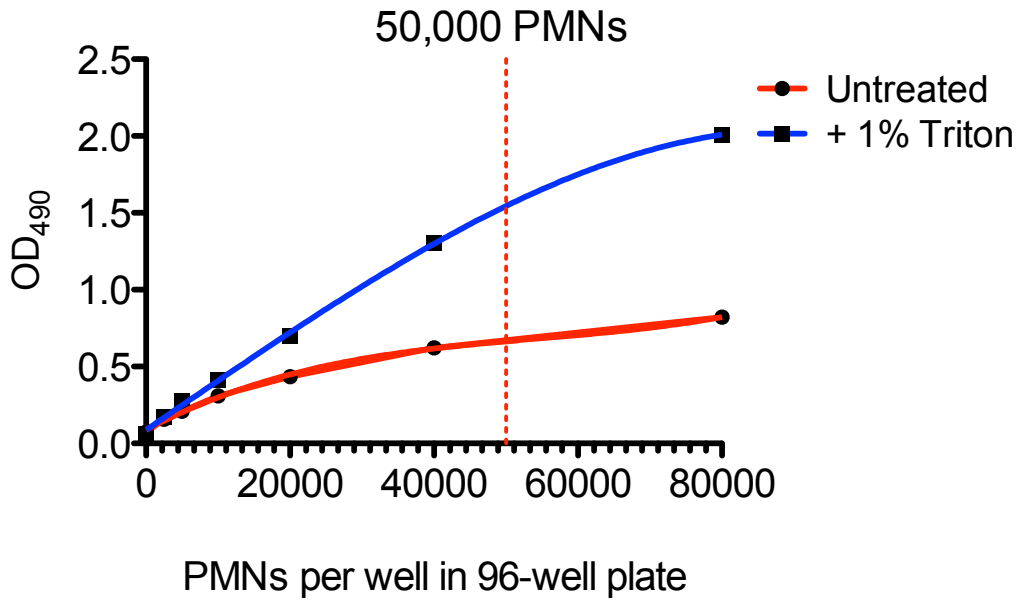

Figure 2-9 Titration experiments for LDH cytotoxicity assay
OD_{490} values for a range of cell densities per individual well of a 96-well plate were compared with OD values from the same concentration of fully lysed cells to determine the optimum cell density of 5×10^4 per well. Data are expressed as the mean of 2 experiments using neutrophils derived from 2 independent volunteers.

2.18 Degranulation Assays

(Chapter 3)

2.18.1 Induction of degranulation

Samples (whole blood or isolated human neutrophils) were stimulated in four separate ways to induce degranulation:

- 100 nM PMA for 20 min
- 10 μM cytochalasin B for 5 min followed by 1 μM fMLP for 10 min
- 100 ng/ml LPS for 30 min (LPS pre-incubated with human serum to provide LPS-binding protein (LBP) for Toll-like receptor 4 (TLR4) ligation)
- Autologous serum-opsonised live PA01 or SA for 30 min

All experiments were carried out in 2 ml round-bottomed eppendorf tubes and incubated at 37^{o}C with continual mixing.

2.18.2 CD63, CD66b and CD11b expression on human neutrophils in whole blood

CD63 is an integral membrane protein expressed on the membrane of azurophil (primary) granules in human neutrophils. It is also expressed in neutrophil lysosomes (Cham et al. 1994). CD66b is a member of the carcinoembryonic antigen family expressed only on the surface membrane of specific (secondary) granules and CD11b/CD18 (Mac-1) is a β_2 integrin expressed across specific, gelatinase (tertiary) and secretory vesicles (Faurschou & Borregaard 2003). All 3 proteins are expressed extracellularly when these granules fuse with the extracellular membrane and can be measured alone or in combination as surrogate markers of degranulation in whole blood flow cytometry assays (Hashiguchi et al. 2005).

A flow cytometry panel of the following antibodies and dyes was set up. Fluorescence compensation values were calculated in separate experiments using single and multi-stained samples.

- PE/Cy7-conjugated mouse anti-human CD16 monoclonal antibody (IgG1, κ) to identify neutrophil population

- DAPI stain to exclude dead cells
- APC-conjugated mouse anti-human CD63 monoclonal antibody (IgG1, κ)
- PE-conjugated mouse anti-human CD66b monoclonal antibody (IgM, κ)
- PerCP/Cy5.5-conjugated mouse anti-human CD11b monoclonal antibody (IgG1, κ)

Briefly, 100 µl of heparinised blood was pre-treated with potential inhibitors or control for 30 min before adding the antibodies listed above at the manufacturer's suggested concentration. Samples were stimulated as described in method 2.18.1 to induce degranulation. The assay was then stopped on ice for 5 min and 1.8 ml of Pharmlyse was added for 15 min at room temperature, before washing twice. 50 µl DAPI was added to each sample 5 min before analysing them on a BD FACSCanto II machine, according to the gating strategy shown in Figure 2-10 below.

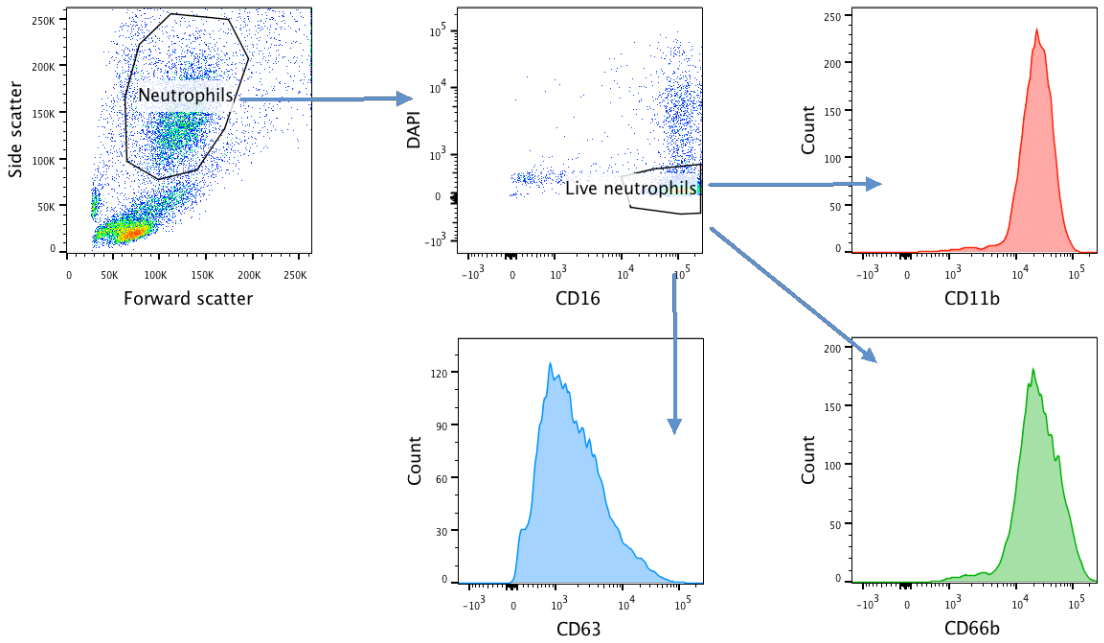

Figure 2-10 Gating strategy used in whole blood assay to measure markers of degranulation in human neutrophils
Live neutrophils are identified by their forward/side scatter properties as well as CD16 positivity and negative DAPI staining, before measuring the relative fluorescence of fluorophore-conjugated antibodies binding live neutrophil CD63 (primary granules), CD66b (secondary granules) and CD11b (secondary, tertiary and secretory granules). Plots from 3 control experiments.

A slight modification in the bacterial preparation method was required when carrying out whole blood assays. In assays involving isolated neutrophils,

healthy blood volunteers were consented and venesected between 08:30 and 09:00 most mornings, giving sufficient time to prepare a subculture of bacteria to early/mid log growth phase and carry out a neutrophil preparation simultaneously. Depending on their growth phase, bacteria can behave very differently in terms of virulence towards immune cells and subsequent viability. To avoid this effect and prepare early/mid log phase bacteria for use with heparinised whole blood by 09:00, bacteria were prepared as shown in Figure 2-11 below.

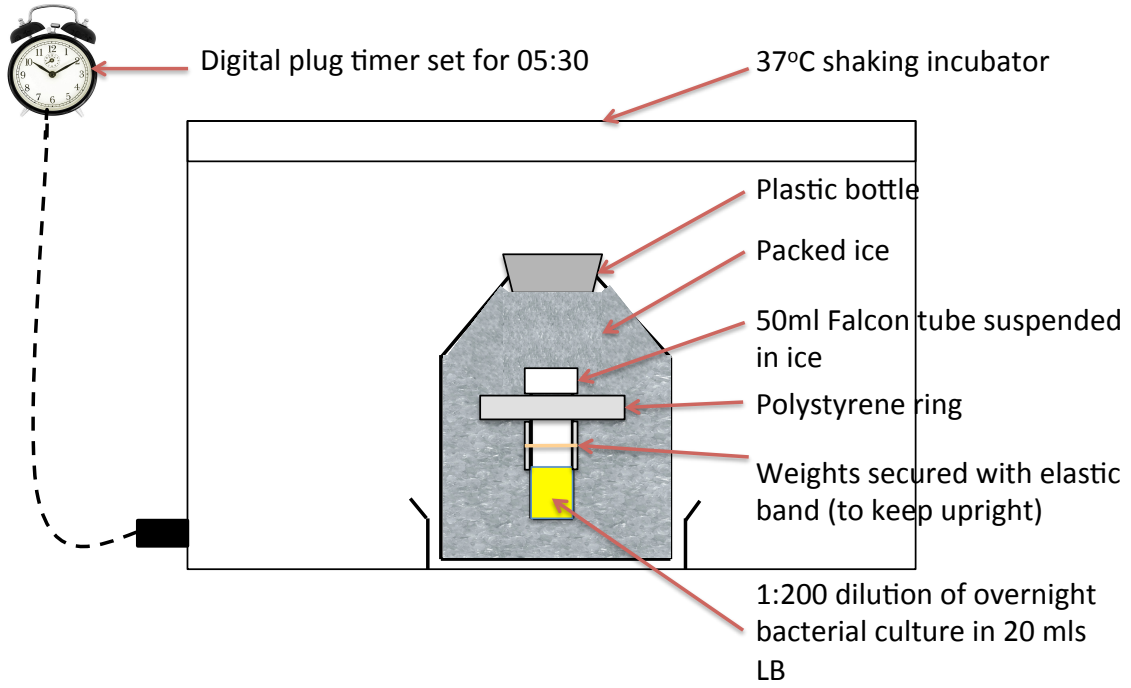

Figure 2-11 Preparation of early/mid log phase bacteria for use in whole blood flow cytometry assays
A 1:200 dilution of an overnight culture was prepared in a weighted 50 ml Falcon tube fitted with a polystyrene ring and suspended in packed ice inside a large plastic bottle (e.g. 5 kg sucrose bottle) in a 37°C incubator at 9pm. A digital timer was set for 05:30, at which point the incubator was turned on, the ice melted and bacterial growth began. At 09:00 the subculture was in early/mid log phase with very similar OD measurements compared to the routine method (see section 2.13)

2.18.3 MPO release assay

To complement the results of measurements of neutrophil degranulation in whole blood, granule components released extracellularly into the supernatant from isolated neutrophils were also measured. MPO is the defining protein of azurophil granules (Bainton & Farquhar 1966) and its presence in cell supernatant can be measured by ELISA, or more simply its enzymatic activity

can be quantified by using an adaptation of the TMB/H_2O_2 colorimetric assay (Palić et al. 2005).

1 x 10^6 neutrophils in IMDM (no phenol red) with 1% autologous serum were stimulated as described in section 2.18.1 in a total assay volume of 1 ml. This allowed simultaneous measurement of live bacterial killing if required. At the end of stimulation, tubes were placed on ice and centrifuged for 5 min at 300g (if neutrophils alone present) or 1 min at 10,000g (if bacteria also present). Cell-free supernatants were transferred to fresh tubes for immediate storage at -80^{o}C for later analysis. 200 µl was used immediately for the MPO release assay. 100 µl of each supernatant was placed in duplicate wells of a 96-well plate and 100 µl of a freshly prepared 1:1 mixture of TMB and H_2O_2 solutions was added to each well and the plates incubated in the dark for 20 min. A separate control sample of 1 x 10^6 neutrophils lysed with 0.1% Triton was used to represent '100% MPO release'. 50 µl of 2N sulphuric acid was added to each well to stop the reaction and the absorbance read at 450 nm using a FLUOstar Omega spectrophotometer, correcting for medium alone.

Results were expressed as % MPO release, defined by:

$$\%\ \boldsymbol{MPO\ release} = 100\% \times \frac{OD\ value\ of\ sample}{OD\ value\ of\ Tritonised\ cells}$$

2.18.4 Lactoferrin ELISA

Lactoferrin is constitutively stored in the specific granules of neutrophils and is released readily in high concentrations upon degranulation. A sandwich ELISA was designed and optimised to measure LTF concentrations in the supernatants generated in experiments above. A mouse anti-human LTF monoclonal antibody (IgG1, κ) at 1 µg/ml was paired with a biotin-conjugated rabbit anti-human LTF polyclonal antibody (IgG) at 0.5 µg/ml, using streptavidin-HRP at 0.5 µg/ml. All the coating and colorimetric steps were as in section 1.1. Lactoferrin standards were prepared with serial 1:2 dilutions of human LTF protein from 320 ng/ml to 10 ng/ml.

Initial titration experiments revealed that both a 1:10 and a 1:20 dilution of thawed supernatants in ELISA assay buffer were required to obtain all sample OD values within the exponential part of the standard curve, depending on the

potency of the stimulant. Results were expressed as ng/ml LTF released per 1 x 10^6 neutrophils.

2.19 L-selectin Shedding

L-selectin (also known as CD62L) is an adhesion molecule expressed on leukocytes with a crucial role in neutrophil recruitment to sites of inflammation. It binds to ligands expressed on vascular endothelium to promote adhesion. When neutrophils are activated by chemokines or by contact with an activated endothelium, or indeed upon initiation of apoptosis, L-selectin is cleaved from neutrophils by the metalloprotease ADAM-17, while expression of the integrin Mac-1 (CD11b/CD18) is increased to promote transmigration through the endothelial cell layer (Li et al. 2006). The degree of L-selectin shedding by neutrophils in response to activation can be measured using a whole blood flow cytometry assay. Briefly, samples of 100 µl of heparinised blood were pre-treated with inhibitors/vehicle control for 30 min at 37^{o}C before staining with APC-conjugated mouse anti-human CD62L monoclonal antibody (IgG, κ) at the manufacturer's suggested concentration for 15 min in the dark at room temperature. Samples were then stimulated with vehicle control or 10 nM fMLP for 15 min at 37^{o}C before placing on ice and adding 2 ml of 1X Pharmlyse to each sample for 15 min at room temperature. The samples were transferred to FACS tubes and washed twice before analysing on a BD FACSCanto II machine. Although CD62L staining in quiescent, unstimulated neutrophils was weak (see Chapter 3 results), there was a sufficient difference between the median fluorescence intensities of stimulated and unstimulated neutrophils to assess an effect of inhibitors on the mechanism.

2.20 Extracellular Superoxide Release (Cytochrome C reduction assay)

The extracellular release of superoxide anions by freshly isolated neutrophils in response to priming by platelet-activating factor (PAF) and activation by fMLP was determined using a cytochrome C reduction assay (Kitchen et al. 1996). Briefly, 50 µl of neutrophils at 1 x 10^7/ml in HBSS+ were placed in 2 ml round-bottomed eppendorf tubes. Potential inhibitors/control and the priming agent PAF (final concentration 100 nM) were placed on the underside of the tube lids before inverting the tubes simultaneously to commence the reaction. Tubes were incubated in a shaking water bath at 37^{o}C for 10 min, before adding fMLP at 100 nM and cytochrome C at 1 mg/ml (end volume 500 µl) and reincubating for a further 15 min. For each sample, a control with 200 U/ml superoxide dismutase (SOD) was included to verify the specificity of cytochrome C reduction by superoxide anions. The reaction was terminated on ice for 5 min and tubes centrifuged at 10,000g for 3 min at 4^{o}C. Triplicate 100 µl samples of supernatant were transferred to a 96-well plate to measure the absorbance at 550 nm in a FLUOstar Omega spectrophotometer. The superoxide dismutase-inhibitable reduction of cytochrome C was determined for each sample using the following equation:

$$Superoxide\ release\ (nanomoles\ of\ O_2^-\ per\ 10^6\ cells) = 159 \times \frac{OD_{550}\ without\ superoxide\ dismutase}{OD_{550}\ with\ superoxide\ dismutase}$$

2.21 Intracellular Oxidative Burst (dihydrorhodamine 123 assay)

The dihydrorhodamine 123 (DHR) assay measures ROS production. Cells readily take up the non-fluorescent compound DHR 123 intracellularly, which is oxidised to the highly fluorescent compound rhodamine 123 by the ROS produced during activation of the oxidative burst (van Pelt et al. 1996). Briefly, 500 µl of freshly isolated healthy neutrophils at 1 x 10^6/ml in HBSS+/1% autologous serum in 2 ml round-bottomed eppendorf tubes were pre-treated with vehicle control or potential inhibitors for 30 min at 37^{o}C before loading with DHR at a final concentration of 1 µM for 15 min in the dark at 37^{o}C. PMA (final concentration 50 nM) or vehicle control were then added and incubated for 15 min at 37^{o}C before transferring the samples to FACS tubes and analysing them on a BD FACSCanto II machine. Data were expressed as the median fluorescence intensity of the neutrophil population at 530 +/- 30 nm, excited by a 488 nm laser.

2.22 In Vivo Murine Experiments

(Chapter 4)

In the absence of an animal project licence within our own research group to test our hypotheses in vivo, we sought collaboration with Dr D Dorward, Clinical Research Fellow in Professor Adriano Rossi's Lung Inflammation research group, Centre for Inflammation Research, Edinburgh University. With another Clinical Research Fellow (Dr C Lucas), Dr Dorward had previously optimised the in vivo murine models of sterile and non-sterile acute lung inflammation described here. The wide range of assays used to measure neutrophil activation, influx and epithelial leak in response to the noxious stimuli were adapted for the purposes of my experiments.

For the *E. coli* experiments using 1 mg/kg and 10 mg/kg dasatinib, and for the acid injury experiment using 5 mg/kg dasatinib, I was present for the duration of the experiments during 3 separate 3-4 day trips to Edinburgh. Dr Dorward performed all work involving direct contact with mice and I assisted him. After culling of mice and harvesting of samples, I worked with Dr Dorward to process the samples immediately. All ELISAs, cytospin counts, slide photography, data preparation and analysis were carried out by myself.

To complete our data set and firmly test our initial hypotheses, Dr Dorward and Dr Lucas kindly carried out the final acid injury experiment at a dose of 10 mg/kg dasatinib, as I was not able to attend on this occasion. For these experiments I analysed all the data.

2.22.1 E. coli model of acute lung inflammation

8-10 week old female C57/BL6 mice were purchased from Harlan UK and were used in all in vivo model experiments, under project licence number PPL 60-4531 and personal licence number PIL 60/12746 (Dr Dorward), according to the Animals (Scientific Procedures) Act 1986.

E. coli (ATCC 25922 strain) was grown in overnight culture by inoculating 10 ml of LB broth with a single colony from a fresh agar plate and placing in a shaking incubator at 37^{o}C. A further 2 hour incubation of a 1:20 sub-dilution in 10 ml of

LB broth was carried out the following morning to reach early log growth phase. The suspension was centrifuged at 4000g for 5 min and the pellet resuspended in 1 ml sterile PBS- in a 1.5 ml eppendorf tube, before washing 3 times in PBS- at 4000g for 1 min. The OD_{600} of the suspension was measured and diluted to a value of exactly 1.0, approximating to an *E. coli* concentration of 2 x 10^8 cfu/ml, as estimated by previously calculated growth curves. From previous experiments carried out by Dr Dorward and Dr Lucas, an intratracheal instillation of 5 µl of an OD_{600}=1.0 suspension per mouse, resuspended in a total volume of 50 µl sterile PBS- (equating to approximately 1 x 10^6 cfu *E. coli* per mouse), was a sufficiently robust stimulus to induce a moderate inflammatory response in the lungs without significant organ dysfunction or systemic sepsis. In each experiment, the actual bacterial concentration of the inoculum was retrospectively calculated by serially diluting it by factors of 10 and pipetting 3 x 10 µl drops of each dilution onto an LB agar plate and incubating overnight at 37^{o}C. An average colony count was taken from a 'countable' dilution and the original inoculum size derived from this value by multiplying by a factor of 50,000 (see Figure 2-12 overleaf). In 2 separate experiments, estimated inoculum total values of 1.3 x 10^6 and 1.5 x 10^6 cfu/mouse were achieved.

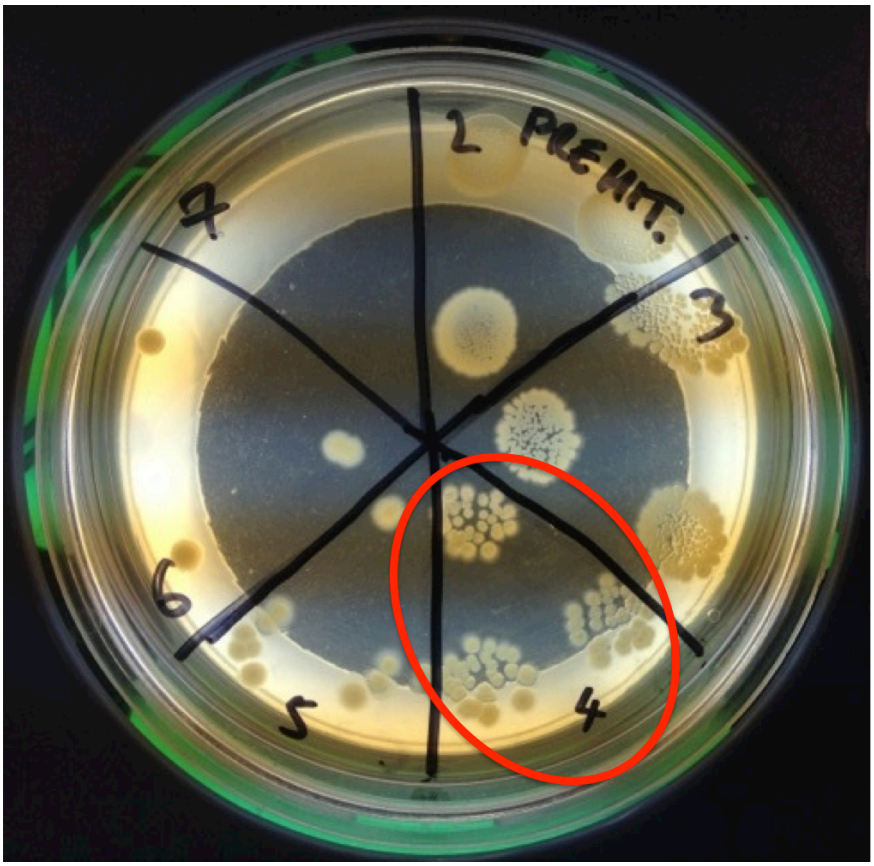

Figure 2-12 Colony counting method for retrospective calculation of total number of viable bacteria inoculated per mouse
In this example, the 1:10^4 dilution of the original bacterial suspension highlighted by the red oval is countable. An average of 3 colony group numbers in 10 µl is calculated (30 colonies) and used to derive the figure of 1.5 x 10^6 cfu of *E. coli* per mouse.

As soon as the *E. coli* suspension was prepared, mice (8-10 per control/treatment group) were pre-treated i.p. with either 20 µl control DMSO or 20 µl dasatinib (at the desired concentration assuming an average weight of 20 g per mouse) dissolved in DMSO. After 30 min, the mice were anaesthetised with i.p. 665 µg ketamine and 8.75 µg medetomidine made up to a final volume of 100 µl with sterile H_2O, then 50 µl of prepared *E. coli* suspension was administered directly to the lungs via the trachea of all mice via a catheter, followed by 2 flushes with 200 µl air (see Figure 2-13 opposite). Anaesthetic was reversed with 200 µl s.c. Antisedan (Atipamezole, 20 µg in 200 µl H2O) after approximately 20 min, before mice were transferred to individually ventilated cages at 28°C, given fresh food and sterile water and observed closely.

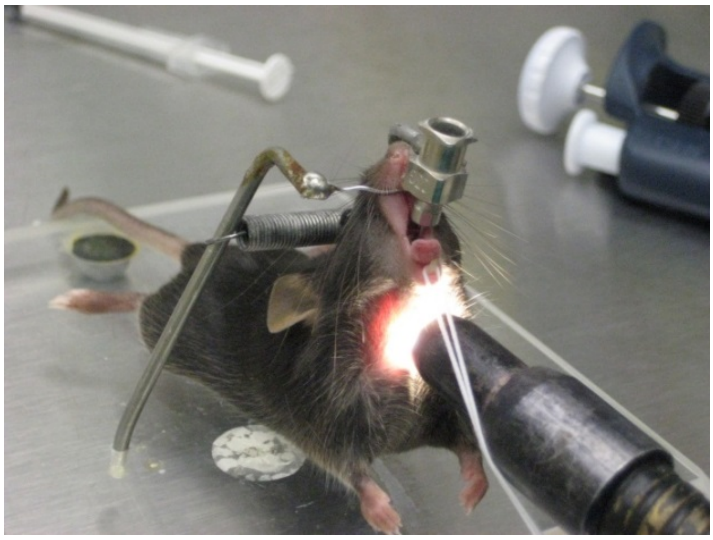

Figure 2-13 Method of intratracheal administration of acid or bacteria in mice
Image reproduced by kind permission of Dr D Dorward.

Dasatinib or control DMSO were readministered i.p. at 12 h. This double treatment regime was based on previous experimental time course data showing that the peak neutrophil influx into the lung interstitium occurs at 12 h compared to 24 h into the BALF (see Figure 2-14 below).

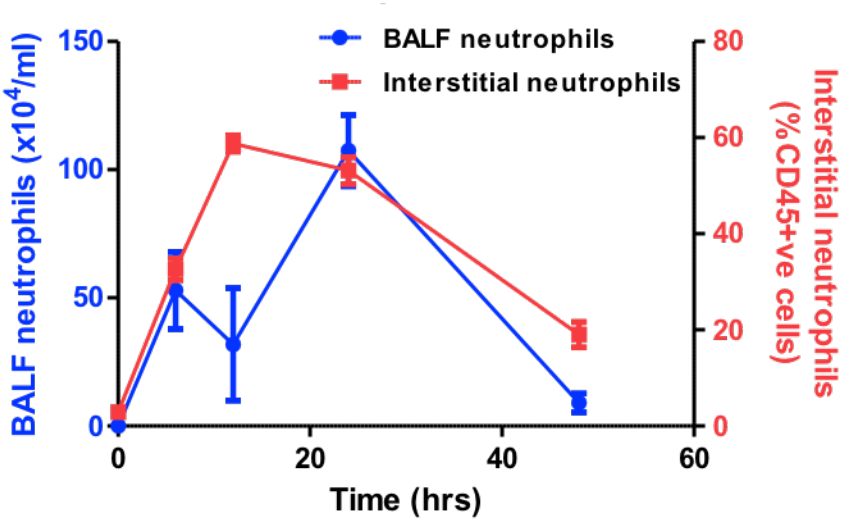

Figure 2-14 Time course experiments showing neutrophil influx into lung interstitium and BALF following i.t. *E. coli*
Data kindly provided by Dr D. Dorward

At 24 h mice were culled with terminal anaesthesia using Avertin with exsanguination. Blood sampling occurred prior to death with BAL and collection of tissues following death of the animal.

Following anaesthesia, the chest wall of the animal was opened by a midline abdominal incision and blood sampled by direct cardiac puncture through the diaphragm into a pre-citrated syringe. 40 µl blood was diluted 1:2 and mixed well with 3.8% sodium citrate solution in a 500 µl eppendorf tube and the remainder used to fill a Microvette CB 300 LH (lithium heparin) serum tube. Next, a tracheostomy was performed and a plastic-coated 25 gauge needle inserted into the trachea as far as the carina and tied securely in place. 3 x sequential 800 µl sterile PBS- lavages were performed, the 1st (cellular) return being placed in a 1.5 ml eppendorf (Tube 1) and the 2nd and 3rd combined into a 2 ml eppendorf tube (Tube 2). The spleen and right lobe of liver were then dissected out and placed in separate 2 ml homogeniser tubes pre-filled with 1 ml sterile PBS- (Precellys Ceramic Kit 1.4mm) before the lung vasculature was flushed anterogradely with 10 ml of sterile, through cannulation of the right ventricle. Once the lungs blanched, the right lung was removed and placed in a 2 ml eppendorf pre-filled with 1 ml sterile PBS- All samples were placed on ice immediately.

2.22.2 Acid model of acute lung inflammation

The experimental plan was very similar to that used in the *E. coli* model (section 2.22.1), with some subtle changes as follows: The acid stimulus used per mouse was 50 µl of pH 2.0 HCl, prepared by diluting a stock solution of pH 1.0 HCl 1:10 in 0.9% NaCl solution. As pH 2.0 acid is a potent pulmonary stimulus, less anaesthetic was used. The resulting acidaemia also affects binding of anaesthetic drugs with serum proteins, prolonging their duration of action and increasing the animal's recovery time. A 200 µl bolus of 0.9% NaCl was administered i.p. as fluid resuscitation, to counteract the immediate effects of fluid shift into the lung parenchyma. Mice were then placed in a humidified chamber supplemented with 2 l/min O_2 at 28^{o}C for 30 min before the anaesthesia was reversed with s.c. Antisedan.

At retrieval, the liver and spleen were not taken, as no bacterial work was required in this model. The left lung was taken in addition to the right lung and placed into a pre-filled homogeniser tube, for cytokine analysis.

2.22.3 *Processing of individual samples in preparation for subsequent assays*

Blood – Serum tubes were centrifuged at room temperature for 5 min at 850g to make serum, which was aliquoted and stored at -80^{o}C for later analysis. 20 µl citrated blood was transferred to individual FACS tubes and stored at 4^{o}C prior to staining.

BALF – The exact volume of BALF returned was measured using scales zeroed to empty 1.5 ml and 2 ml eppendorf tubes, then both tubes were centrifuged at 850g for 5 min at room temperature. Supernatants from the 1.5 ml (Tube 1) and 2 ml (Tube 2) eppendorfs were aliquoted and stored separately at -80^{o}C, with some fresh supernatant taken for immediate use. The remaining cell pellets from tubes 1 and 2 were combined and resuspended in 500 µl PBS- for use in subsequent assays.

Liver and spleen – In the *E. coli* model, these samples were homogenised by placing the tubes in a Precellys homogeniser (Bertin Technologies, France) and disaggregated with three cycles of 6800 rpm for 30 s.

Right lung – Lung samples were cut into smaller pieces and incubated in 500 µl of 5 mg/ml collagenase D for 1 h at 37°C in a shaking heat block at 400 rpm. After disaggregation through a 19 gauge needle, samples were centrifuged at 300g for 5 min, resuspended in 500 µl ACK lysis buffer and incubated for 5 min on ice, before washing in 500 µl PBS- at 300g for 5 min. Cells were then resuspended in 1 ml of PBS- and passed through a 40 µm cell sieve. The cells were resuspended in 250 µl PBS- and incubated for 10 min with 2.5 µl rat anti-mouse CD16/32 Fc blocking monoclonal antibody (IgG2a, λ) prior to antibody staining.

Left lung – In the acid model experiment using 5 mg/kg dasatinib, the left lung was also taken and homogenised as described above, spun at 850g for 5 min and the supernatant aliquoted and stored at -80^{o}C for subsequent cytokine analysis.

2.22.4 Measurement of neutrophil/cellular influx into alveolar space

50 µl of the resuspended cellular pellet from BALF Tube 1 was placed in a round-bottomed 96 well plate and 50 µl of both ChemoMetec reagent A-100 and reagent B added. The sample was loaded onto a Nucleocassette and cell concentration measured using a NucleoCounter© NC-100™ machine (ChemoMetec A/S, Allerod, Denmark). Using the previously measured total BALF volume, a cellular concentration expressed in cells/µl BALF could be calculated. To determine cell purity, cytocentrifuge preparations of 7.5 x 10^5 cells were fixed with methanol, stained with Reastain Diff-Quik for 1 min in each solution, mounted with DPX and viewed at x1000 using a conventional benchtop light microscope, counting the % neutrophils in 3 randomly selected fields of at least 100 cells.

2.22.5 Measurement of neutrophil activation and recruitment by flow cytometry

Citrated blood (20 µl), BALF cell suspension (20 µl) and digested lung parenchymal cells (20 µl) in individual FACS tubes were stained with FITC-conjugated rat anti-mouse CD11b monoclonal antibody (IgG2b, κ), PE-conjugated rat anti-mouse CD63 monoclonal antibody (IgG2a, κ), Pacific Blue-conjugated rat anti-mouse Ly6G monoclonal antibody (IgG2a, κ) for 30 min at 4^{o}C in the dark, before adding 2 ml of 1X FACSLyse solution and storing at 4^{o}C in the dark overnight for analysis the following day. Immediately before analysis, the samples were centrifuged at 300g for 5 min and the cells resuspended in 200 µl PBS-. 50 µl of Beckman Coulter flow check beads were added to each sample, mixed well and analysed on a BD FACSAria II machine, capturing a total 5000 beads with all associated events. The gating strategy is shown in Figure 2-15 opposite.

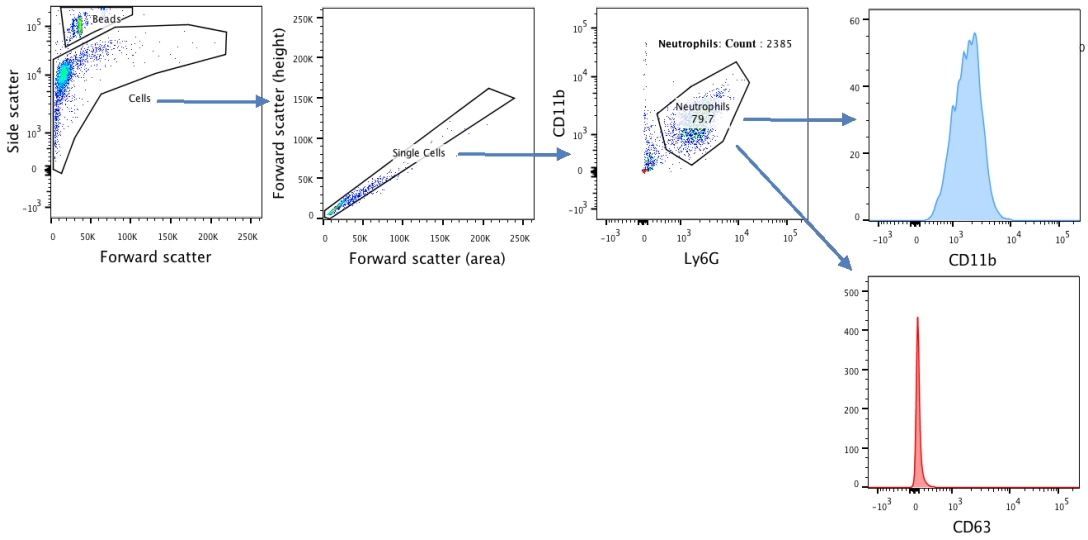

Figure 2-15 Gating strategy used to analyse total neutrophil number, % of total cells and activation markers within 3 compartments: peripheral blood, BALF and lung parenchyma
Single neutrophils are gated by their forward/side scatter properties, from which $CD11b^+$ $Ly6G^+$ cells are selected and analysed for CD63 and CD66b staining. Representative plot from 4 experiments.

2.22.6 Measurement of epithelial damage/leak

Duplicate 10 µl samples of BALF from tube 1 were used to measure total protein content with a Pierce BCA Protein Assay Kit against a set of standard concentrations (31.25-2000 µg/ml), according to the manufacturer's instructions. BALF stored at -80°C was analysed 48 h later using a soluble IgM ELISA kit, according to the manufacturer's instructions. Multiple dilutions of single samples were tested to obtain accurate results within the ELISA standard curve.

2.22.7 Measurement of bacterial survival

3 x 10 µl drops of citrated blood were placed on a LB agar plate and incubated overnight to look for evidence of bacteraemia. BALF, homogenised liver, lung and spleen samples were all serially diluted 1:10 in LB Broth and 3 x 10 µl drops of each were incubated on LB agar to assess for local and distant bacterial spread. As described in section 2.22.1, colony counts were used to calculate bacterial concentrations.

2.22.8 Measurement of systemic toxicity

As surrogate measures of systemic sepsis and drug toxicity, prepared plasma samples were tested for levels of lactate in mmol/l and alanine transaminase (ALT) in u/l. Briefly, samples of citrated blood were centrifuged at 850g for 3 min. Plasma was aliquoted and stored at -80^{o}C for later analysis by Dr Forbes Howie, Edinburgh University. ALT and lactate were quantified by using commercial kits (from Alpha Laboratories Ltd, Eastleigh, UK and Randox Laboratories Ltd, Crumlin, UK respectively) adapted for use on a Cobas Fara centrifugal analyser (Roche Diagnostics Ltd, Burgess Hill, UK).

2.22.9 Measurement of inflammatory cytokines in BALF and homogenised lung

The MPO content of the BALF was measured in two ways. 50 µl of fresh BALF from Tube 1 was placed in a 96-well plate and 100 µl of a premixed 1:1 TMB/H_2O_2 solution was added and incubated in the dark at room temperature for 20 min or until no further blue colour developed. The reaction was stopped with 50 µl of 2N sulphuric acid and the absorbance measured at 450nm. Frozen BALF and homogenised lung (in the acid model only) samples were thawed and analysed for the presence of MPO using a MPO ELISA kit, in addition to LTF, IL-6, KC, CCL-2, IL-10 and TNFα with their respective ELISA kits. As before, multiple dilutions of single samples were tested to obtain appropriate OD values.

2.23 Statistical Analysis and Graphical Presentation of Data

Flow cytometry data were analysed using Flojo version 10.0.7 (Ashland, OR, US). Statistical analysis and graphical presentation were carried out using Prism version 5.0f (Graphpad Software, La Jolla, CA, US).

Parametric data were analysed with the student's T-test when comparing two conditions and with a repeated measures Analysis of Variance (ANOVA) for greater than two conditions, using Dunn's post-hoc analysis test to compare individual conditions with the control condition. 2-way ANOVA analysis was used when two simultaneous variables were tested.

Non-parametric data were analysed with the Mann Whitney test for two conditions and with either the Kruskal-Wallis test or Friedman test for greater than two conditions, also using Dunn's post-hoc analysis test to compare individual conditions with the control condition. A significance level of less than 5% was used in all statistical tests.

Data are presented in tabular or graphical form as medians with range or interquartile range (IQR) if taken from non-parametrically distributed populations, or means with standard deviations (SD)/standard errors (SE) if taken from parametrically distributed populations. The graphical results of optimisation or control experiments are generally displayed in black and white, whereas the results of experiments used to test hypotheses are displayed in colour, in which the control conditions are displayed in red.

Chapter 3. An Investigation into the Effects of Src Kinase Inhibitors on Neutrophil Function In Vitro

3.1 Chapter Overview

This chapter details the work I carried out to investigate the effects of src kinase inhibition on in vitro neutrophil function in acute inflammation and infection. The following hypothesis was tested:

"*In vitro *src kinase inhibition of human neutrophils reduces extracellular degranulation in response to both chemical and live bacterial stimuli, without impairing efficient neutrophil phagocytosis and intracellular killing of bacteria"

The experiments initially focus on the key process of neutrophil degranulation, establishing an optimum concentration of PP1 required to attenuate extracellular degranulation from healthy volunteer neutrophils in response to a number of 'physiological' chemical and bacterial stimuli.

The key experiments are then repeated to establish an optimum concentration of a clinically licensed src kinase inhibitor to use subsequently in further in vitro functional assays.

Throughout the results chapters, I have endeavoured to keep a standardised structure to aid the reader in interpreting the results. Within each subsection, where possible, I generally detail the experiment rationale, design and the results in the text opposite each figure and legend, together with comments analysing the results and explaining how they led onto the next experiment. Details of experimental methods have not been repeated, and can be referred to in Chapter 2 on page 31.

The results are discussed in relation to published data throughout each chapter, before concluding with a summary of the key findings.

3.1.1 Parametric and non-parametric data

When examining the in vitro data in Chapters 3 and 5, it is important for the reader to consider that each experiment was typically repeated a maximum of 3

- 6 times due to a limited supply of blood donors and the logistics of performing several different assays within the limited lifespan of neutrophils. With such small experimental numbers, it is impossible to carry out any meaningful test of normality, so if values were reproducible between individual healthy volunteers, I chose to make the assumption that the sample was taken from a normally distributed population and have therefore displayed the data as mean +/- SD/SE and analysed them with t-tests and ANOVAs. Conversely, in some assays such as apoptosis by cell morphology (Section 3.5.2) and superoxide release (Section 3.5.8), there was little reproducibility of values between individual volunteers and the data are presented as median +/- IQR and analysed with Mann Whitney tests or Friedman/Kruskal-Wallis tests.

As expected, values from ex vivo experiments involving neutrophils from critically ill patients (Section 5.3) showed marked variability and as such were displayed and analysed as non-parametric data.

In vivo murine experiments (Chapter 4) were carried out using 8 – 10 animals per group. Given the larger sample numbers and reliability of the assays, these data have been displayed and analysed as parametric in distribution for all except the bacterial survival assays.

3.2 Experimental Techniques to Stimulate Human Neutrophil Degranulation with Sterile and Non-sterile Stimuli

There are numerous effective techniques of experimentally inducing human neutrophil degranulation via different intracellular pathways, using chemical stimuli in vitro, some of which are more physiologically relevant. I chose to use the following stimulants:

3.2.1 Cytochalasin B/fMLP

In Ca^{2+}-replete neutrophils pre-treated with cytochalasin B, the bacterial protein-derived chemoattractant, fMLP, ligates its G protein-coupled receptor FPR1, inducing both phospholipase C (PLC) and phospholipase D (PLD) activation in a PI3K-dependent manner. The resulting secondary messengers inositol-1,4,5-triphosphate (IP_3) and 1,2-diradyl-sn-glycerol (DG) activate protein kinase C (PKC) and mobilise intracellular Ca^{2+} stores to initiate degranulation (Mullmann et al. 1993; Mansfield et al. 2002; Lacy 2006).

3.2.2 Phorbol myristate acetate

Phorbol myristate acetate (PMA) is a potent PKC agonist that can be used to study the mechanisms controlling NADPH oxidase assembly and degranulation in both the plasma membrane and the granule membrane. The traditional theory is that PMA acts independently of PI3K, however there is some evidence to show that PMA-induced superoxide production is PI3K-dependent in the granule membrane and PI3K-independent at the plasma membrane (Karlsson et al. 2000). The same observation has yet to be demonstrated in the mechanisms controlling neutrophil degranulation, which is usually measured by extracellular release.

3.2.3 Lipopolysaccharide

In the presence of LPS-binding protein, LPS released from the outer membrane of Gram negative organisms ligates CD14 on macrophages, neutrophils and monocytes, which, via its co-receptor TLR4, initiates intracellular signalling resulting in activation of NF-κB (Kitchens 2000; Lu et al. 2008). Although lipopolysaccharides from different Gram negative bacteria differ in their

molecular weight depending on their carbohydrate content, LPS from *E. coli* is capable of inducing neutrophil extracellular degranulation at a concentration of 100 ng/ml (Hayashi et al. 2003; Sabroe et al. 2005). LPS has also long been studied in in vivo models of sepsis and acute lung inflammation.

3.2.4 Live bacteria

Live bacteria represent the most physiologically relevant stimuli of neutrophil degranulation. They are less studied in the literature due to a number of factors including: variation in individual pathogen, strain virulence strategies and host-pathogen interactions, the challenge of obtaining reproducible results due to the sensitivity of bacteria to their immediate environment and the interference of bacterial presence (and ongoing multiplication) on assay performance. I chose to use PA and SA as they represent Gram negative and Gram positive organisms commonly isolated from the lungs of critically ill patients. They comprised the two most common organisms isolated in 1689 cases of ventilator-associated pneumonia (VAP) in a series of 24 studies with an isolation frequency of 24.4% and 20.4% respectively (Chastre & Fagon 2002). I used serum-opsonised live bacteria and was therefore predominantly studying complement receptor (CR3)-mediated phagocytosis and degranulation (Caron & Hall 1998).

3.3 Src Kinase Inhibition of Neutrophil Degranulation with PP1

Initial experiments sought to replicate previously published data showing that the specific src tyrosine kinase inhibitor, PP1, can inhibit adhesion-dependent degranulation (Mócsai et al. 1999) and fMLP-induced degranulation (Mócsai et al. 2000) and establish an optimum concentration of PP1 for use in subsequent experiments.

3.3.1 PP1 inhibits c-src Tyr^{416} phosphorylation in stimulated neutrophils without affecting p38 MAPK phosphorylation

When c-src is activated, Tyr^{527} is dephosphorylated, allowing destabilisation of its regulatory SH2 and SH3 domains, revealing the kinase required for the autophosphorylation of Tyr^{416} (Cooper et al. 1986).

Results: Figure 3-1 opposite suggests that at concentrations of 10 μM and above, PP1 inhibits autophosphorylation of c-src Tyr^{416} in purified neutrophils both unstimulated or stimulated by 100 ng/ml LPS, with no effect on activation of the control p38 MAPK pathway.

Comments: It is interesting to observe that in these experiments, the control neutrophils without PP1 pre-treatment demonstrate a relatively high degree of baseline c-src Tyr^{416} phosphorylation, irrespective of LPS stimulation and despite the addition of phosphatase inhibitors to the lysis buffer. This may be caused by unavoidable activation during the Percoll method of neutrophil purification.

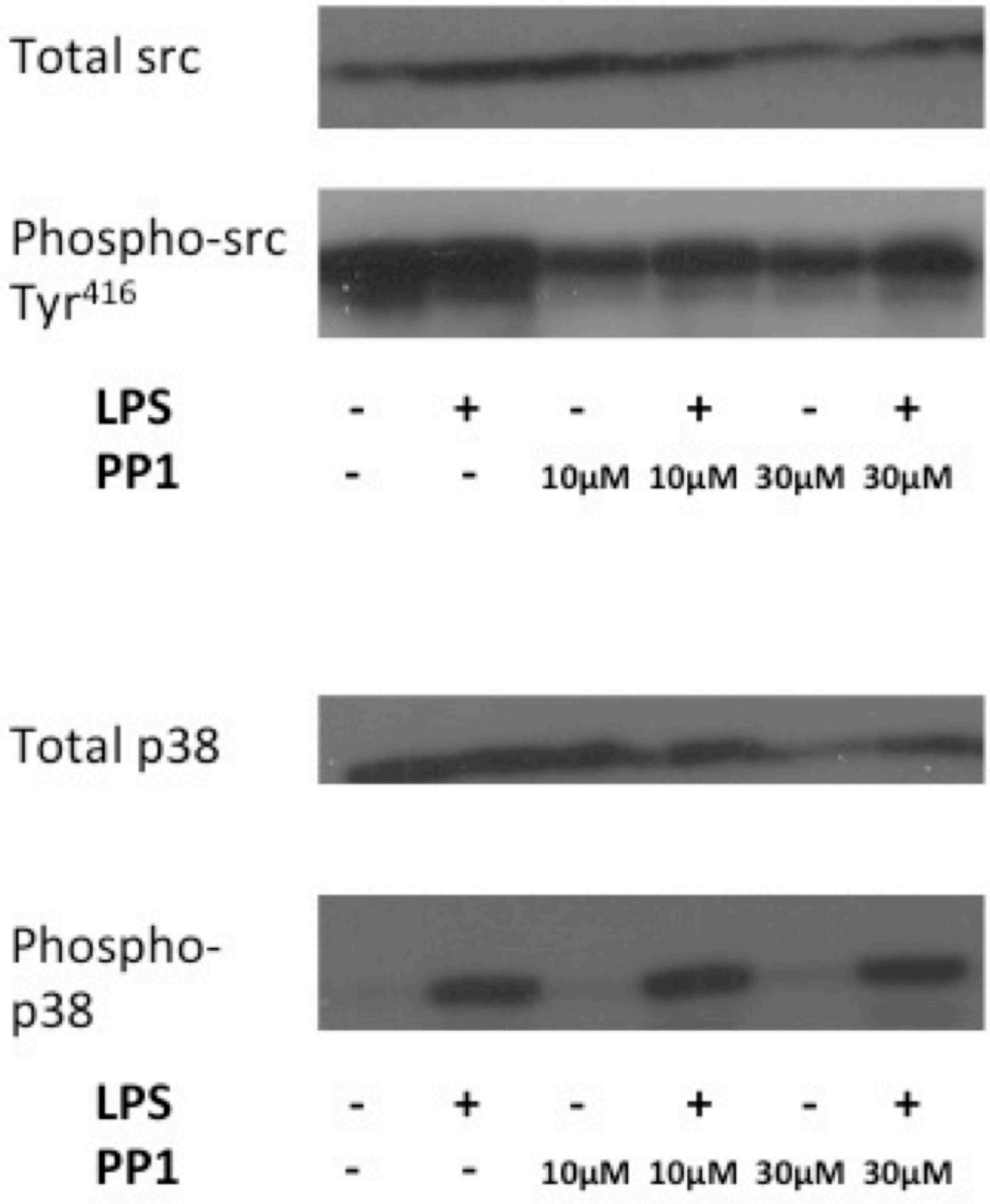

Figure 3-1 PP1 inhibits src kinase activity in human neutrophils stimulated with LPS

Western blot of lysates from 5 x 10^6 neutrophils (from healthy volunteers) pre-treated with control, 10 μM PP1 or 30 μM PP1 and stimulated for 15 min with 100 ng/ml LPS or control. Lysates were probed with antibodies directed towards phospho-src Tyr^{416}, total src kinase, phospho-p38 MAPK and total p38 MAPK. Representative image from one of three separate experiments using neutrophils from independent volunteers.

3.3.2 PP1 inhibits neutrophil degranulation of primary granules in response to fMLP in a dose dependent fashion

I used MPO as a surrogate marker of primary granule degranulation as its relative activity in extracellular fluid can be measured simply by exploiting its ability to reduce H_2O_2 in the colorimetric TMB/H_2O_2 assay. Using this method makes the assumptions that the MPO activity is directly proportional to the amount of actual enzyme present **and** that the MPO released by neutrophil degranulation in response to the various stimulants is all functional. In the murine experiments in chapter 5 I therefore modified my methods to measure both MPO antigen presence using ELISA and activity using the TMB/H_2O_2 assay.

Results: Figure 3-2 opposite shows that neutrophils adherent to tissue culture plastic (B) and in free suspension (C) release significantly less MPO in response to fMLP when pre-treated with at least 10 μM (C) and 30 μM (B) of PP1.

Comments: The control experiment in A demonstrates that this effect cannot be explained by an inhibitory effect of high concentrations of PP1 itself on the enzymatic activity of MPO in the TMB/H_2O_2 assay.

Control adherent neutrophils appear to release less than half the amount of functional MPO released by neutrophils in suspension. The mechanism of adhesion via integrin activation and ligation represents an important stimulator of degranulation. I used 1 x 10^6 neutrophils in both adherent and suspension conditions: 1 x 10^6 neutrophils adherent to the base of a single well of a 24-well plate represents a very crowded fit. It is therefore conceivable that any MPO released is either taken up by adjacent neutrophils or remains within the neutrophil monolayer rather than being circulated into suspension in the media.

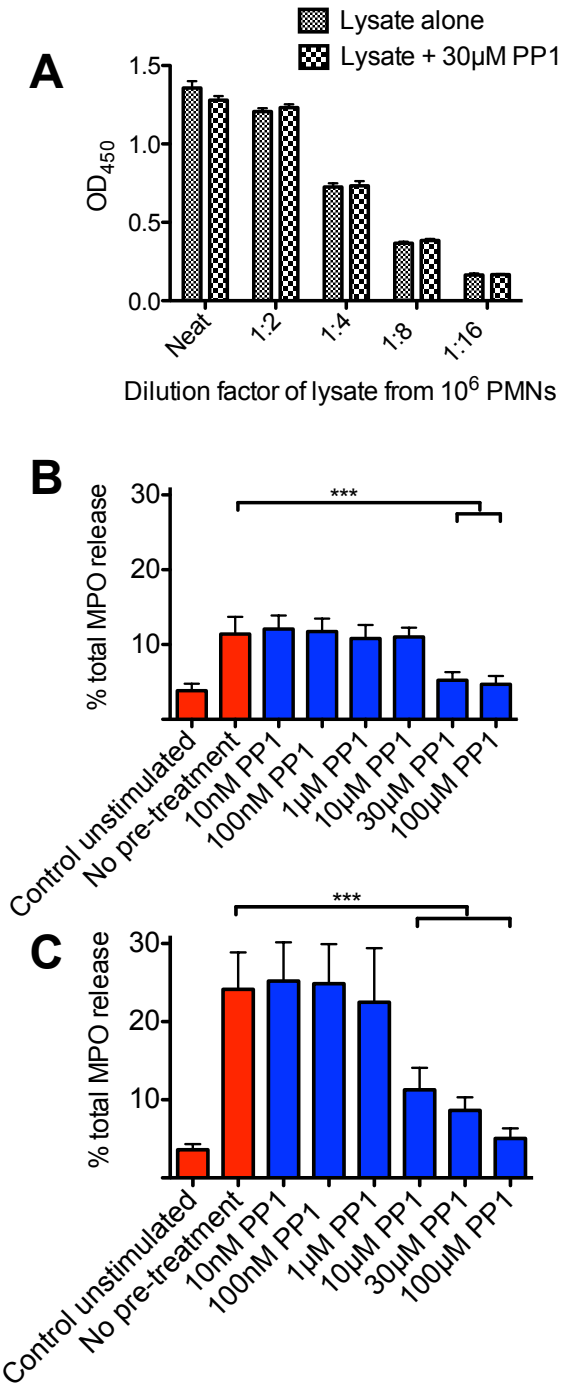

Figure 3-2 PP1 inhibits primary granule release of MPO from neutrophils in response to cytochalasin B/fMLP

Control experiment to demonstrate no effect of the presence of 30 μM PP1 on the reduction of H_2O_2 by MPO in the TMB/H_2O_2 assay (A). Data show mean + SD of OD values of the neutrophil lysates from 3 independent healthy volunteers. Dose response of PP1 pre-treatment on MPO release from 10^6 neutrophils (from healthy volunteers) stimulated with 10 μM cytochalasin B for 5 min followed by 1 μM fMLP for 10 min, adherent to tissue culture plastic (B) and in suspension (C). All conditions except the left-hand column were stimulated with cytochalasin B+fMLP. Data show mean and SD values of samples from 5 experiments using neutrophils from 5 independent volunteers. $p<0.0001$ by repeated measures ANOVA ***$p<0.001$ by Dunn's post-hoc test comparing with 'no pre-treatment' control.

3.3.3 *PP1 inhibits neutrophil degranulation of secondary granules in response to fMLP*

Lactoferrin was chosen as a surrogate marker for secondary granule release. Although secondary granules are released ahead of primary granules both temporally and in magnitude, both granules are released within the experimental endpoint of 30 min (Lacy & Eitzen 2008).

Results: Figure 3-3 below shows very similar inhibitory thresholds of PP1 as for MPO release. Again, considerably less LTF is detected in the supernatant from adherent neutrophils than from suspension neutrophils.

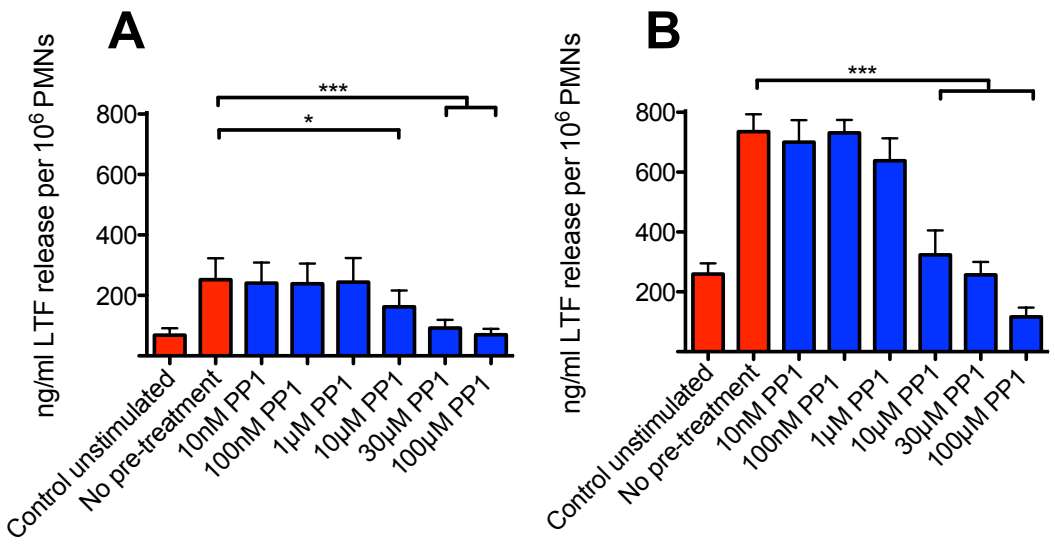

Figure 3-3 PP1 inhibits secondary granule release of LTF from neutrophils in response to cytochalasin B/fMLP
Dose response of PP1 pre-treatment on LTF release from 10^6 neutrophils (from healthy volunteers) stimulated with 10 μM cytochalasin B for 5 min followed by 1 μM fMLP for 10 min in adherent (A) and suspension (B) conditions. All conditions except the left-hand column were stimulated with cyto B+fMLP. Data show mean and SD values from 5 experiments using neutrophils from 5 independent volunteers. $p<0.0001$ by repeated measures ANOVA; *$p<0.05$, ***$p<0.001$ by Dunn's post-hoc test comparing with 'no pre-treatment' control.

3.3.4 *PP1 inhibits neutrophil degranulation in whole blood in response to fMLP*

To reproduce these observations using a second experimental method, the relative expression of CD63 (primary granules), CD66b (secondary granules) and CD11b (a commonly studied marker of neutrophil activation expressed on secondary, tertiary and secretory vesicles) on the extracellular membranes of neutrophils in heparinised blood was assessed using flow cytometry. It should

be noted that I used one timepoint of 30 min stimulation. In reality there is continual cycling of membrane proteins from intracellular vesicles to the plasma membrane with subsequent degradation by ubiquitination (Bonifacino & Weissman 1998) but this 'snapshot' measurement gives an estimation of the degree of granule translocation and fusion with the plasma membrane in response to stimuli.

Results: Although the effect of PP1 in whole blood appears less marked than in purified neutrophils, there is significant reduction of all three markers when pre-treated with at least 30 μM PP1, as shown in Figure 3-4 below.

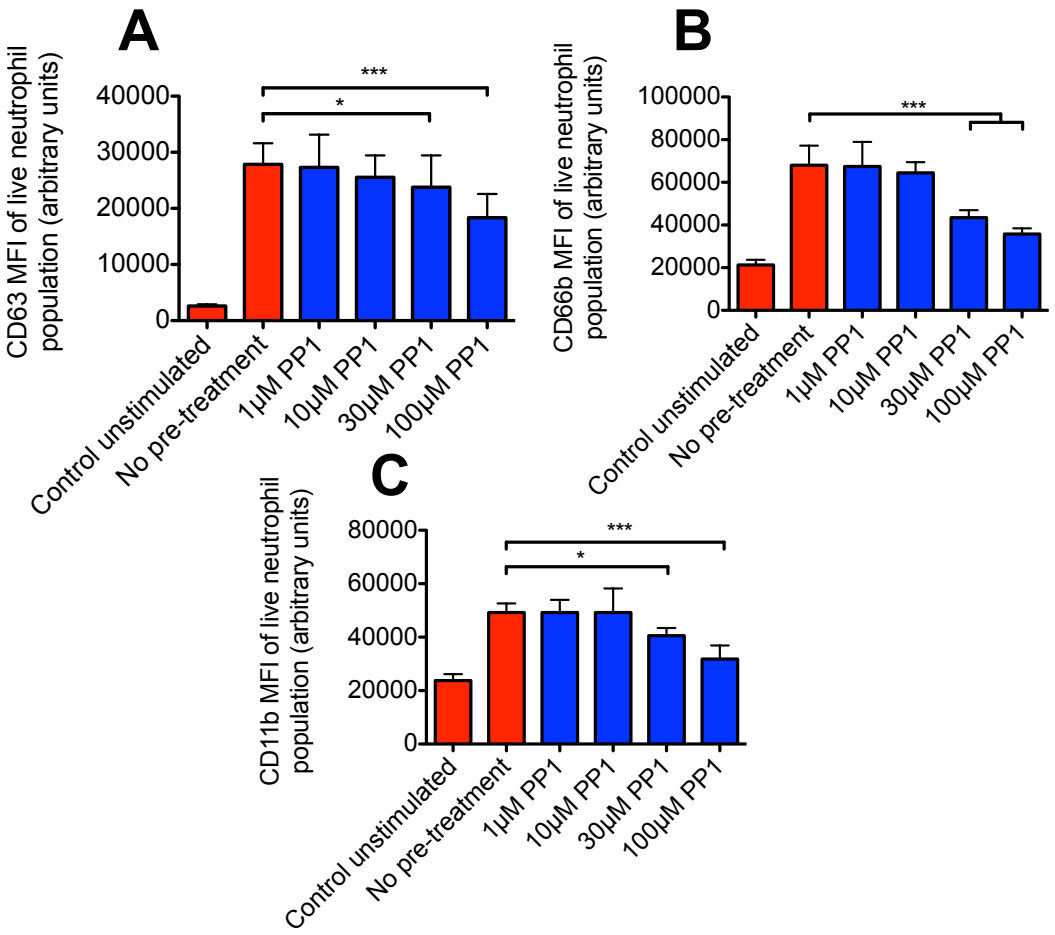

Figure 3-4 PP1 inhibits primary and secondary granule extracellular fusion in response to cytochalasin B/fMLP
Dose response of PP1 pre-treatment on extracellular expression of the primary granule marker CD63 (A), the secondary granule marker CD66b (B) and the secondary/tertiary granule/secretory vesicle marker CD11b (C) by neutrophils in whole blood (from healthy volunteers), in response to cytochalasin B/fMLP stimulation. All conditions except the left-hand column were stimulated with cyto B+fMLP. Data show mean and SE MFI values from 4 experiments using samples from 4 independent volunteers. $p<0.0001$ by repeated measures ANOVA; *$p<0.05$, ***$p<0.001$ by Dunn's post-hoc test comparing with 'no pre-treatment' control.

3.3.5 *PP1 inhibits neutrophil degranulation of primary and secondary granules in response to LPS in a dose dependent fashion*

I chose to perform subsequent degranulation experiments on neutrophils in suspension and in whole blood only because the relative release of primary and secondary granules was significantly blunted in adherent conditions.

Results: Pre-treatment with at least 10 μM PP1 is capable of significantly reducing both MPO and LTF release from purified neutrophils in response to 100 ng/ml LPS, but a higher concentration of 30 μM is required to significantly reduce CD63, CD66b and CD11b expression (Figure 3-5 below and Figure 3-6 opposite).

Comments: LPS induces similar levels of CD66b and CD11b expression to stimulation with cytochalasin B/fMLP, but markedly less CD63 expression. This observation is also, to a lesser extent, seen in the MPO/LTF values and is likely to be explained by differences in the relative timing and speed of granule release with and without the addition of the co-stimulant cytochalasin B, as shown in the original granule kinetic studies (Bentwood & Henson 1980).

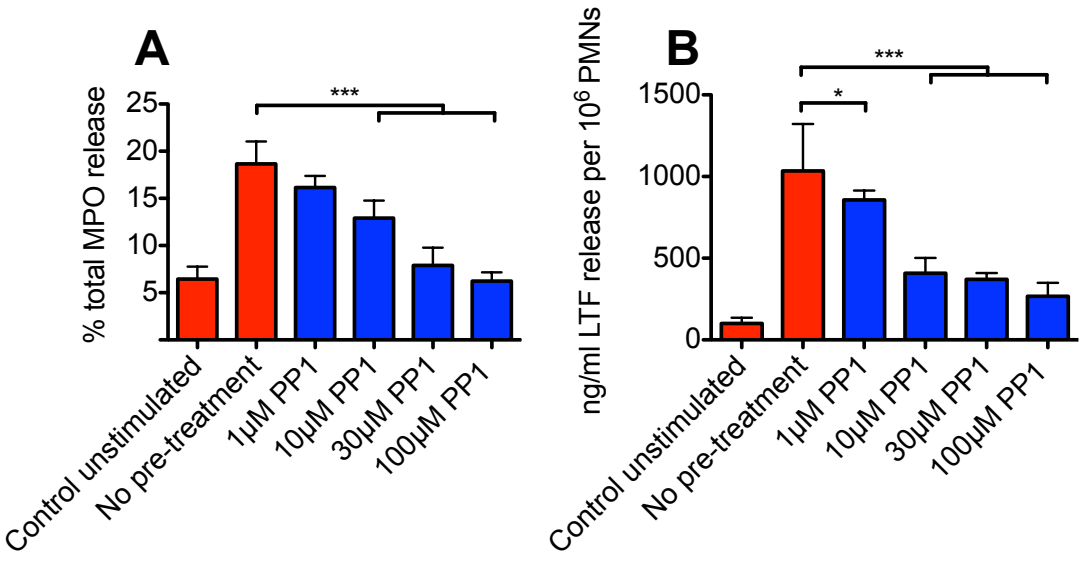

Figure 3-5 PP1 inhibits primary granule MPO release and secondary granule LTF release in response to LPS
Dose response of PP1 pre-treatment on MPO (A) and LTF (B) release from 10^6 neutrophils (from healthy volunteers) in suspension stimulated with 100 ng/ml LPS for 30 min. All conditions except the left-hand column were stimulated with LPS. Data show mean and SD values from 5 experiments using samples from 5 independent volunteers. $p<0.0001$ by repeated measures ANOVA; *$p<0.05$, ***$p<0.001$ by Dunn's post-hoc test comparing with 'no pre-treatment' control.

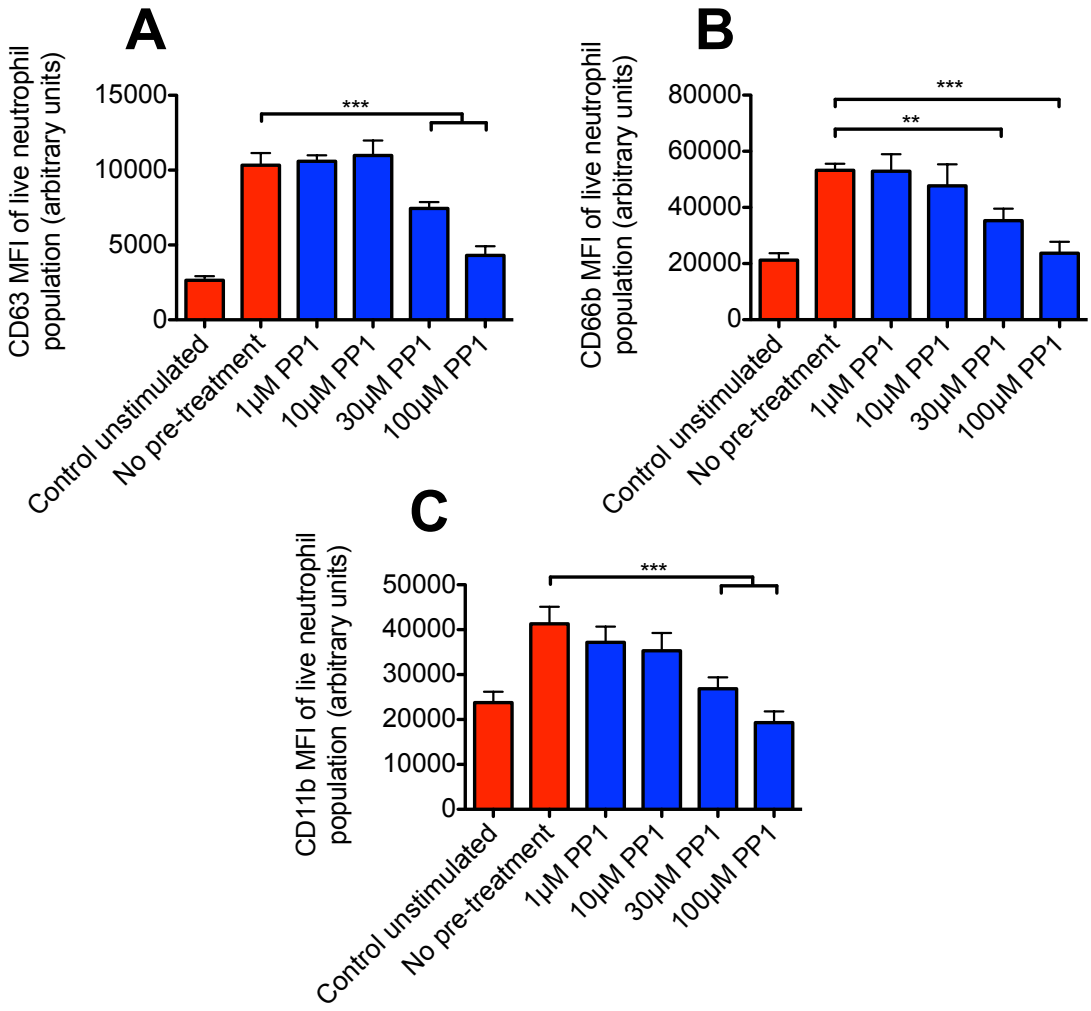

Figure 3-6 PP1 inhibits primary and secondary granule extracellular fusion in response to LPS

Dose response of PP1 pre-treatment on extracellular expression of CD63 (A), CD66b (B) and CD11b (C) by neutrophils in whole blood (from healthy volunteers), in response to 100 ng/ml LPS stimulation. All conditions except the left-hand column were stimulated with LPS. Data show mean and SE MFI values from 4 experiments using samples from 4 independent volunteers. $p<0.0001$ by repeated measures ANOVA; $^{**}p<0.01$, $^{***}p<0.001$ by Dunn's post-hoc test comparing with 'no pre-treatment' control.

3.3.6 PP1 does not inhibit PMA-induced neutrophil degranulation

Results: As expected, PP1 pre-treatment only reduces neutrophil degranulation (MPO and LTF release; CD63 and CD11b expression) in response to PMA at an exceptionally high concentration of 100 μM (see Figure 3-7 below and Figure 3-8 opposite).

Comments: PMA is a potent PKC agonist and stimulates neutrophil degranulation independent of src kinases. This important experimental control shows that src kinase inhibition with PP1 does not globally inhibit neutrophil inflammatory pathways and functions.

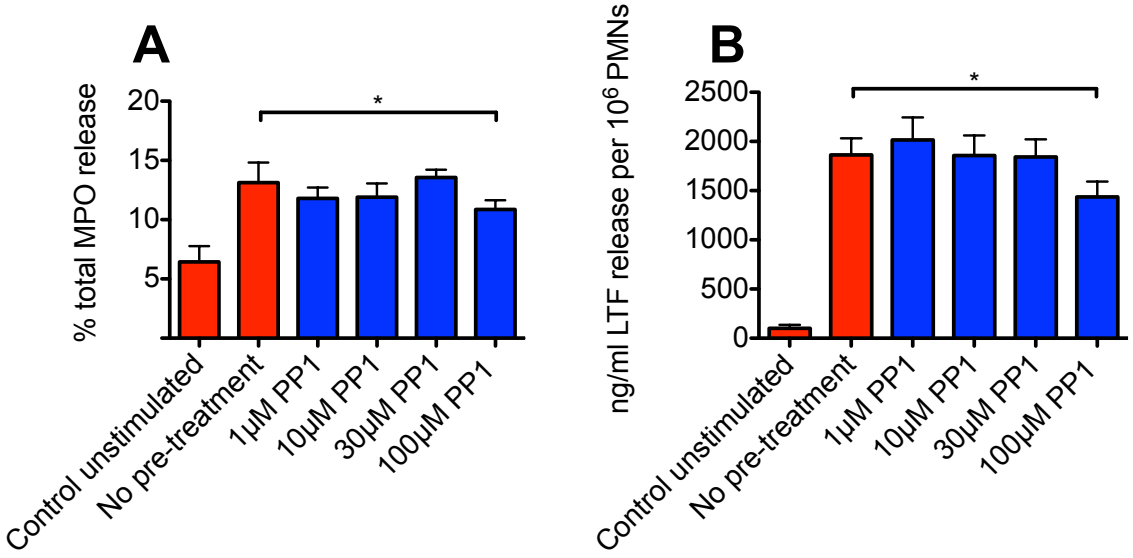

Figure 3-7 PP1 only inhibits primary granule MPO release and secondary granule LTF release in response to PMA at high concentrations
Dose response of PP1 pre-treatment on MPO (A) and LTF (B) release from 10^6 neutrophils (from healthy volunteers) in suspension stimulated with 100 nM PMA for 30 min. All conditions except the left-hand column were stimulated with PMA. Data show mean and SD values from 5 experiments using samples from 5 independent volunteers. p=0.007 (A) and p=0.0017 (B) by repeated measures ANOVA, *p<0.05 by Dunn's post-hoc test comparing with 'no pre-treatment' control.

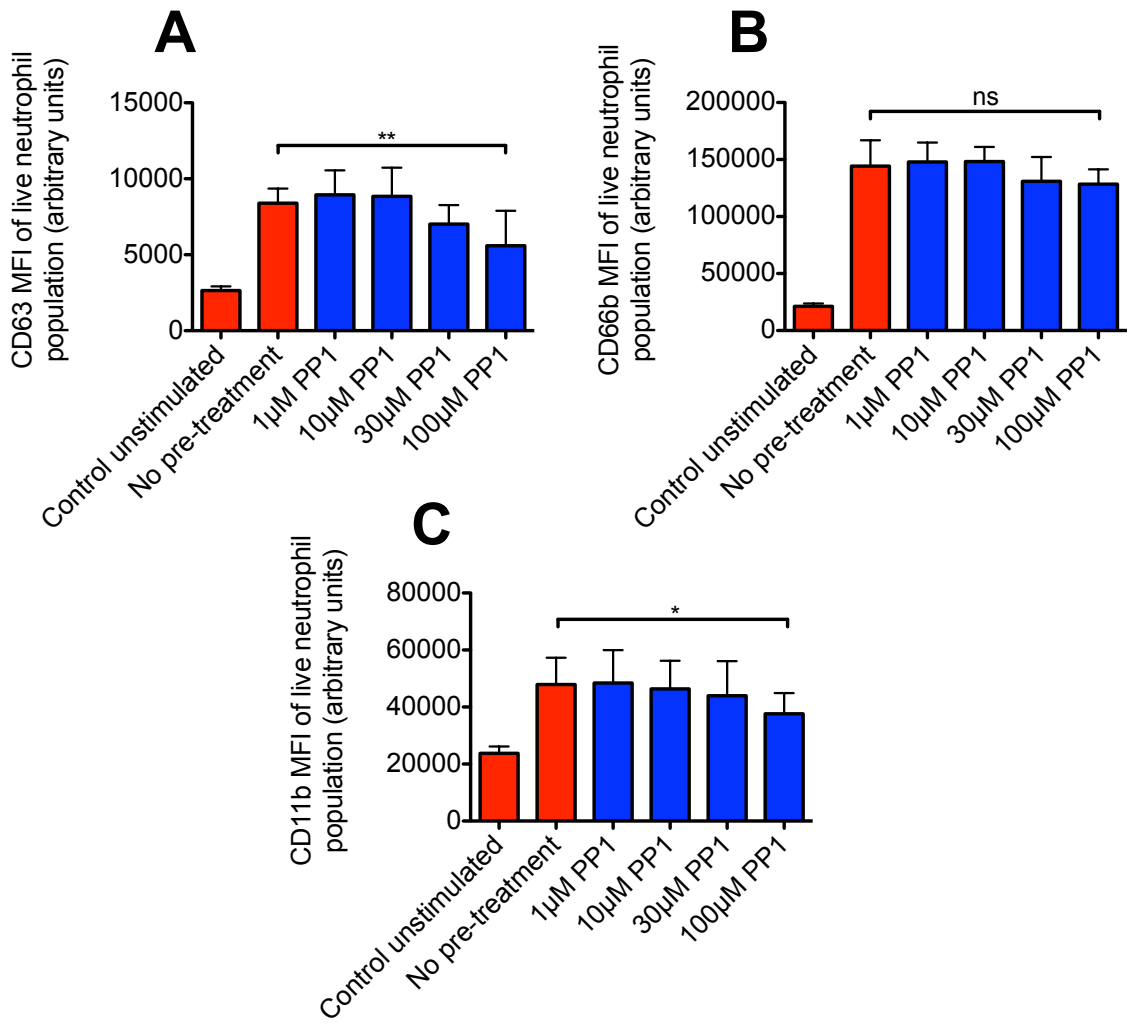

Figure 3-8 PP1 only inhibits primary and secondary granule extracellular fusion in response to PMA at high concentrations

Dose response of PP1 pre-treatment on extracellular expression of CD63 (A), CD66b (B) and CD11b (C) by neutrophils in whole blood (from healthy volunteers), in response to 100 nM PMA stimulation. All conditions except the left-hand column were stimulated with PMA. Data show mean and SE MFI values from 4 experiments using samples from 4 independent volunteers. $p=0.0024$ (A), $p=0.0063$ (B) and $p=0.015$ (C) by repeated measures ANOVA; $^{*}p<0.05$, $^{**}p<0.01$ by Dunn's post-hoc test comparing with 'no pre-treatment' control.

3.3.7 PP1 inhibits neutrophil degranulation in response to live bacteria

Novel data came from challenging degranulation experiments involving live bacteria. I chose to use the *P. aeruginosa* strain PA01 rather than clinically isolated strains as it is a relatively predictable non-virulent laboratory strain commonly used in scientific research. However in whole blood flow cytometry experiments, direct inoculation of blood with live PA01 resulted in rapid neutrophil death, as evidenced by high % DAPI staining (data not shown). For whole blood experiments I therefore used the *S. aureus* strain SA NCTC 8325 that did not induce significant cell death in this assay.

An MOI of approximately 10 bacteria per neutrophil was used because preliminary data showed that at this ratio, significant neutrophil degranulation occurred with net bacterial killing. At lower MOIs, the bacteria were all killed too rapidly and did not offer a robust stimulus whereas at higher MOIs the bacteria multiplied too quickly during the assay and overwhelmed the neutrophils (data not shown), consistent with earlier published observations (Li et al. 2002; Li et al. 2004). As such, results from experiments in which the retrospectively estimated MOI was markedly different from 10:1 were excluded for analysis. I found that after careful practice and strict timings, this potential variable was minimised.

As shown in Figure 3-9 opposite, I carried out degranulation experiments on purified neutrophils both in free suspension on a tube rotator (B+D) and adherent to plastic (A+C). Whole blood measurements of CD63/66b/11b expression were in suspension. Serum-opsonised bacteria initiate phagocytosis and neutrophil degranulation upon ligation of the opsonin C3bi with its receptor CR3 on neutrophils. In this very simple in vitro model of alveolar infection and inflammation, purified neutrophils maintained in free suspension or in whole blood were chosen to represent neutrophils within extracellular or alveolar fluid, whilst adherent neutrophils represented activated neutrophils adherent to capillary endothelial cells or alveolar epithelial cells via integrin expression and ligation.

Results: In both experimental conditions, at least 10 μM PP1 is required to significantly inhibit both primary and secondary granule release in response to

live PA01. A similar effect is observed when studying CD63, CD66b and CD11b expression on neutrophils in suspension in whole blood (Figure 3-10 overleaf).

Comments: These observations will be discussed together with the phagocytosis and killing data presented in sections 3.5.7 to 3.5.9 below.

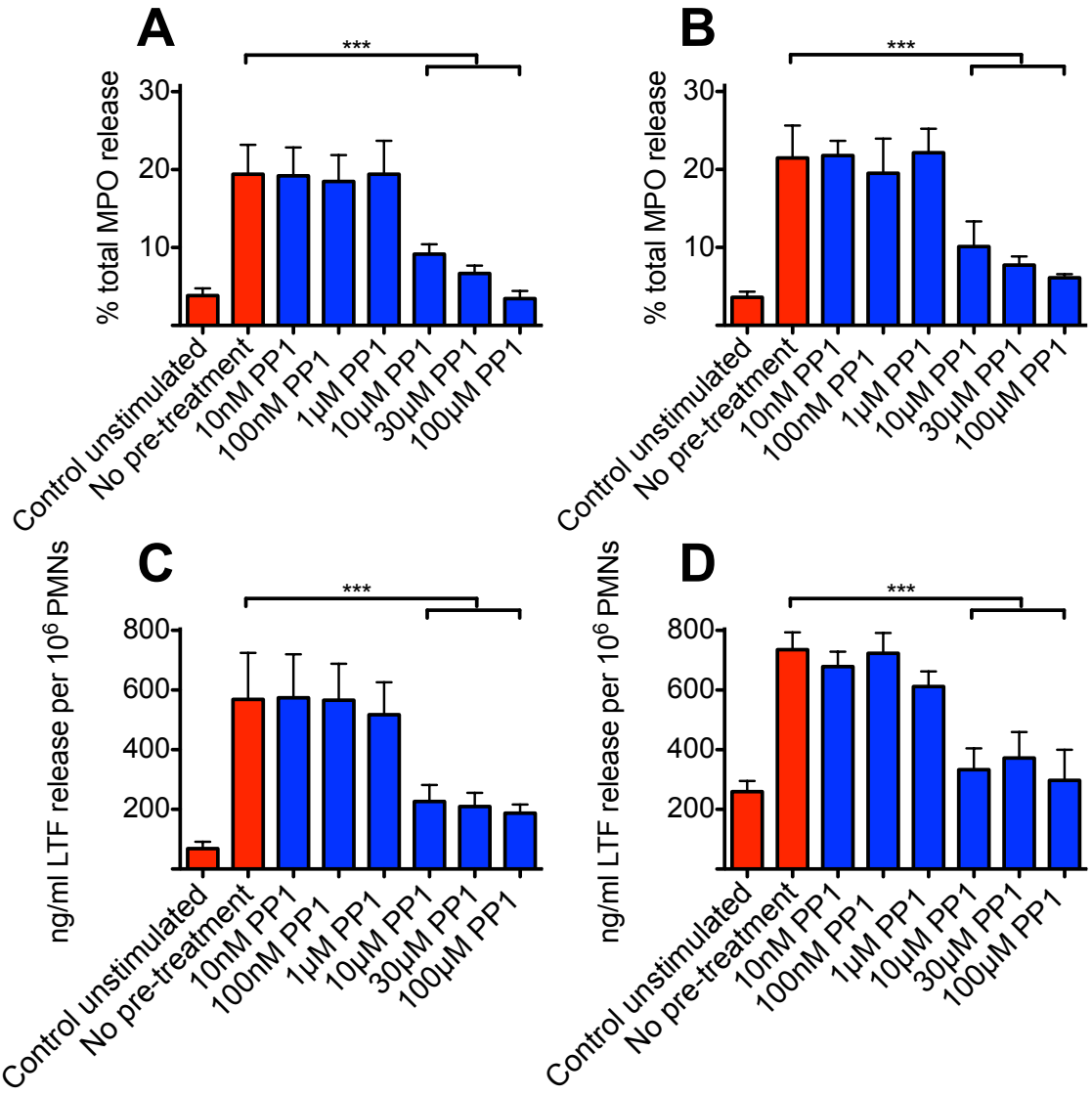

Figure 3-9 PP1 inhibits primary granule MPO release and secondary granule LTF release in response to live serum-opsonised bacteria
Dose response of PP1 pre-treatment on MPO (A+B) and LTF (C+D) release from 10^6 neutrophils (from healthy volunteers) adherent to tissue culture plastic (A+C) or in suspension (B+D), stimulated with serum-opsonised *P. aeruginosa* (MOI~10 PA01: 1 polymorphonuclear leukocyte - PMN) for 30 min. All conditions except the left-hand column were stimulated with PA01. Data show mean and SD values from 5 experiments using samples from 5 independent volunteers. $p<0.0001$ by repeated measures ANOVA; ***$p<0.001$ by Dunn's post-hoc test comparing with 'no pre-treatment' control.

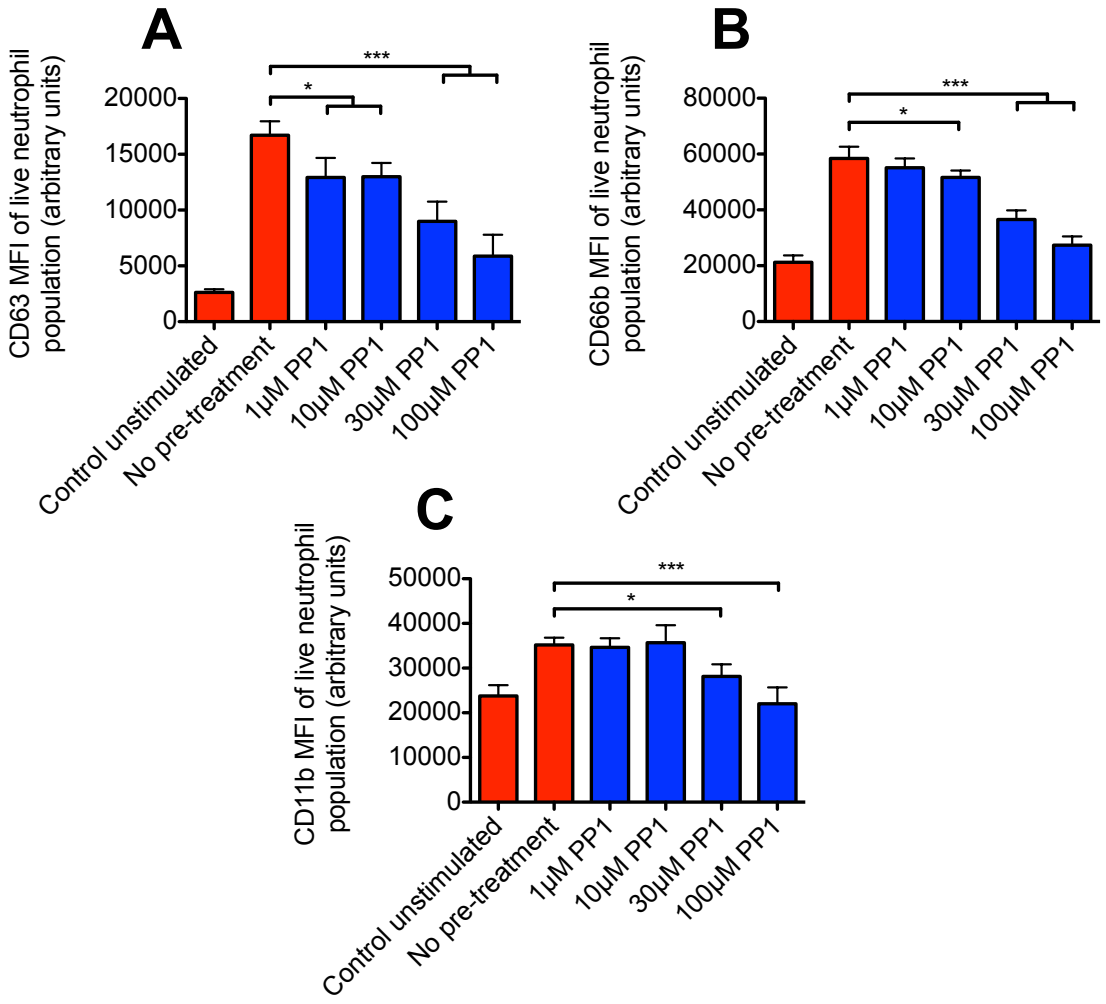

Figure 3-10 PP1 inhibits primary and secondary granule extracellular fusion in response to live serum-opsonised bacteria

Dose response of PP1 pre-treatment on extracellular expression of CD63 (A), CD66b (B) and CD11b (C) by neutrophils in whole blood (from healthy volunteers), in response to stimulation by live *S. aureus*. All conditions except the left-hand column were stimulated with *S. aureus*. Data show mean and SE MFI values from 4 experiments using samples from 4 independent volunteers. $p<0.0001$ by repeated measures ANOVA; *$p<0.05$, ***$p<0.001$ by Dunn's post-hoc test comparing with 'no pre-treatment' control.

3.4 Src Kinase Inhibition of Neutrophil Degranulation with Clinically Licensed Src Kinase Inhibitors

The next set of experiments aimed to test whether the observations made using PP1 were replicated using other src kinase inhibitors. I specifically chose two safe, clinically licensed src kinase inhibitors: dasatinib and bosutinib. The experiments were designed to identify a drug to take forward into in vivo murine models of acute lung inflammation (Chapter 4) as well as an optimum in vitro concentration for use in further in vitro experiments (Chapter 5). Although dasatinib inhibits the non-receptor tyrosine kinases Abl, c-src and c-kit with an IC_{50} of 0.6 nM, 0.8 nM and 79 nM respectively, these concentrations were established using in vitro kinase autophosphorylation assays on glutathionine-sepharose beads (O'Hare 2005; Shah et al. 2006) and higher concentrations are required in cellular assays to act intracellularly. Indeed, at least 10 nM was required to observe an effect in functional assays on human neutrophils (Futosi et al. 2012).

Bosutinib is considered a potent dual inhibitor of c-src and Abl with comparable IC_{50} values to dasatinib in kinase assays: 1.2 nM and 1.0 nM respectively (Boschelli et al. 2001; Golas et al. 2003). It has also been shown to inhibit other members of the src family kinases such as Hck, Fgr, Lyn that are found only on haematopoietic cells (Remsing Rix et al. 2009).

An initial concentration range of 10 nM to 1 μM of both dasatinib and bosutinib was therefore used for the majority of the initial experiments that follow.

3.4.1 The src/Abl kinase inhibitors dasatinib and bosutinib inhibit c-src Tyr^{416} phosphorylation in stimulated neutrophils

Results: The Western blots reproduced opposite in Figure 3-11 show a marked attenuation in c-src Tyr^{416} autophosphorylation when human neutrophils are pre-treated with 100 nM dasatinib and a complete absence of c-src kinase activity using a concentration of 1 μM.

With bosutinib there appears to be a biphasic response with increased c-src kinase activation at lower concentrations (100 nM) but a significant reduction at 1 μM. The experiments below were carried out at the same time and the observations reproduced using neutrophils from 3 different healthy volunteers on 3 separate days.

Comments: The results of the bosutinib Western blot will be interpreted in light of functional assay data shown below in section 3.4.2.

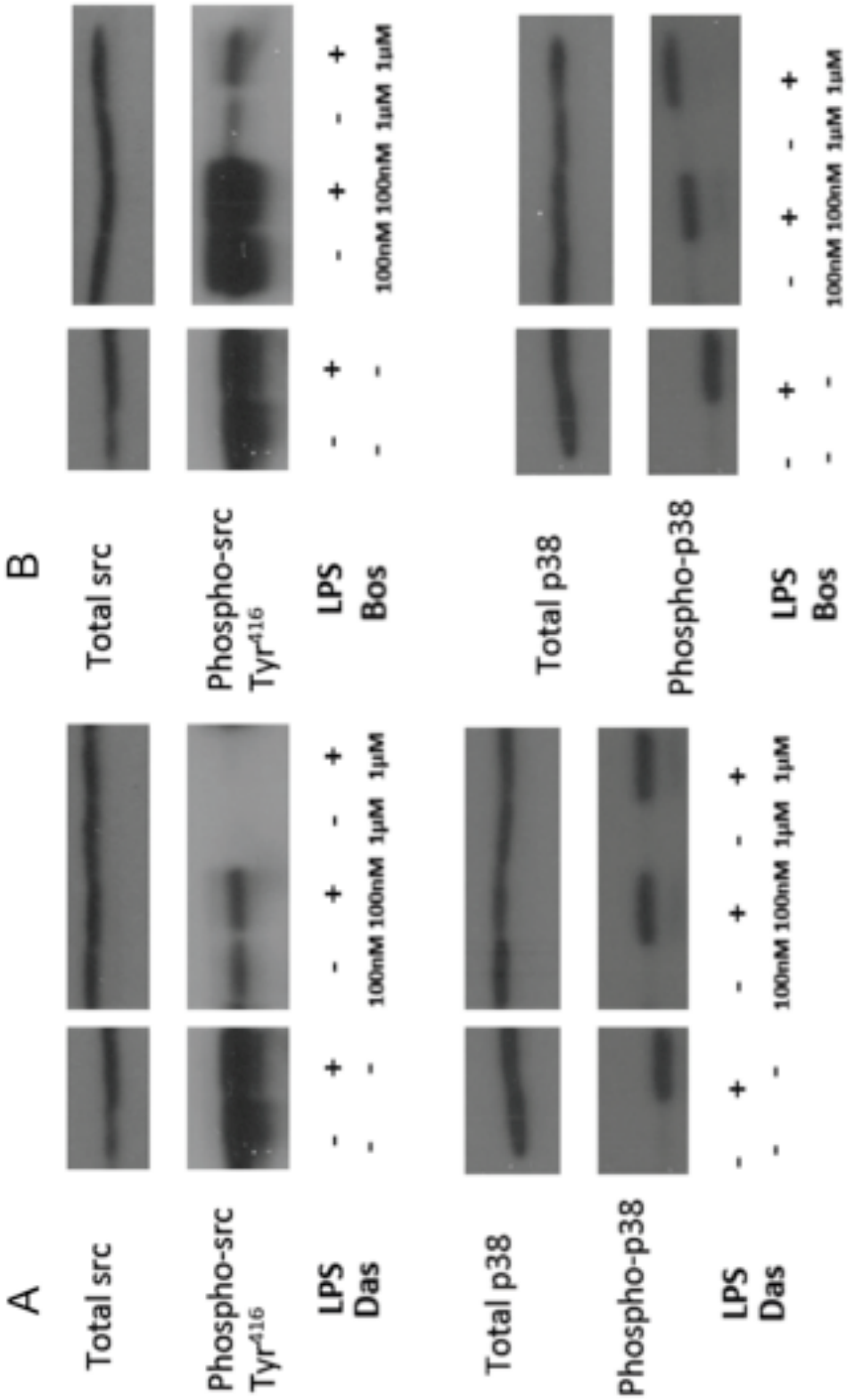

Figure 3-11 Dasatinib and bosutinib inhibit src kinase activity in human neutrophils stimulated with LPS

Western blot of lysates from 5 x 10^6 neutrophils (from healthy volunteers) pre-treated with control, 100 nM or 1 μM dasatinib, 100 nM or 1 μM bosutinib and stimulated for 15 min with 100 ng/ml LPS or control. Lysates were probed with antibodies directed towards phospho-src Tyr^{416}, total src kinase, phospho-p38 MAPK and total p38 MAPK. Representative image from one of three separate experiments using neutrophils from independent volunteers.

3.4.2 Effect of dasatinib and bosutinib on lactoferrin release from stimulated neutrophils

I decided to measure only LTF as a surrogate marker of degranulation because it was released more readily and reliably than MPO in response to all stimuli tested in the PP1 experiments above. It is a stable molecule resistant to protein degradation (Brock et al. 1976) and can be measured accurately by ELISA.

Results: In dose response experiments shown opposite (Figure 3-12), pre-treatment with at least 100 nM dasatinib is required to inhibit LTF release from neutrophils stimulated by cytochalasin B/fMLP, LPS or live *S. aureus*, with a trend towards an effect at 10 nM. Little effect is seen with bosutinib except at a concentration of 1 μM.

Comments: My observations build on those made by Futosi et al. by the addition of live bacteria as a stimulus (Futosi et al. 2012). Similar to PP1, no effect is seen with PMA stimulation, demonstrating specificity in dasatinib's action. The equivalent results for bosutinib are consistent with the Western blot shown in Figure 3-11 and suggest that concentrations of at least 1 μM of bosutinib are required to observe an inhibitory effect in functional assays.

Figure 3-12 Dasatinib and bosutinib (at very high concentrations) inhibit LTF release from neutrophils in response to both sterile and non-sterile stimuli

Dose response of dasatinib (A,C,E,G) and bosutinib (B,D,F,H) pre-treatment on LTF release from 10^6 neutrophils (from healthy volunteers) in suspension, stimulated by cytochalasin B 10 μM/fMLP 1 μM (A+B), LPS 100 ng/ml (C+D), PMA 100 nM (E+F) and serum-opsonised live *S. aureus* (MOI~10 SA: 1 PMN) (G+H). All conditions except the left-hand column were stimulated. Data show mean and SD values from 4 experiments using samples from 4 independent volunteers. $p<0.001$ by repeated measures ANOVA; $^{**}p<0.01$, $^{***}p<0.001$ by Dunn's post-hoc test comparing with 'no pre-treatment' control.

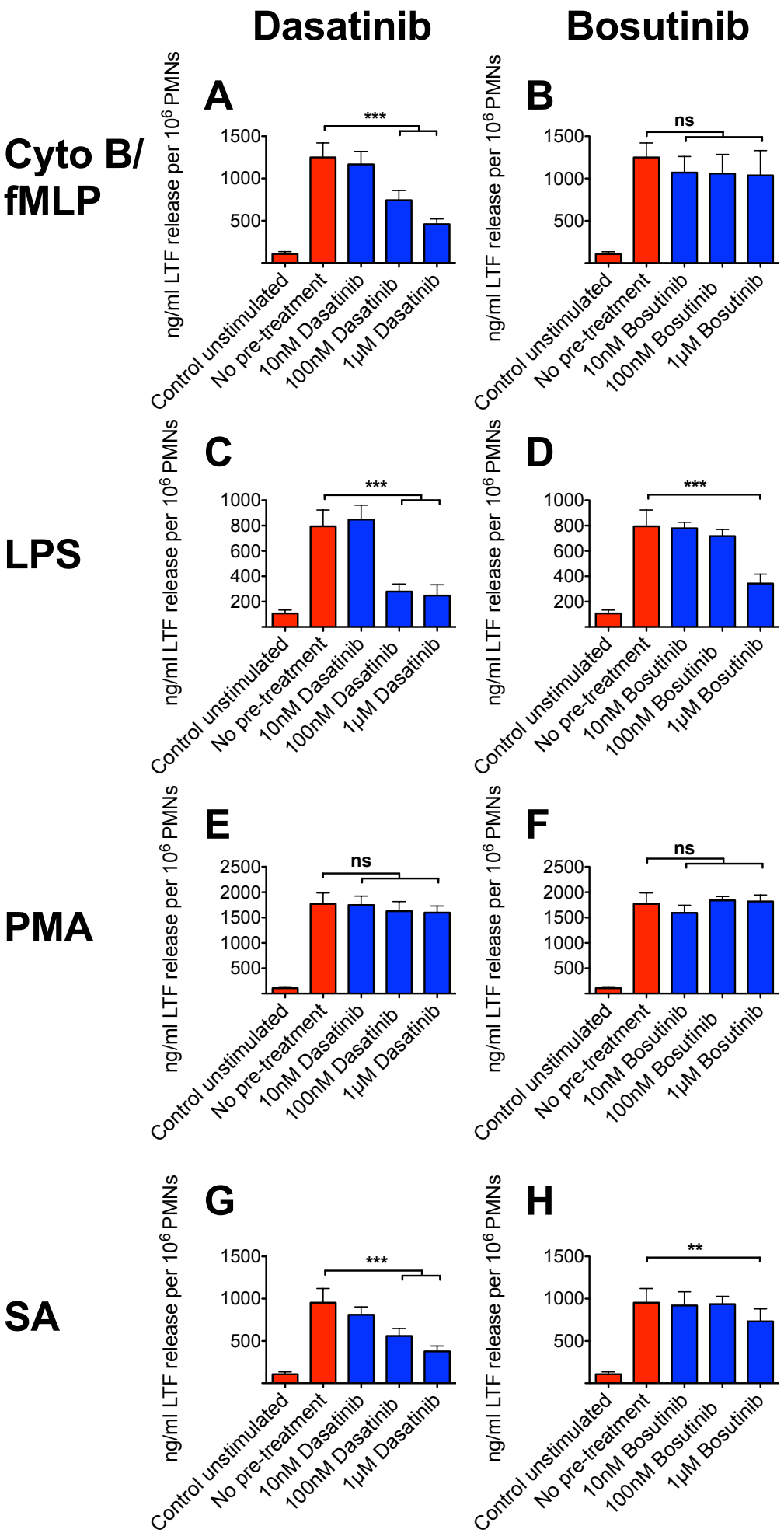
Dasatinib
Bosutinib
Cyto B/ fMLP
LPS
PMA
SA
A
B
C
D
E
F
G
H
ng/ml LTF release per 10^6 PMNs
***
ns
**
Control unstimulated
No pre-treatment
10nM Dasatinib
100nM Dasatinib
1μM Dasatinib
10nM Bosutinib
100nM Bosutinib
1μM Bosutinib

3.4.3 Effect of dasatinib on CD63/CD66b/CD11b expression on stimulated neutrophils

Based on the results in sections 3.4.1 and 3.4.2 above, dasatinib was a better option than bosutinib to take forward into further in vitro and in vivo experiments.

Results: In whole blood degranulation assays (Figure 3-13 opposite), dasatinib reliably exerts an inhibitory effect on CD63 and CD66b expression at concentrations of 100 nM and above, in response to stimulation with cytochalasin B/fMLP, LPS and live *S. aureus*, with no effect on PMA stimulation. CD11b expression is only affected by dasatinib in response to live *S. aureus*.

Comments: These results complement the lactoferrin release data shown above in Figure 3-12. They show that both primary (CD63) and secondary (CD66b) granule exocytosis is inhibited by dasatinib. Dissimilar to the PP1 data, dasatinib only inhibits CD11b expression in response to CR3 (integrin-mediated) serum-opsonised *S. aureus* stimulation, with no effect on fMLP (G-protein coupled receptor-mediated) activation or LPS-mediated activation. Reassuringly, Futosi et al. showed similar findings, using different assays involving isolated adherent neutrophils (Futosi et al. 2012)

As briefly discussed previously, the validity of these in vitro observations depends entirely on demonstrating that the drugs themselves are not directly cytotoxic to neutrophils at the equivalent concentrations shown to inhibit degranulation. At a final PP1 concentration of 100 μM in IMDM, I often observed that the drug precipitated when diluted 1:100 from its stock concentrate (10 mM in DMSO). A 1 in 100 dilution of DMSO is usually sufficient to avoid the inhibitory effects of the diluent itself on neutrophil function.

Figure 3-13 Dasatinib inhibits primary and secondary granule extracellular fusion in response to sterile and non-sterile stimuli
Dose response of Dasatinib pre-treatment on extracellular expression of CD63 (A-D), CD66b (E-H) and CD11b (I-L) by neutrophils in whole blood (from healthy volunteers), in response to stimulation by cytochalasin B 10 μM/fMLP 1 μM (A,E,I), LPS 100 ng/ml (B,F,J), PMA 100 nM (C,G,K) and serum-opsonised live *S. aureus* (MOI~10 SA: 1 PMN) (D,H,L). Data show mean and SE MFI values from 4 experiments using samples from 4 independent volunteers. $p<0.001$ by repeated measures ANOVA; *$p<0.05$, **$p<0.01$ and ***$p<0.001$ by Dunn's post-hoc test comparing with 'no pre-treatment' control.

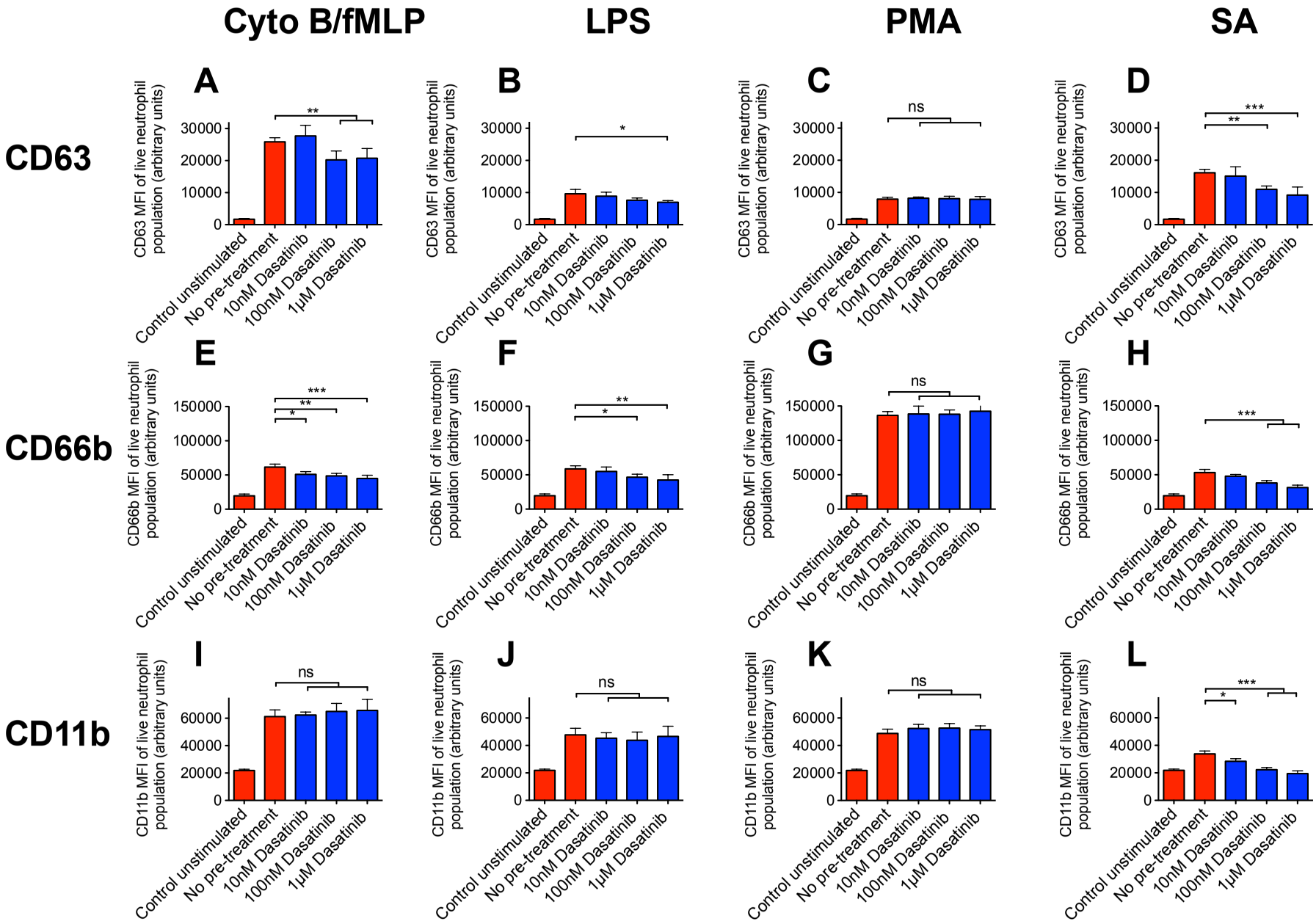
Cyto B/fMLP
LPS
PMA
SA
CD63
CD66b
CD11b
A
B
C
D
E
F
G
H
I
J
K
L
CD63 MFI of live neutrophil population (arbitrary units)
CD66b MFI of live neutrophil population (arbitrary units)
CD11b MFI of live neutrophil population (arbitrary units)
Control unstimulated
No pre-treatment
10nM Dasatinib
100nM Dasatinib
1μM Dasatinib
ns

3.5 Effect of Src Kinase Inhibition on Cell Viability

The total duration of exposure to PP1 or dasatinib in the functional assays was typically 60 min (30 min pre-treatment followed by 30 min assay), so I chose to assess direct drug-induced cytotoxicity by LDH release after 60 min exposure. I also assessed neutrophil apoptosis at 30 min, as well as the traditional timepoints of 6 h and 24 h using both Annexin V/PI staining and cell morphology.

3.5.1 Direct drug-induced cytotoxicity

Results: As shown in Figure 3-14 opposite, dasatinib is not directly cytotoxic to neutrophils at all concentrations tested. However PP1 exposure induces a small but nevertheless significant rise in LDH release at 10 μM, but over double the control level (~10% to 20%) at concentrations of 30 μM and above, in excess of the positive control using 100 nM PMA.

Comments: How a doubling of the relatively low background rate of cell lysis (as measured by LDH release) would affect the functional release of granule products is hard to predict, but it seems more likely to reduce neutrophil function, and may partly explain the inhibitory effect of PP1 seen at 30 μM. One can therefore conclude that the optimum effective in vitro concentration of PP1 in these assays must lie somewhere in a tight ‘therapeutic window’ between 10 μM and 30 μM.

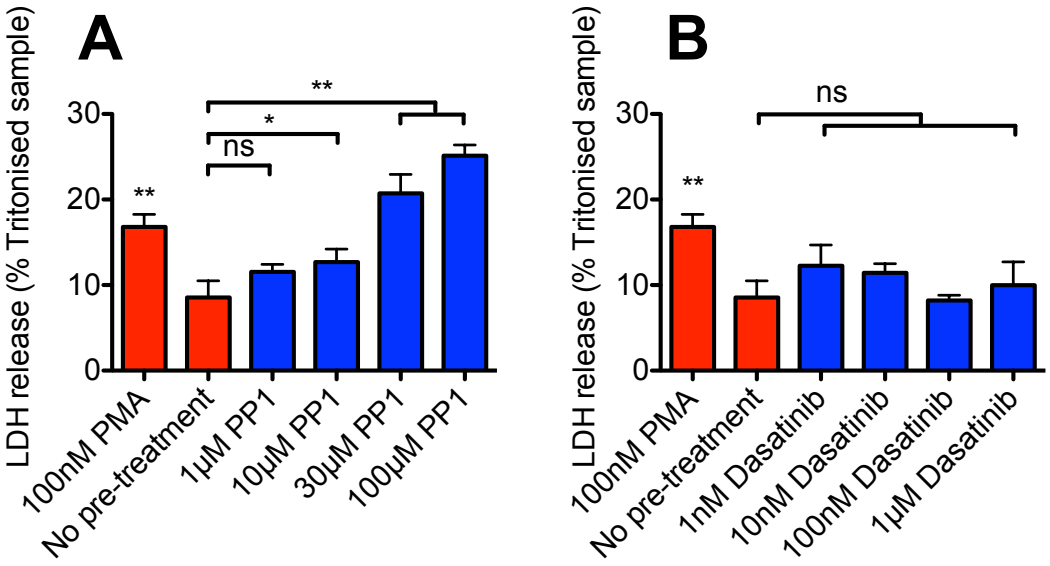

Figure 3-14 PP1, but not dasatinib, induces direct neutrophil cytotoxicity at high concentrations

Dose response of PP1 (A) and dasatinib (B) pre-treatment on extracellular release of LDH from 5 x 10^4 neutrophils (from healthy volunteers), expressed as a percentage of the total LDH released from the same number of cells lysed with 1% Triton X-100. Data show mean and SE values from 3 experiments using triplicate samples from 3 independent volunteers. $p<0.001$ by repeated measures ANOVA; *$p<0.05$, **$p<0.01$ by Dunn's post-hoc test comparing with 'No pre-treatment control'

3.5.2 Neutrophil apoptosis

Results: Figure 3-15 opposite shows the relative proportion of neutrophils that are alive (Ann V^-/PI^-), early apoptotic (Ann V^+/PI^-) or late apoptotic/dead (Ann $V^{+/-}/PI^+$) after 30 min, 6 h and 24 h exposure to 10 μM PP1 or 100 nM dasatinib at 37^{o}C. Even at 30 min, PMA induces the production of cell debris, explaining why the bars do not approximate to 100%.

Comments: In these experiments, 30 min and 6 h are too early for apoptosis to occur, and only by 24 h are there significant levels of neutrophil apoptosis. The death rates do not correlate directly with the LDH release data shown above; however the two assays measure cytotoxicity in different ways. Lactate dehydrogenase is a stable cytoplasmic enzyme released extracellularly only when plasma membrane damage occurs. PI binds exposed deoxyribonucleic acid (DNA) in damaged and dead cells to become fluorescent and therefore potentially offers a more accurate count of dead cells in a population.

Figure 3-15 PP1 and dasatinib treatment does not affect neutrophil apoptosis, as assessed by Annexin V/PI staining
Neutrophils (from healthy volunteers), at 10^6/ml, were treated with control, 100 nM PMA, 10 μM PP1 or 100 nM dasatinib and aliquots removed at 30 min (A), 6 h (B) and 24 h (C) before staining with Annexin V APC and PI and assessed using a BD FACSCanto II machine. Data show mean and SD values for % alive, early apoptotic and late apoptotic/dead neutrophils from 5 experiments using samples from 5 independent volunteers. p=1.00 (A+B), p=0.373 (C) by 2-way ANOVA, using treatment and viability as variables.

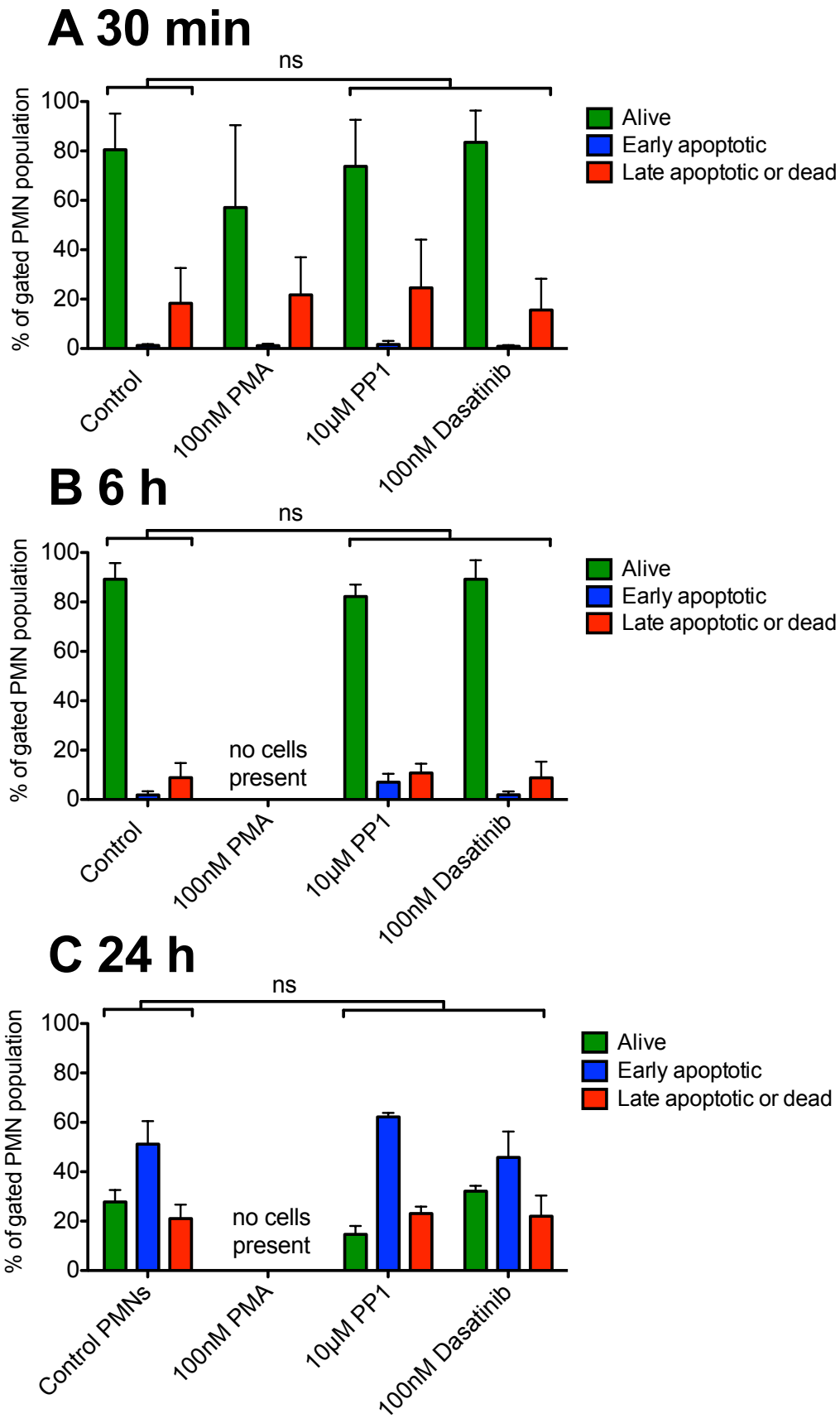
A 30 min
ns
% of gated PMN population
100
80
60
40
20
0
Control
100nM PMA
10μM PP1
100nM Dasatinib
Alive
Early apoptotic
Late apoptotic or dead
B 6 h
ns
% of gated PMN population
100
80
60
40
20
0
no cells present
Control
100nM PMA
10μM PP1
100nM Dasatinib
Alive
Early apoptotic
Late apoptotic or dead
C 24 h
ns
% of gated PMN population
100
80
60
40
20
0
no cells present
Control PMNs
100nM PMA
10μM PP1
100nM Dasatinib
Alive
Early apoptotic
Late apoptotic or dead

Results: Figure 3-16 opposite and Figure 3-17 overleaf support the flow cytometry data using a different experimental technique. After 30 min and 6 h exposure, there are minimal levels of apoptosis as assessed by cell morphology on cytospin staining. 24 h exposure to PP1 or dasatinib does not increase or decrease levels of apoptosis from control levels.

Comments: Taken together, the cytotoxicity and apoptosis data are crucial as they show that at therapeutic concentrations of 10 μM PP1 and 100 nM dasatinib, there is no significant change in background apoptosis or necrosis rates in unstimulated healthy human neutrophils, suggesting that any inhibitory effect on degranulation or other functional responses is a true effect. At higher concentrations of PP1 (over 30 μM) the drug exerts a direct cytotoxicity effect. This finding may explain some of the inhibitory effects observed previously at such concentrations of PP1.

In the context of ARDS, this is important as it means that src kinase inhibition with either drug should not induce excessive neutrophil death at the site of lung inflammation, nor should it result in an imbalance in the resolution phase of acute lung inflammation.

Figure 3-16 PP1 and dasatinib treatment does not affect neutrophil apoptosis, as assessed by cell morphology
Neutrophils (from healthy volunteers) at 10^6/ml, were treated with control, 100 nM PMA, 10 μM PP1 or 100 nM dasatinib and aliquots removed at 30 min (A), 6 h (B) and 24 h (C) for cytocentrifuge preparation and counting of % apoptotic neutrophils by morphology under light microscopy. Data show median and IQR values from 4 experiments using samples from 4 independent volunteers. p=0.0329 (A), p=0.0046 (B) and p=0.0417 (C) by Friedman test, excluding PMA positive control values.

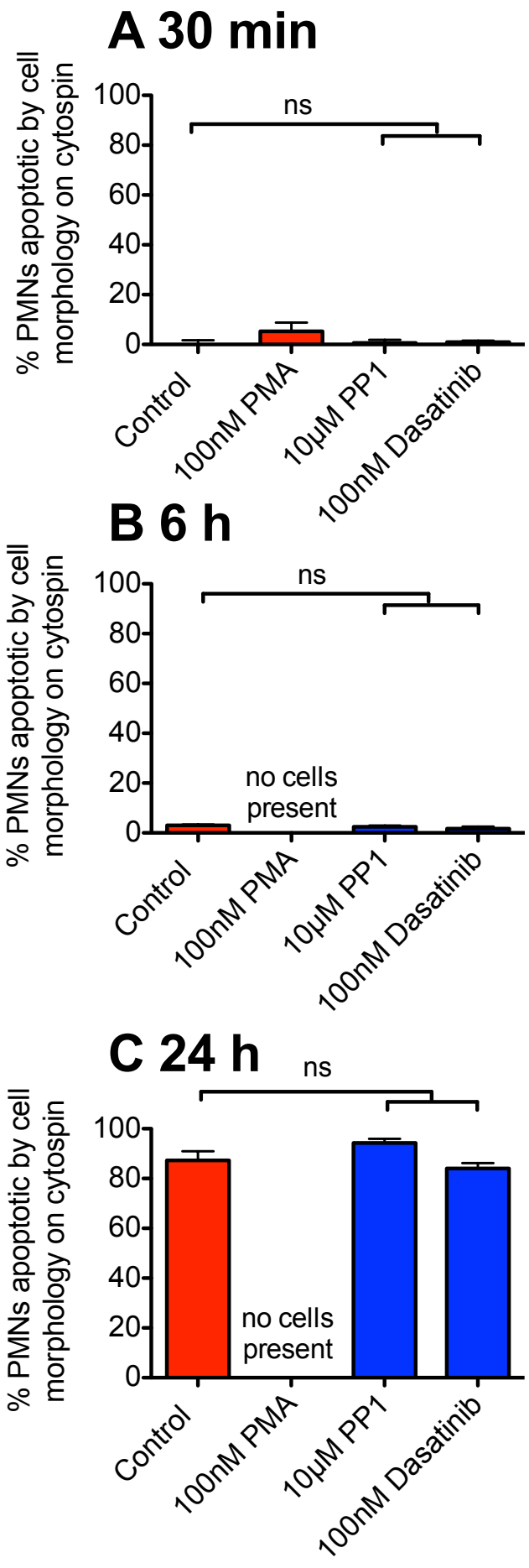
A 30 min
% PMNs apoptotic by cell morphology on cytospin
100
80
60
40
20
0
ns
Control
100nM PMA
10μM PP1
100nM Dasatinib
B 6 h
% PMNs apoptotic by cell morphology on cytospin
100
80
60
40
20
0
ns
no cells present
Control
100nM PMA
10μM PP1
100nM Dasatinib
C 24 h
% PMNs apoptotic by cell morphology on cytospin
100
80
60
40
20
0
ns
no cells present
Control
100nM PMA
10μM PP1
100nM Dasatinib

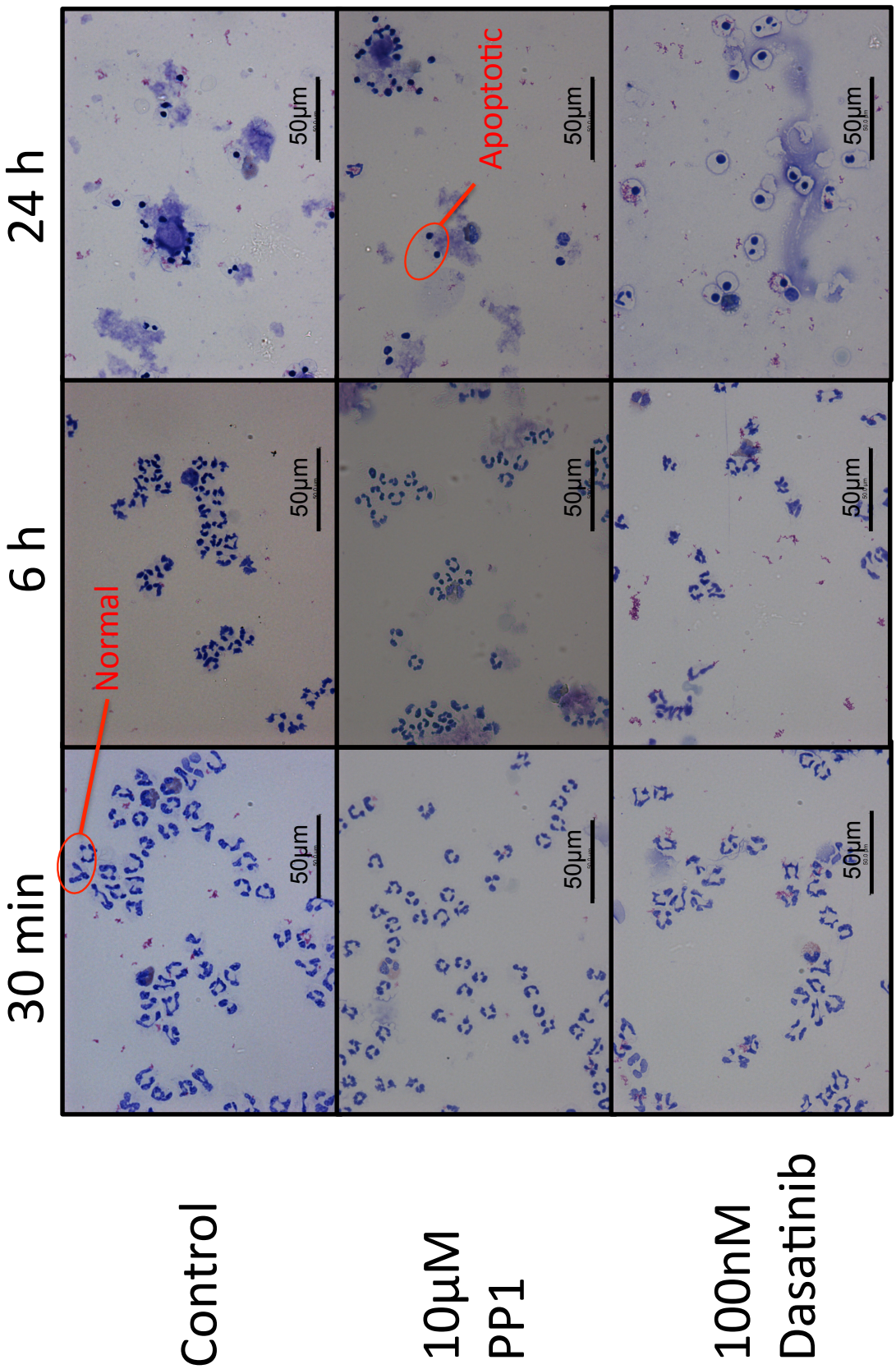

Figure 3-17 PP1 and dasatinib treatment has no effect on neutrophil apoptosis

X400 images of cytocentrifuge preparations of neutrophils exposed to control, 10 µM PP1 or 100 nM dasatinib for 30 min, 6 h and 24 h. Representative images from one of three separate experiments using neutrophils from independent volunteers.

3.5.3 Effect of Src Kinase Inhibition on Key Neutrophil Functions

Having established reliable inhibitory concentrations of both PP1 and dasatinib in degranulation assays, I proceeded to test the effect of src kinase inhibition on a number of pro-inflammatory functions of neutrophils.

Neutrophils are recruited to the inflamed lung through interaction with the inflamed endothelium, using first selectin and then integrin activation. The src family kinases and downstream Syk kinases are integral to the intracellular signalling pathways that induce adhesion, spreading, chemotaxis, and superoxide production through oxidative burst (Zarbock & Ley 2008). It would therefore follow that src kinase inhibition results in reduced neutrophil recruitment to site of lung inflammation. In ARDS, where excessive neutrophil recruitment and degranulation is a major factor in the pathogenesis of the condition, this effect may prove beneficial.

3.5.4 Cell adhesion

Results: Using a simple assay to test adhesion of neutrophils to tissue culture plastic in response to 50 nM fMLP in the presence of 1% autologous serum (Figure 3-18 opposite), the results show that src kinase inhibition with at least 30 μM PP1 or 100 nM dasatinib results in significantly reduced levels of adhesion.

Comments: Adhesion is inhibited to near the level of the negative control with cytochalasin D. Cytochalasin D is a potent inhibitor of actin polymerisation and prevents any degree of neutrophil shape change required for effective adhesion (Casella et al. 1981). Seen through inverted microscopy, the effect is marked, with the majority of treated neutrophils remaining spherical in free suspension or loosely adherent, rather than firmly adherent and spread over the plastic surface.

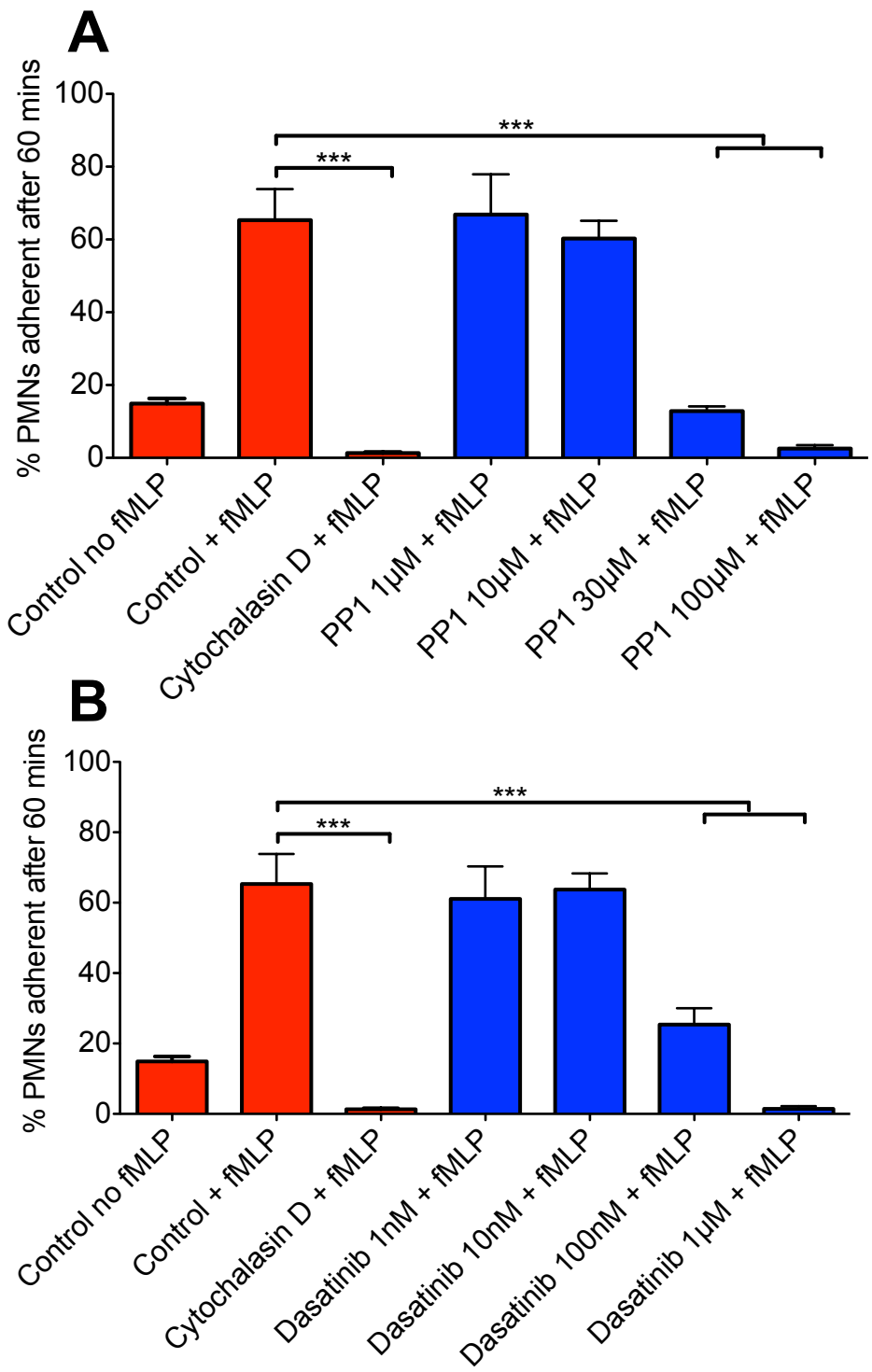

Figure 3-18 PP1 and dasatinib inhibit neutrophil adhesion to tissue culture plastic at higher concentrations

Dose response of PP1 (A) and dasatinib (B) treatment on the ability of neutrophils (from healthy volunteers) in suspension to become adherent to tissue culture plastic when stimulated for 60 min with 50 nM fMLP in the presence of 1% autologous serum. Data show mean and SE values from 3 experiments using samples from 3 independent volunteers. $p<0.001$ by repeated measures ANOVA; ***$p<0.001$ by Dunn's post-hoc test comparing with 'Control + fMLP'.

3.5.5 L-selectin shedding

L-selectin (CD62L) is constitutively expressed at high levels on neutrophil plasma membranes and is one of the first adhesion molecules to interact with inducible ligands on the inflamed endothelium. Once neutrophils become firmly adherent, they become activated to allow transmigration and L-selectin is 'shed' by enzymatic cleavage with a subsequent increase in β_2 integrin expression (Allport et al. 1997).

Downregulation of surface CD62L expression in response to fMLP can be measured simply by flow cytometry.

Results: Figure 3-19 opposite demonstrates that neutrophil stimulation with just 10 nM fMLP reduces CD62L fluorescence to near the level of the isotype control antibody.

Comments: In these experiments the maximum fluorescence in unstimulated neutrophils is surprisingly low (~400 arbitrary units) which may indicate weak binding or brightness of the CD62L APC antibody. Despite this, there is a sufficiently wide fluorescence intensity range to observe an inhibition of L-selectin shedding at 30 μM PP1 but no effect at 10 μM PP1 or 100 nM dasatinib.

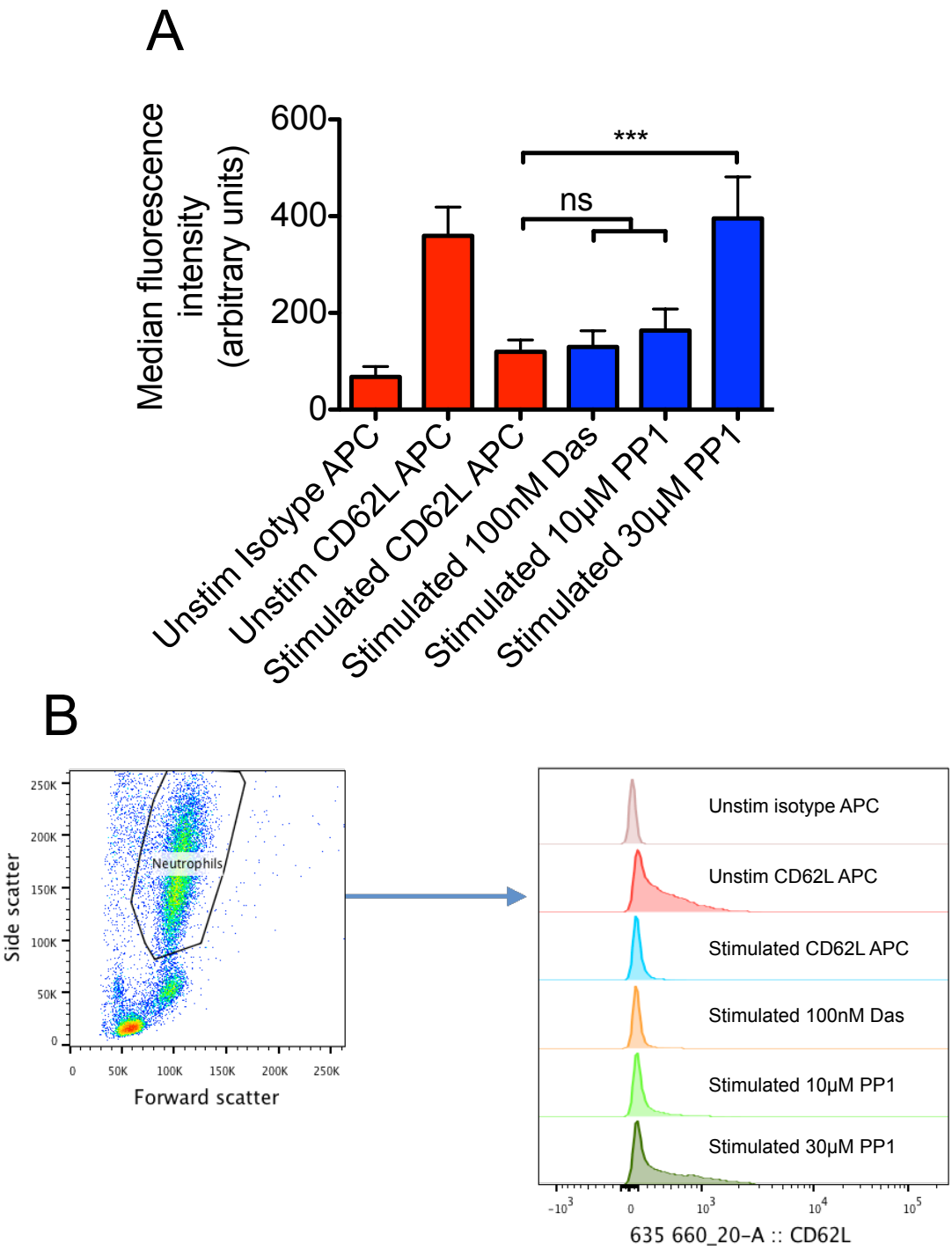

Figure 3-19 PP1, but not dasatinib, inhibits L-selectin shedding from neutrophils in response to fMLP at high concentrations

Heparinised blood samples (from healthy volunteers) were pre-treated with control, 10 μM or 30 μM PP1, or 100 nM dasatinib before staining with anti-human CD62L APC (L-selectin) and stimulating with 10 nM fMLP or control. Data show mean and SD MFI values from 4 experiments using samples from 4 independent volunteers (A) and a representative image showing gating strategy and a fluorescence overlay plot (B). $p<0.0001$ by repeated measures ANOVA; ***$p<0.001$ by Dunn's post-hoc test comparing with 'Stimulated CD62L APC' condition.

3.5.6 Chemotaxis

The next logical investigatory step was to investigate neutrophil transmigration through Transwell pore membranes or through monolayers of endothelial or epithelial cells. I was unable to optimise the experimental technique involving Transwell membranes. However Futosi et al. were able to show that dasatinib does not affect migration through membranes and only chemotaxis and adhesion are inhibited, suggesting that there is redundancy in the role of src kinases and that several other (unidentified) protein tyrosine kinases regulate the complex mechanisms of transmigration (Futosi et al. 2012; Zarbock 2012).

Instead I measured chemotaxis across a glass slide toward the chemoattractant fMLP using the under-agarose technique.

Results: As expected, and consistent with previously published data, src kinase inhibition with both PP1 and dasatinib significantly reduces neutrophil chemotaxis across glass towards the chemoattractant fMLP (Figure 3-20 below).

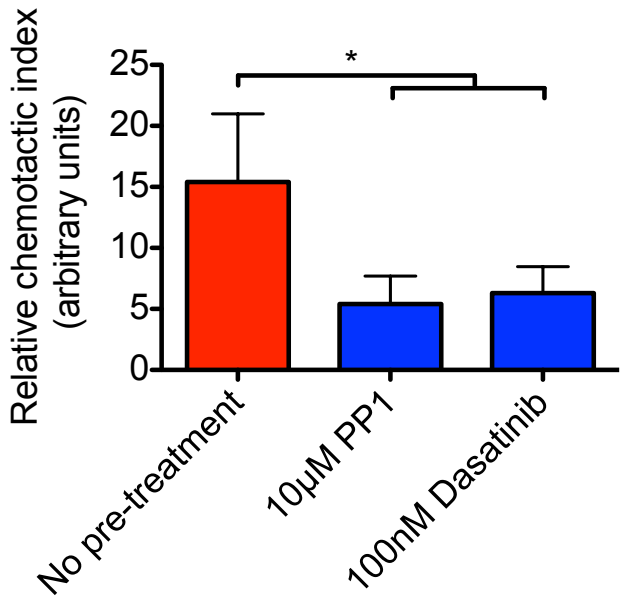

Figure 3-20 Both PP1 and dasatinib inhibit neutrophil chemotaxis towards the chemoattractant fMLP
Neutrophils (from healthy volunteers) were treated with control, 10 μM PP1 or 100 nM dasatinib and their chemotaxis measured along a chemotactic gradient towards a peak concentration of 100 nM fMLP. Data shown are mean and SD values from 3 experiments using duplicate samples from 3 independent volunteers. p=0.0293 by repeated measured ANOVA; *p<0.05 by Dunn's post-hoc test comparing with 'no pre-treatment' control.

3.5.7 Phagocytosis

I examined the effect of PP1 and dasatinib on neutrophil phagocytosis of fluorescent killed pHrodo *S. aureus* and *E. coli* particles in adherent conditions (Figure 3-21 overleaf) and in heparinised blood (Figure 3-22 overleaf). These killed bacteria offer physiologically relevant Gram +ve and Gram –ve phagocytic stimuli and allow a controllable stimulus size. The bacteria are bound to a pHrodo 'pH-sensitive' fluorogenic dye that only becomes fluorescent upon acidification within a phagolysosome, so it is possible to discriminate phagocytosed from adherent or extracellular particles. Other methods I tried involved quenching extracellular fluorescence from alternative fluorescent particles with trypan blue or crystal violet, but the methodology was less reproducible. The pHrodo phagocytosis experiment also depends on a functioning NADPH oxidase system, so it can indirectly give some insight into NADPH oxidase function.

Results: In adherent neutrophils there is a significant effect of PP1 on phagocytosis of both SA and EC particles at all concentrations tested, to the level of the negative control (cytochalasin D) at higher concentrations. Dasatinib concentrations of 100 nM and above also reduce phagocytosis to both stimuli. In heparinised whole blood, modest concentrations of PP1 (10 μM) and dasatinib (100 nM) have absolutely no effect on phagocytosis.

Comments: From earlier degranulation experiments it has already been shown that both drugs are exerting an effect on neutrophils in whole blood at such concentrations. Futosi et al. also found no effect of using up to 1 μM dasatinib on phagocytosis of live green fluorescent protein (GFP)-expressing *S. aureus* by purified neutrophils in suspension but did not assess adherent neutrophils (Futosi et al. 2012).

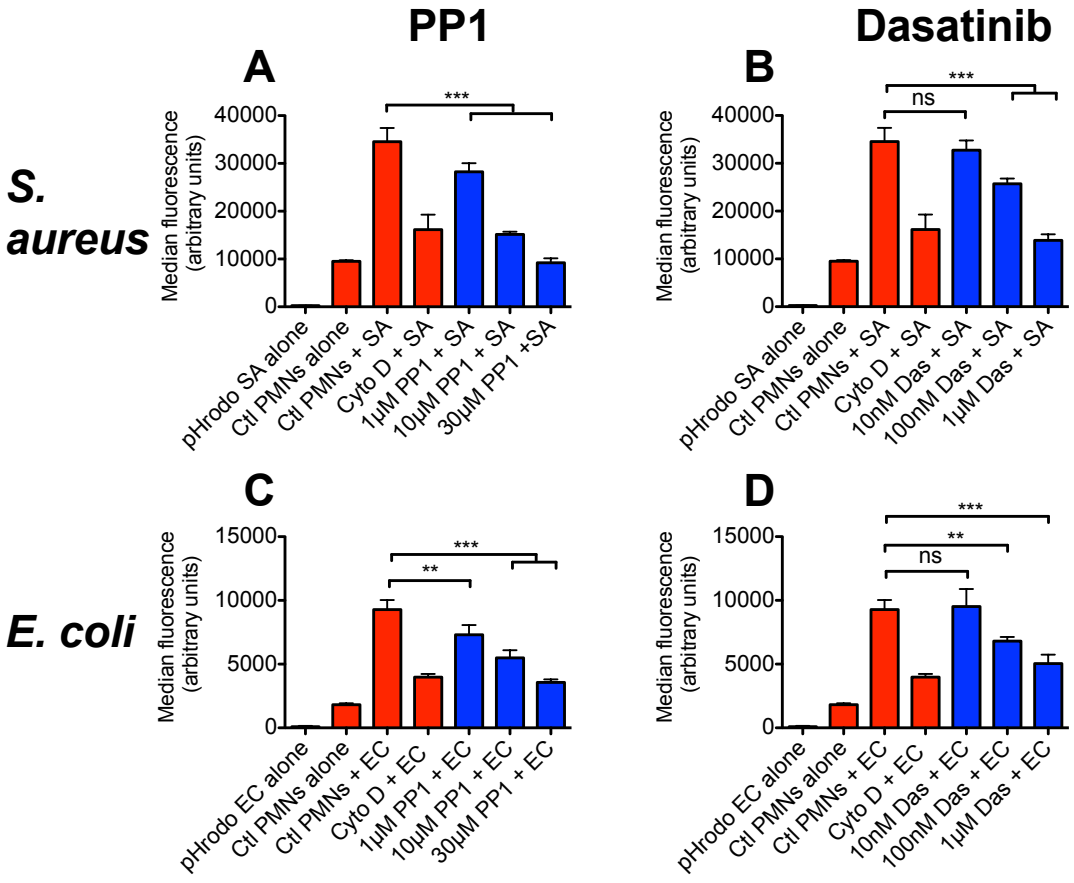

Figure 3-21 PP1 and dasatinib inhibit phagocytosis of pHrodo *S. aureus* and *E. coli* particles by adherent neutrophils
Effect of PP1 (A+C) and dasatinib (B+D) treatment on adherent neutrophils (from healthy volunteers) exposed to pHrodo *S. aureus* (A+B) and *E. coli* (C+D) particles. Data shown are mean and SE MFI values from 4 experiments using triplicate samples from 4 independent volunteers. $p<0.0001$ by repeated measures ANOVA; $^{**}p<0.01$, $^{***}p<0.001$ by Dunns post-hoc test comparing with 'Control PMNs + EC/SA' and excluding cyto D control values.

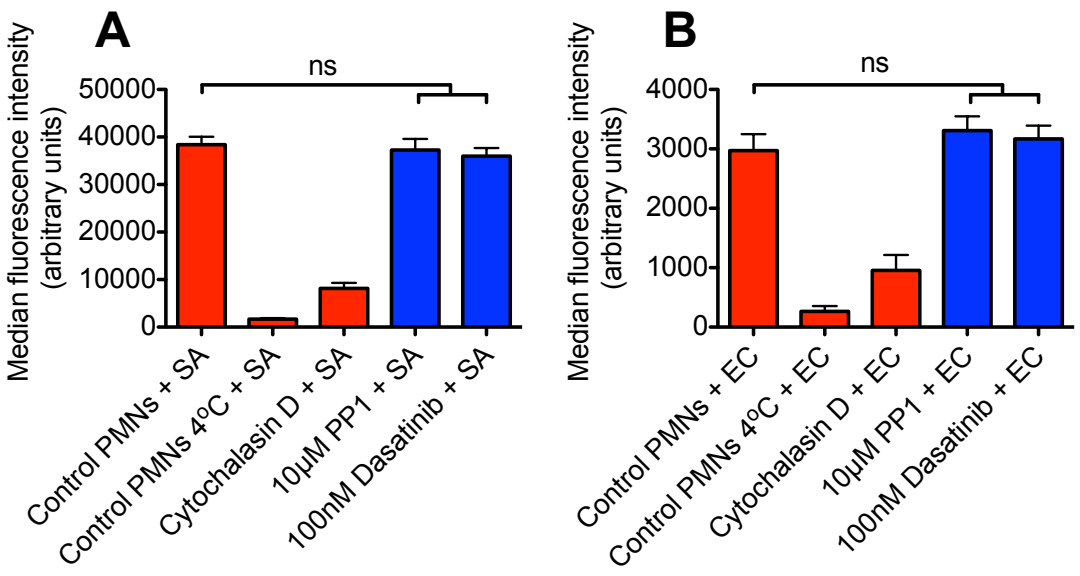

Figure 3-22 PP1 and dasatinib do not affect phagocytosis of pHrodo *S. aureus* and *E. coli* particles by neutrophils in suspension in heparinised blood

Heparinised blood samples (from healthy volunteers) pre-treated with 10 μM PP1 or 100 nM dasatinib were exposed to pHrodo *S. aureus* (A) and *E. coli* (B) particles. Data shown are mean and SE MFI values from 4 experiments using samples from 4 independent volunteers. p=0.0919 (A) and p=0.288 (B) by repeated measures ANOVA comparing with 'Control PMNs + EC/SA' and excluding 4°C and cytochalasin D control values.

3.5.8 Oxidative burst

Results: Figure 3-23A opposite shows that both PP1 and dasatinib inhibit extracellular superoxide release, a marker of oxidative burst, after priming of neutrophils in suspension with PAF and stimulation with fMLP.

We have already seen from the degranulation experiments that the mechanisms of PMA-induced degranulation are independent of src kinases, so the results shown in Figure 3-23B are not unexpected.

Comments: This finding suggests that src kinase inhibition impairs the assembly of NADPH oxidase, an observation also made by Futosi et al, who showed similar results using a lucigenin assay to detect extracellular superoxide release in response to fMLP, anaphylatoxin C5a, LPS and TNFα (Futosi et al. 2012).

Figure 3-23 Both PP1 and dasatinib impair extracellular superoxide release in response to PAF/fMLP but do not affect intracellular ROS production in response to PMA
Extracellular superoxide release from isolated neutrophils (from healthy volunteers) pre-treated with control, 10 μM PP1 or 100 nM dasatinib and stimulated with 100 nM PAF followed by 100 nM fMLP, as measured by the cytochrome C reduction assay (A). Intracellular ROS production by neutrophils in heparinised blood (from healthy volunteers) loaded with 1 μM DHR 123 and pre-treated with control, 10 μM PP1 or 100 nM dasatinib before stimulation with 50 nM PMA, as measured on a FACSCanto II machine by neutrophil fluorescence generated by the oxidation of intracellular DHR 123 to rhodamine 123 (B). Data shown are median and IQR (A) and mean and SD MFI (B) values from 5 (A) and 4 (B) experiments using samples from 5 (A) and 4 (B) independent volunteers. p=0.0023 by Friedman test; *p<0.05 by Dunn's post-hoc test (A) and p=0.336 by repeated measures ANOVA, excluding no PMA and diphenyleneiodonium (DPI) control values (B).

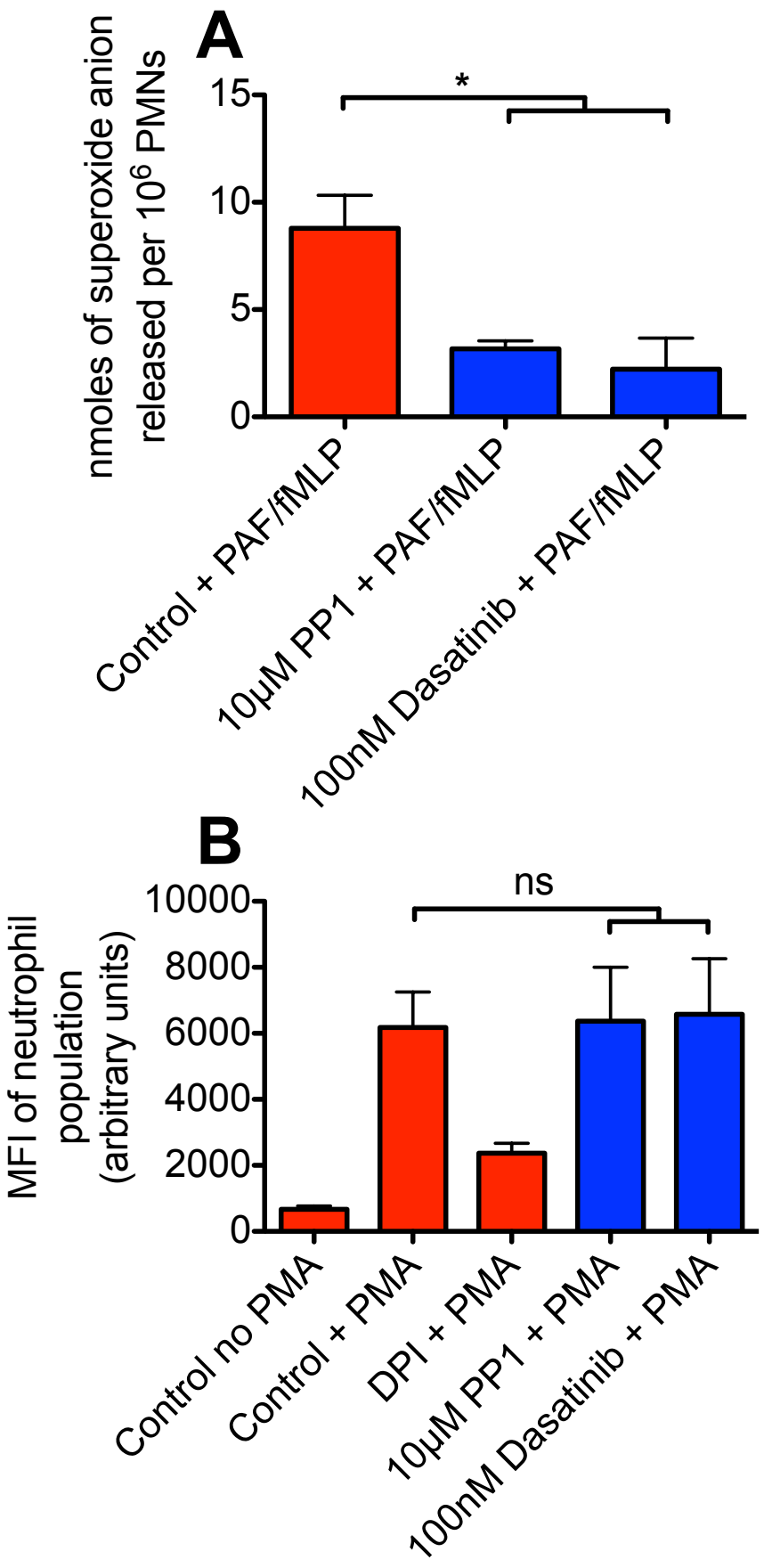
A
nmoles of superoxide anion released per 10^6 PMNs
15
10
5
0
*
Control + PAF/fMLP
10μM PP1 + PAF/fMLP
100nM Dasatinib + PAF/fMLP
B
MFI of neutrophil population (arbitrary units)
10000
8000
6000
4000
2000
0
ns
Control no PMA
Control + PMA
DPI + PMA
10μM PP1 + PMA
100nM Dasatinib + PMA

3.5.9 Live bacterial killing

The final neutrophil function to test in vitro is perhaps the most important: live bacterial killing. I initially started doing the PP1 bacterial killing experiments using PA01 (Figure 3-25 overleaf), but found the organism's growth curve and behaviour in such assays less predictable than those of SA NCTC 8325, and therefore changed to using this pathogen strain for subsequent killing assays (Figure 3-24).

The results graphs below can be difficult to interpret at first glance. Aliquots of the neutrophil/pathogen co-culture are taken at 2 timepoints = 0 min and 30 min, the neutrophils lysed to release all viable intracellular bacteria and the samples diluted appropriately, spread on agar plates and cultured overnight before counting colonies to estimate the initial concentration of viable bacteria in each sample (in cfu/ml). The fold change in the concentration after 30 min therefore measures the net growth or death of the bacterial population during this time period.

Results: Figure 3-24A opposite is a control experiment showing that 1 μM dasatinib does not affect natural *S. aureus* growth and survival in short-term culture. However with the addition of healthy neutrophils at an MOI of ~10 SA:1 PMN, the neutrophils are approximately 'bacteriostatic' and there is neither net growth or death of the bacterial population at 30 min. Interestingly, Figure 3-24B shows that pre-treatment of healthy neutrophils with 10 nM, 100 nM or 1 μM dasatinib has no effect on their killing efficacy in suspension.

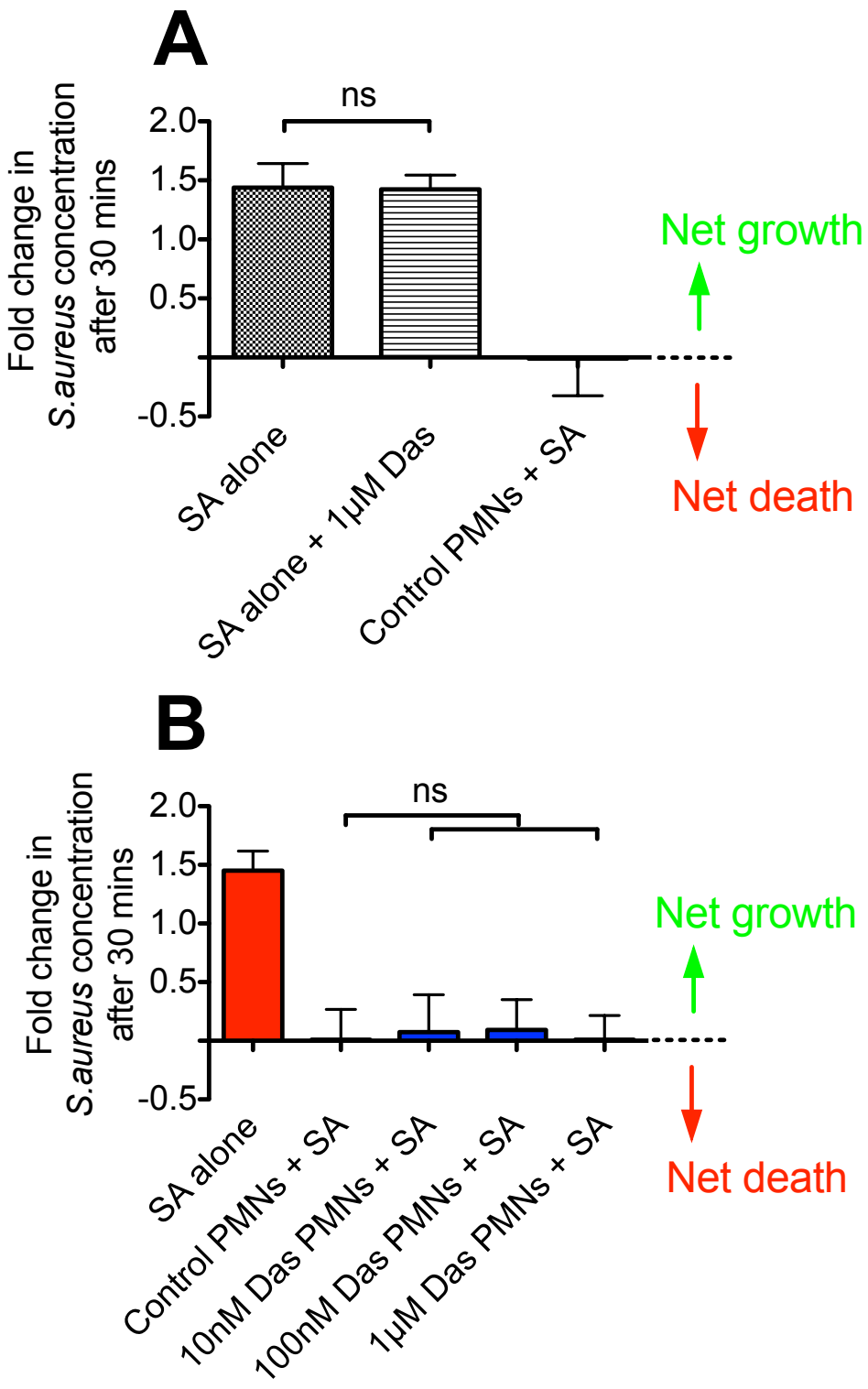

Figure 3-24 Dasatinib does not impair live killing of serum-opsonised *S. aureus* by neutrophils in suspension

Control experiment (A) in which live serum-opsonised *S. aureus* was incubated in medium alone, with 1 μM dasatinib (no neutrophils) or with 10^6 neutrophils (MOI~10 SA: 1 PMN) and net growth after 30 min measured. Dose response of dasatinib treatment on neutrophil killing of live *S. aureus* in suspension (B). Data shown are mean and SE values from 3 (A) and 4 (B) experiments using samples from 3 (A) and 4 (B) independent volunteers. p=0.1 by Mann-Whitney test (A) and p=0.938 by repeated measures ANOVA (B)

Results: The results for PP1 are displayed opposite in Figure 3-25. Again PP1 has no effect on natural growth and survival of PA01 (A) and only significantly impairs bacterial killing in adherent (B) and suspension (C) conditions at very high concentrations (100 μM).

Comments: This effect may well be attributable to excessive neutrophil death due to PP1, as demonstrated earlier in section 3.5.1. It should be noted that these killing assays are unable to distinguish intracellular bacterial killing from extracellular killing by NETs formation. NETs formation is an NADPH-dependent mechanism that takes around 4 h in vitro (Gray et al. 2013) so it is unlikely to be a factor in short 30 min killing assays.

Figure 3-25 PP1 only impairs live killing of serum-opsonised *P. aeruginosa* by neutrophils at a concentration of 100 μM
Control experiment (A) in which live serum-opsonised *P. aeruginosa* was incubated in medium alone, with 30 μM PP1 (no neutrophils) or with 10^6 neutrophils (MOI~10 PA01: 1 PMN) and net growth after 30 min measured. Dose response of PP1 treatment on neutrophil killing of live *P. aeruginosa* in adherent conditions (B) or suspension conditions (C). Data shown are mean and SD values from 3 (A) and 6 (B+C) experiments using samples from 3 (A) and 6 (B+C) independent volunteers. p=0.1 by Mann-Whitney test (A) and p<0.0001 by repeated measures ANOVA; ***p<0.001 by Dunn's post-hoc test comparing with 'Control PMNs + PA01' and excluding PA01 control condition (B+C).

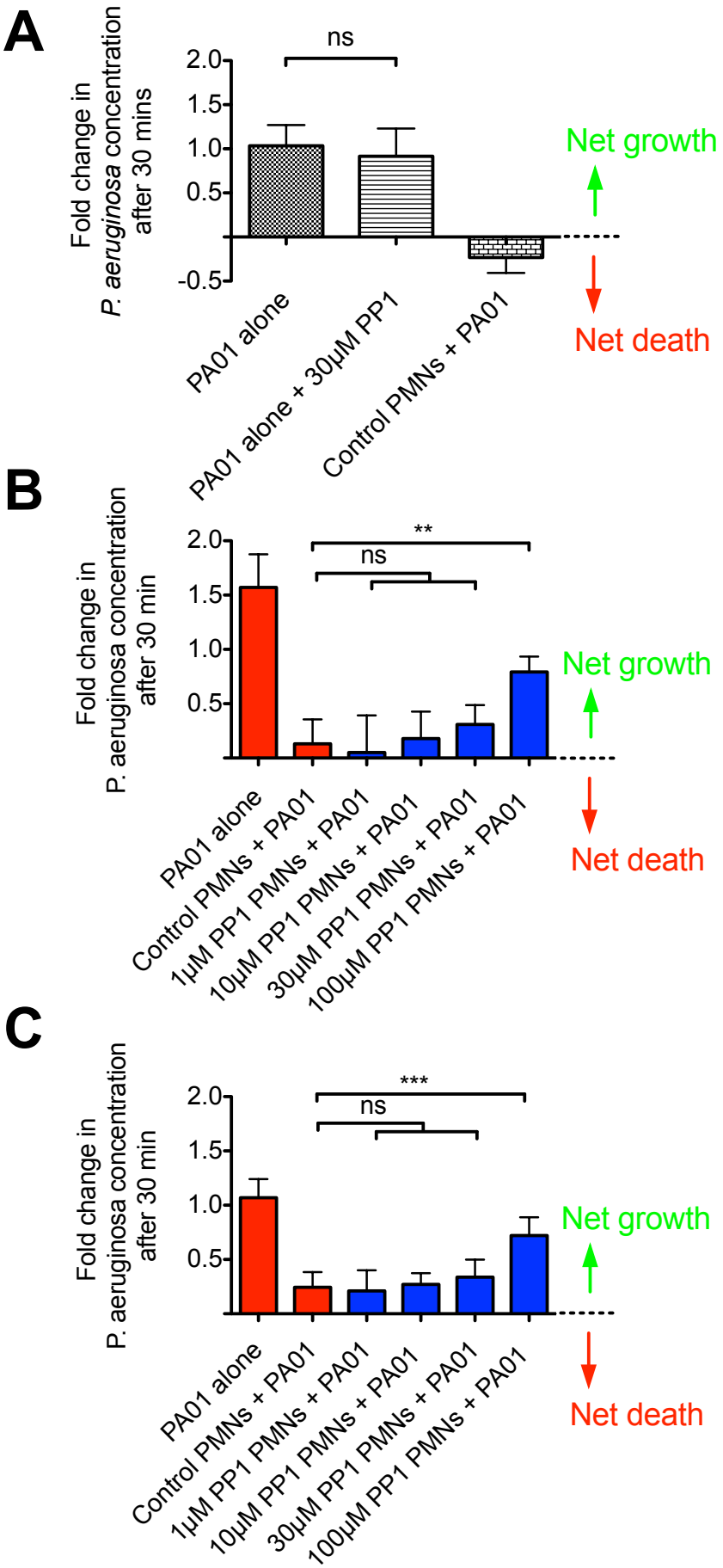
A
Fold change in
P. aeruginosa concentration
after 30 mins
ns
2.0
1.5
1.0
0.5
-0.5
Net growth
Net death
PA01 alone
PA01 alone + 30μM PP1
Control PMNs + PA01
B
Fold change in
P. aeruginosa concentration
after 30 min
**
ns
2.0
1.5
1.0
0.5
Net growth
Net death
PA01 alone
Control PMNs + PA01
1μM PP1 PMNs + PA01
10μM PP1 PMNs + PA01
30μM PP1 PMNs + PA01
100μM PP1 PMNs + PA01
C
Fold change in
P. aeruginosa concentration
after 30 min
***
ns
2.0
1.5
1.0
0.5
Net growth
Net death
PA01 alone
Control PMNs + PA01
1μM PP1 PMNs + PA01
10μM PP1 PMNs + PA01
30μM PP1 PMNs + PA01
100μM PP1 PMNs + PA01

3.5.10 Clinical relevance of findings

Taken together, my in vitro findings imply that careful src kinase inhibition of neutrophils with drugs such as PP1 or dasatinib, can theoretically reduce neutrophil recruitment to sites of lung inflammation, whilst attenuating the degree of extracellular degranulation from recruited cells and maintaining effective bacterial killing.

Patients with chronic myeloid leukaemia (CML) taking dasatinib have an increased risk of developing mild to moderate infections (EMEA 2015) but consistent with our data, Futosi et al. found that there was only a modest decrease to 75% control killing values using concentrations as high as 1 μM dasatinib with a negligible effect at 100 nM (Futosi et al. 2012).

Interestingly, the most common daily dose of dasatinib in patients with CML is 100 mg/day. In pharmacokinetic studies, a 70 mg/day dose resulted in a maximum serum dasatinib concentration of 50-100 ng/ml, equating to approximately 100-200 nM (Demetri et al. 2009).

These findings suggest that any increased infection frequency in patients taking dasatinib is unlikely to be due to impaired bacterial killing by neutrophils but may be due to impaired recruitment to sites of infection.

3.6 Summary of Key Findings

These data confirm previously published findings regarding the potent effect of src kinase inhibition on neutrophil function in in vitro models of acute inflammation as well as providing many further insights into its effect in more clinically relevant models of infection involving live and killed bacteria, as well as the action of the clinically licensed src kinase inhibitor, dasatinib.

My key findings are summarised as follows:

1. Src kinase inhibition of healthy human neutrophils with concentrations of PP1 in excess of 10μM reliably inhibits in vitro neutrophil degranulation stimulated by:
   - G-protein coupled formyl peptide receptor activation
   - Toll-like receptor-4 ligation by LPS
   - Contact with live serum-opsonised PA01 and *S. aureus,*

   but not by PKC-mediated PMA activation.

2. At lower concentrations of PP1 (10 μM) that are capable of inhibiting degranulation, only certain key neutrophil functions of chemotaxis, adherent phagocytosis and extracellular superoxide anion release are impaired. At moderately high concentrations (30 μM), further functions are affected, including a minor but significant effect on cell viability (but not apoptosis), cell adhesion and L-selectin shedding. Only at very high concentrations of PP1 (100 μM) is effective killing of PA01 affected in both adherent and suspension conditions, in part due to its cytotoxic effect at this concentration.

3. Taking the findings in 1 and 2 above together, one can speculate that there is an optimum concentration range of src kinase inhibition with PP1 (estimated between 10 μM and 30 μM) at which extracellular degranulation to sterile and non-sterile stimuli is impaired without a significant effect on efficient bacterial killing or cell viability. This concept has exciting implications for potential anti-inflammatory treatment strategies in conditions such as ARDS where maintaining an effective innate immune response to primary or secondary lung infection is crucial.

4. These findings can be replicated using a less specific, but clinically licensed, src/Abl kinase inhibitor, dasatinib. Consistent with previously published data (Futosi et al. 2012), 100 nM dasatinib, which equates to plasma concentrations found when taking a daily oral dose of less than 70mg, inhibits degranulation from healthy neutrophils stimulated by fMLP and LPS but not PMA. My data extend these observations to degranulation assays involving stimulation with live *Staphylococcus aureus.* 100 nM dasatinib also impairs only adhesion, chemotaxis, extracellular superoxide release and adherent phagocytosis with no effect on viability, apoptosis, L-selectin shedding and bacterial killing of *S. aureus.*

My original hypothesis:

"*In vitro src *kinase inhibition of human neutrophils reduces extracellular degranulation in response to both chemical and live bacterial stimuli, without impairing efficient neutrophil phagocytosis and intracellular killing of bacteria"

has therefore been satisfied in all aspects except that src inhibition affects phagocytosis by adherent neutrophils with no effect on purified neutrophils in suspension or in whole blood.

These data were sufficiently robust to proceed to test my second hypothesis in in vivo models of sterile and non-sterile acute lung inflammation, which I will describe in chapter 4.

Chapter 4. An Investigation into the Effect of the Src Kinase Inhibitor Dasatinib on In Vivo Models of Bacteria and Acid-Induced Acute Lung Inflammation

4.1 Chapter Overview

This chapter describes the experiments I carried out to test the following hypothesis:

"Inhibition of the* src *kinase pathway attenuates neutrophil recruitment to the alveolar and interstitial spaces, neutrophil degranulation and endothelial cell injury and leak in in vivo models of bacteria and acid-induced acute lung inflammation"

In Chapter 3, dasatinib was identified as a safe and effective in vitro src kinase inhibitor of human neutrophils. In mice, the drug has been shown to exert an inhibitory effect on ex vivo leukocyte adhesion to foetal calf serum-coated plates in response to TNFα at doses of 5 mg/kg and above when administered orally (Futosi et al. 2012). Each experiment that follows compares a group of mice treated with i.p. dasatinib (at various concentrations) with a control group of mice treated with control vehicle alone (DMSO). The paired 'dasatinib' and 'control' groups were both stimulated in separate experiments by direct intratracheal administration of either i) live *E. coli* (Section 4.2) or ii) pH 2.0 hydrochloric acid (Section 4.3). Specific details of experimental methods used can be referred to in Chapter 2 on page 31.

4.2 Effect of Dasatinib on an In Vivo Murine Model of *E. coli*-induced Acute Lung Inflammation

E. coli was used as the bacterial stimulus for these experiments because it represents a thoroughly studied gram negative pathogen with a rapid and predictable growth rate, able to survive in many growth conditions. It is also a commonly isolated pathogen in sepsis, ventilator-associated pneumonia and ARDS. Professor Rossi's group, with whom I collaborated on these experiments, had optimised the methods using this pathogen.

As discussed in Chapter 2 (Materials and Methods), experiments plotting the time course of neutrophil influx into the alveolar and interstitial space in response to i.t. *E. coli* demonstrated an initial 6 h peak influx (alveolar) followed by a 12 h peak (interstitial) with a second wave of alveolar neutrophils (and persistently high interstitial neutrophils) at 24 h.

Pharmacokinetic data obtained in rats show that peak plasma concentrations of dasatinib are achieved within 1 hour of i.p. administration at both 1 mg/kg and 10 mg/kg with the serum concentrations falling to 50% of the peak concentration by 10 h (Seferian et al. 2013). These experiments also measured peak plasma concentrations of 100 ng/ml (~200 nM) and 1 μg/ml (~2 μM) using doses of 1 mg/kg and 10 mg/kg respectively, similar to the dose range used in my in vitro experiments.

Using these figures, we decided to treat the mice twice with up to 10 mg/kg i.p. dasatinib or control at 0h and 12 h to correspond to neutrophil influx into alveolar and interstitial spaces at these timepoints and cull the mice at 24 h. Based on the results of the intial 10 mg/kg experiment, the experiment was repeated using a lower dose of 1 mg/kg. The results are presented together but the experiments were carried out on separate occasions using different batches of mice. In all experiments between 8 and 10 mice were used per group. This group size was calculated from previous experiments by Drs Dorward and Lucas as the minimum number of mice required to observe a significant difference between control and treated groups, assuming a normally distributed spread of data within each group.

4.2.1 Cellular influx to alveolar space: control experiments

Important control experiments shown in Figure 4-1 and Figure 4-2 overleaf were initially carried out to confirm that i.p. treatment with 1 mg/kg and 10 mg/kg dasatinib itself (using the dual dosing strategy at 0 h and 12 h) does not itself cause a meaningful cellular influx into the alveolar space in mice untreated with i.t. *E. coli*.

Comments: As expected, lavages from unstimulated mice are relatively acellular, containing predominantly alveolar macrophages alone in very small total numbers. This can be appreciated by comparing the graph scale used in Figure 4-2 (approximately 20 cells/μL of BALF) with the scale used in Figure 4-3A (over 400 cells/μL fluid in stimulated mice).

Figure 4-1 shows the expected BALF cytospin appearance of control mice exposed to *E. coli* (neutrophilic influx with some capillary haemorrhage into the alveolar space). Interestingly, treatment with 10 mg/kg dasatinib appears to result in more haemorrhage (than 1 mg/kg or control). This was readily apparent from the macroscopic appearance of the fluid, but was not formally quantified.

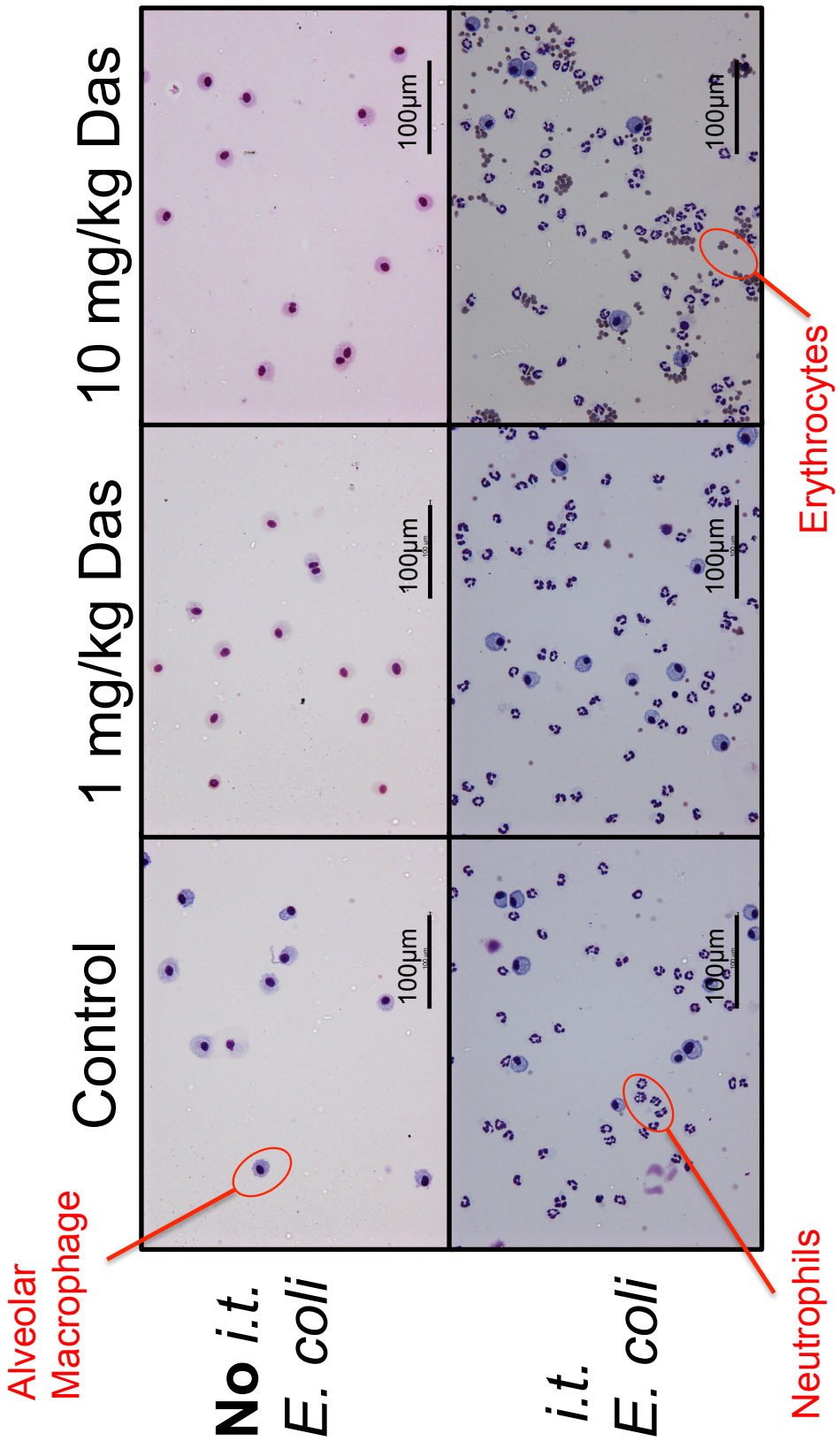

Figure 4-1 Neutrophilic influx into the alveolar space accompanies i.t. *E. coli* delivery in mice
Representative x200 images of cytocentrifuge preparations of BALF retrieved from mice treated with i.p. control vehicle, 1 mg/kg dasatinib or 10 mg/kg dasatinib and exposed to either i.t. *E. coli* or no stimulus. Images taken from 1 experiment using 1 mouse per condition (top row) and 2 experiments using >8 mice per condition (bottom row)

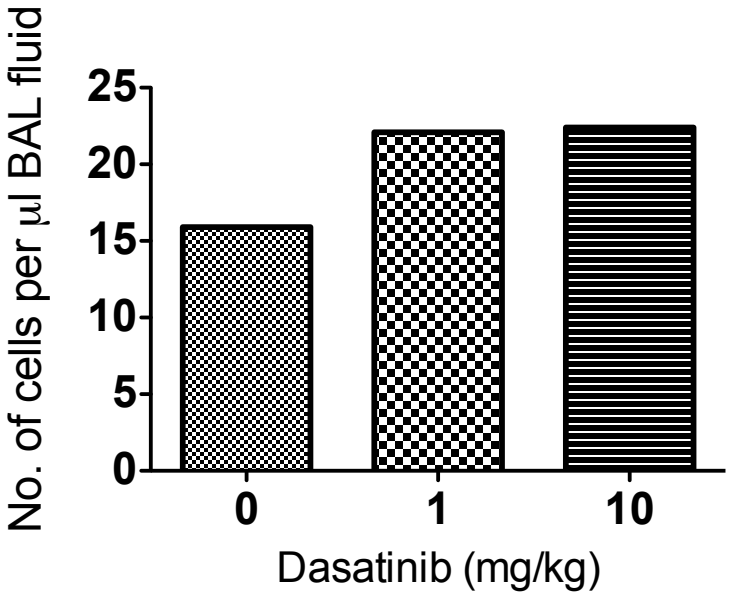

Figure 4-2 Dasatinib itself does not induce a significant cellular influx into the alveolar space of control mice

Dose response control experiment to demonstrate no meaningful effect of i.p. dasatinib treatment on cellular influx in control mice unexposed to i.t. *E. coli,* n=1 mouse per condition. Results obtained using NucleoCounter© machine method.

4.2.2 Cellular influx to alveolar space: effect of dasatinib

Results: Figure 4-3 opposite shows that treatment with both 1 mg/kg and 10 mg/kg dasatinib does not attenuate cellular influx into the alveolar space in response to *E. coli*. Specifically both the total number of neutrophils and the percentage neutrophil content of the BALF is not affected.

Comments: This result is unexpected given the clear effect of dasatinib on neutrophil adhesion and integrin-mediated activation in vitro.

Reassuringly, the inter-experiment control group variability is relatively good in these assays (indicated by the red dotted significance bars), with only a slight difference in % neutrophils in BALF as assessed by flow cytometry (Figure 4-3C).

The Figure 4-3A values were obtained very shortly after sample retrieval using the Nucleocounter method and the Figure 4-3B values the following day using flow cytometry. This may explain any apparent discrepancies in estimated total cell and total neutrophil numbers in the same samples. The same can be said for any discrepancies between % neutrophil values obtained using flow cytometry or cell morphology on cytospin. In the case of any major discrepancy, results obtained by cell morphology are favoured.

Figure 4-3 Dasatinib treatment does not affect cellular influx into the alveolar space in response to *E. coli*
Effect of i.p. treatment with 1 mg/kg dasatinib (left panel) and 10 mg/kg dasatinib (right panel) on the total number of cells (A), the total number of neutrophils (B) and the % neutrophils (C+D) in BAL samples from mice exposed to i.t. *E. coli*. Results obtained using NucleoCounter© machine method (A), flow cytometry (B+C) and cell morphology on cytospin staining (D). Data show mean and SD values from 2 experiments using samples from 8 mice per group; the 1 mg/kg+control and 10 mg/kg+control values are separate experiments. Control vs dasatinib: p=0.221 (1 mg/kg), p=0.931 (10 mg/kg) (A); p=0.398, p=0.450 (B); p=0.457, p=0.056 (C); p=0.274, p=0.497 (D). Inter-experiment control group difference: p=0.661 (A), 0.548 (B), **p=0.0028 (C) and p=0.967 (D) by unpaired t-test.

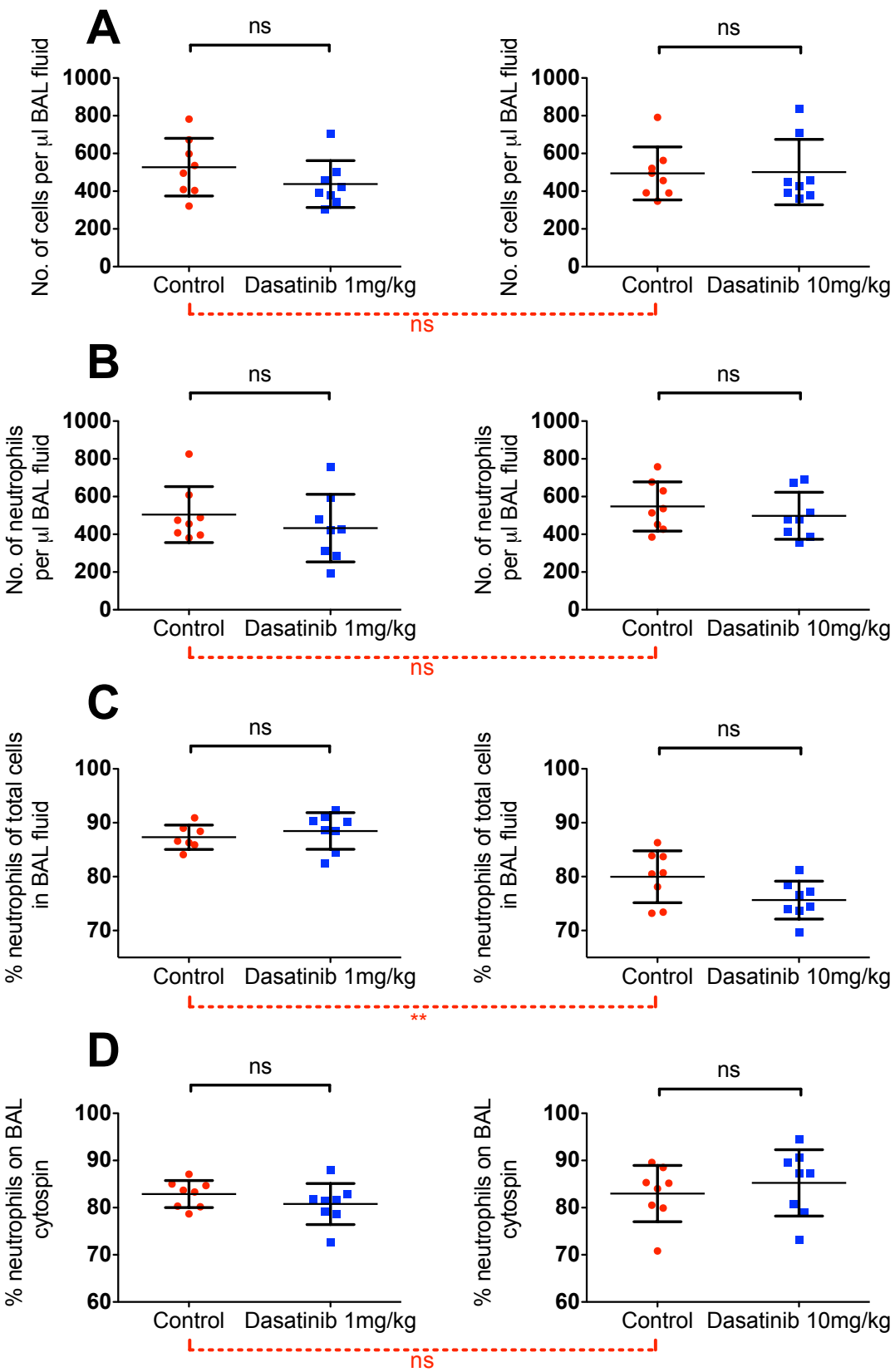
A
ns
No. of cells per µl BAL fluid
1000
800
600
400
200
0
Control
Dasatinib 1mg/kg
ns
Dasatinib 10mg/kg
ns
B
No. of neutrophils per µl BAL fluid
C
% neutrophils of total cells in BAL fluid
100
90
80
70
**
D
% neutrophils on BAL cytospin
60

4.2.3 Cellular influx to lung interstitium

This method of measuring neutrophil influx into the lung interstitium estimates the number of activated neutrophils migrating through activated endothelium into the interstitial space. The lung samples are taken after BAL and right ventricular/pulmonary artery flushing and therefore the counts obtained should exclude cells present in these other inflamed spaces. It is known that murine lungs harbour a considerable number of marginated neutrophils in the vascular and interstitial compartments of the lung in the stable state and that these can mobilise into the alveolar space in response to inflammation (Barletta et al. 2012).

Results: Figure 4-4A opposite shows that treatment with 10 mg/kg dasatinib induces a neutrophilia in peripheral blood in response to *E. coli* challenge, presumably due to bone marrow release.

At the lower dose of 1 mg/kg, there is a small significant drop of approximately 5% in the percentage of neutrophils present in the lung interstitium, with no change in the total number of neutrophils present. It is unknown which other types of cell undergo a corresponding increase, by inference. There is possibly an associated trend to an effect on the equivalent percentage of neutrophils in the alveolar space in Figure 4-3D above.

Comments: A neutrophil percentage of 10-20% of total leukocytes, although appearing low compared to human blood (where the figure is much higher at 50-70%), is in keeping with expected values in C57/Black 6 mice, in which lymphocytes comprise 75-90% of the total leukocytes (Doeing et al. 2003).

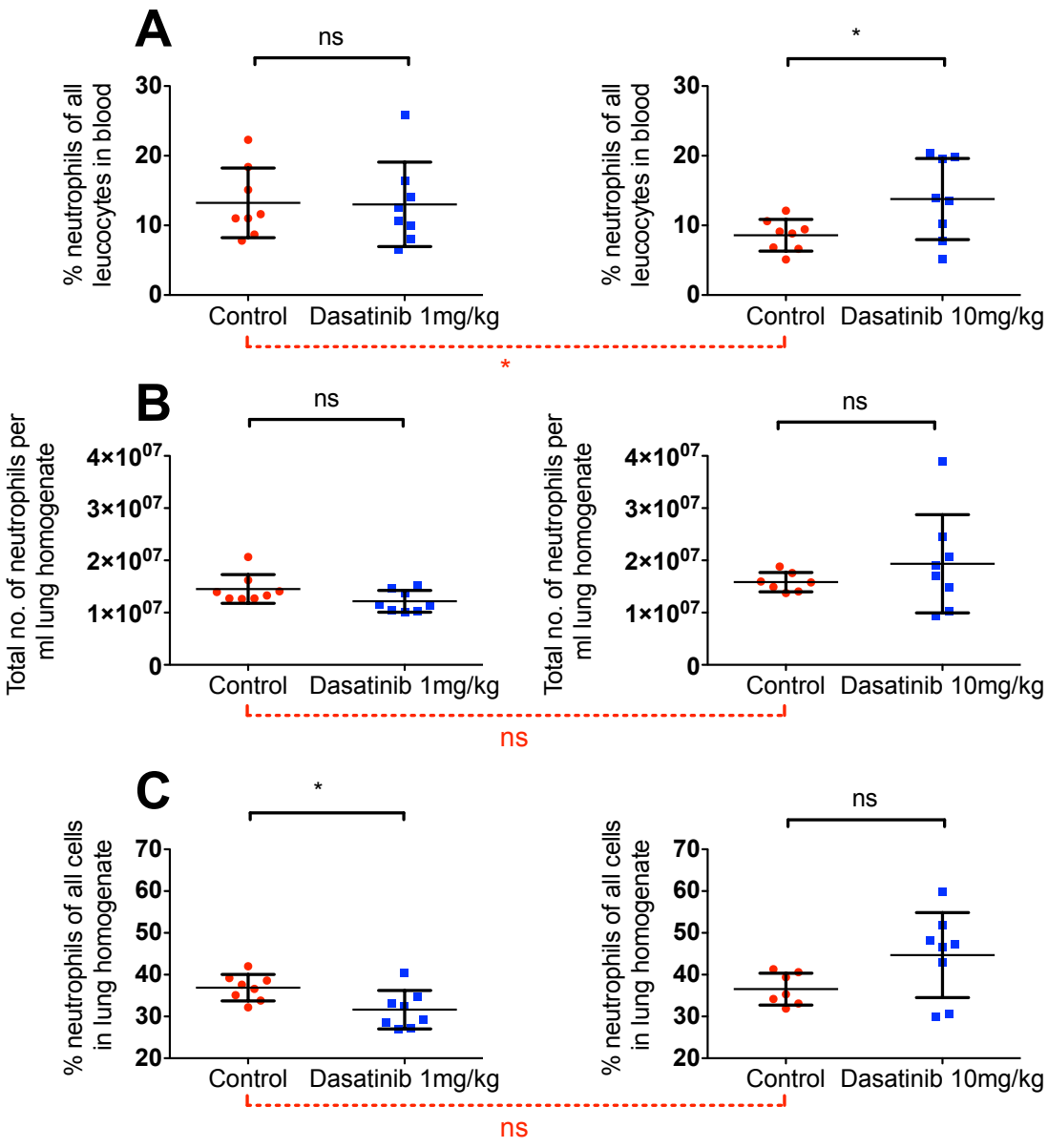

Figure 4-4 Treatment with 1 mg/kg Dasatinib reduces neutrophil influx into the lung interstitium in response to i.t. *E. coli*

Effect of i.p. treatment with 1 mg/kg dasatinib (left panel) and 10 mg/kg dasatinib (right panel) on the % neutrophils of all leukocytes in peripheral blood (A), the total number of neutrophils in lung homogenate (B) and the % neutrophils of all cells in lung homogenate (C) samples from mice exposed to i.t. *E. coli*. Data show mean and SD values from 2 experiments using samples from 8 mice per group; the 1 mg/kg+control and 10 mg/kg+control values are separate experiments. Control vs dasatinib: p=0.939 (1 mg/kg), *p=0.034 (10 mg/kg) (A); p=0.074, p=0.351 (B); *p=0.018, p=0.068 (C). Inter-experiment control group difference: *p=0.0313 (A), 0.305 (B), p=0.851 (C) by unpaired t-test.

4.2.4 Evidence of neutrophil degranulation

Although dasatinib does not appear to significantly affect the neutrophil influx into the interstitial space, does it affect the degree of degranulation of primary and secondary granules as assessed by surface CD63 expression (primary granule release) and CD11b expression (surrogate for secondary granule release) on Ly6+ lung homogenate cells (Ly6 is specific for murine neutrophils)?

Results: As shown in Figure 4-5 opposite, dasatinib does not have any effect on degranulation of Ly6+ neutrophils in the interstitial space at both 1 mg/kg and 10 mg/kg doses. Baseline control values, although significantly different between the two experiments, show a degranulation response to *E. coli* exposure compared to unexposed mice (data not shown).

Comments: Of note, levels of CD63 expression (Figure 4-5B) are consistently low throughout all experiments, possibly reflecting either poor antibody-receptor affinity or weakly fluorescent PE.

It is possible that the homogenisation process itself affects surface receptor expression. Neither proteases nor protease inhibitors were used in the process except collagenase and those released by the tissue itself. Theoretically these may exert an autocrine effect on receptor expression.

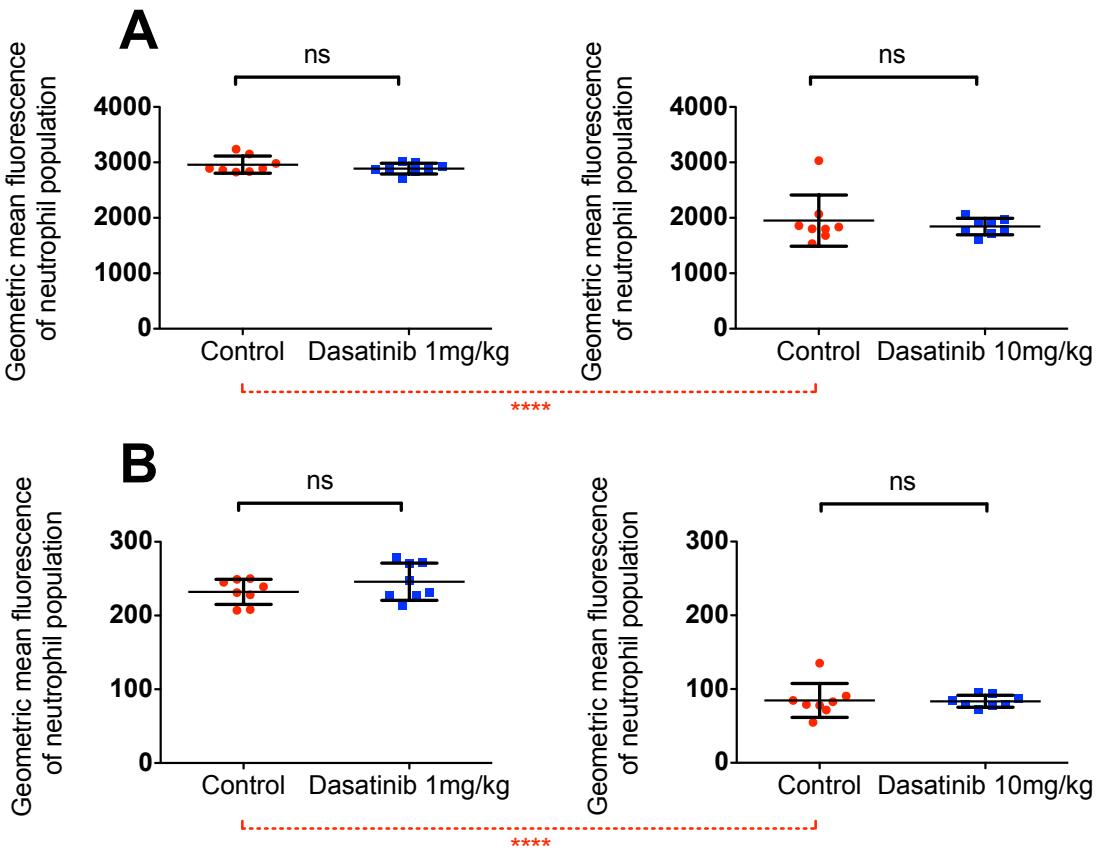

Figure 4-5 Dasatinib treatment does not affect neutrophil degranulation in the lung interstitium

Effect of i.p. treatment with 1 mg/kg dasatinib (left panel) and 10 mg/kg dasatinib (right panel) on neutrophil expression of CD11b (A) and CD63 (B) in lung homogenate samples from mice exposed to i.t. *E. coli*. Data show mean and SD values from 2 experiments using samples from 8 mice per group; the 1 mg/kg+control and 10 mg/kg+control values are separate experiments. Control vs dasatinib: p=0.289 (1 mg/kg), p=0.542 (10 mg/kg) (A); p=0.228, p=0.900 (B). Inter-experiment control group difference: ****p<0.0001 (A), ****p<0.0001 (B) by unpaired t-test.

Similarly, does dasatinib affect the degree of degranulation of neutrophils entering the alveolar space?

Results: When measured by CD63 and CD11b expression, it appears not, as is shown below in Figure 4-6. There is a modest increase in CD63 expression in mice treated with 10 mg/kg dasatinib, though it is difficult to know how to interpret this, when the control group fluorescence values are so low and there is apparent inter-experiment control group variability.

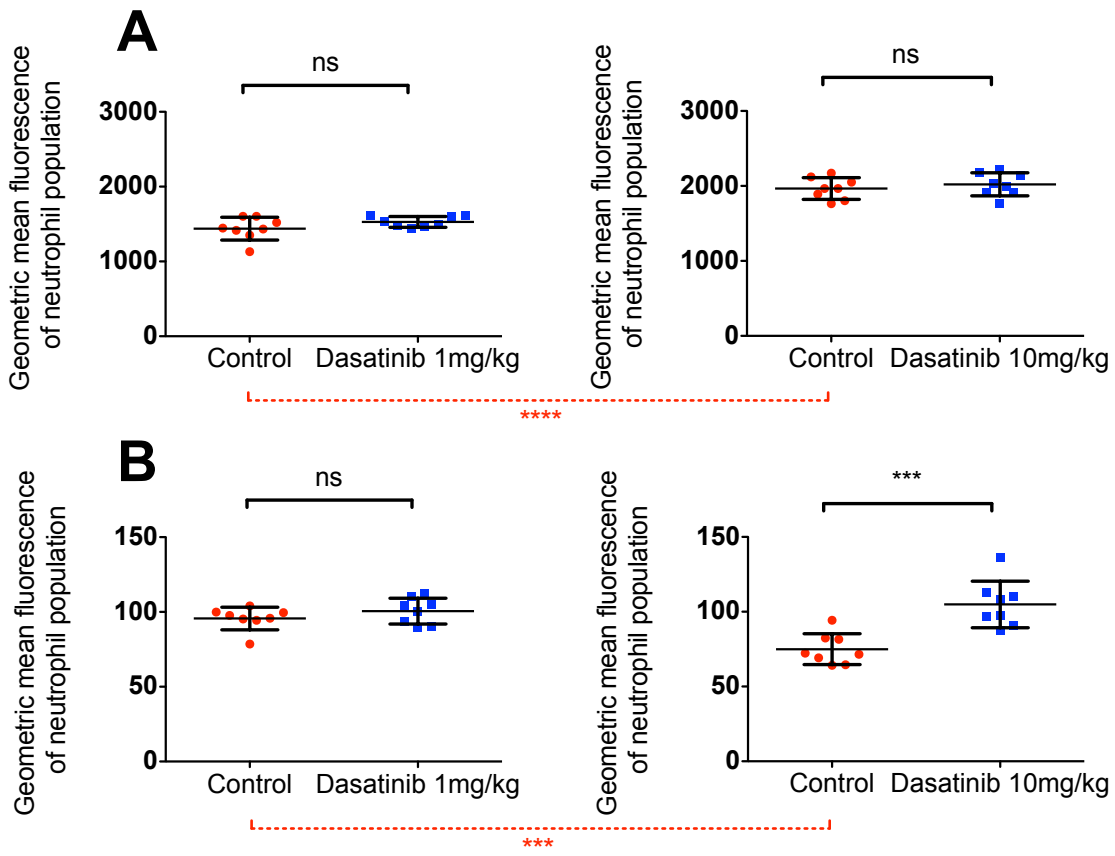

Figure 4-6 Treatment with 10 mg/kg, but not 1 mg/kg of Dasatinib, increases neutrophil degranulation in the alveolar space
Effect of i.p. treatment with 1 mg/kg dasatinib (left panel) and 10 mg/kg dasatinib (right panel) on neutrophil expression of CD11b (A) and CD63 (B) in BAL samples from mice exposed to i.t. *E. coli*. Data show mean and SD values from 2 experiments using samples from 8 mice per group; the 1 mg/kg+control and 10 mg/kg+control values are separate experiments. Control vs dasatinib: p=0.152 (1 mg/kg), p=0.473 (10 mg/kg) (A); p=0.242, ***p=0.0005 (B). Inter-experiment control group difference: ****p<0.0001 (A), ***p=0.0004 (B) by unpaired t-test.

Although there is no observed effect of dasatinib on degranulation, as measured by flow cytometry, we also determined levels of degranulation by measuring MPO activity (Figure 4-8A overleaf), MPO concentration (Figure 4-8B overleaf) and LTF concentration (Figure 4-7 below) in cell-free alveolar fluid, but not in the interstitial space. As it is an assumption that all MPO antigen detected by ELISA is associated with a functional enzyme and that methods of measuring MPO activity are inconsistent and dependent on sample acquisition techniques (Pulli et al. 2013), we also calculated a separate measurement of MPO activity per unit of MPO enzyme, expressed in arbitrary units (BAL MPO concentration ÷ OD_{450} value) as shown in Figure 4-8C overleaf.

Results: The results below show that at 1 mg/kg, dasatinib significantly reduces BALF MPO concentration but has no effect on MPO activity or LTF concentration. At 10 mg/kg, BALF MPO activity is markedly higher with no apparent corresponding difference in enzyme concentration. BALF LTF concentration is significantly reduced compared to control values, but these results should be interpreted with caution as the 10 mg/kg control group values are significantly higher than the 1 mg/kg control group values and may account for this apparent difference.

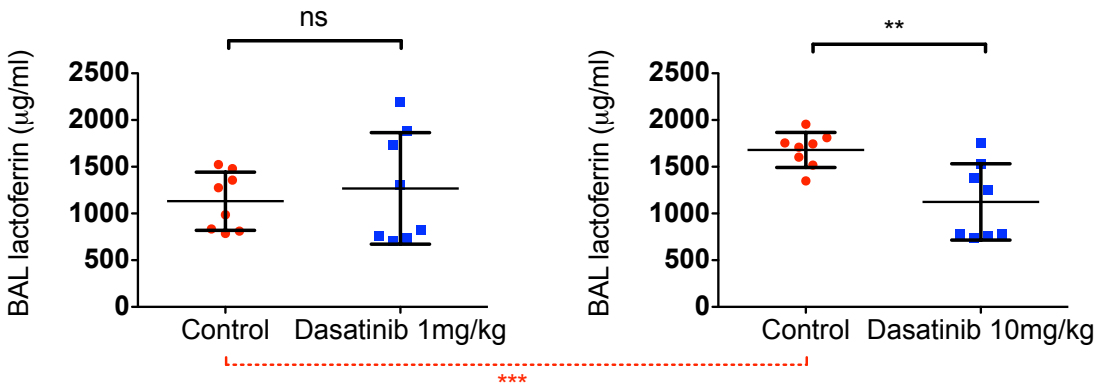

Figure 4-7 Treatment with 10 mg/kg Dasatinib reduces lactoferrin concentration in the alveolar space
Effect of i.p. treatment with 1 mg/kg dasatinib (left panel) and 10 mg/kg dasatinib (right panel) on the LTF concentration in BAL samples from mice exposed to i.t. *E. coli*. Data show mean and SD values from 2 experiments using samples from 8 mice per group; the 1 mg/kg+control and 10 mg/kg+control values are separate experiments. Control vs dasatinib: p=0.576 (1 mg/kg), **p=0.003 (10 mg/kg). Inter-experiment control group difference: ***p=0.0008 by unpaired t-test.

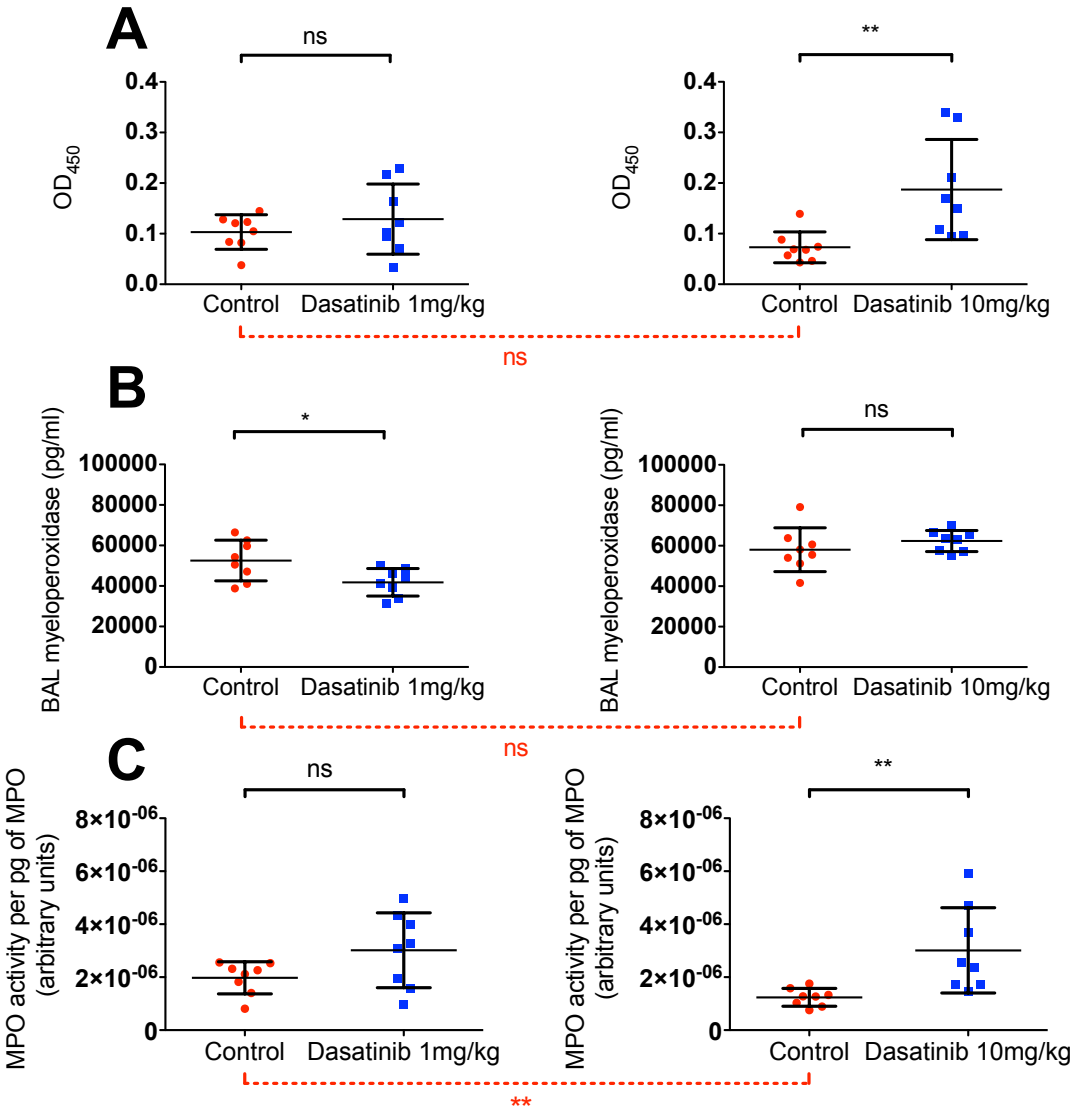

Figure 4-8 Treatment with 1 mg/kg Dasatinib reduces MPO concentration with no effect on enzyme activity, but 10 mg/kg dasatinib increases MPO activity, in the alveolar space

Effect of i.p. treatment with 1 mg/kg dasatinib (left panel) and 10 mg/kg dasatinib (right panel) on total MPO activity (A), MPO concentration (B) and effective MPO activity per unit of MPO enzyme (C) in BAL samples from mice exposed to i.t. *E. coli*. Data show mean and SD values from 2 experiments using samples from 8 mice per group; the 1 mg/kg+control and 10 mg/kg+control values are separate experiments. Control vs dasatinib: p=0.364 (1 mg/kg), **p=0.008 (10 mg/kg) (A); *p=0.025, p=0.338 (B); p=0.076, **p=009 (C). Inter-experiment control group difference: p=0.0825 (A), p=0.314 (B) and **p=0.0093 (C) by unpaired t-test.

4.2.5 Bacterial survival

The effect of dasatinib on bacterial survival is perhaps of most practical interest and will help to put some of the degranulation results above in context.

Results: Looking at the results displayed overleaf in Figure 4-9, it is immediately clear that treatment with 10 mg/kg results in increased bacterial survival and spread. Not only are the bacteria not cleared from the alveolar space, but the total concentration of bacteria in the interstitial space is considerably increased compared to control, by a factor of 100. Bacteria are also seen in the liver and spleen of some mice, suggesting haematogenous or lymphatic spread.

At the lower dose of 1 mg/kg there is no apparent spread outside of the lungs and the alveolar space remains virtually sterile, but there is a marginal but significant increase in bacteria surviving within the lung interstitium by a factor of approximately 2.

Comments: Interpreting these data, it is clear that dasatinib impairs bacterial clearance after i.t. *E. coli* exposure and this effect is dose-dependent. It is highly unlikely that dasatinib itself promotes bacterial growth, as demonstrated by in vitro experiments in Chapter 3. At higher doses of dasatinib, the delicate balance between bacterial replication, invasion and spread on one hand, and bacterial killing by the innate immune system on the other hand, favours the bacteria, allowing relatively unrestrained exponential bacterial growth.

I would hypothesise that this dynamic process subsequently presents a significantly larger inflammatory stimulus to the immune system, leading to accelerated inflammation and tissue damage. This theory may well explain some of the results presented above, including the increased BALF MPO activity, alveolar neutrophil CD63 expression, increased peripheral blood neutrophilia and increased alveolar haemorrhage in mice treated with 10 mg/kg dasatinib.

In this in vivo model, dasatinib is administered systemically and is therefore likely to be acting to varying degrees on every murine cell, as src kinases are known to be ubiquitously expressed in all mammalian cells. Granulocytes constitutively express certain src kinases specifically involved in acute

inflammation (Hck, Lyn, Fgr). It is impossible to conclude from these experiments whether this apparent immunoparalysis is specifically due to an in vivo effect on neutrophil function. There are no published experiments investigating the direct in vitro or in vivo effect of dasatinib on any immune cells except neutrophils (Futosi et al. 2012) and murine monocyte-derived macrophages (MDMs) and bone marrow-derived macrophages (BMDMs) (Fraser et al. 2009; Ozanne et al. 2014), but we know from work involving other src kinase inhibitors such as PP1 that src kinases are crucial in macrophage and monocyte (Byeon et al. 2012), pulmonary endothelial cell (Chang et al. 2008; Han et al. 2013), and alveolar epithelial cell (Li et al. 1998; Huang et al. 2003) function.

Figure 4-9 Treatment with 10 mg/kg Dasatinib reduces bacterial killing and increases extrapulmonary dissemination
Effect of i.p. treatment with 1 mg/kg dasatinib (left panel) and 10 mg/kg dasatinib (right panel) on bacterial presence and survival in peripheral blood (A), spleen (B), liver (C) and lung homogenates (D) and BALF (E) from mice exposed to i.t. *E. coli*. Data show median and IQR values from 2 experiments using samples from 8 mice per group; the 1 mg/kg+control and 10 mg/kg+control values are separate experiments. Control vs dasatinib: p=1.00 (1 mg/kg+10 mg/kg) (A); p=1.00, p=0.077 (B); p=1.00, p=0.382 (C); *p=0.05, ***p=0.0002 (D); p=0.111, ***p=0.0004 (E). Inter-experiment control group difference: p=1.00 (A,B,C), p=0.140 (D) and *p=0.0129 (E) by Mann Whitney test.

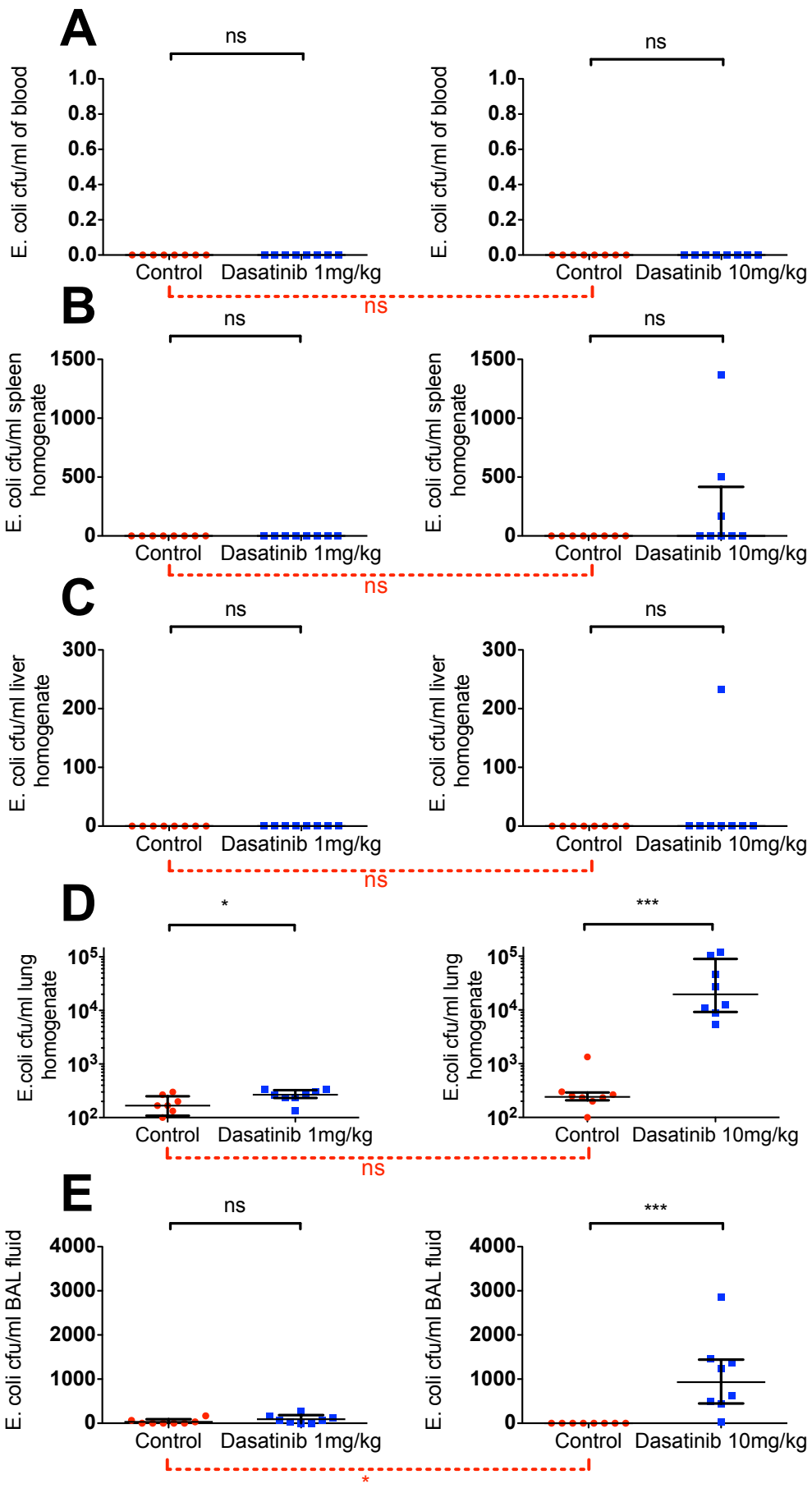
A
ns
E. coli cfu/ml of blood
1.0
0.8
0.6
0.4
0.2
0.0
Control
Dasatinib 1mg/kg
Dasatinib 10mg/kg
ns
B
E. coli cfu/ml spleen homogenate
1500
1000
500
0
C
E. coli cfu/ml liver homogenate
300
200
100
D
*
***
E.coli cfu/ml lung homogenate
10^5
10^4
10^3
10^2
E
E. coli cfu/ml BAL fluid
4000
3000
2000
1000

4.2.6 Alveolar leak

Alveolar protein leak is another detrimental effect of alveolar inflammation and represents a direct marker of alveolar-capillary injury, which can be also detected in conditions less severe than ARDS. A control experiment in Figure 4-10 below shows that dasatinib at both 1 mg/kg and 10 mg/kg does not itself induce meaningful alveolar protein leak in unexposed mice (BAL protein in unstimulated mice receiving 1mg/kg dasatinib ~200µg/ml compared with ~400µg/ml in mice exposed to *E. coli*).

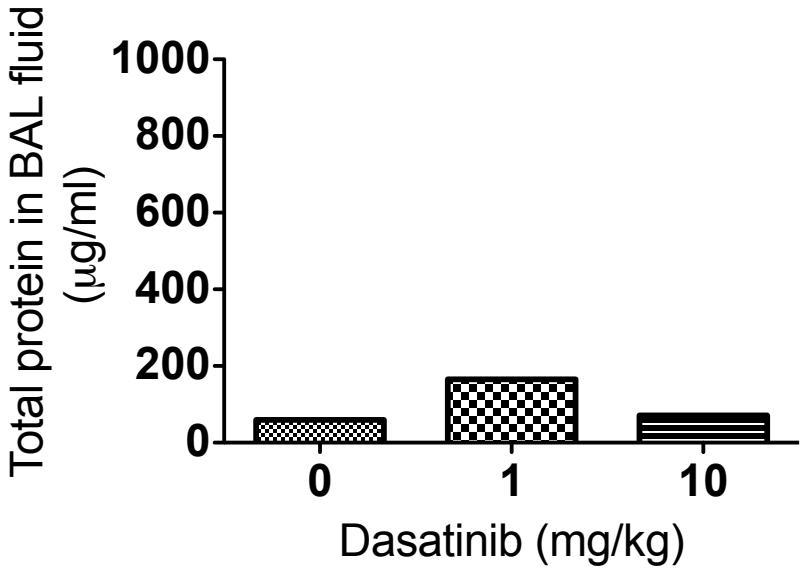

Figure 4-10 Dasatinib itself does not induce significant protein leak into the alveolar space of control mice
Dose response control experiment to demonstrate no meaningful effect of i.p. dasatinib treatment on protein levels in the alveolar space of mice unexposed to i.t. *E. coli,* n=1 mouse per condition.

Protein leak was measured by two methods: i) immediate total protein measurement of the cell-free BALF using a BCA assay and ii) mouse soluble IgM concentration of frozen cell-free BALF samples using ELISA.

Results: Both techniques demonstrate considerably higher protein content in BALF from mice treated with 10 mg/kg dasatinib, with no effect at 1 mg/kg (Figure 4-11 opposite).

Comments: This is likely to be a direct effect of increased bacterial survival and pathogenicity in these mice.

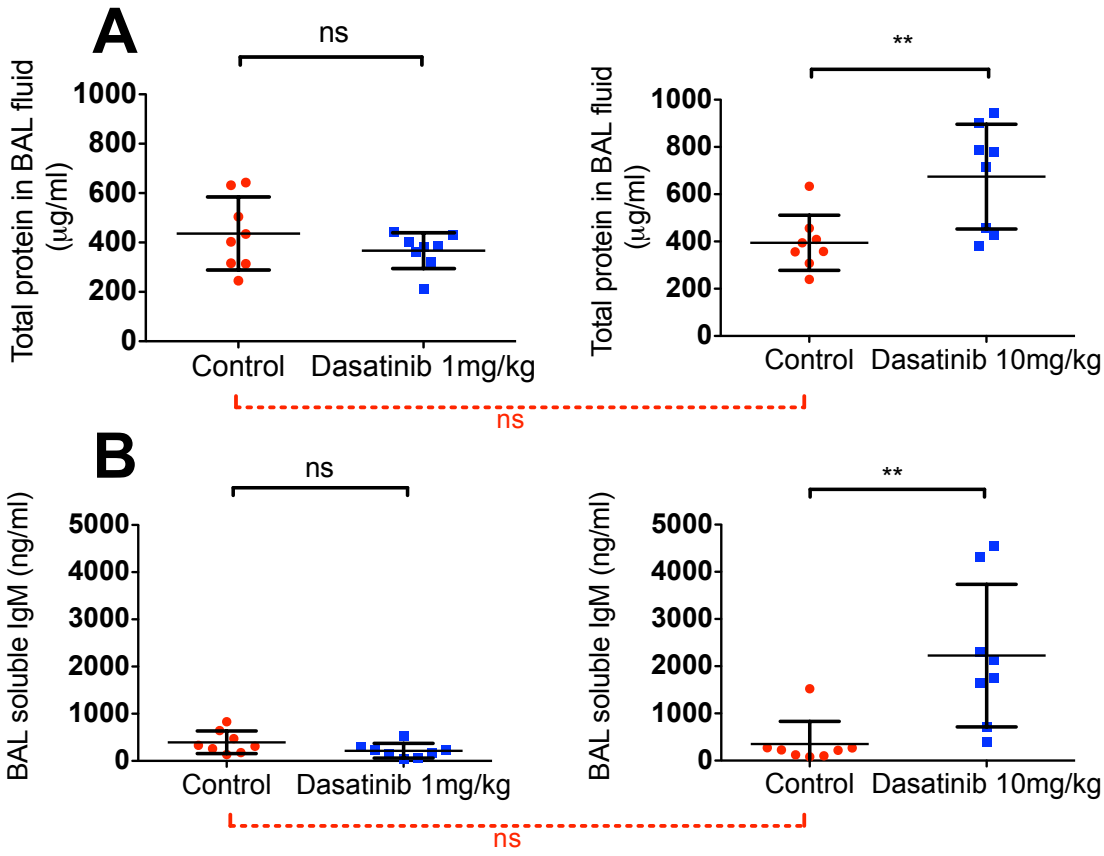

Figure 4-11 Treatment with 10 mg/kg Dasatinib increases alveolar protein leak in response to i.t. *E. coli*

Effect of i.p. treatment with 1 mg/kg dasatinib (left panel) and 10 mg/kg dasatinib (right panel) on the total protein concentration (A) and soluble IgM concentration (B) in BAL samples from mice exposed to i.t. *E. coli*. Data show mean and SD values from 2 experiments using samples from 8 mice per group; the 1 mg/kg+control and 10 mg/kg+control values are separate experiments. Control vs dasatinib: p=0.250 (1 mg/kg), **p=0.0069 (10 mg/kg) (A); p=0.0959, **p=0.0048 (B). Inter-experiment control group difference: p=0.536 (A), p=0.824 (B) by unpaired t-test.

4.2.7 Pro/anti-inflammatory cytokines in BALF

The balance of pro- and anti-inflammatory cytokines present in BALF after stimulation gives important, but non-specific information on the degree of inflammation present as well as any 'counter-inflammatory' or 'resolutionary' processes that may be occurring simultaneously. The 3 pro-inflammatory cytokines we chose to measure were:

- **KC** or CXCL1 (chemokine C-X-C motif ligand 1). This murine cytokine is expressed by neutrophils, macrophages and epithelial cells and is a potent neutrophil chemoattractant (Moser et al. 1990). It is the murine equivalent of human IL-8.
- **MCP-1** (monocyte chemotactic protein 1). This is a potent chemokine that regulates the recruitment and infiltration of monocytes, macrophages, memory T lymphocytes and natural killer (NK) cells. It is mainly produced by monocytes and macrophages themselves at sites of inflammation, but can also be produced by many other immune cells (Deshmane et al. 2009). Although not able to directly cause neutrophil influx and degranulation, MCP-1 levels regulate activation of different cellular components of the innate immune system. In a murine model of LPS-induced acute lung inflammation, 3 methods of monocyte depletion attenuated the observed late neutrophil influx by as much as 82% from control (Dhaliwal et al. 2012). However, when these findings were translated into a randomised-controlled trial of peripheral blood monocyte depletion in a human model of LPS-induced lung inflammation, no significant effects on neutrophil influx were observed (Barr et al. 2013).
- **TNFα** (tumor necrosis factor alpha). TNFα is potently released by activated macrophages and neutrophils as well as other cell types in response to LPS, bacterial products and IL-1 (Walsh et al. 1991). It has numerous local and systemic pro-inflammatory effects.

The anti-inflammatory cytokine we chose to measure was:

- **IL-10** This is primarily produced by monocytes and in unstimulated tissues the expression is minimal. It is generally synthesised in response to pathogenic stimuli (Mosser & Zhang 2008).

Results: Figure 4-12 overleaf shows that at high doses of dasatinib, there are higher levels of pro-inflammatory cytokine production (KC and TNFα) in the alveolar space, with no activation of IL-10. At a dose of 1 mg/kg, there is slightly less TNFα production in dasatinib-treated mice, but no change in MCP-1 or KC production. Again IL-10 is undetectable.

Comments: It is possible that a 24 h timepoint is too early to observe markers of resolution such as IL-10 release, as suggested by the neutrophil influx graph in Chapter 2 that shows peak neutrophil levels in interstitial and alveolar spaces falling back to normal between 24 h and 48 h. Although monocyte (the primary source of IL-10) counts were not quantified in these 2 spaces, very few monocytes were observed on cytospins of BALF.

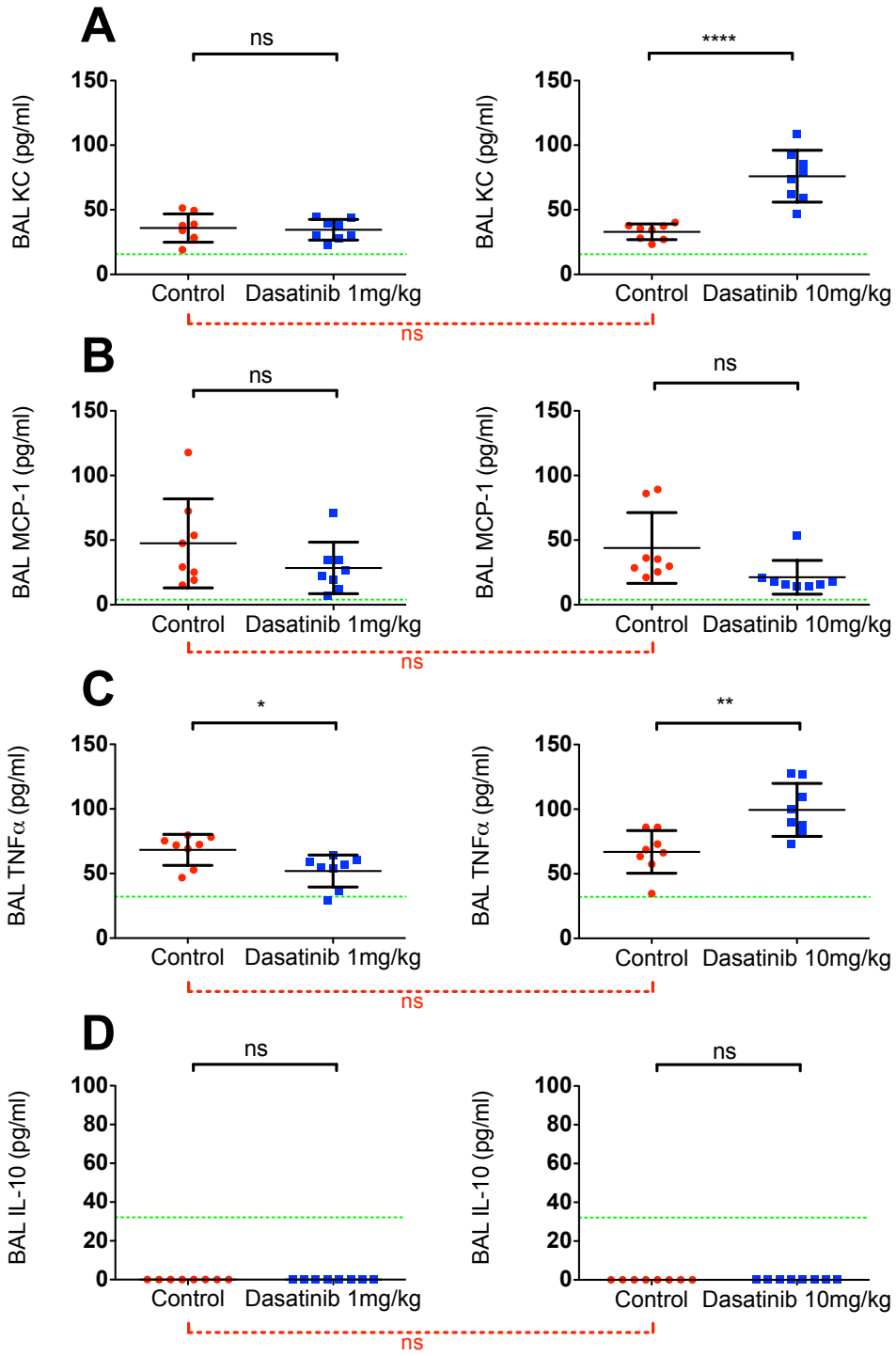

Figure 4-12 Effect of dasatinib treatment on the pro/anti-inflammatory cytokine profile of the alveolar space

Effect of i.p. treatment with 1 mg/kg dasatinib (left panel) and 10 mg/kg dasatinib (right panel) on the concentration of KC (A), MCP-1 (B), TNFα (C) and IL-10 (D) in BAL samples from mice exposed to i.t. *E. coli*. Data show mean and SD values from 2 experiments using samples from 8 mice per group; the 1 mg/kg+control and 10 mg/kg+control values are separate experiments. The horizontal dotted green lines indicate the lower level of detection for each ELISA kit. Control vs dasatinib: p=0.786 (1 mg/kg), ****p<0.0001 (10 mg/kg) (A); p=0.197, p=0.0528 (B); *p=0.177, **p=0.0035 (C); p=1.00 (D). Inter-experiment control group difference: p=0.523 (A), p=0.823 (B), p=0.852 (C) and p=1.00 (D) by unpaired t-test.

4.2.8 Evidence of extrapulmonary toxicity

Results: As expected, mice treated with 10 mg/kg dasatinib are visibly more unwell than control mice due to an increased bacterial burden and this is reflected in simple markers of extrapulmonary toxicity or 'sepsis': serum lactate (a marker of suboptimal supply of oxygen to the peripheral tissues) and ALT (a direct marker of liver inflammation) levels, as shown below in Figure 4-13 below.

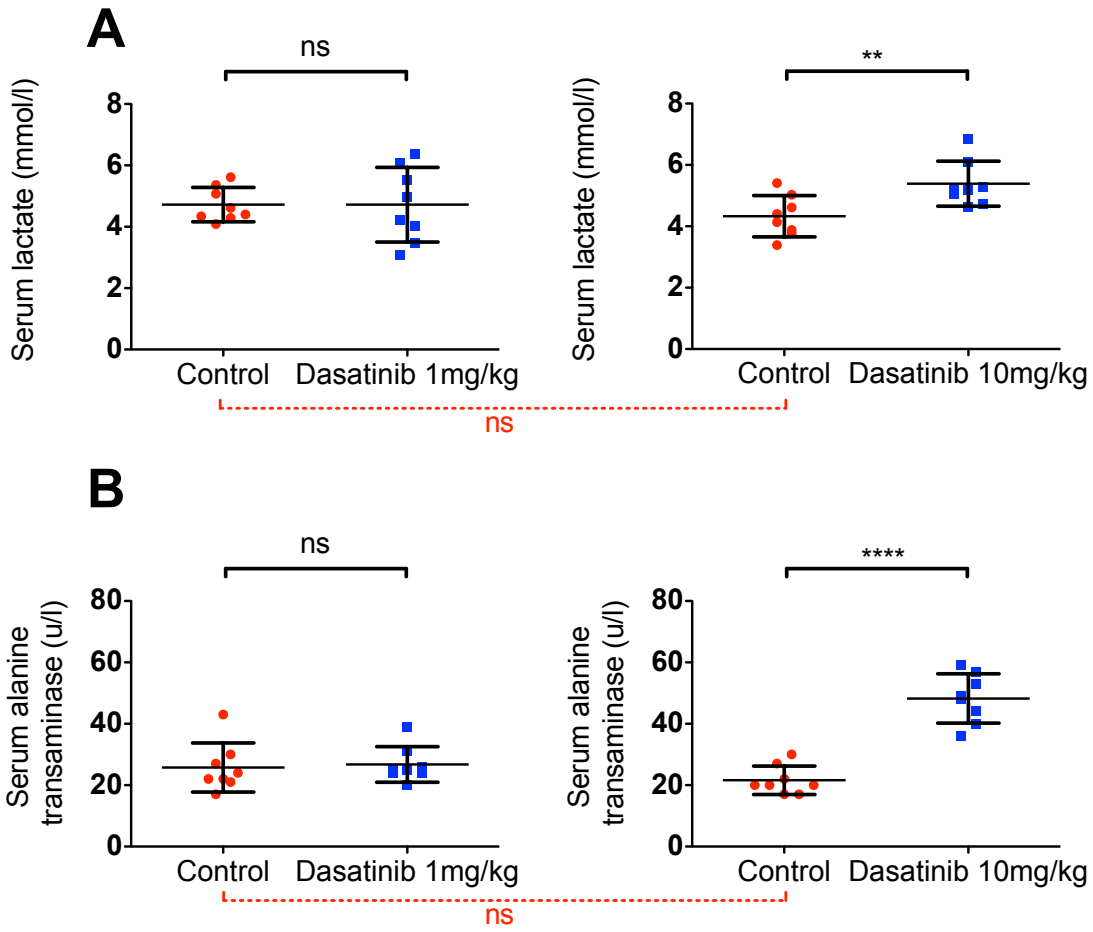

Figure 4-13 Treatment with 10 mg/kg Dasatinib increases markers of extrapulmonary toxicity in *E. coli*-treated mice
Effect of i.p. treatment with 1 mg/kg dasatinib (left panel) and 10 mg/kg dasatinib (right panel) on the serum concentration of lactate (A) and ALT (B) in mice exposed to i.t. *E. coli*. Data show mean and SD values from 2 experiments using samples from 8 mice per group; the 1 mg/kg+control and 10 mg/kg+control values are separate experiments. Control vs dasatinib: p=0.992 (1 mg/kg), **p=0.0095 (10 mg/kg) (A); p=0.779, ****p<0.0001 (B). Inter-experiment control group difference: p=0.224 (A), p=0.227 (B) by unpaired t-test.

4.3 Effect of Dasatinib on an In Vivo Murine Model of Acid-induced Acute Lung Inflammation

I investigated the second part of my hypothesis by using a sterile model of acute lung inflammation. One reason for sterility was to remove the potentially complicating factor of simultaneous bacterial replication and invasion encountered in the model described above. Also, acid inhalation represents the second most common cause of direct lung injury that may lead to ARDS (Ware & Matthay 2000) and is therefore a clinically relevant model to study.

Direct acid instillation into murine lungs results in a robust TNFα dependent neutrophilic alveolitis with alveolar oedema from increased vascular and epithelial permeability that usually heals with fibrosis, in a similar way to human ARDS (Maniatis et al. 2012). However in humans, ARDS caused by acid aspiration is invariably complicated by primary lung infection (upper airway commensals mixed with regurgitated stomach contents at the time of aspiration) or secondary lung infection (subsequent bacterial/fungal invasion of a damaged alveolar epithelial cell layer in the context of acquired immune cell dysfunction) so it is rarely a true 'sterile' condition. Interestingly, neutrophil recruitment in acid models is partly β_2-integrin dependent and partly mediated by platelet-neutrophil interactions though P-selectin (Zarbock et al. 2006). We expected to see an effect of dasatinib in this model.

Based on our results from the *E. coli* model, we chose to start with a modest dasatinib dose of 5 mg/kg and increase the group size to 10 to ensure any subtle effects were picked up in the data. We chose the higher dose of 10 mg/kg for the second experiment (kindly carried out by Drs Dorward and Lucas in my absence; all data analysis and interpretation carried out by me) based on the results of the 5 mg/kg experiment. Only 9 mice per group were available for the 5 mg/kg experiment.

Certain assays (e.g. alveolar and interstitial fluid cytokine levels, MPO and LTF levels) carried out in the 5 mg/kg experiment were not repeated in the 10 mg/kg experiment as we decided that the extra data would not offer any more insight into the effects of dasatinib. It is practically too difficult for 2 operators to carry out these experiments on more than 2 groups (of 8+ mice) at once, without compromising the experimental accuracy and reliability, so the 2 experiments

were carried out separately. Despite this, inter-experiment control variability was once again good.

4.3.1 Cellular influx to alveolar space

Using identical methods to the *E. coli* experiments, cellular influx to the alveolar space in response to acid injury was measured. The total cell/neutrophil influx in response to acid was lower than to *E. coli.*

Results: At 5 mg/kg there is no effect on total cell and total neutrophil influx (Figure 4-14A and B opposite) but there is an observed reduction in the percentage of neutrophils on BAL cytospin (Figure 4-14D).

Comments: This finding is not observed using the flow cytometric method, however the control group variability in these experiments means these figures should be interpreted with care (Figure 4-14C). As discussed in section 4.2.2 above, in such cases of discrepancy, the results obtained by cell morphology are favoured. However, it should be indicated again that as the total number of neutrophils in BALF is the same between control and 5 mg/kg dasatinib, the cytospin results again suggest that there is a corresponding relative increase in other unidentified cell types.

Results: 10 mg/kg dasatinib results in increased total cell and total neutrophil influx compared to control. Data is missing for the 10 mg/kg cytospins as the slides were inadvertently disposed of before counting.

Figure 4-14 Treatment with 5 mg/kg Dasatinib reduces % neutrophilia in the alveolar space but 10 mg/kg Dasatinib increases cellular influx to the alveolar space
Effect of i.p. treatment with 5 mg/kg dasatinib (left panel) and 10 mg/kg dasatinib (right panel) on the total number of cells (A), the total number of neutrophils (B) and the % neutrophils (C+D) in BAL samples from mice exposed to i.t. hydrochloric acid. Results obtained using NucleoCounter© machine method (A), flow cytometry (B+C) and cell morphology on cytospin staining (D). Cytospin slides for 10 mg/kg+control experiment were mislaid before counting. Data show mean and SD values from 2 experiments using samples from 10 mice per group (5 mg/kg experiment) and 9 mice vs 8 mice due to a failed lavage (10 mg/kg experiment); the 5 mg/kg+control and 10 mg/kg+control values are separate experiments. Control vs dasatinib: p=0.997 (5 mg/kg), *p=0.037 (10 mg/kg) (A); p=0.602, *p=0.0197 (B); p=0.550, p=0.191 (C); ***p=0.0002 (D). Inter-experiment control group difference: *p=0.047 (A), p=0.061 (B), ***p=0.0008 (C) by unpaired t-test.

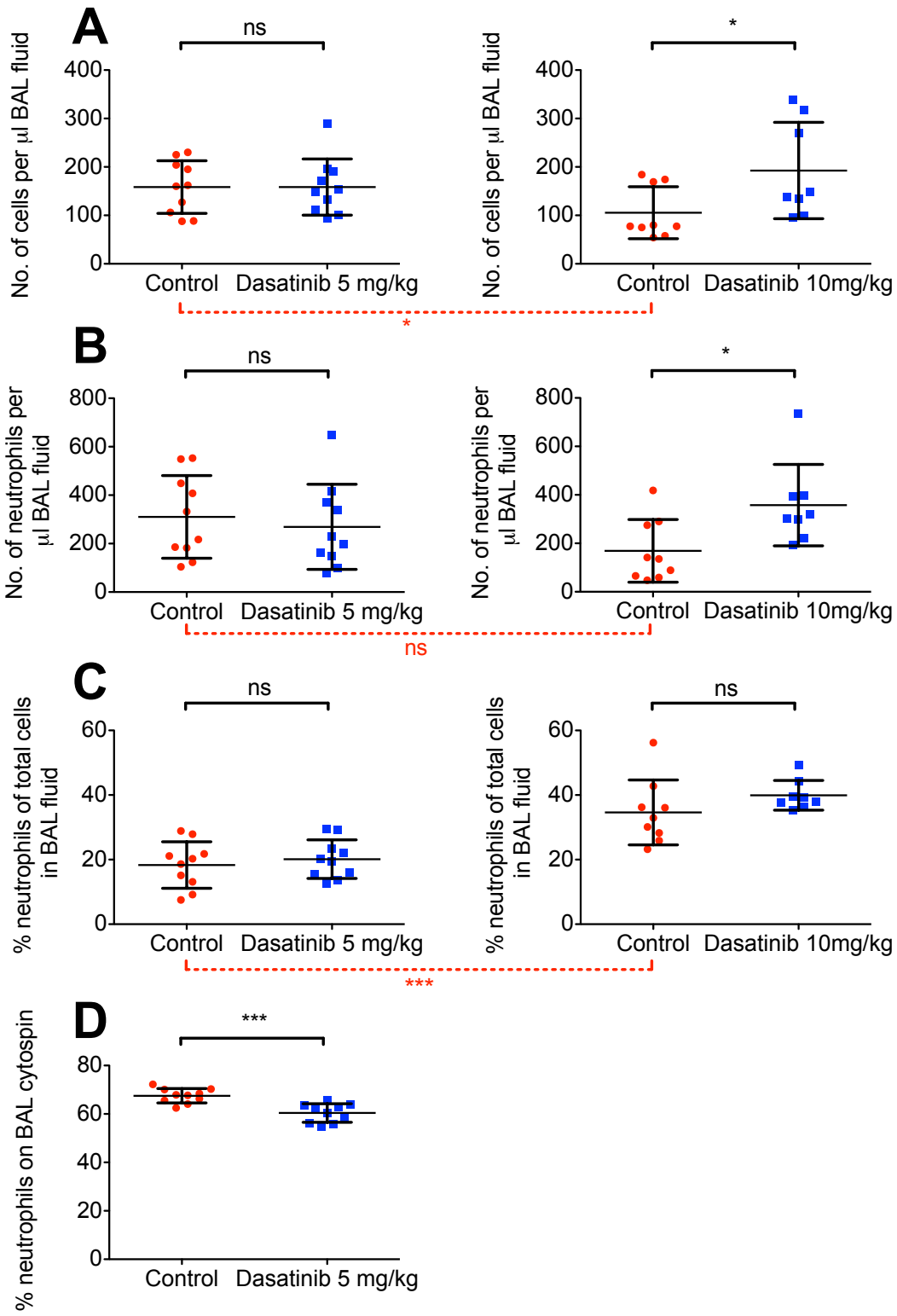
A
ns
*
No. of cells per µl BAL fluid
400
300
200
100
0
Control
Dasatinib 5 mg/kg
Dasatinib 10mg/kg
*
B
ns
*
No. of neutrophils per µl BAL fluid
800
600
400
200
0
Control
Dasatinib 5 mg/kg
Dasatinib 10mg/kg
ns
C
ns
ns
% neutrophils of total cells in BAL fluid
60
40
20
0
Control
Dasatinib 5 mg/kg
Dasatinib 10mg/kg
***
D
***
% neutrophils on BAL cytospin
80
60
40
20
0
Control
Dasatinib 5 mg/kg

4.3.2 Cellular influx to lung interstitium

Results: As shown in Figure 4-15 opposite, 5 mg/kg dasatinib has no effect on cellular influx into the lung interstitium, but 10 mg/kg results in a clear increase in total and % neutrophil content in the interstitial space, matching the response seen in the alveolar space.

Comments: Total neutrophil influx to the lung interstitium is considerably less than for *E. coli* (see Figure 4-4), by a factor of over 10^{-1}. However the influx appears to be more neutrophilic in composition, with a control group mean % neutrophil content of 64% (acid) vs 38% (*E. coli*). See Figure 4-4 above and Figure 4-15 opposite.

Together these data suggest enhanced recruitment of neutrophils to the alveolar and interstitial spaces in mice treated with 10 mg/kg dasatinib.

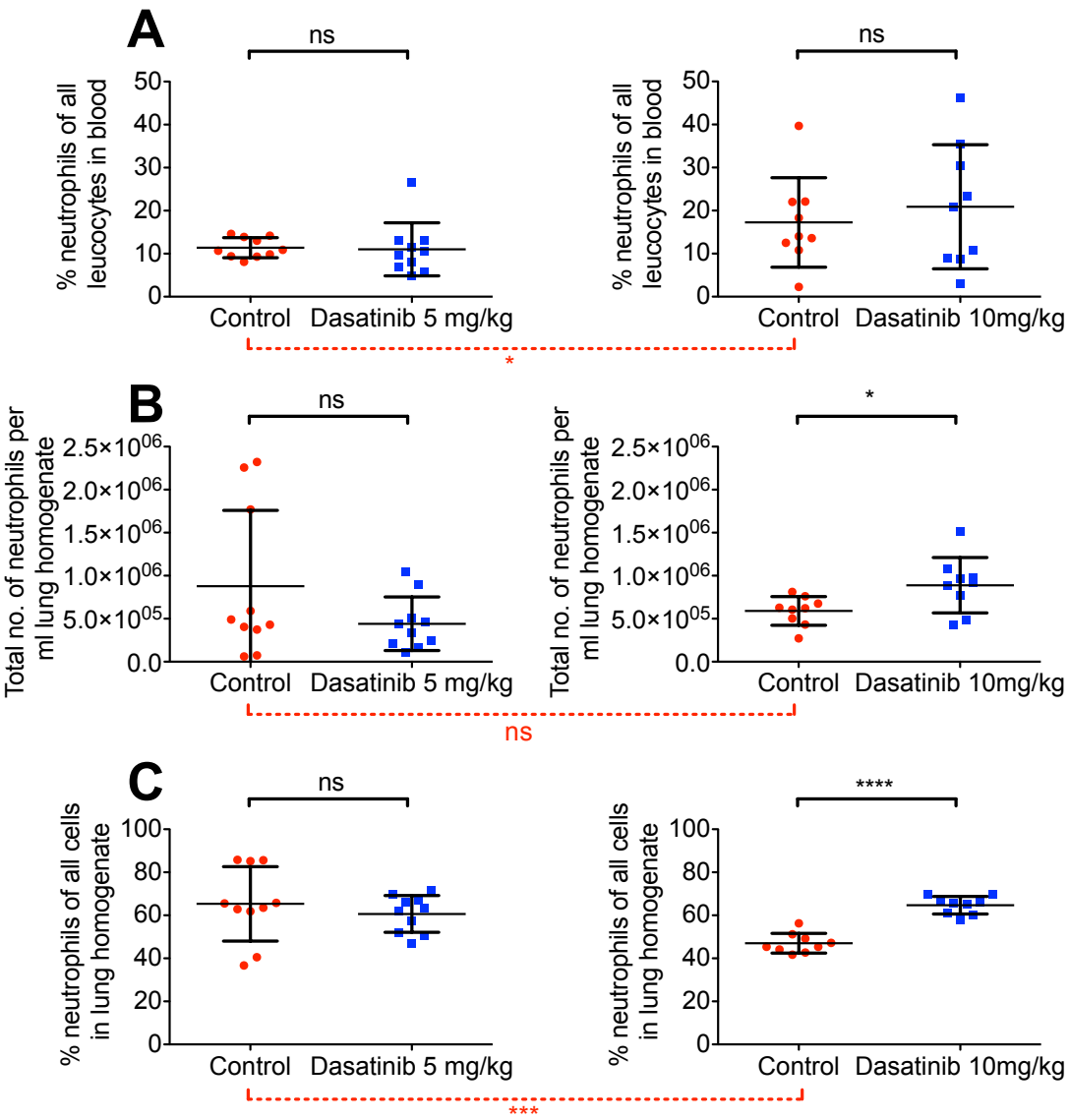

Figure 4-15 Treatment with 10 mg/kg Dasatinib increases neutrophil influx into the lung interstitium in response to acid injury

Effect of i.p. treatment with 5 mg/kg dasatinib (left panel) and 10 mg/kg dasatinib (right panel) on the % neutrophils in blood (A), the total number of neutrophils (B) and the % neutrophils (C) in lung homogenates from mice exposed to i.t. hydrochloric acid. Data show mean and SD values from 2 experiments using samples from 10 mice per group (5 mg/kg experiment) and 9 mice vs 8 mice due to a failed lavage (10 mg/kg experiment); the 5 mg/kg+control and 10 mg/kg+control values are separate experiments. Control vs dasatinib: p=0.853 (5 mg/kg), p=0.547 (10 mg/kg) (A); p=0.158, *p=0.0249 (B); p=0.453, ****p<0.0001 (C). Inter-experiment control group difference: p=0.101 (A), p=0.351 (B), **p=0.007 (C) by unpaired t-test.

4.3.3 Evidence of neutrophil degranulation

Due to the weakly fluorescent PE-CD63 antibody in the *E. coli* experiments, we chose to measure only CD11b expression on neutrophils in the acid-injury model.

Results: 5 mg/kg dasatinib reduces CD11b expression on interstitial neutrophils with no effect on alveolar neutrophils. 10 mg/kg dasatinib, on the other hand, causes significantly higher expression of CD11b in the interstitium, indicating increased activation and degranulation (Figure 4-16 below).

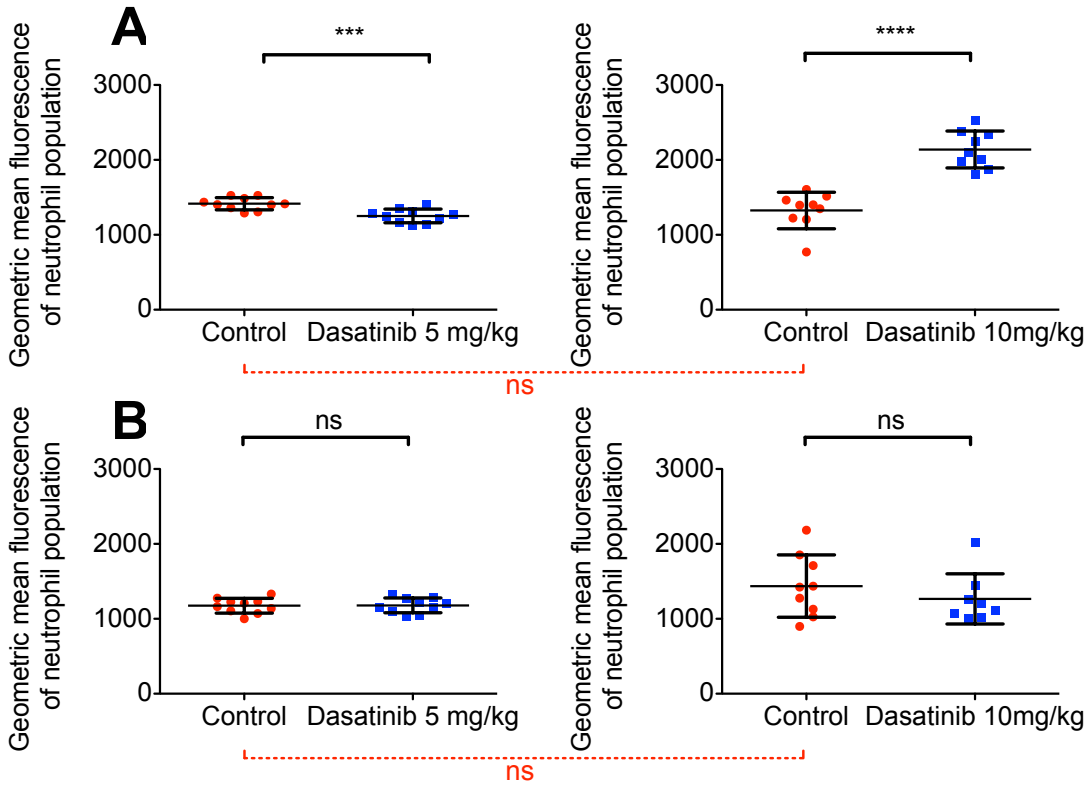

Figure 4-16 CD11b expression on neutrophils in the lung interstitium in response to acid injury is reduced by treatment with 5 mg/kg Dasatinib but increased with 10 mg/kg Dasatinib
Effect of i.p. treatment with 5 mg/kg dasatinib (left panel) and 10 mg/kg dasatinib (right panel) on neutrophil expression of CD11b in lung homogenate (A) and BAL (B) samples from mice exposed to i.t. HCl. Data show mean and SD values from 2 experiments using samples from 10 mice per group (5 mg/kg experiment) and 9 mice vs 8 mice due to a failed lavage (10 mg/kg experiment); the 5 mg/kg+control and 10 mg/kg+control values are separate experiments. Control vs dasatinib: ***p=0.0005 (5 mg/kg), ****p<0.0001 (10 mg/kg) (A); p=0.931, p=0.368 (B). Inter-experiment control group difference: p=0.29 (A), p=0.07 (B) by unpaired t-test.

In a variation to the *E. coli* experiments, we also measured MPO concentration in the cell-free lung homogenate fluid in the 5 mg/kg experiment.

Results: Although there is no effect on alveolar or interstitial MPO concentration using 5 mg/kg dasatinib, there is evidence of significantly reduced LTF (secondary granule) release into BALF, indicating an effect on neutrophil degranulation (Figure 4-17 below).

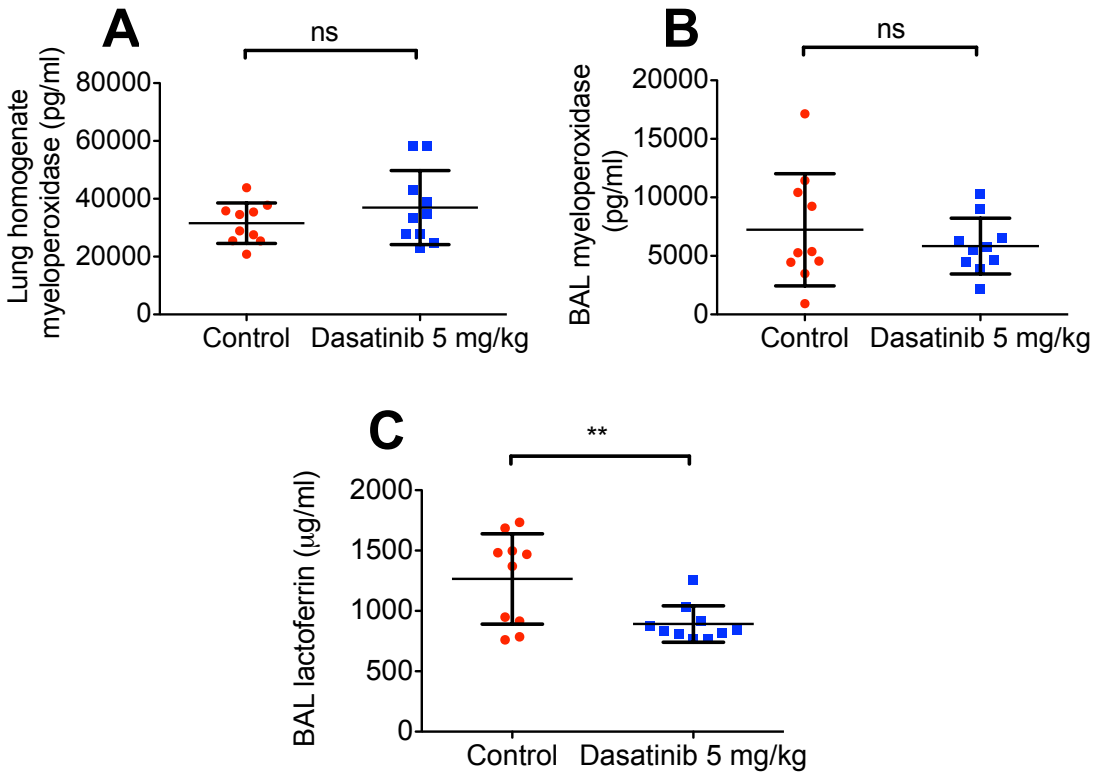

Figure 4-17 Treatment with 5 mg/kg dasatinib reduces alveolar lactoferrin release in response to acid injury
Effect of i.p. treatment with 5 mg/kg dasatinib on the concentration of MPO in lung homogenates (A) and the concentration of MPO (B) and LTF (C) in BAL samples from mice exposed to i.t. HCl. Data show mean and SD values from 1 experiment using samples from 10 mice per group. LTF concentration only measured in BALF. Both assays only carried out in initial 5 mg/kg+control experiment. p=0.257 (A), p=0.422 (B) and **p=0.009 (C) by unpaired t-test.

4.3.4 Alveolar leak

Mice receiving 10 mg/kg dasatinib with acid injury were visibly more unwell at 12 h than the control group with more haemorrhagic lavage fluid. Their large bowel appeared more ischaemic.

Results: Although there is no significant effect on alveolar leak at both doses (as measured by total protein concentration in the BALF), there is a clear trend towards an effect at 10 mg/kg, indicating increased epithelial and endothelial cell dysfunction (Figure 4-18 below).

Comments: This may be due to a direct effect of src kinase inhibition on barrier function. In response to LPS in mice, c-src and Yes kinases have been shown to mediate vascular leakage with an opposing effect of Lyn kinase activation in stabilising endothelial adherens junctions (Han et al. 2013).

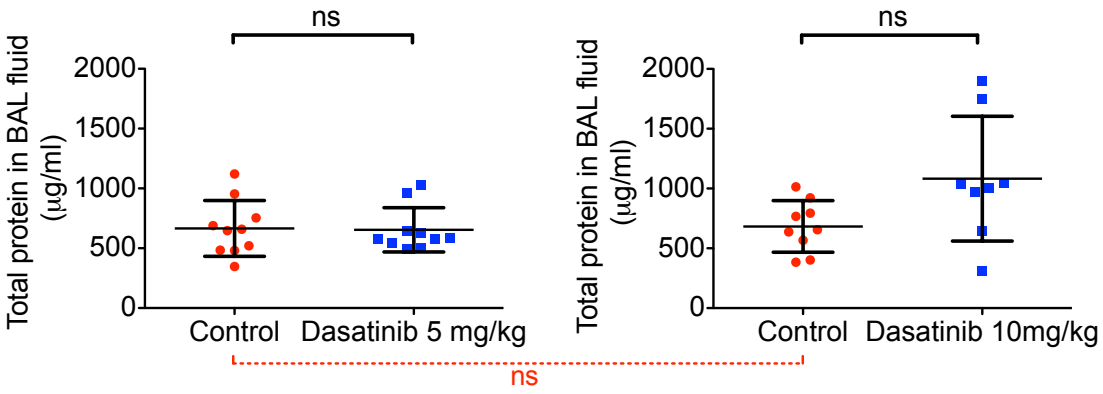

Figure 4-18 Treatment with dasatinib has no effect on alveolar leak in response to acid injury
Effect of i.p. treatment with 5 mg/kg dasatinib (left panel) and 10 mg/kg dasatinib (right panel) on the total protein concentration in BAL samples from mice exposed to i.t. HCl. Data show mean and SD values from 2 experiments using samples from 10 mice per group (5 mg/kg experiment) and 9 mice vs 8 mice due to a failed lavage (10 mg/kg experiment). Control vs dasatinib: p=0.905 (5 mg/kg) and p=0.052 (10 mg/kg). Inter-experiment control group difference: p=0.872 by unpaired t-test.

4.3.5 Pro/anti-inflammatory cytokines in BALF and lung interstitium

Cytokines were measured in both cell-free alveolar and interstitial fluid in the 5 mg/kg experiment, but not in the subsequent 10 mg/kg experiment (Figure 4-19 overleaf).

Results: As shown, dasatinib significantly reduces MCP-1 production in the alveolar space with no effect in the interstitial space.

Comments: All other cytokine levels are unchanged in both compartments, although alveolar TNFα and IL-10 values are below the minimum detection levels of their respective ELISA kits. However, the positive values obtained in Figure 4-19H indicate that the IL-10 ELISA kit was indeed working.

A more sensitive method of measuring IL-10 in lavage samples, such as a cytometric bead array (CBA) kit or a more sensitive ELISA kit may have revealed more information about anti-inflammatory processes.

It is difficult to know how to interpret the significant effect of dasatinib treatment on BALF MCP-1 values in the context of the normal levels of other cytokines. The graph in Figure 4-19C does however demonstrate a marked effect. If the effect is real, it suggests that dasatinib inhibits alveolar monocyte and macrophage activation, most likely through Hck, Fgr or Lyn kinase inhibition (Okutani et al. 2006).

Taken with the other findings above, it does suggest a modest anti-inflammatory effect of 5 mg/kg dasatinib in response to sterile acid injury through inhibition of neutrophil degranulation.

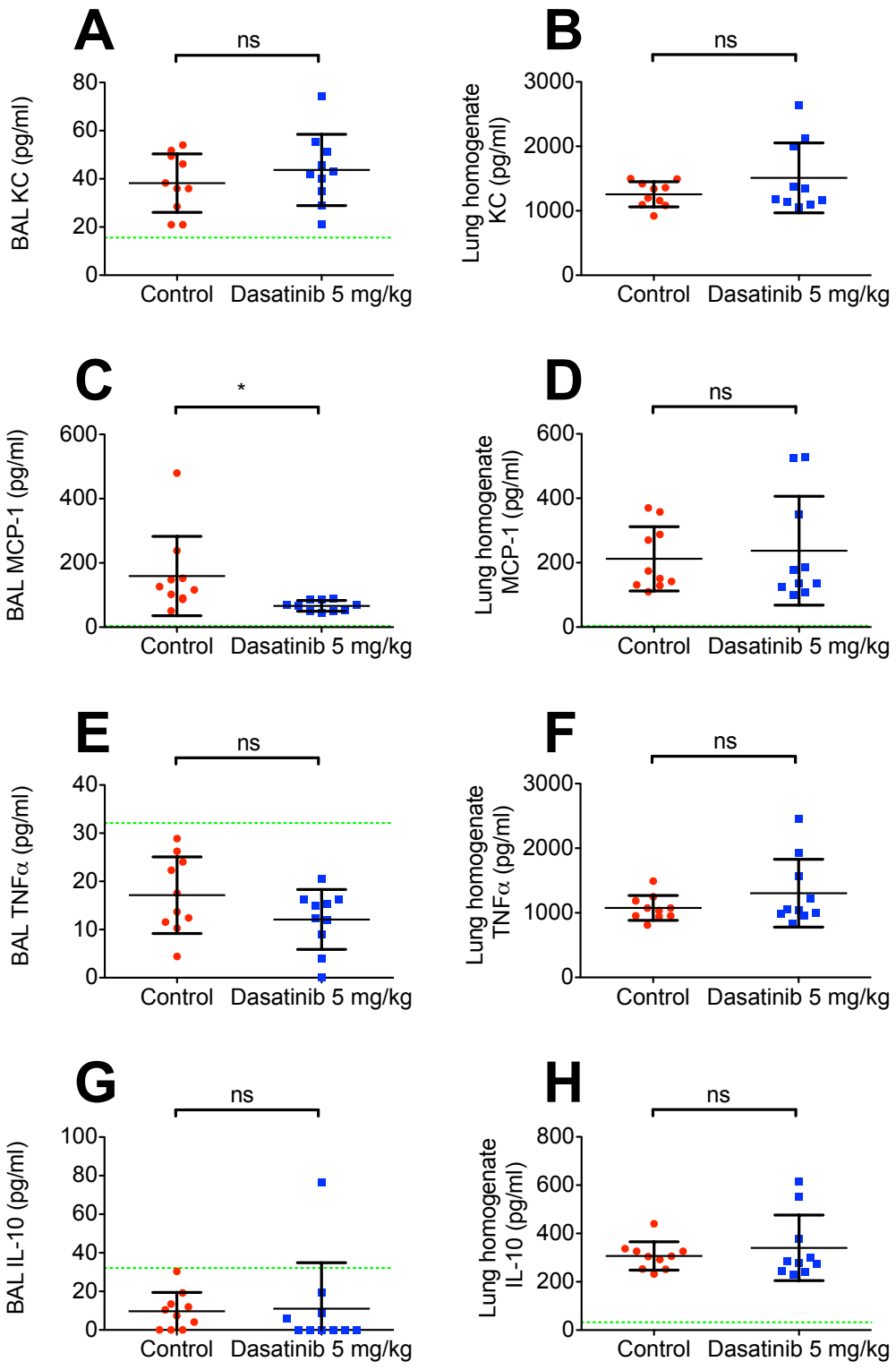

Figure 4-19 Treatment with 5 mg/kg dasatinib reduces alveolar MCP-1 release in response to acid injury

Effect of treatment with 5 mg/kg dasatinib on the concentration of KC (A+B), MCP-1 (C+D), TNFα (E+F) and IL-10 (G+H) in BAL (A, C, E and G) and lung homogenate (B, D, F and H) samples from mice exposed to i.t. HCl. Data show mean and SD values from 1 experiment using samples from 10 mice per group. The horizontal dotted green lines indicate the lower level of detection for each ELISA. Assays only carried out in initial 5 mg/kg+control experiment. p=0.376 (A), p=0.179 (B), *p=0.0301 (C), p=0.699 (D), p=0.131 (E), p=0.216 (F), p=0.874 (G), p=0.483 (H) by unpaired t-test.

4.3.6 Evidence of extrapulmonary toxicity

Results: Perhaps surprisingly, 5 mg/kg dasatinib appears to reduce markers of impaired tissue perfusion (lactate) but increase markers of liver inflammation (ALT), whereas 10 mg/kg dasatinib results in increased liver toxicity alone.

Comments: The control group variability in ALT levels may account for this unexpected result in the 5 mg/kg experiment.

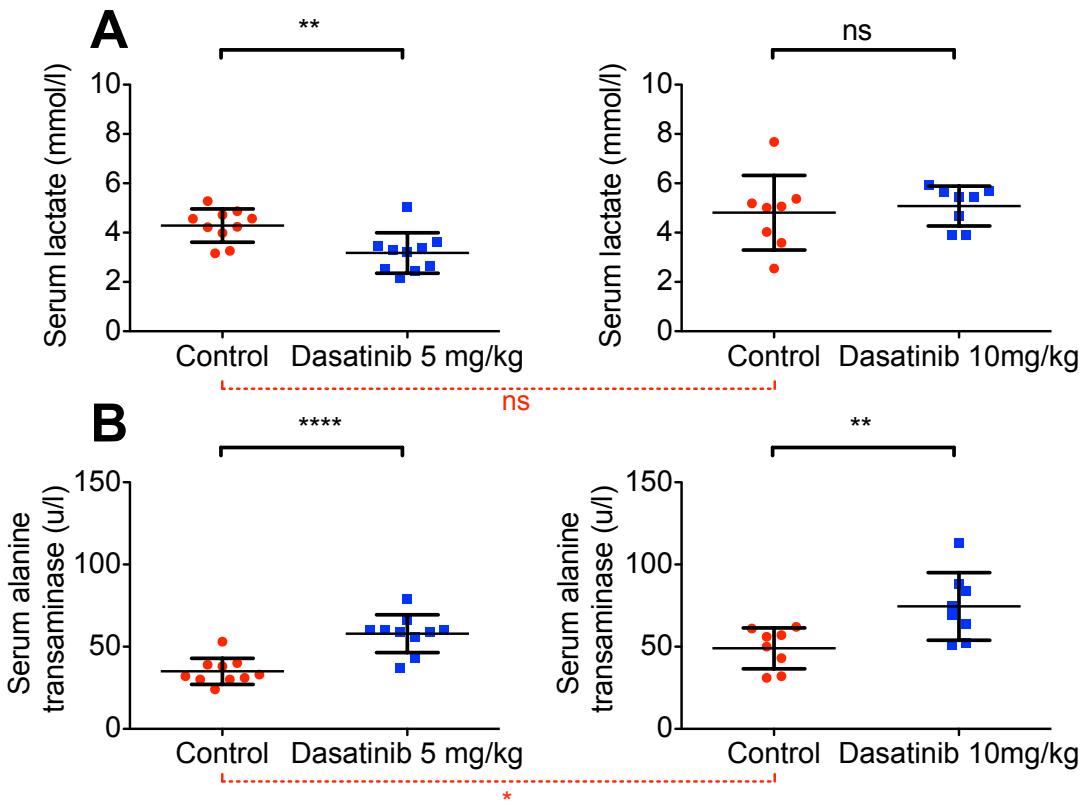

Figure 4-20 Treatment with dasatinib increases liver toxicity in response to acid injury
Effect of i.p. treatment with 5 mg/kg dasatinib (left panel) and 10 mg/kg dasatinib (right panel) on the concentration of lactate (A) and ALT (B) in serum from mice exposed to i.t. HCl. Data show mean and SD values from 2 experiments using samples from 10 mice per group (5 mg/kg experiment) and 8 per group due to insufficient samples (10 mg/kg experiment); the 5 mg/kg+control and 10 mg/kg+control values are separate experiments. Control vs dasatinib: **p=0.0040 (5 mg/kg), p=0.664 (10 mg/kg) (A); ****p<0.0001, **p<0.0094 (B). Inter-experiment control group difference: p=0.34 (A), *p=0.010 (B) by unpaired t-test.

4.4 Summary of Key Findings

These experiments have tested my hypothesis in two in vivo murine models of *E. coli and* acid-induced acute lung inflammation. My key findings are summarised as follows:

1. Intratracheal instillation of live *E. coli* into healthy mice reproducibly causes intense neutrophilic influx into the alveolar and interstitial spaces with evidence of degranulation, inflammation and alveolar leak. Treatment with dasatinib has a variable effect dependent on the dose administered. At low dose (1 mg/kg) there is reduced interstitial neutrophil content, reduced alveolar release of MPO and TNFα but slightly increased bacterial survival in the lung interstitium, with no effect on other markers. At high dose (10 mg/kg) there is a clear detrimental effect that is likely to be due to increased bacterial survival and exponential growth in all compartments of the lung as a result of impaired neutrophil phagocytosis and killing. The dose threshold of this effect is however unknown.

2. In a sterile model of lung inflammation using acid instillation, a moderate dose of dasatinib (5 mg/kg) reduces alveolar neutrophil content, degranulation of LTF and MCP-1 release, with reduced interstitial neutrophil CD11b activation and no major effect on other markers. Again, the higher dose of 10 mg/kg induces a detrimental effect, with increased alveolar and interstitial neutrophil influx and degranulation, and increased alveolar haemorrhage.

Therefore in these experiments, my hypothesis:

"Inhibition of the* src *kinase pathway attenuates neutrophil recruitment to the alveolar and interstitial spaces, neutrophil degranulation and endothelial cell injury and leak in in vivo models of bacteria and acid-induced acute lung inflammation"

has not been fully satisfied. Instead src inhibition has a moderating effect on the composition of the inflammatory cell infiltrate in both models, with reduced markers of degranulation at lower doses and no effect on endothelial cell injury

and leak. At higher doses, src inhibition has the opposite effect with increased neutrophil influx, degranulation and alveolar leak.

These findings will be further discussed in Chapter 6 (General Discussion), particularly with regard to their significance in further understanding the pathogenesis of ARDS.

Chapter 5. An Investigation into the Effect of Src Kinase Inhibitors on the Processes of Neutrophil-Mediated Epithelial Cell Damage and Macrophage Efferocytosis of Apoptotic Cells

5.1 Chapter Overview

This chapter describes the work I carried out to test my third hypothesis:

"*In vitro *src kinase inhibition of human neutrophils attenuates neutrophil-mediated epithelial cell damage whilst promoting a pro-resolutionary environment, allowing efficient apoptotic cell clearance"

I investigated whether PP1 or dasatinib affected secondary epithelial cell inflammation as well as alveolar repair, processes that are important in the pathogenesis and resolution of ARDS. Section 5.2 details the optimisation and implementation of an in vitro model of neutrophil-mediated epithelial cell injury, using bacterial stimulation to simulate an infected alveolus, to extend my in vitro work from Chapter 3. Section 5.3 describes experiments to confirm that ex vivo neutrophils from critically ill patients are dysfunctional and pro-inflammatory, and test whether this behaviour can be inhibited with src kinase inhibitors. Finally, in Sections 5.4 and 5.5, I investigate the effects of src kinase inhibition on alveolar repair, by incorporating an apoptotic cell efferocytosis assay into the experimental design.

As the experimental design in this chapter is particularly complex, I have detailed it both pictorially and in text throughout this chapter to aid the reader in interpreting the results. Methods for routine techniques such as ELISA, flow cytometry, neutrophil phagocytosis and bacterial killing and cell culture are not repeated, and can be referred to in Chapter 2 on page 31.

5.2 Effects on Epithelial Cell Inflammation and Damage

Aim: The experimental aim was to test whether src kinase inhibition of human neutrophils exposed to live bacteria indirectly affected epithelial cell inflammation and damage.

5.2.1 Experimental design

This description refers to Figure 5-1 opposite. Briefly, 2 x 10^6 neutrophils in serum-free IMDM (no phenol red) from healthy volunteers were treated for 30 min at 37^{o}C in a shaking water bath with 10 μM PP1 or 100 nM dasatinib with appropriate controls (**Step 1**).

The cells were then washed twice in warm PBS- to remove the effect of the inhibitors for the remainder of the experiment, before resuspending at the same concentration in IMDM. Each condition was then stimulated with serum-opsonised *S. aureus* (NCTC 8325) *or E. coli* (K-12 strain) for 30 min at 37^{o}C in a shaking water bath at an MOI of ~10 bacteria: 1 neutrophil (**Step 2**).

Each individual co-culture supernatant was filter-sterilised through a separate 0.2 μm filter and transferred to an individual well of a 24-well plate containing cultured, adherent A549 epithelial cells at ~70% confluence in serum-free conditions. From further preliminary experiments, I found that serum-free conditions were required to observe evidence of damage and inflammation in the epithelial cell monolayer. The A549s were cultured in the supernatants for 24 h at 37^{o}C, 5% CO_2 (**Step 3**).

At this point, photographs of the monolayer integrity were taken using inverted light microscopy before transferring each supernatant to a fresh eppendorf tube. The tubes were centrifuged at 10,000g for 3 min and the upper debris-free supernatants were transferred to fresh eppendorf tubes and frozen at -80^{o}C for later analysis. The samples were tested in duplicate for inflammatory cytokine release (IL-8 and MCP-1) and cytotoxicity (LDH release) (**Step 4**).

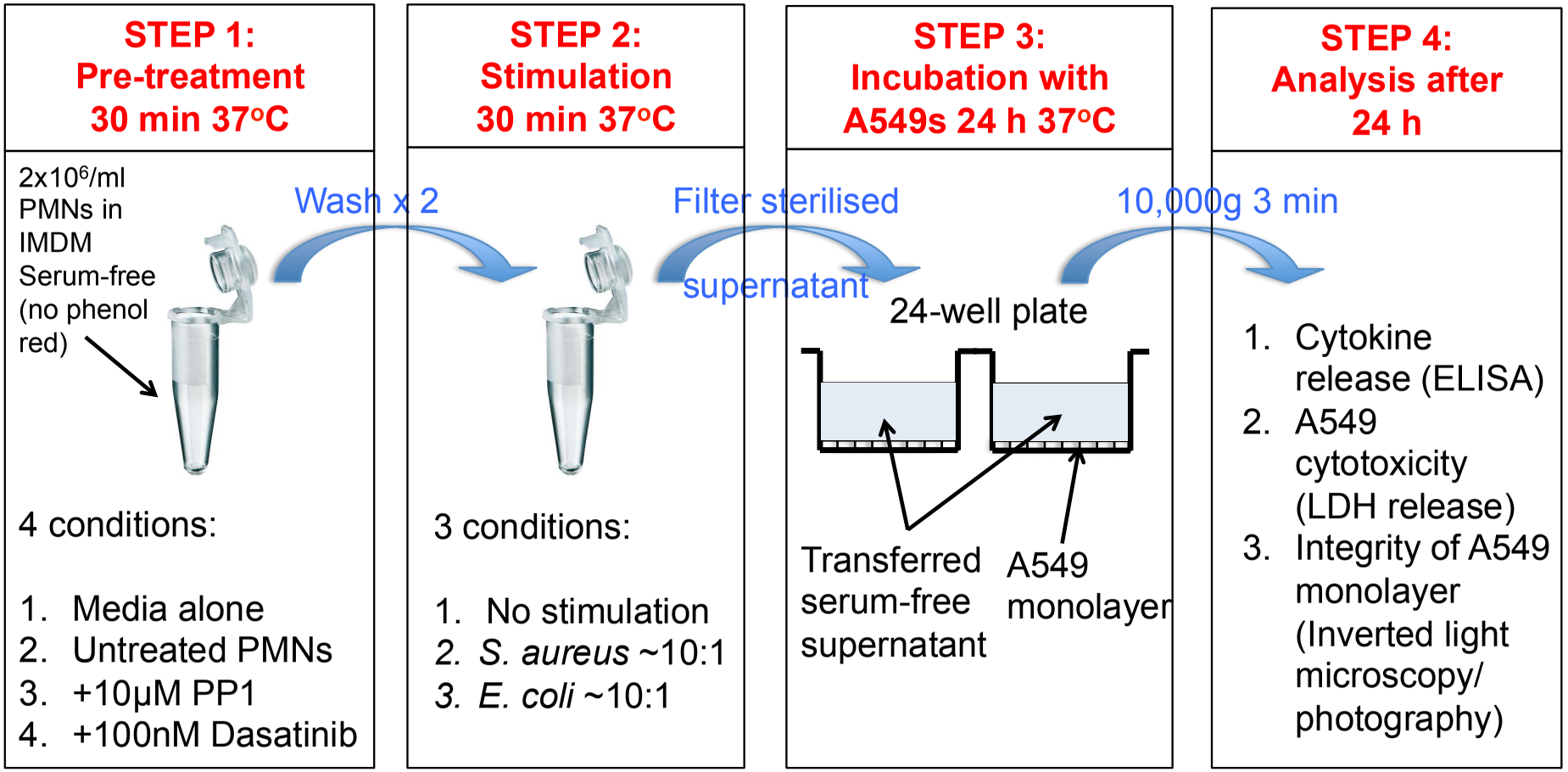

Figure 5-1 Experimental design for section 5.2

5.2.2 Src kinase inhibition of neutrophils: effect on epithelial cell monolayer integrity in an in vitro model of infection

From my preliminary experiments and previously published data (Conway Morris et al. 2009), it was observed that LPS-stimulated neutrophils induce A549 cell monolayer disruption with inflammatory cytokine and LDH release through both direct membrane-mediated effects and when the cells are separated by a permeable membrane, suggesting the effect is partly due to a soluble factor.

Results: Figure 5-2 opposite shows representative images of the A549 monolayer integrity after 24 h incubation with filter-sterilised supernatants from various combinations of src kinase-treated healthy neutrophils with live SA or EC and appropriate controls.

Comments: The top 2 rows of Figure 5-2 demonstrate two important control observations:

- A549s at 70% confluence incubated in serum-free media alone reach near 100% confluence at 24 h. The supernatant of unpre-treated, unstimulated healthy neutrophils has no obvious effect on this growth.
- When the src kinase inhibitors, PP1 and dasatinib are ‘carried over’ in the supernatant from treated neutrophils to A549 cells, the inhibitors themselves appear to cause disruption of the A549 monolayer. The cells are clumped and spherical with some detachment into suspension.

This effect is not observed when PP1 and dasatinib-treated neutrophils are washed before they are incubated for a further 30 min in media alone and their supernatant is transferred to the A549s, suggesting it is due to a direct effect of the inhibitors. This would be expected, given the importance of src family kinases in integrin function. For this reason, the inhibitors were routinely washed from the cells for all subsequent experiments, as shown in Figure 5-1 above.

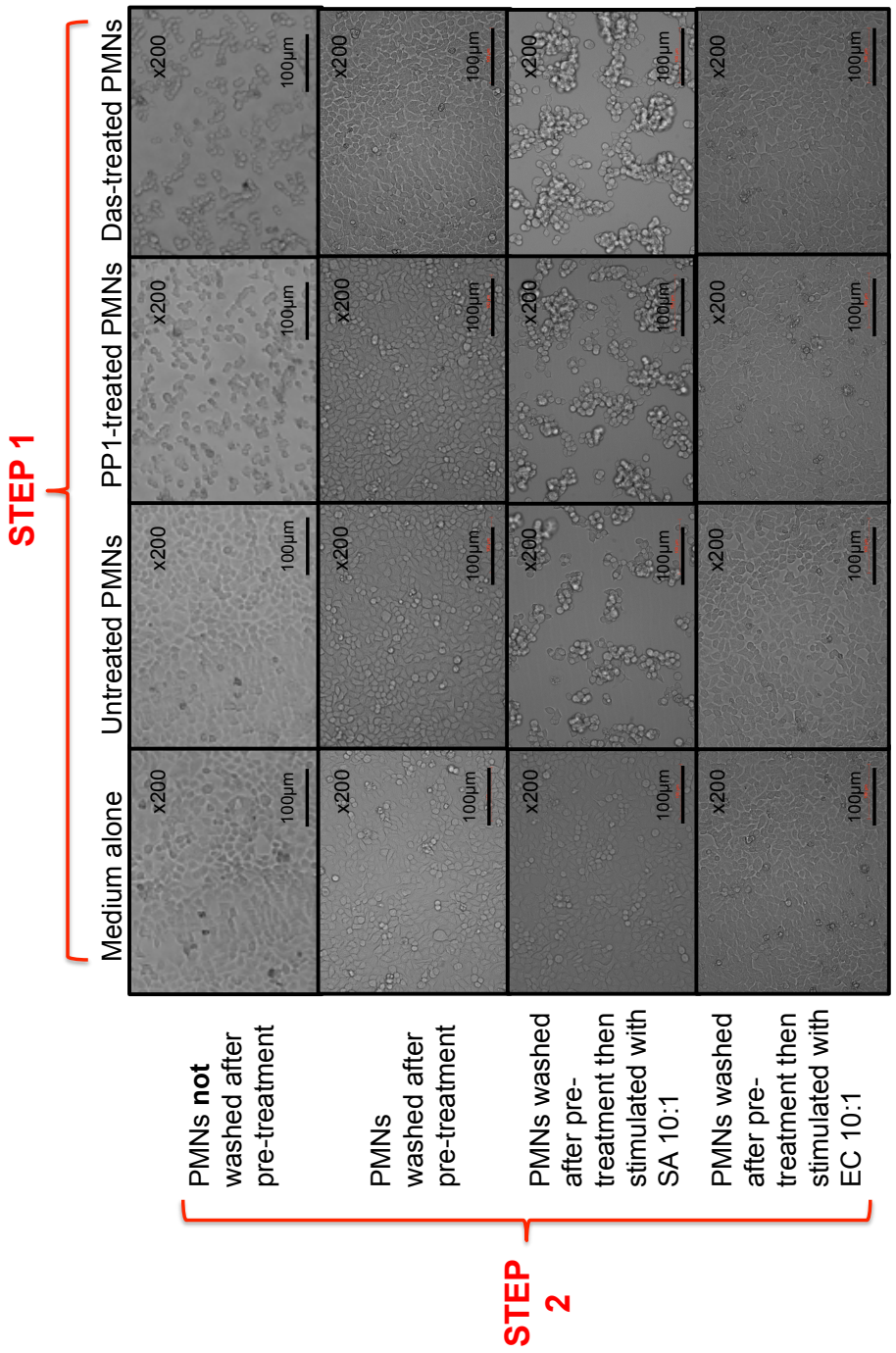

Figure 5-2 Products of the interaction of neutrophils with PP1, Dasatinib and SA disrupt A549 monolayer integrity

X200 representative images of confluent A549 monolayers incubated for 24 h in the filter-sterilised, serum-free supernatant of the following neutrophil interactions: Neutrophils (from healthy volunteers) pre-treated for 30 min with control medium, 10 µM PP1 or 100 nM dasatinib before being washed twice in PBS- to remove the effects of drugs (second row) or left unwashed (top row). Healthy neutrophils pre-treated for 30 min with control medium, 10 µM PP1 or 100 nM dasatinib, washed twice in PBS- and subsequently stimulated for 30 min with SA (MOI~10 SA:1 PMN) (third row) or EC (MOI~10:1) (bottom row). An extra set of control conditions tested neutrophil-free control medium with or without bacteria (first column). Representative images from 3 experiments using neutrophils from 3 independent volunteers.

The photos displayed in the 3rd and 4th rows in show an interesting effect:

- The supernatant of live SA and EC alone does not cause any monolayer disruption, but the supernatant of untreated neutrophil/SA co-culture severely disrupts the monolayer, suggesting this effect is caused by soluble factors released by neutrophils and/or SA in response to their interaction. This observation is not seen when using a neutrophil/*E. coli* co-culture. The SA effect is not reversed when neutrophils are pre-treated with 10 μM PP1 or 100 nM dasatinib, using precisely the same experimental conditions (PP1/dasatinib concentration and MOI) as in Chapter 3. This suggests that the causative soluble factors are not products of neutrophil degranulation.

Although I did not test this theory, it is possible that these results are explained by the release of lipoteichoic acid (LTA) in the SA experiments. LTA is a cell wall component in Gram-positive organisms such as *S. aureus* released upon bacteriolysis by leukocytes and mediates inflammation through ligation of TLR2. Gram-negative organisms such as *E. coli* do not contain LTA. At 30 μg/ml, LTA is known to induce production and release of the opsonin surfactant protein A through NF-κB activation from A549 cells in vitro, though without any effect on cell viability (Liu et al. 2012). It also induces a dose-dependent increase in cyclooxygenase-2 (COX-2) and prostaglandin E_2 (PGE_2) expression and activity (Lin et al. 2001). So although LTA has not been previously shown to disrupt epithelial cell barrier function, it does however induce endothelial cell barrier dysfunction in pulmonary microvessel endothelial cell monolayers through generation of ROS/Reactive nitrogen species (RNS) (Pai et al. 2012).

It is also possible that the effect seen is due to virulence factors specific to *S. aureus* NCTC 8325 that are not exhibited by *E. coli* K-12 strain. For example, *S. aureus* releases several leukotoxins such as leukocidin in response to neutrophil interaction that can induce both NETs production and breakdown (Malachowa et al. 2013; Thammavongsa et al. 2013).

5.2.3 LDH/cytokine release from epithelial cells: control experiments

I carried out the following control experiments to assess two potential confounding factors:

The first control experiment investigated whether relative cytokine or LDH release from A549s cells may simply be dependent on the exact number of cells present in each well.

Results: These are summarised in Figure 5-3A opposite. The results confirm that neither pre-treatment of the neutrophils in Step 1, nor stimulation of the neutrophils with bacteria (only SA used in this control experiment) in Step 2, significantly affect the total protein concentration of the lysed A549 monolayer harvested in Step 4 of the experimental protocol. Total protein concentration gives a crude but fairly accurate comparison of the total number of A549 cells present.

Comments: As the results were consistent, I did not measure this parameter again in subsequent experiments and attributed any difference in relative cytokine or LDH levels between experimental conditions to an actual difference in A549 cell expression and release.

The second control experiment investigated whether the majority of IL-8 measured in the final A549 supernatant in Step 4 was released by A549 cells rather than neutrophils, a known source of vigorous IL-8 release.

Results: These are summarised in Figure 5-3B opposite. As shown in the left hand condition, quiescent neutrophils release relatively low levels of IL-8, with or without 30 min of live bacterial stimulation. The middle condition also shows that quiescent A549 cells release low levels of background IL-8, even when exposed to SA supernatant. IL-8 release from A549s is increased approximately 3-fold by exposure to the supernatant of SA-stimulated neutrophils. This effect is dependent on neutrophil stimulation.

Comments: In subsequent experiments, these control conditions were not repeated and any relative differences in cytokine release in Step 4 were therefore attributed to true effects on A549 cell expression and release.

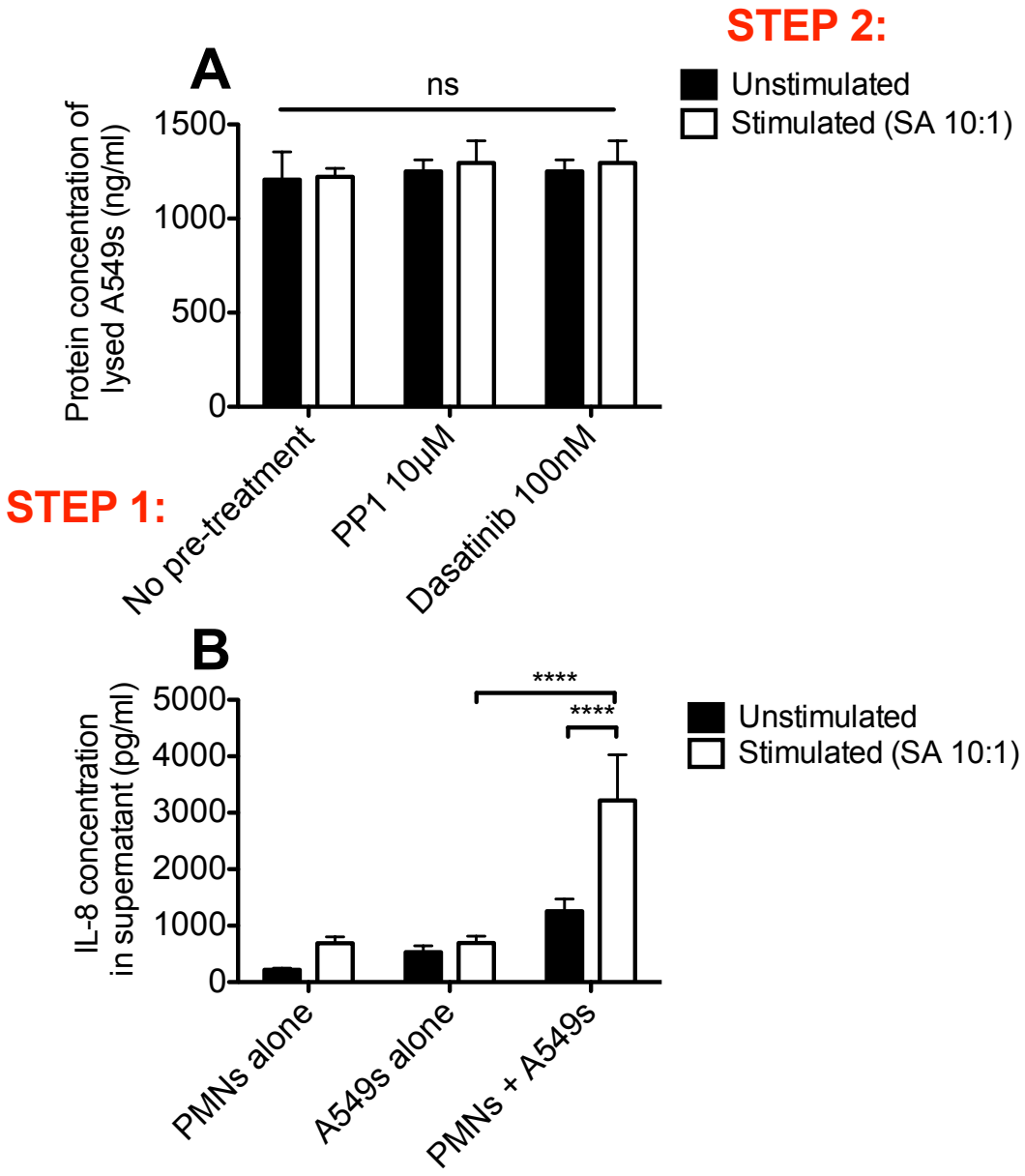

Figure 5-3 Neutrophil/bacterial supernatants do not significantly affect the A549 monolayer total protein content or contribute to IL-8 generation in the absence of A549s

Protein concentration of washed A549 monolayers incubated for 24 h in the filter-sterilised, serum-free supernatant of neutrophils pre-treated for 30 min with control medium, 10 μM PP1 or 100 nM dasatinib before washing twice with PBS- and being left unstimulated or stimulated for 30 min with live serum-opsonised SA (A). Data show mean and SD values from 3 experiments using duplicate samples from 3 independent volunteers. p=0.836 by 2-way ANOVA. IL-8 concentration in the supernatant of unstimulated and SA-stimulated neutrophils (left hand condition), A549s incubated for 24 h in the filter-sterilised supernatant of control medium or SA alone (middle condition) and A549s incubated for 24 h in the filter-sterilised supernatant of unstimulated neutrophils or neutrophils exposed to live SA (right hand condition) (B). Data show mean and SD values of duplicate ELISA wells from 3 experiments using samples from 3 independent volunteers. ****p<0.0001 by 2-way ANOVA.

5.2.4 Effect of src kinase inhibition on neutrophil-mediated epithelial inflammation

Results: Figure 5-4 opposite, Figure 5-5 (overleaf) and Figure 5-6 (overleaf) show IL-8, MCP-1 and LDH release from A549 cells in Step 4 respectively. In Figure 5-4 A and B, PP1 and dasatinib pre-treatment appears to attenuate the release of an unknown pro-inflammatory soluble factor from neutrophils exposed to SA, indirectly leading to significantly reduced release of pro-inflammatory IL-8 from A549 cells.

Comments: Interestingly, supernatant from neutrophil:SA interactions induces the release of almost double the amount of IL-8 from A549 cells than from neutrophil:EC interactions, also suggesting that SA NCTC 8325 is more virulent and pathogenic at a similar MOI.

These observations are consistent with the A549 monolayer appearances displayed in Figure 5-2 except that the indirect reduction in IL-8 release due to src kinase inhibition of neutrophils is not matched by improved monolayer integrity.

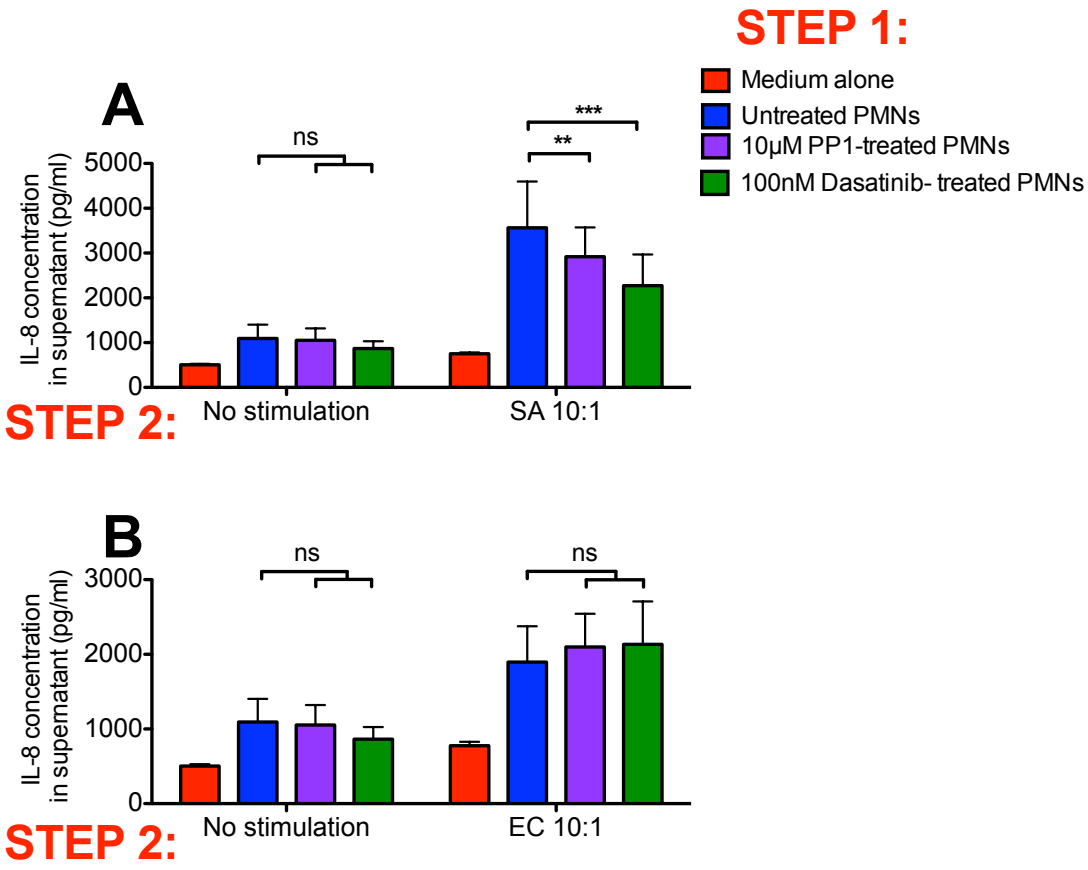

Figure 5-4 PP1 and Dasatinib treatment of neutrophils exposed to SA results in an attenuated IL-8 release from A549 cells

IL-8 release from A549s incubated for 24 hours in filter-sterilised, serum-free supernatants from healthy neutrophils pre-treated with 10 μM PP1 or 100 nM dasatinib and exposed to live SA (A) or live EC (B). Data show mean and SD values of duplicate ELISA wells from 2 experiments, each using samples from 3 independent volunteers (total n=6). $p<0.0001$ (A) and $p=0.0316$ (B) by repeated measures ANOVA; $^{**}p<0.01$, $^{***}p<0.001$ by Dunn's post-hoc test comparing treated with control untreated neutrophils.

Comments: MCP-1 is released by endothelial cells. There is some in vitro evidence to suggest it can actually be released by neutrophils in response to the products of GM-CSF-treated mononuclear cells and may represent the link between neutrophils and the adaptive immune response (Yamashiro et al. 1999). As discussed in Chapter 4, it may be of particular importance in ALI and ARDS because monocyte recruitment appears to control the later phases of neutrophil migration in established murine LPS-induced acute lung inflammation (Dhaliwal et al. 2012). In Figure 5-5 opposite, the opposite pattern to IL-8 occurs, in that the intial pre-treatment of neutrophils with PP1 and dasatinib in Step 1 appears to indirectly result in increased MCP-1 release from A549s when the neutrophils are stimulated by SA in Step 2. Similar findings are not seen with *E. coli*.

The finding in Figure 5-5A is difficult to explain but there is evidence to suggest that in epithelial cells, MCP-1 is conversely anti-inflammatory in its action, promoting airway epithelial cell repair. In cultured bronchial epithelial cells, MCP-1 is expressed in response to monolayer injury and acts in an autocrine manner on its CCR2B receptor to promote proliferation and haptotaxis (Lundien et al. 2002). This repair mechanism may also be present in alveolar epithelial cells and may explain my findings, suggesting indirect ‘pro-resolutionary’ effects of src kinase inhibition of neutrophils.

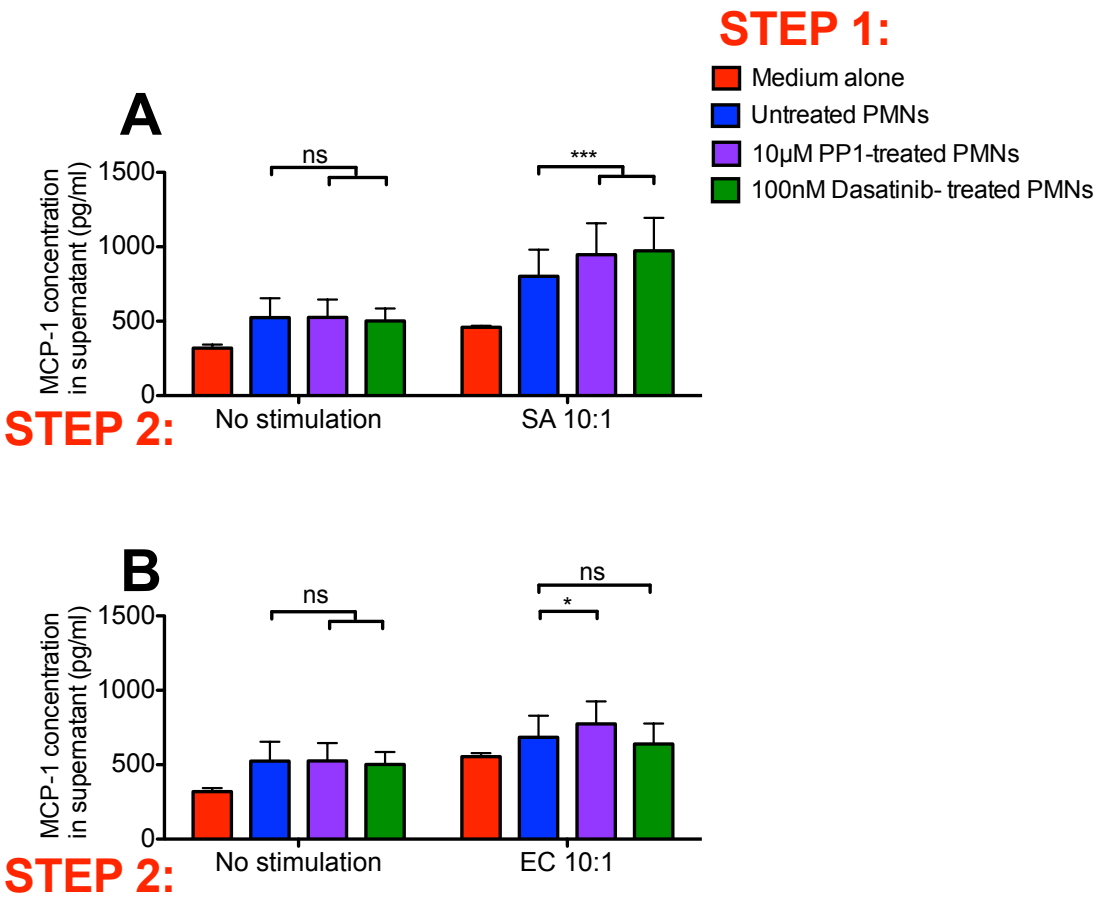

Figure 5-5 PP1 and Dasatinib treatment of neutrophils exposed to SA and EC results in an increased MCP-1 release from A549 cells

MCP-1 release from A549s incubated for 24 hours in filter-sterilised, serum-free supernatants from healthy neutrophils pre-treated with 10 μM PP1 or 100 nM dasatinib and exposed to live SA (A) or live EC (B). Data show mean and SD values of duplicate ELISA wells from 2 experiments, each using samples from 3 independent volunteers (total n=6). p=0.0003 (A) and **p=0.0011 (B) by repeated measures ANOVA; **p<0.01, ***p<0.001 by Dunn's post-hoc test comparing treated with control untreated neutrophils.

Comments: To estimate epithelial cell damage, I also measured relative LDH release from A549s in the experiments above. In Figure 5-6 below, supernatant from untreated neutrophil:bacterial interaction induces LDH release from A549s, when both SA or EC are used. Pre-treatment of the neutrophils with PP1 or dasatinib reduces this indirect A549 damage when using SA, in the same pattern as IL-8. Such an effect is not seen when using EC; indeed dasatinib appears to potentiate the damage. As with IL-8 release, the difference in effect between SA and EC is likely to be related to their differing mechanisms of virulence.

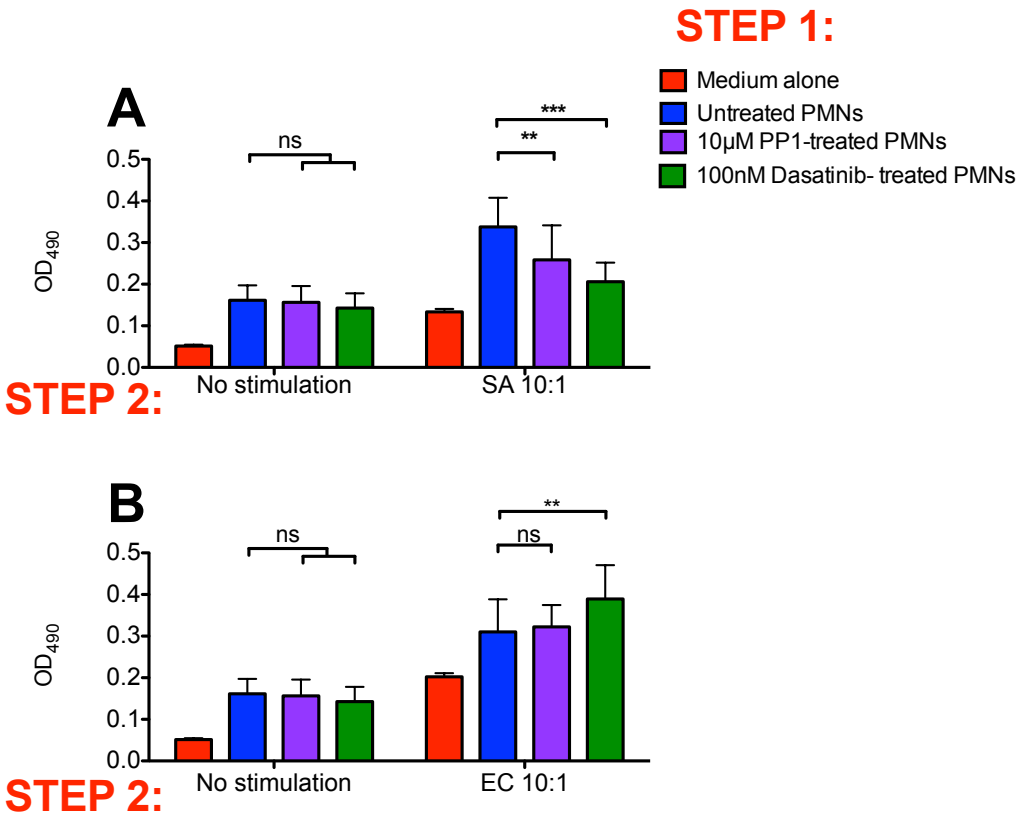

Figure 5-6 PP1 and Dasatinib treatment of neutrophils exposed to SA results in reduced A549 cell damage
LDH release from A549s incubated for 24 hours in filter-sterilised, serum-free supernatants from healthy neutrophils pre-treated with 10 μM PP1 or 100 nM dasatinib and exposed to live SA (A) or live EC (B). Data show mean and SD values of duplicate LDH assay wells from 2 experiments, each using samples from 3 independent volunteers (total n=6). ***p=0.0003 (A) and **p=0.003 (B) by repeated measures ANOVA; **p<0.01, ***p<0.001 by Dunn's post-hoc test comparing treated with control untreated neutrophils.

5.3 Can Src Kinase Inhibition of Neutrophils from Critically Ill Patients Reduce Toxicity to A549 cells?

In these experiments I translated my findings from Section 5.2 into a clinical setting to test whether src kinase inhibition of neutrophils from critically ill patients affects their ability to induce indirect damage and inflammation in epithelial cells. Such patients are a very heterogenous group, with numerous different sterile and non-sterile precipitating factors. As discussed in the methods in Chapter 2, these patients were all admitted to an ICU within the previous 48 hours, with evidence of SIRS and requiring support of at least one organ, and expected to survive beyond a further 48 hours after recruitment.

5.3.1 *Neutrophils from critically ill patients exhibit impaired phagocytosis and bacterial killing*

Patients: Neutrophils from a total of 6 critically ill patients were used in experiments. As patient recruitment was unpredictable and usually limited to 1 patient at once, I recruited non-matched healthy controls on the same day and carried out the experiments simultaneously. In total, 5 experiments were carried out, 1 of which involved 2 critically ill patients and 1 healthy volunteer and another involved 1 critically ill patient and 2 healthy volunteers.

As neutrophils from critically ill patients show marked variability in experimental assays, any statistical comparisons were made using non-parametric tests (Mann Whitney test for 2 conditions and the Kruskal-Wallis test with Dunn's post-hoc correction for >2 conditions).

Results: Table 5-1 shows the basic demographic data of the two groups together with some basic measures of neutrophil phagocytic and killing function. The patients were significantly older with poorer in vitro neutrophil function. They were a relatively unwell group, with a median APACHE II score of 24.5, predicting an in-hospital mortality rate of 40% (Knaus et al. 1985). Four patients had pneumonia, one patient had pancreatitis and one patient had just undergone an emergency laparotomy.

	Critically ill patients	Healthy controls	p value
Number	6	6	
Age (yrs): median (range)	76 (43-82)	30 (23-34)	**0.0022
APACHE II score: median (range)	24.5 (15-30)	n/a	n/a
Phagocytosis of zymosan particles (%): median (range)	51 (44.1-64)	74 (63.9-76.2)	**0.0043
Bacterial killing (SA fold change after 30 min): median (range)	0.18 (-0.143 to +0.349)	-0.34 (-0.623 to +0.002)	*0.026

Table 5-1 Demographics, neutrophil phagocytosis and bacterial killing rates of critically ill and control groups
Groups compared using Mann Whitney test

Results: Figure 5-7 below and Figure 5-8 A overleaf show the results of Table 5-1 in graphical form. The control group is poorly matched for age and this may have a bearing on inherent neutrophil function.

Comments: It is well described that increasing age is associated with reduced phagocytic and bactericidal activity, perhaps due to increased calcium concentration in resting neutrophils. This age effect is actually minimal in assays involving live *E. coli,* in which mean phagocytic and bactericidal activities are 74% and 59% respectively in a 62-83 yr old age group compared to 91% and 64% in a 21-36 yr old group (Wenisch et al. 2000). An age effect has previously been demonstrated in the opsonised zymosan assay, in which mean zymosan phagocytosis drops from 61% (21-45 yr old group) to 39% (66-94 yr old group) (Mege et al. 1988). However, using identical experimental protocols to myself, Conway Morris showed that neutrophil phagocytosis was 36% lower in 72 critically ill patients than 21 sex and age-matched healthy volunteers and that the effect is associated with level of C5a exposure (Conway Morris et al. 2009). I observed a comparable level of reduction of 23% using a smaller unmatched group size, suggesting that in these assays, differences are mainly due to critical illness. Other additional factors such as concurrent pharmacological treatment should be considered when interpreting the results.

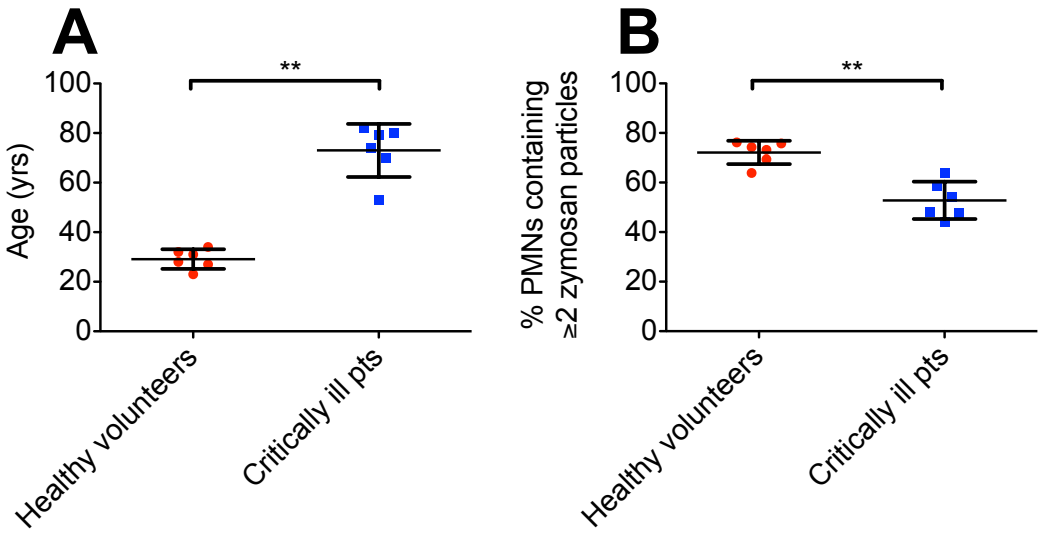

Figure 5-7 Critically ill patients are significantly older with poorer neutrophil phagocytosis
Comparison of ages of healthy volunteers and critically ill patients (A). Neutrophils isolated from healthy volunteers or critically ill patients containing at least 2 serum-opsonised zymosan particles after 30 min exposure (B). Data show median and IQR values from 5 experiments using a total of 6 individuals per group. **p=0.0022 (A), **p=0.0043 (B) by Mann Whitney test.

Results: As shown in Figure 5-8 B opposite, pre-treatment of neutrophils from critically ill patients with PP1 or dasatinib neither improved nor reduced ex vivo killing of live PA01 in suspension.

Comments: The results are consistent with the in vitro findings in healthy neutrophils described in Chapter 3, but they contradict the in vivo findings described in Chapter 4, in which bacterial clearance is impaired by treatment with dasatinib.

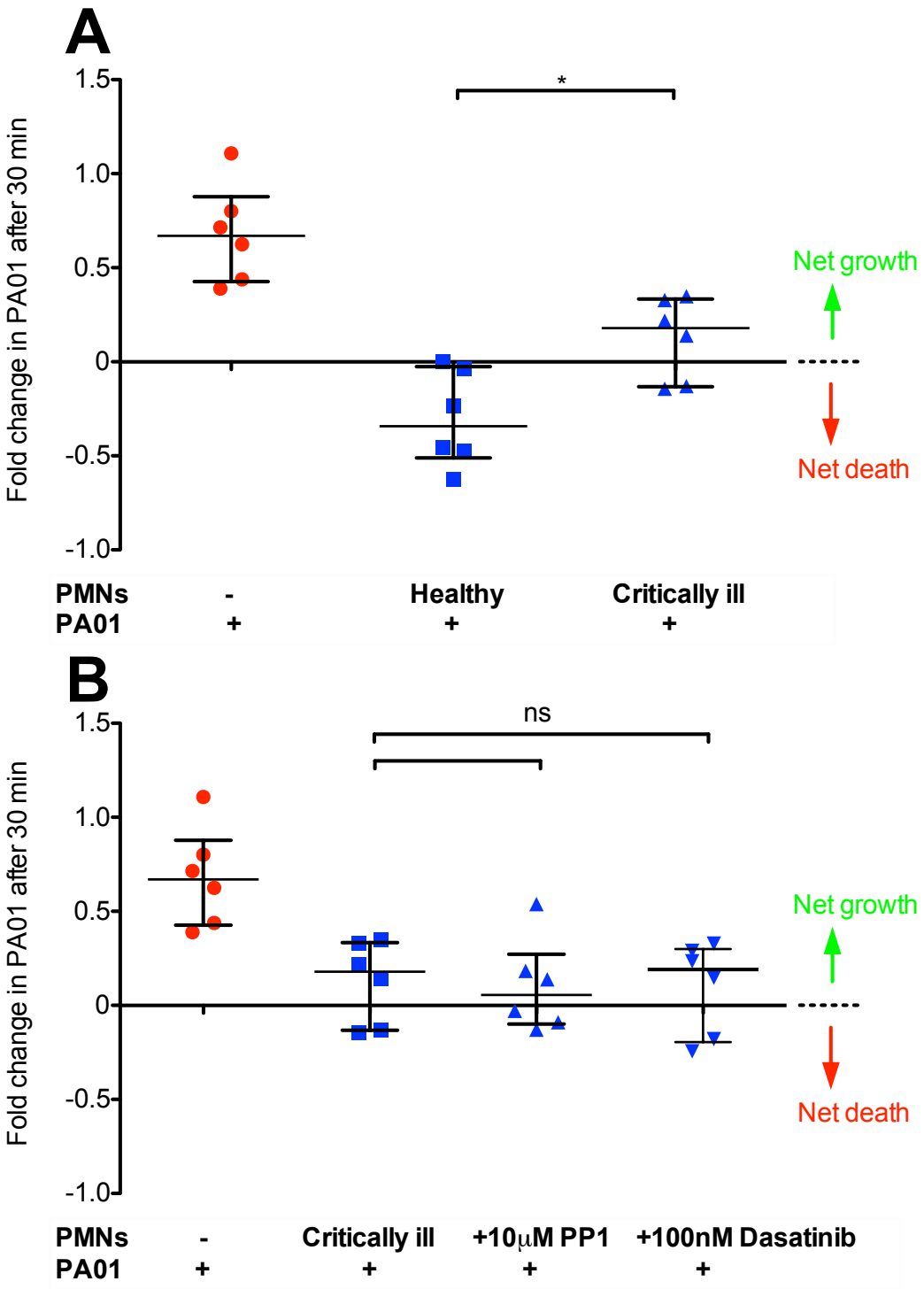

Figure 5-8 Impaired bacterial killing by neutrophils from critically ill patients is not affected by treatment with PP1 or Dasatinib

Viable PA01 in cfu/ml after 30 min incubation in control medium and with neutrophils from healthy volunteers or critically ill patients (MOI~10 PA01:1 PMN) (A). Viable PA01 after incubation in control medium and with neutrophils from critically ill patients pre-treated with control medium, 10 μM PP1 or 100 nM dasatinib (B). Data show median and IQR values of duplicate colony counts from 5 experiments using neutrophils from 6 individual patients and 6 volunteers. *p=0.026 by Mann Whitney test (A) and p=0.8948 by Kruskal-Wallis test (B).

5.3.2 Variation in experimental design

Figure 5-9 opposite shows the slight variation in the experimental protocol described above that I used to be able to test whether neutrophils from critically ill patients induce more epithelial cell inflammation and damage, and if so, whether treatment with PP1 or dasatinib attenuates this. The 30 min step involving bacterial stimulation was therefore removed. Both healthy volunteer and patient neutrophils were left untreated or exposed to 10 μM PP1 or 100 nM dasatinib for 30 min (**Step 1**), before washing twice to remove PP1/dasatinib. In these experiments the neutrophils themselves were transferred to separate wells on a 24 well plate containing A549 epithelial cells at ~70% confluence.

The reasons for changing the protocol to use neutrophils themselves rather than their supernatant were: i) the model was more representative of an inflamed alveolus in which neutrophils and alveolar epithelial cells are in direct contact and ii) a clear difference in baseline neutrophil function between the two groups was demonstrated and I felt that this difference would not adequately be transmitted to A549 cells via a 30 min release into fresh supernatant without stimulation.

Neutrophils were initially placed both in direct contact with the A549s and suspended just above them by a 0.4 μm pore-sized Transwell filter, through which only soluble factors can cross. Fresh serum-free IMDM (no phenol red) was added to each well and the cells incubated for 24 h (**Step 2**). A549 cell inflammation and damage were measured in the same way as described in Section 5.2.1 (**Step 3**)

Figure 5-9 Experimental design for section 5.3

5.3.3 Neutrophils from critically ill patients disrupt epithelial cell integrity

Results: Interestingly, neutrophils from both healthy volunteers and patients induce a similar degree of A549 monolayer disruption and this effect appears slightly less marked when neutrophils are separated from the A549s by a filter (Figure 5-10 opposite 2nd and 3rd rows). After 24 h incubation in culture medium, around 50% of neutrophils become apoptotic with some cell death (see Figure 5-16 below); that may account for this effect. Src kinase inhibition has no effect on rates of apoptosis in vitro (Chapter 3). Neutrophil pre-treatment with PP1 (4th row) or dasatinib (5th row) appears to have no effect on A549 monolayer disruption in both groups.

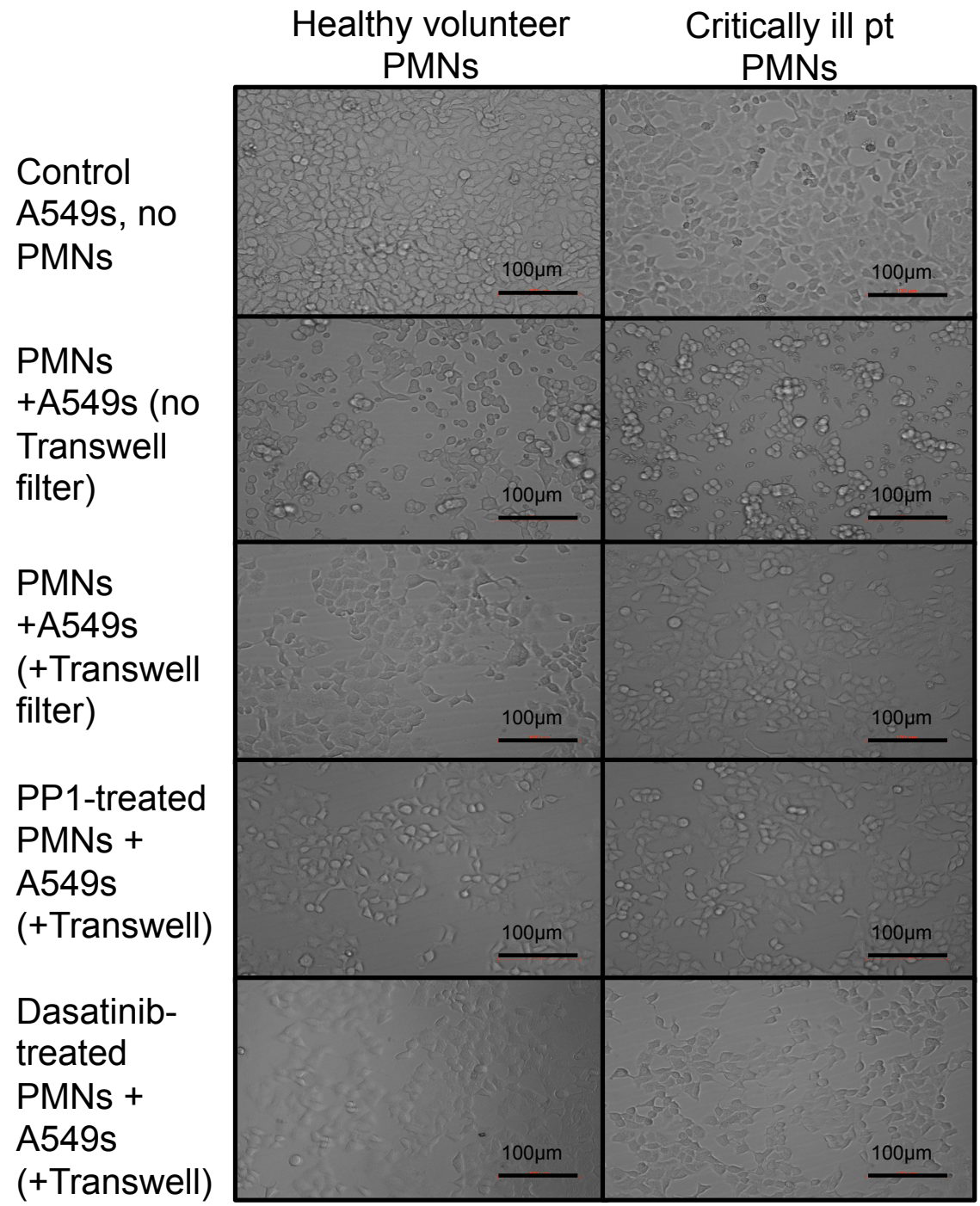

Figure 5-10 Treatment of neutrophils from healthy volunteers or critically ill patients with PP1 and Dasatinib does not reduce neutrophil-mediated inflammatory damage to A549 epithelial cell monolayer

X200 representative images of confluent A549 monolayers incubated for 24 hours either in serum-free medium (top row), or with direct contact with neutrophils isolated from healthy volunteers or critically ill patients (second row), or neutrophils suspended above a 0.4µm Transwell filter (third row), pre-treated with 10 µM PP1 (fourth row) or 100 nM dasatinib (bottom row). Images taken from 5 experiments using samples from 6 critically ill patients and 6 independent volunteers per group.

5.3.4 Neutrophils from critically ill patients induce more epithelial cell inflammation: control experiments

I carried out the following control experiment to investigate whether measured IL-8, MCP-1 or LDH was released from A549s or neutrophils, or both.

Results: Figure 5-11 opposite shows that A549 cells release significant quantities of IL-8, MCP-1 and LDH when exposed to neutrophils from critically ill patients. This effect is more marked when the neutrophils are in direct contact with the A549 cells.

Comments: Although quiescent neutrophils or A549s incubated on their own for 24 h release minimal IL-8 and LDH, it is highly likely that in co-culture the release of these markers comes from both cell types. However the peak levels were approximately 4000pg/ml (IL-8) and an OD_{490} of ~0.4 (LDH), similar to the levels released over 24 h by A549s alone in the experiments displayed in section 5.2.4 above, suggesting that the majority of the release is likely to come from A549 cells. MCP-1 has only been shown to be expressed by neutrophils in response to stimulated mononuclear cells, so any release observed in these experimental conditions should come from A549 cells alone.

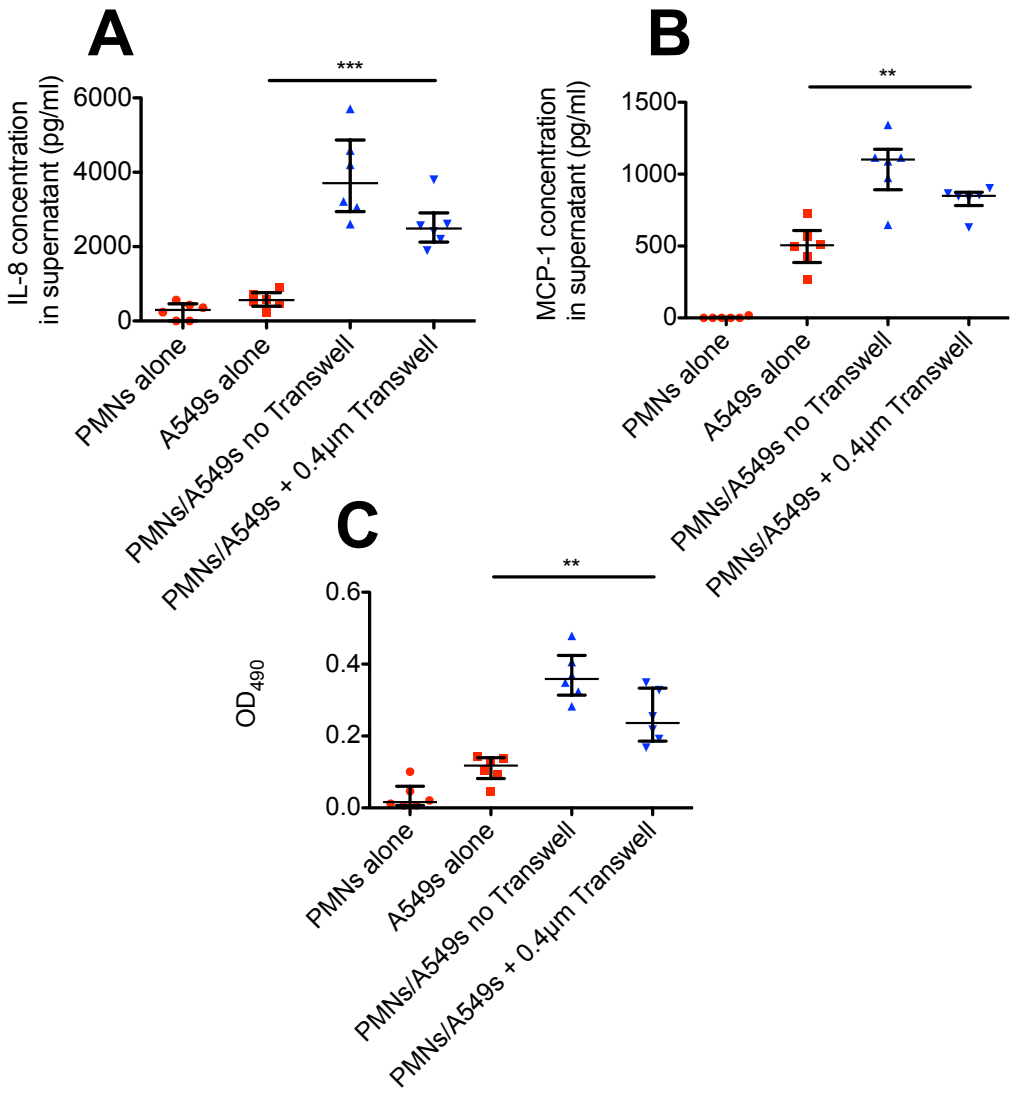

Figure 5-11 Control experiments to demonstrate A549 cell inflammation and damage from interaction with neutrophils

Supernatants from critically ill neutrophils alone, A549s cells alone, A549s and neutrophils in direct contact, or separated by 0.4µm Transwell filters tested for IL-8 levels (A), MCP-1 levels (B) and LDH activity (C). Data show median and IQR values from 5 experiments using samples from 6 critically ill patients in duplicate assay wells. ***p=0.001 (A), **p=0.002 (B) and **p=0.002 (C) by Kruskal-Wallis test comparing all conditions except PMNs alone.

5.3.5 Neutrophils from critically ill patients induce more epithelial cell inflammation and damage

Results: Comparing the effect of neutrophils from both groups on epithelial cells in Figure 5-12 opposite, it is clear that neutrophils from critically ill patients induce more IL-8 and LDH release, with a small increase in MCP-1 release when separated by a filter membrane.

Comments: As discussed, this pattern of results could conceivably be explained by release of IL-8 and LDH directly from activated neutrophils themselves in the critically ill patient group. It seems more likely to come from the A549s in response to a soluble factor released from the neutrophils. My results are consistent with a previous member of our research group (Dr Conway Morris, personal communication).

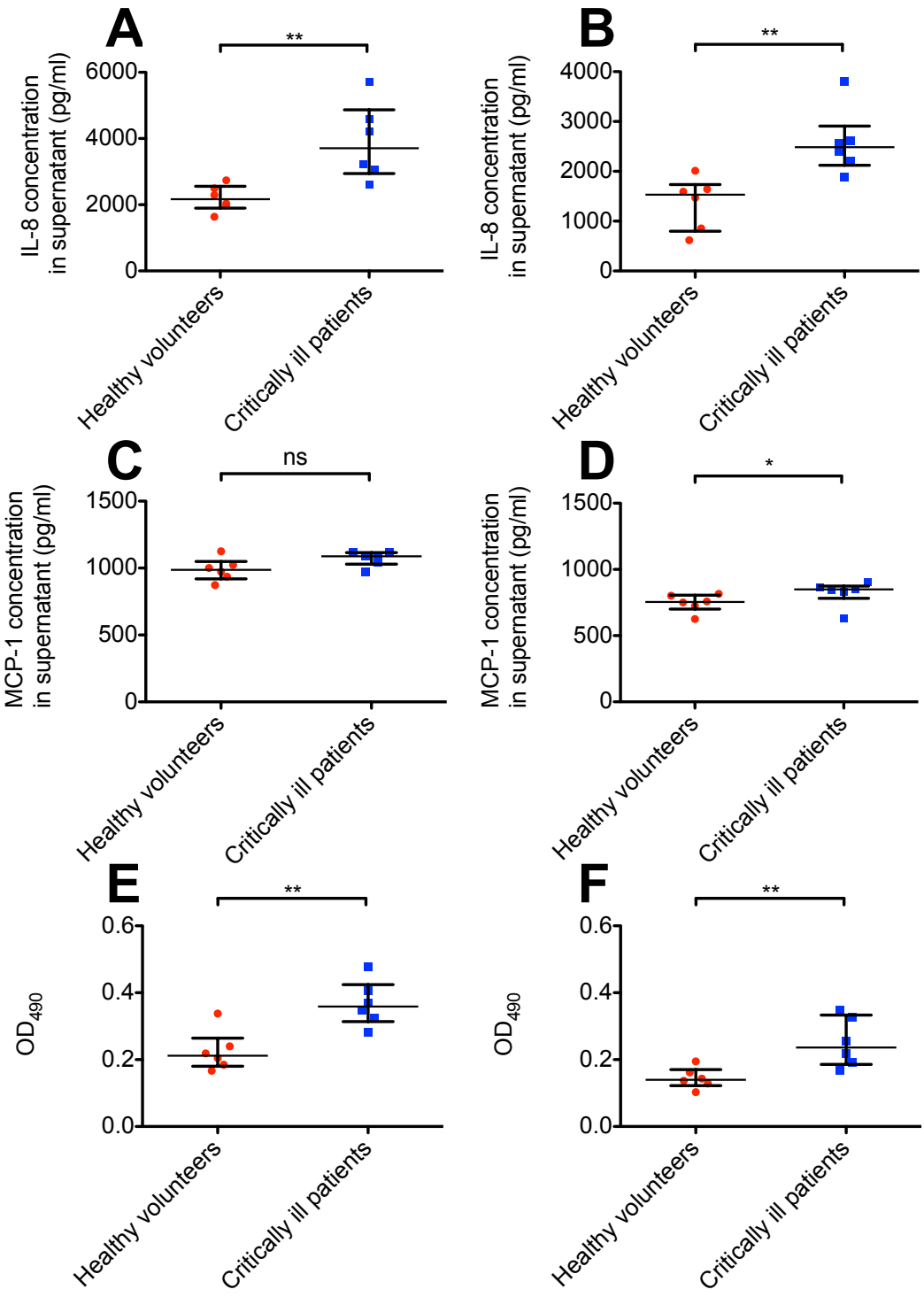

Figure 5-12 Neutrophils from critically ill patients induce more epithelial cell inflammation and damage through release of a soluble factor

Supernatants from A549 monolayers incubated for 24 hours with neutrophils from healthy volunteers or from critically ill neutrophils maintained in direct contact (A, C and E) or separated by 0.4μm Transwell filters (B, D and F) tested for IL-8 levels (A+B), MCP-1 levels (C+D) and LDH activity (E+F). Data show median and IQR from 5 experiments using samples from 6 critically ill patients and 6 independent volunteers in duplicate assay wells. **p=0.0043 (A), **p=0.0043 (B), p=0.132 (C), *p=0.0411 (D), **p=0.0087 (E), **p=0.0087 (F) by Mann Whitney test.

5.3.6 Neutrophils from critically ill patients induce more epithelial cell inflammation and damage: effect of src kinase inhibition

If there is a direct pro-inflammatory and cytotoxic effect of neutrophils from critically ill patients on alveolar epithelial cells, can this effect be reduced by src kinase inhibition? For these experiments, I chose to only pre-treat neutrophils separated from A549s by a filter with PP1 and dasatinib because the effects on A549 cells appeared less marked and could potentially be manipulated.

Results: In Figure 5-13 opposite there is a small, but non-significant, effect of both PP1 and dasatinib pre-treatment on both IL-8 and LDH release, with no effect on MCP-1 release.

Comments: With more samples per group, there may be a significant effect. Again, it is impossible to confidently conclude that any effect is not due to a direct inhibitory effect of PP1 or dasatinib on neutrophil release of IL-8 or LDH.

Assuming that src kinase inhibition with PP1 or dasatinib inhibits degranulation of neutrophils from critically ill patients in a similar way to healthy volunteer neutrophils, the results above suggest that the soluble factor(s) responsible for epithelial cell inflammation is unlikely to be a product of neutrophil degranulation. There are many potential culprits, including ROS/RNS, cytokines and chemokines, serine proteases such as neutrophil elastase, matrix metalloproteinases such as MMP-8 and MMP-9, neutrophilic-derived cationic peptides such as LTF, LL-37 and defensins (Grommes & Soehnlein 2011).

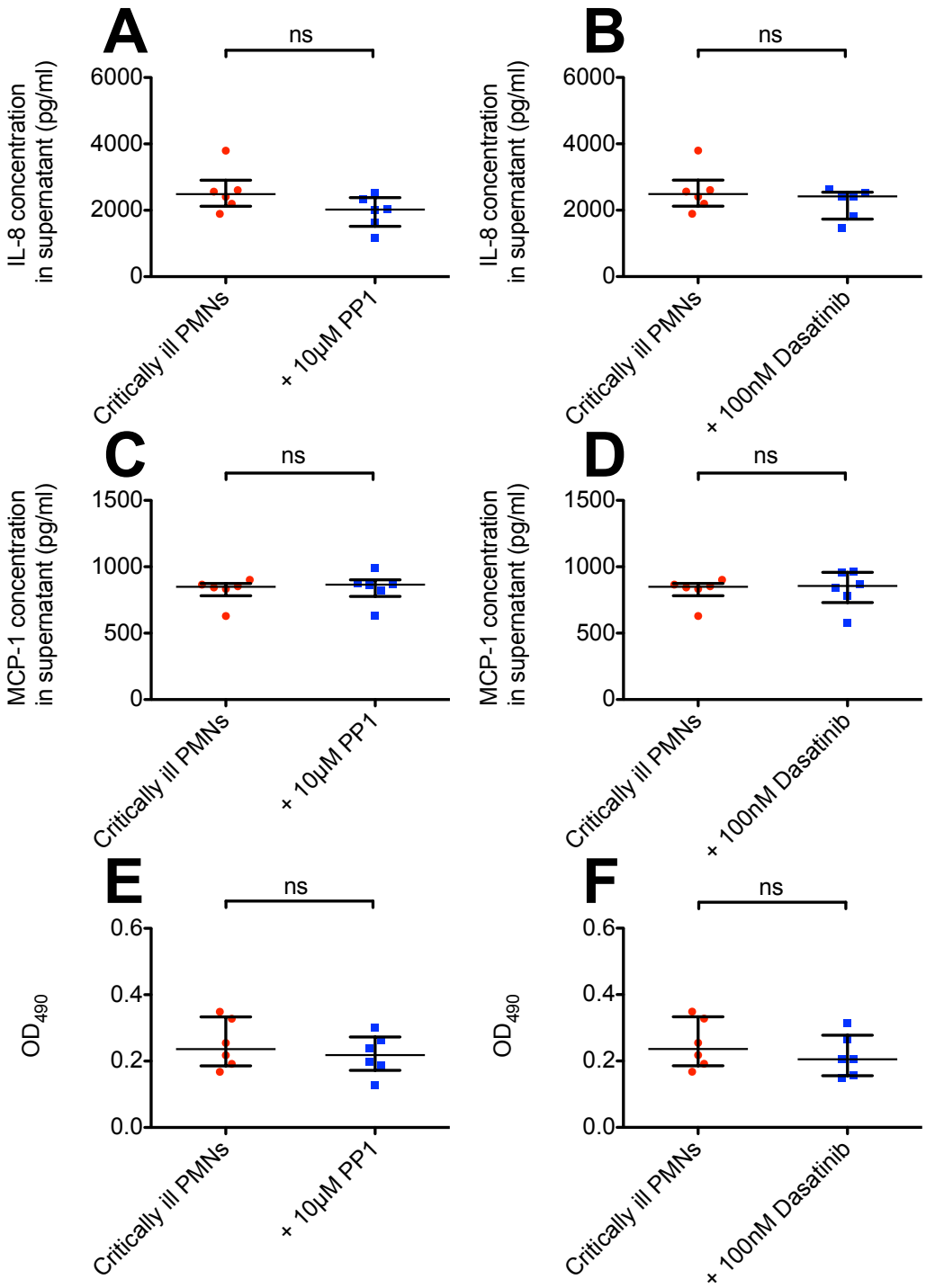

Figure 5-13 Treatment of neutrophils from critically ill patients with PP1 or Dasatinib does not reduce epithelial cell inflammation and damage

Supernatants from A549 monolayers separated by a 0.4μm Transwell filter from untreated neutrophils from critically ill patients and neutrophils pre-treated with 10 μM PP1 (A, C and E) and 100 nM dasatinib (B, D and F) tested for IL-8 levels (A+B), MCP-1 levels (C+D) and LDH activity (E+F). Data show median and IQR values from 5 experiments using samples from 6 critically ill patients. p=0.0931 (A), p=0.589 (B), p=0.589 (C), p=0.818 (D), p=0.589 (E), p=0.394 (F) by Mann Whitney test.

5.4 Indirect Effects of Src Kinase Inhibition on Macrophage Efferocytosis of Apoptotic Cells

This section describes my final experiments aimed to test the effect of src kinase inhibition of neutrophils on a vital component of 'normal' acute lung inflammation: alveolar repair and efferocytosis of apoptotic cells. I hypothesised that an anti-inflammatory treatment such as this would push the balance towards resolution and result in improved apoptotic cell clearance in a simple in vitro model of macrophage efferocytosis of apoptotic neutrophils.

5.4.1 Experimental design and assay optimisation

Experimental methods for culturing apoptotic neutrophils and measuring macrophage phagocytosis of apoptotic neutrophils by staining for neutrophilic expression of MPO are described in detail on page 54. The basic experimental protocol used in section 5.2 above was adjusted slightly as shown below in Figure 5-14 opposite.

As previously, neutrophils from healthy volunteers were pre-treated with 10 μM PP1 or 100 nM dasatinib with appropriate controls (**Step 1**), before washing twice to remove PP1/dasatinib and stimulating with *S. aureus* or *E. coli* at an MOI of ~10:1 with an unstimulated control (**Step 2**). The filter-sterilised supernatant of each tube was transferred to separate wells of a 24 well plate containing 7 day old cultured MDMs from a different healthy volunteer and the medium supplemented with 10% serum (autologous to the MDM volunteer). Apoptotic neutrophils cultured overnight from a separate healthy volunteer were washed thoroughly before adding to the MDMs at an MOI of 4 apoptotic neutrophils: 1 MDM (**Step 3**). Autologous serum was found to be necessary to opsonise the non-autologous apoptotic cells for optimum levels of phagocytosis. In serum-free conditions I observed a complete absence of MDM phagocytosis.

After 24 h culture at 37^{o}C at 5% CO_2, each supernatant was carefully removed, centrifuged to remove cell debris and the supernatant frozen at -80^{o}C for cytokine analysis. Each well containing MDMs was washed gently with warm PBS- to remove non-adherent apoptotic neutrophils before drying, fixing and staining for MPO (**Step 4**).

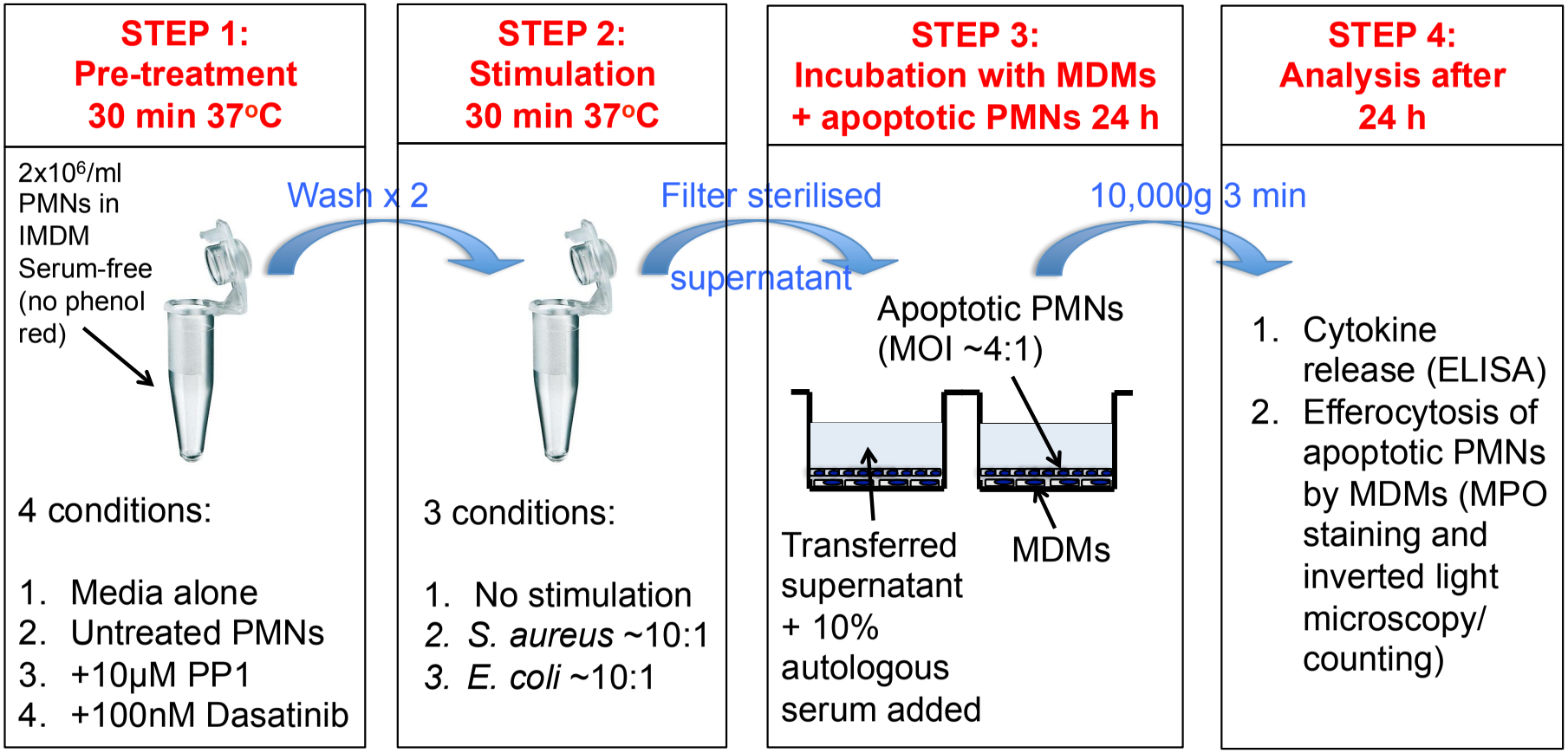

Figure 5-14 Experimental design for section 5.4

Figure 5-15 A-D opposite show the dramatic change in appearance and size as peripheral blood mononuclear cells (A and C) differentiate and mature into the typical “fried egg” appearance of MDMs (B and D) by day 7 in culture. Images E and F show the change in morphology from peripheral blood neutrophils to apoptotic cells after overnight culture, with condensation of nuclear material into dark-staining nuclear bodies. Image G shows the typical appearances of ‘normal’ in vitro MDM phagocytosis of apoptotic neutrophils and image H shows impaired clearance.

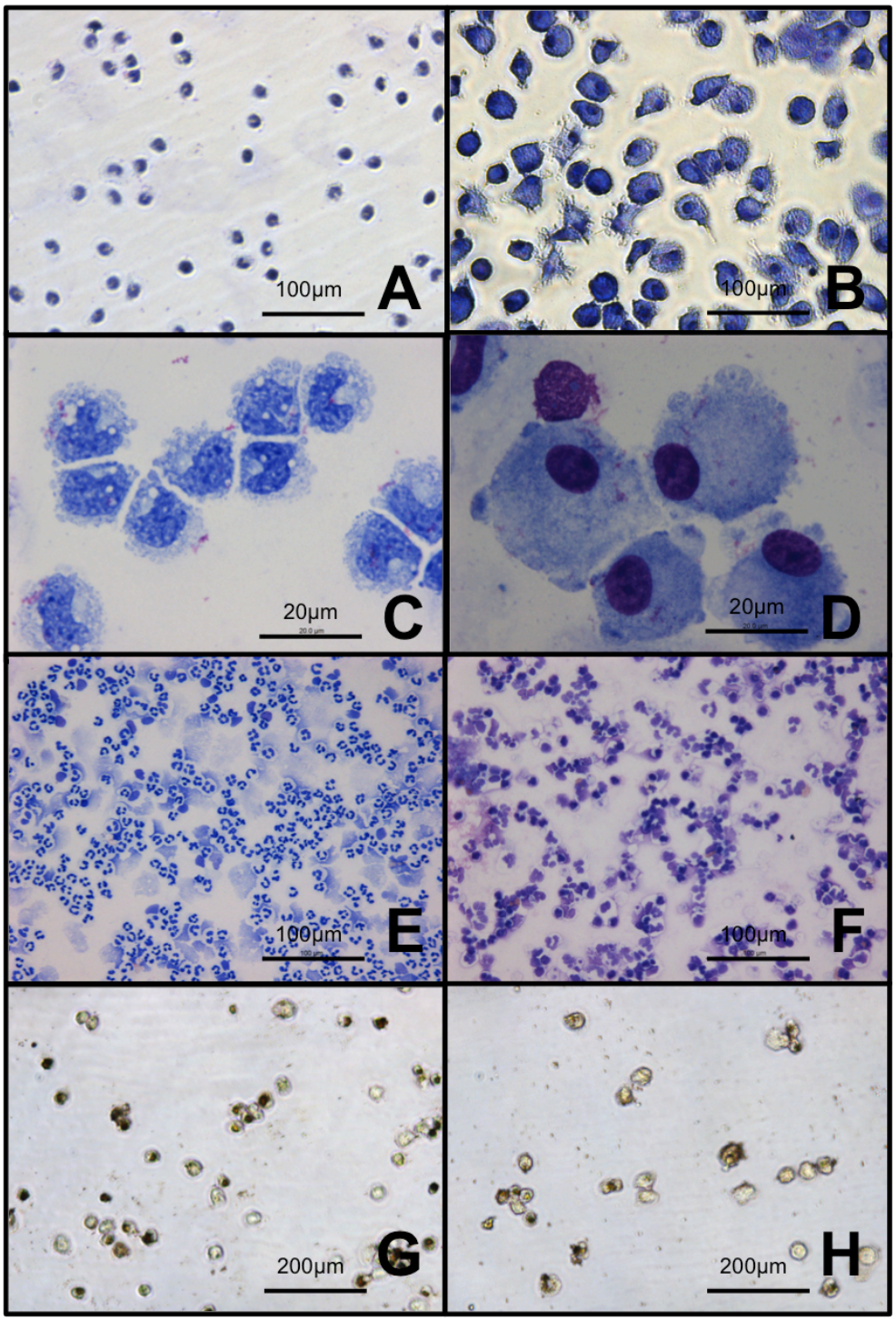

Figure 5-15 Culture of MDMs, apoptotic neutrophils and phagocytosis of apoptotic neutrophils by MDMs

X200 representative images of purified monocytes adherent to tissue culture plastic on day 0 (A) and after 7 days in culture to differentiate into MDMs (B). X1000 representative images of cytocentrifuge preparations of purified monocytes at day 0 (C) and after 7 days in culture to differentiate into MDMs (D). X200 representative images of cytocentrifuge preparations of purified neutrophils using Percoll method (E) and after 24 h of culture in IMDM/0.5% BSA at 37^{o}C/5% CO_2 to promote neutrophil apoptosis (F). X100 representative images of MDMs (clear cells) demonstrating normal (G) and impaired (H) phagocytosis of apoptotic neutrophils (brown dots), after MPO staining with H_2O_2 and dimethoxybenzidine. Images taken from > 8 individual experiments.

Figure 5-16 below shows a typical percentage of neutrophils of ~50% undergoing apoptosis in overnight culture in my optimisation experiments. Other groups quote higher rates of at least 70-80% (Professor A Rossi's group, Edinburgh, UK, personal communication). It is possible that these relatively low rates of apoptosis are due to inadvertent neutrophil activation during the isolation process from citrated blood.

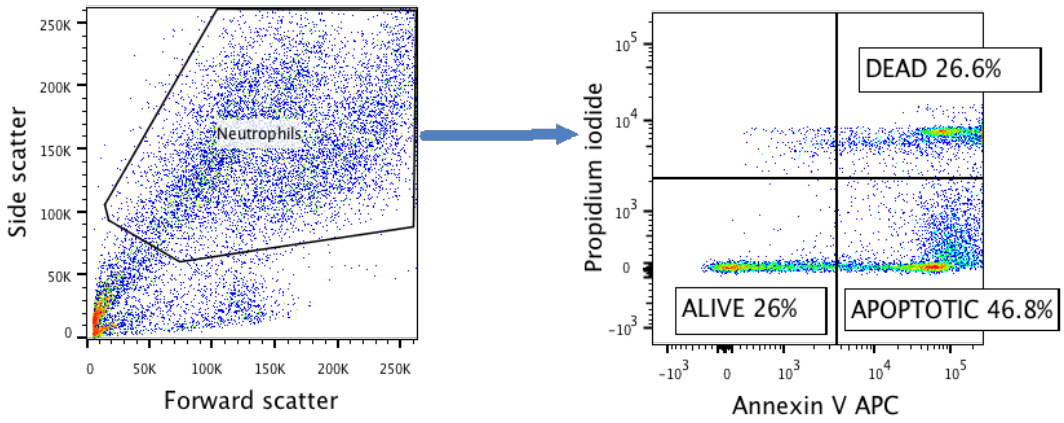

Figure 5-16 Neutrophils become apoptotic after 24 h in culture
Representative flow cytometric plot showing PI and Annexin V APC staining on neutrophils incubated for 24 h in IMDM/0.5% BSA at 37°C/5% CO_2. Almost half of all gated neutrophil events are apoptotic with high Annexin V staining but low PI staining. Representative plot taken from 3 control experiments.

5.4.2 Effects on MDM pro/anti-inflammatory cytokine release: control experiments

As discussed in the methods in Chapter 2, a combination of pro-inflammatory (IL-6, IL-8, TNFα, MCP-1, IL-1β) and anti-inflammatory (IL-1RA, IL-10) cytokines were initially tested in the MDM/apoptotic cell supernatant. TNFα, IL-6, IL-1β and IL-10 were virtually undetectable even in neat media in control experiments. This may be due to using a relatively low concentration of 2.5 x 10^5 MDMs per well in a total medium volume of 750µl.

IL-8 (neutrophil recruitment) and MCP-1 (monocyte recruitment) were therefore routinely assayed in addition to IL-1RA. IL-1RA is a natural inhibitor of the pro-inflammatory cytokine IL-1β released by epithelial cells and immune cells. In vitro, its release from macrophages is associated with an alternatively activated 'M2 phenotype' that is broadly immunoregulatory in nature, in contrast to a classically activated 'M1 phenotype' macrophage that is associated with tissue destruction (Mantovani 2006).

It is important to consider when interpreting these experiments that peripheral blood monocytes spontaneously differentiating into MDMs after 7 days in autologous serum exhibit two distinctly different morphologies and phenotypes: i) round cells with higher efferocytosis capacity and IL-10 expression (reminiscent of the M2 phenotype) and ii) spindle-shaped cells with increased oxidative burst potential and chemokine expression (similar to the pro-inflammatory M1 phenotype) (Eligini et al. 2013). This effect was readily apparent on inverted microscopy in my experiments and although not formally quantified, the majority of MDMs at day 7-8 appeared round in morphology (see Figure 5-15B above).

The aim of my control experiments was to investigate the relative contribution of MDMs, 10% serum, neutrophil supernatant and apoptotic neutrophils towards the production of the three measured cytokines.

Results: Figure 5-17 opposite displays the results.

Comments: Apoptotic neutrophils release background IL-8 when incubated on their own, however this is likely to be from residual 'alive' neutrophils (~26% of 'apoptotic cell' population were Annexin V^-/PI^- after 24 h culture – see Figure 5-16 above). Similarly 10% serum alone contains detectable MCP-1 but no IL-8 or IL-1RA.

Peak IL-8 and MCP-1 release, together with a reduced release of IL-1RA appears to occur when MDMs are exposed to both neutrophil supernatant and apoptotic neutrophils. Neutrophil pre-treatment with PP1 or dasatinib does not appear to have an effect on MDM release in the absence of apoptotic neutrophils. Surprisingly, MCP-1 is measurable in the supernatant of both unstimulated and stimulated neutrophils, well above the ELISA assay detection limit of 15.6 pg/ml.

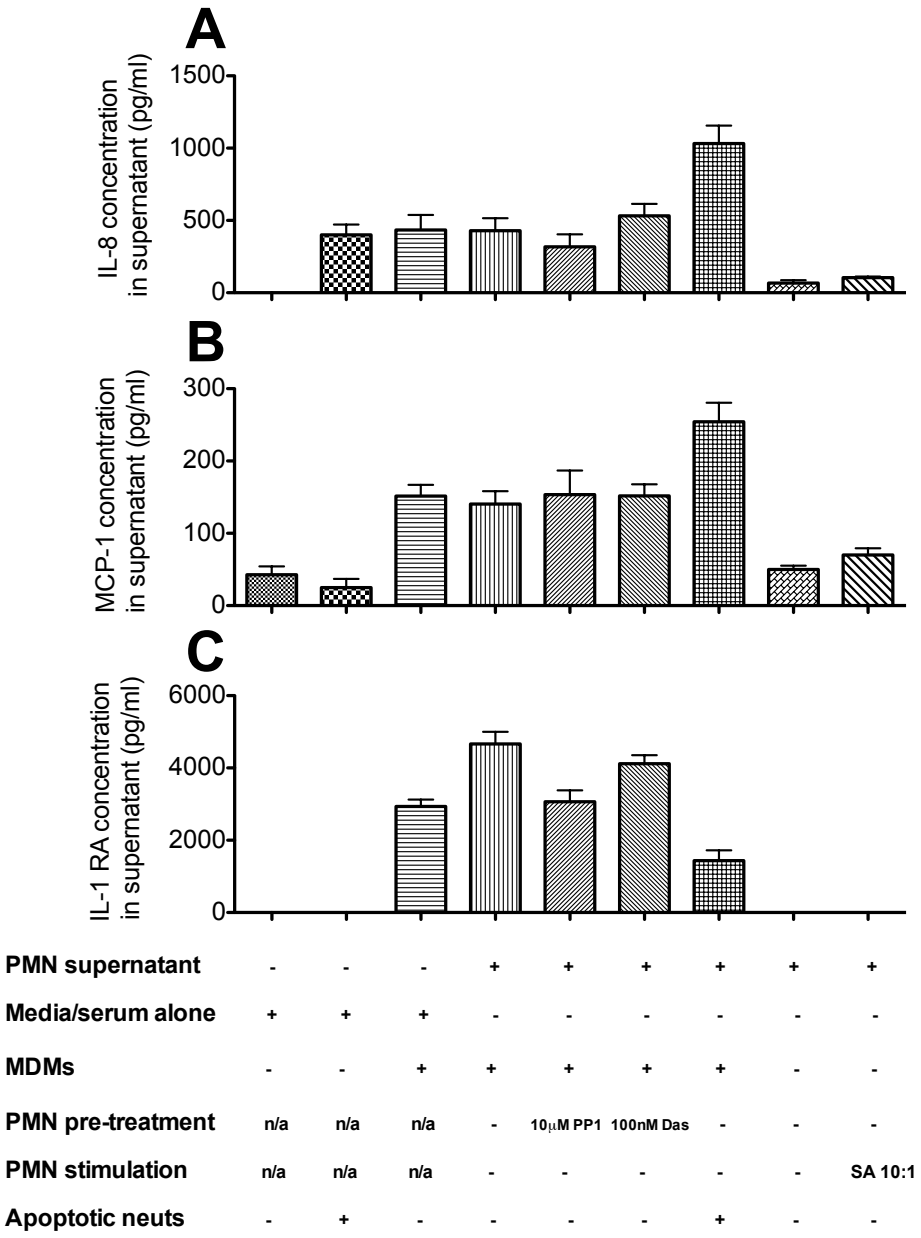

Figure 5-17 Control experiments to demonstrate cytokine release from MDMs

Supernatants for the listed control conditions were tested for the concentrations of IL-8 (A), MCP-1 (B) and IL-1RA (C). Pre-treated and stimulated neutrophils were washed twice in PBS- and the filter-sterilised supernatant transferred to washed MDMs in culture, where indicated. Data show mean and SE values of one control experiment using MDMs from 3 individual volunteers.

5.4.3 Src kinase inhibition of neutrophils: effect on MDM pro/anti-inflammatory cytokine release

Results: In Figure 5-18 opposite and Figure 5-19 overleaf, it is unclear from the pattern of results whether PP1 or dasatinib exert any overall effect.

Comments: Supernatants from bacteria-stimulated neutrophils increase IL-8 release from MDMs in response to apoptotic neutrophils compared to supernatants from unstimulated neutrophils. PP1 or dasatinib pre-treatment of the neutrophils attenuates this effect when either SA (Figure 5-18A) or EC (Figure 5-19A) are used to stimulate the neutrophils. The IL-RA levels are pretty similar across all conditions, with some variability between volunteers, suggesting no major effect. There is no effect on MCP-1 levels when using *S. aureus* and a slight increase in levels with PP1 when using *E. coli*, but no significant effect of dasatinib.

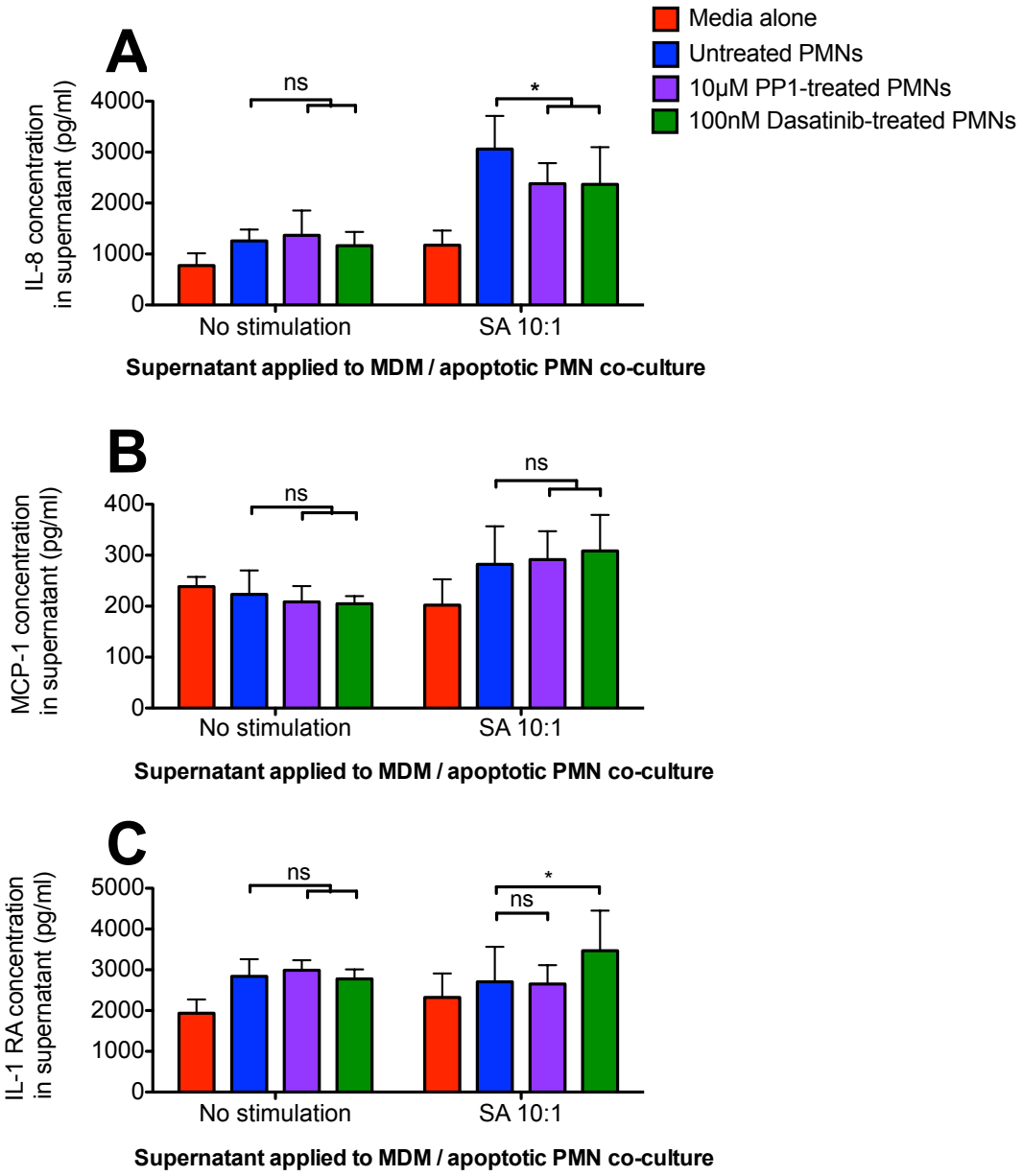

Figure 5-18 PP1 and Dasatinib treatment of neutrophils exposed to SA results in an attenuated IL-8 release from MDMs exposed to apoptotic neutrophils

Il-8 (A), MCP-1 (B) and IL-1RA (C) release from MDMs incubated with non-autologous apoptotic neutrophils for 24 hours in filter-sterilised, 10% autologous serum-supplemented supernatants from healthy neutrophils pre-treated with 10 μM PP1 or 100 nM dasatinib and exposed to live SA. Data show mean and SD values of duplicate ELISA wells from 6 replicate sets of conditions. The 6 replicates were from 2 separate experiments: in each, MDMs were derived from 3 volunteers, apoptotic neutrophils were derived from another volunteer and further donor gave fresh neutrophils to derive supernatants (total n=6). *p=0.0134 (A), p=0.625 (B) and *p=0.0294 (C) for stimulated conditions by repeated measures ANOVA; *p<0.05 by Dunn's post-hoc test comparing treated with control untreated neutrophils.

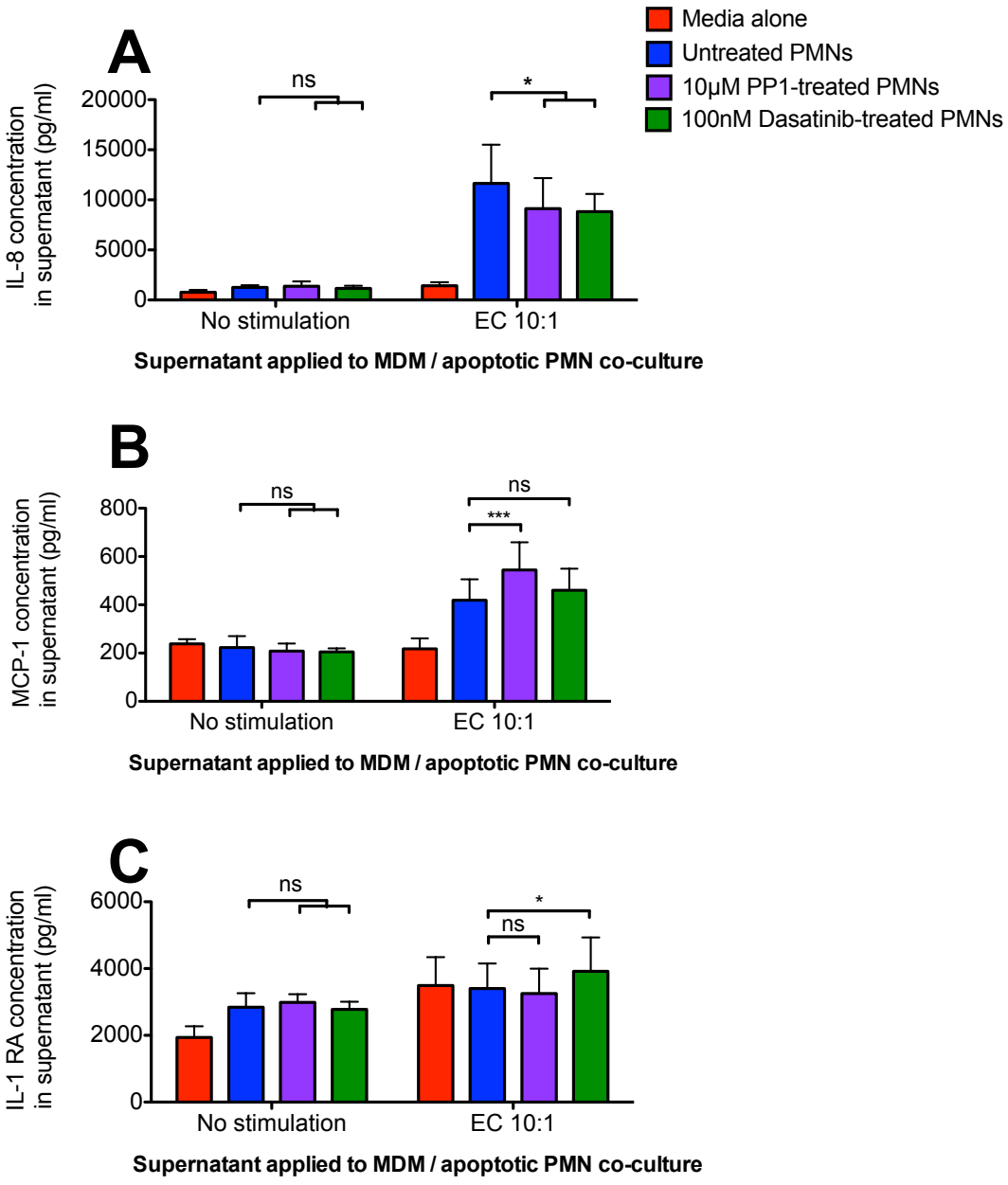

Figure 5-19 PP1 and Dasatinib treatment of neutrophils exposed to EC results in an attenuated IL-8 release from MDMs exposed to apoptotic neutrophils

Il-8 (A), MCP-1 (B) and IL-1RA (C) release from MDMs incubated for 24 hours with non-autologous apoptotic neutrophils in filter-sterilised, 10% autologous serum-supplemented supernatants from healthy neutrophils pre-treated with 10 μM PP1 or 100 nM dasatinib and exposed to live EC. Data show mean and SD values of duplicate ELISA wells from 6 replicate sets of conditions. The 6 replicates were from 2 separate experiments: in each, MDMs were derived from 3 volunteers, apoptotic neutrophils were derived from another volunteer and further donor gave fresh neutrophils to derive supernatants (total n=6). *p=0.0196 (A), *p=0.0146 (B) and **p=0.01 (C) for stimulated conditions by repeated measures ANOVA; *p<0.05, ***p<0.001 by Dunn's post-hoc test comparing treated with control untreated neutrophils.

5.4.4 Src kinase inhibition of neutrophils: effect on MDM efferocytosis of apoptotic neutrophils

Of particular interest was the effect of initial PP1 and dasatinib treatment on the subsequent efferocytosis capacity of the MDMs in these experiments.

Results: Figure 5-20A opposite clearly shows that an unknown soluble factor released from neutrophil:bacteria interactions impairs effective MDM efferocytosis.

Comments: Either neutrophils or bacteria release the unknown factor. It may act on the MDM itself, or it may exert an effect on the “Find me” and “Eat me” mechanisms used by the apoptotic neutrophil to facilitate its ingestion (Poon et al. 2014).

Figure 5-20B shows that the impaired efferocytosis shown in A is ‘reversed’ by pre-treating the neutrophils with either PP1 or dasatinib, to near expected levels. The finding is novel and suggests that release of the unknown factor from neutrophils is inhibited by src kinase inhibition.

It provides further evidence of an anti-inflammatory role of src kinase inhibition in promoting resolution after bacterial infection in the lung.

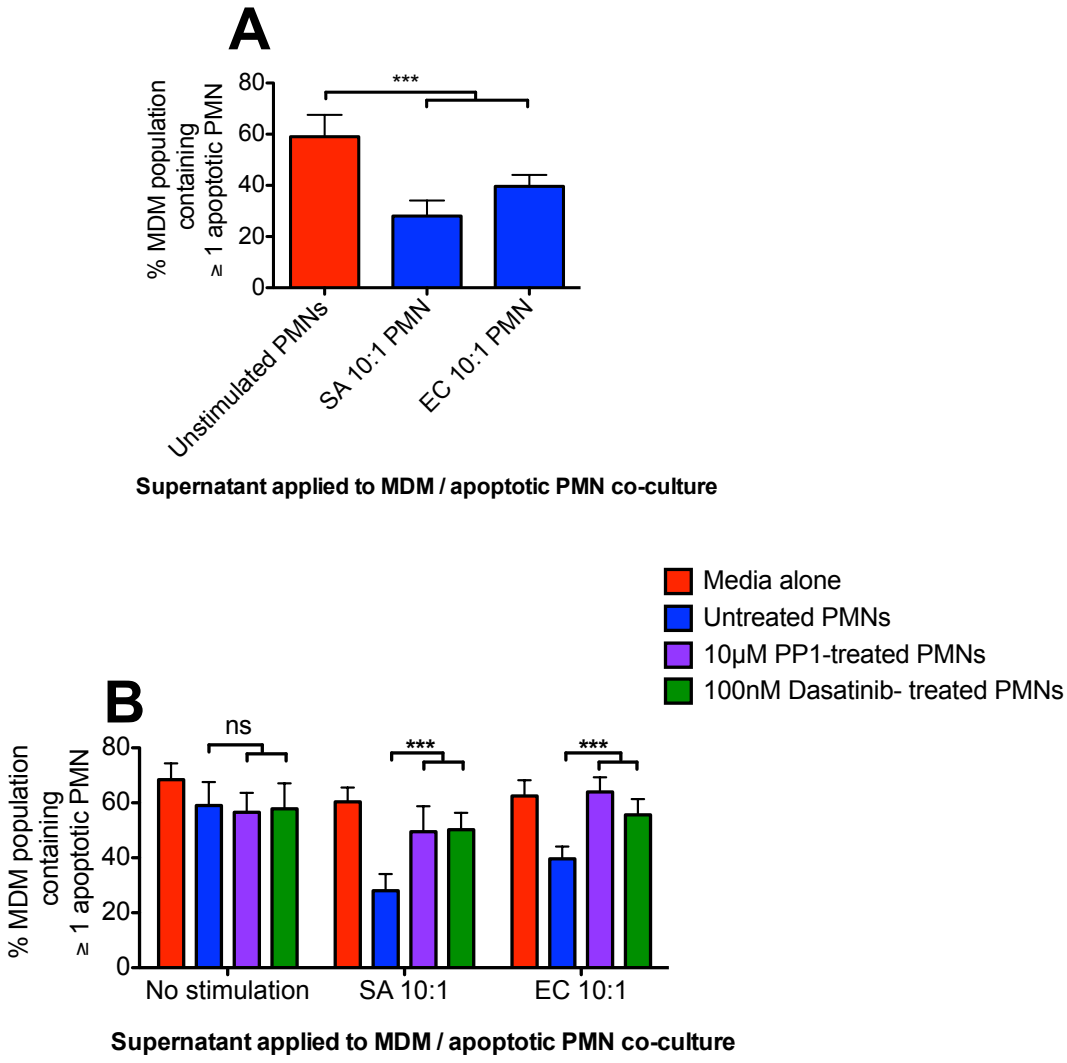

Figure 5-20 PP1 and Dasatinib treatment of neutrophils exposed to SA or EC results in improved efferocytosis of apoptotic neutrophils

Rates of phagocytosis of apoptotic neutrophils by MDMs incubated for 24 hours in filter-sterilised, 10% autologous serum-supplemented supernatants from healthy neutrophils exposed to live SA or EC (A). Phagocytosis rates of MDMs incubated in supernatants from healthy neutrophils pre-treated with 10 μM PP1 or 100 nM dasatinib and exposed to live SA or EC (B). Data show mean and SD values of samples from 2 separate experiments, each using MDMs from 3 volunteers and a single donor of non-autologous apoptotic neutrophils (total n=6). ***p<0.001 (A), p=0.0959 (Unstimulated), ***p<0.001 (SA and EC) (B) by repeated measures ANOVA; ***p<0.001 by Dunn's post-hoc test comparing treated with control untreated neutrophils.

5.5 Investigation of the Soluble Factors Released From Neutrophil/Bacterial Interaction

For these final experiments I attempted to investigate the nature of this unknown factor. There are many possibilities but I chose to test the following: LTF, serine proteases (specifically HNE) and ROS.

Lactoferrin inhibits chemotaxis of granulocytes and is the only known “Keep out” signal regulating efferocytosis, being released by apoptotic neutrophils themselves (Bournazou et al. 2009). It is also a product of neutrophil degranulation inhibited by PP1 and dasatinib, as shown in Chapter 3.

Neutrophil serine proteases such as cathepsin G, HNE and proteinase 3 are released at sites of infection and inflammation by degranulation. Conventionally it is believed that any extracellular immunomodulatory properties are neutralised by potent, naturally-occurring serine protease inhibitors, or ‘serpins’, present in serum. The experiments I carried out all used 10% autologous serum, which might be expected to provide enough serine protease inhibition to discount these enzymes as culprits. However there is some evidence to suggest that proteases can be released so readily that they can overwhelm and inactivate their inhibitors (Pham 2006).

Similarly, ROS produced by activated neutrophils is known to activate RhoA in surrounding phagocytes. RhoA negatively regulates efferocytosis and this mechanism is well described in the literature (Nakaya et al. 2006; McPhillips et al. 2007; Poon et al. 2014). The antioxidant N-acetylcysteine inhibits ROS production, RhoA activation and promotes apoptotic cell clearance in LPS-mediated murine lung inflammation (Moon et al. 2010).

5.5.1 Variation in experimental design

I adjusted the basic experimental protocol again to inhibit these mediators as shown in Figure 5-21 overleaf. I chose to measure only efferocytosis without associated cytokine release.

Supernatants from 'untreated neutrophils' in **Steps 1** and **2** were treated with either 1 μg/ml of a mouse anti-human LTF monoclonal antibody (IgG1, κ), a mouse anti-human IgG1 isotype control antibody at the same concentration, the pan-serine protease inhibitor 4-(2-Aminoethyl) benzenesulfonyl fluoride hydrochloride (AEBSF) at 1 mM, the specific HNE inhibitor sivelestat at 100 μg/ml or N-acetylcysteine at 10 μM. The drugs were present in the supernatant for the entire efferocytosis stage **(Step 4)**. The intention was to test whether any of the inhibitors mimicked the effect of src kinase inhibition in improving efferocytosis.

Unfortunately due to the complexity of the experiments, with limited time available, I carried out the experiments on a single day, using MDMs from 3 separate healthy volunteers and apoptotic and healthy neutrophils from 2 further separate volunteers.

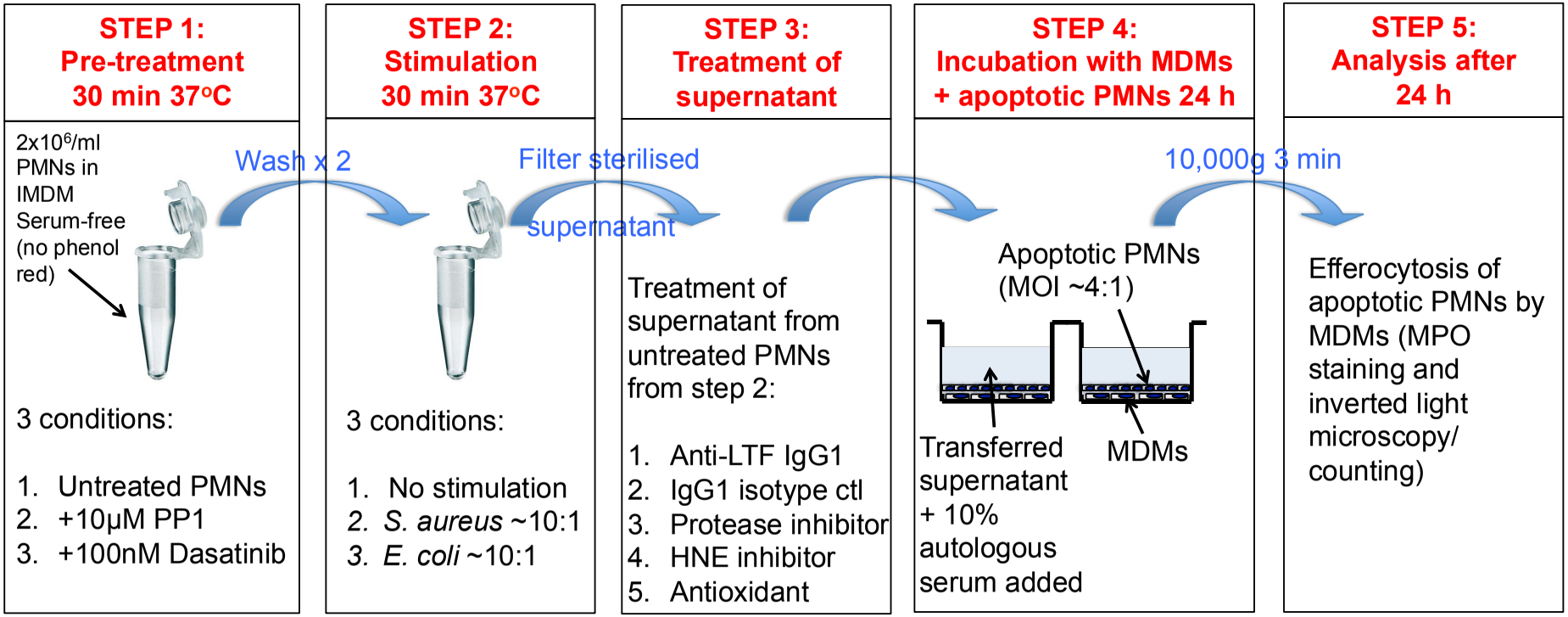

Figure 5-21 Experimental design for section 5.5

5.5.2 Lactoferrin

Results: Figure 5-22 below demonstrates 2 main findings: the two antibodies themselves have no effect on baseline rates of efferocytosis. Additionally they do not reverse the effect seen in stimulated neutrophils, suggesting that LTF is not responsible for this effect.

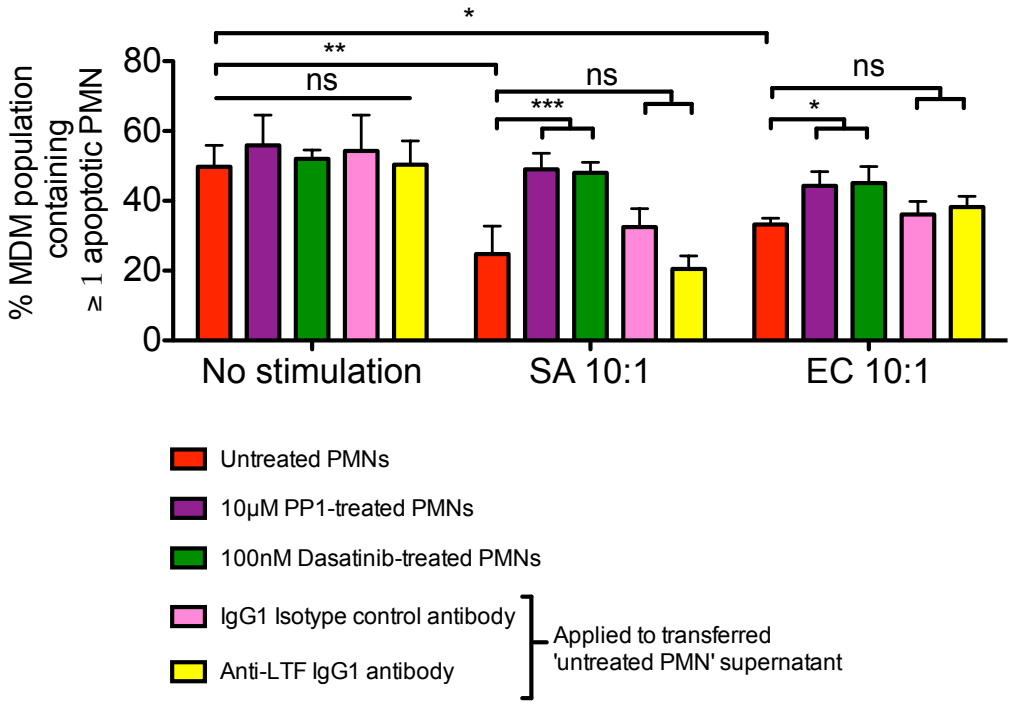

Figure 5-22 Lactoferrin is not responsible for impaired efferocytosis by MDMs

Rates of phagocytosis of apoptotic neutrophils by MDMs incubated for 24 hours in filter-sterilised, 10% autologous serum-supplemented supernatants from healthy neutrophils exposed to live SA or EC. In an additional 2 conditions, 1 μg/ml IgG1 isotype control antibody (pink) and 1 μg/ml anti-LTF IgG1 antibody (yellow) was added to the supernatant prior to transfer to MDM plate. Data show mean and SE values of samples from 1 experiment, each using MDMs from 3 volunteers and a single donor of non-autologous apoptotic neutrophils (total n=3). ***p<0.001 by repeated measures ANOVA; *p<0.05 and **p<0.01 by Dunn's post-hoc test comparing SA and EC-exposed neutrophils with control unstimulated neutrophils. p=0.842 (Unstimulated), ***p<0.001 (SA) and *p=0.014 (EC) by repeated measures ANOVA; *p<0.05, ***p<0.001 by Dunn's post-hoc test comparing treated neutrophils or supernatant with control untreated neutrophils.

5.5.3 Serine proteases

Results: In contrast, there is a very marked effect of the water-soluble, pan-serine protease inhibitor, AEBSF, as shown in Figure 5-23 opposite, even when added to unstimulated neutrophil supernatant.

Comments: One interpretation might be that serine proteases themselves are actually required to drive efferocytosis and that the AEBSF is neutralising all activity in the 10% serum added. This is not a recognised phenomenon; however there is in vitro evidence to suggest that both macrophages and neutrophils, which are both capable of phagocytosing and clearing apoptotic autologous neutrophils, are inhibited by the serpin plasminogen activator inhibitor-1 (PAI-1) (Park et al. 2008). I used 1 mM AEBSF, a concentration at the highest end of the dose range suggested on the product information sheet and it is possible that the drug itself is toxic to MDMs at this concentration. Dose response experiments would be required to further investigate this finding.

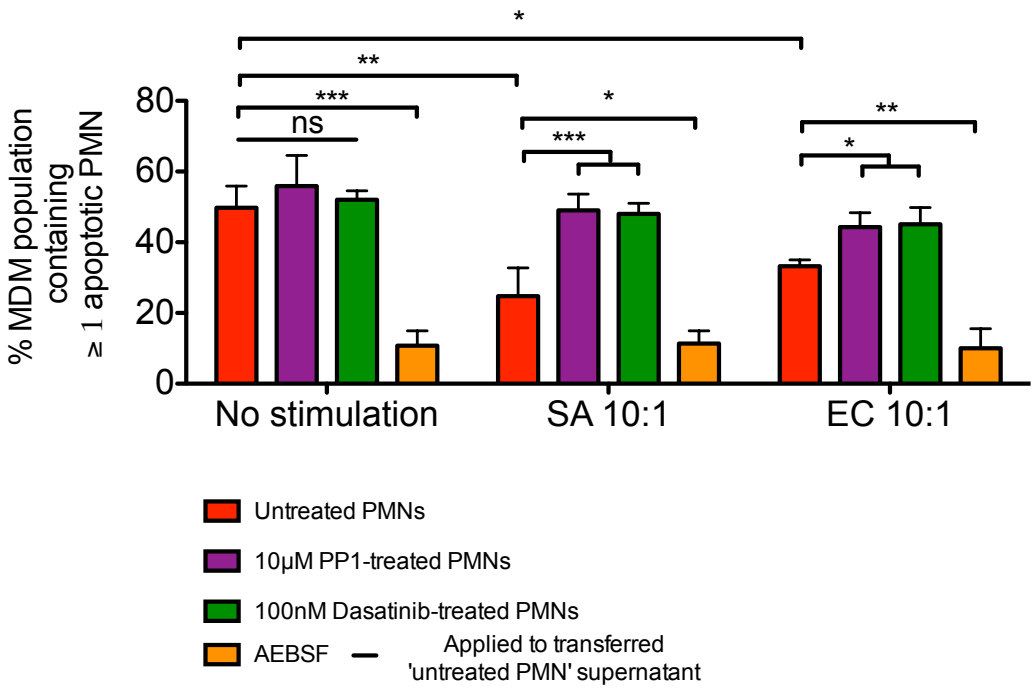

Figure 5-23 The pan-serine protease inhibitor, AEBSF, has direct effects on MDM function

Rates of phagocytosis of apoptotic neutrophils by MDMs incubated for 24 hours in filter-sterilised, 10% autologous serum-supplemented supernatants from healthy neutrophils exposed to live SA or EC. In an additional condition, the pan-serine protease inhibitor, 1 mM AEBSF (orange), was added to the supernatant prior to transfer to MDM plate. Data show mean and SE values of samples from 1 experiment, each using MDMs from 3 volunteers and a single donor of non-autologous apoptotic neutrophils (total n=3). ***p<0.001 by repeated measures ANOVA; *p<0.05 and **p<0.01 by Dunn's post-hoc test comparing SA and EC-exposed neutrophils with control unstimulated neutrophils. ***p=0.0005 (Unstimulated), ***p<0.001 (SA) and ***p=0.0002 (EC) by repeated measures ANOVA; *p<0.05, **p<0.01, ***p<0.001 by Dunn's post-hoc test comparing treated neutrophils or supernatant with control untreated neutrophils.

5.5.4 Human neutrophil elastase

Results: Figure 5-24 below shows that HNE is also not responsible for the impaired MDM efferocytosis.

Comments: I used a concentration of 100 µg/ml of sivelestat, that inhibited 80% of neutrophil elastase activity in ex vivo pleural effusions post lobectomy (Sakuma et al. 1998), so I am confident that any HNE present in the supernatants was effectively inhibited.

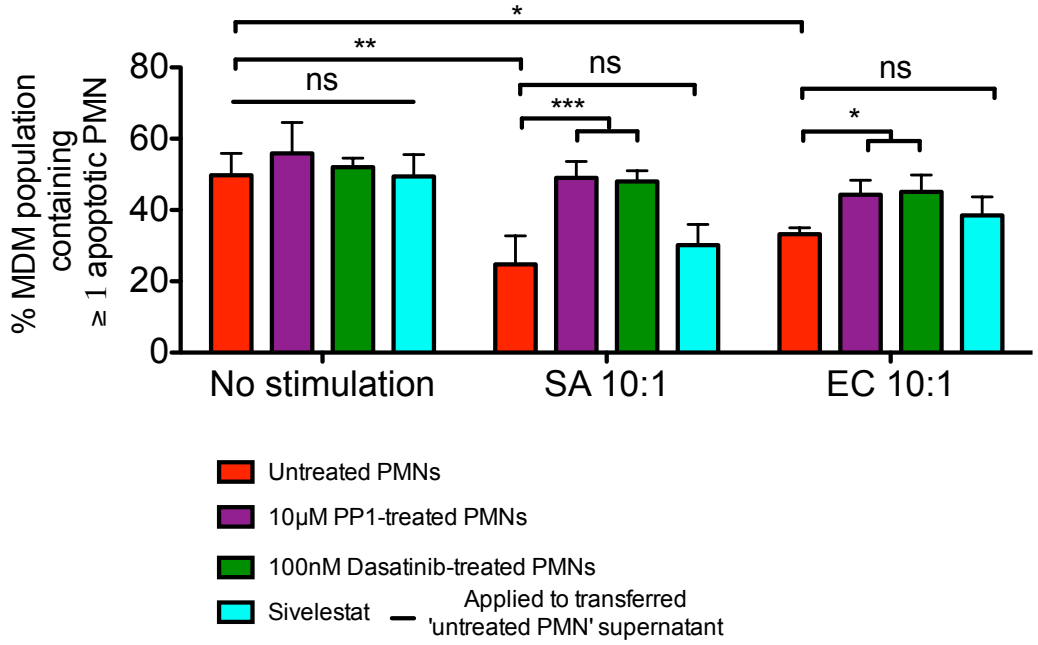

Figure 5-24 Neutrophil elastase is not responsible for impaired efferocytosis by MDMs
Rates of phagocytosis of apoptotic neutrophils by MDMs incubated for 24 hours in filter-sterilised, 10% autologous serum-supplemented supernatants from healthy neutrophils exposed to live SA or EC. In an additional condition, 100 µg/ml sivelestat, a specific neutrophil elastase inhibitor (violet), was added to the supernatant prior to transfer to MDM plate. Data show mean and SE values of samples from 1 experiment, each using MDMs from 3 volunteers and a single donor of non-autologous apoptotic neutrophils (total n=3). ***p<0.001 by repeated measures ANOVA; *p<0.05 and **p<0.01 by Dunn's post-hoc test comparing SA and EC-exposed neutrophils with control unstimulated neutrophils. p=0.682 (Unstimulated), ***p=0.0003 (SA) and **p=0.0041 (EC) by repeated measures ANOVA; *p<0.05, ***p<0.001 by Dunn's post-hoc test comparing treated neutrophils or supernatant with control untreated neutrophils.

5.5.5 Reactive oxygen species

Results: Unexpectedly, 10 μM N-acetylcysteine also has no effect on the impaired efferocytosis (Figure 5-25 overleaf).

Comments: This in vitro concentration was extrapolated from studies showing impaired neutrophil release of elastase, IL-8 and ROS in response to fMLP and PMA using 10 μM N-acetylcysteine (Sadowska et al. 2006). I had initially contemplated whether the N-acetylcysteine is unable to neutralise extracellular ROS and that it should have been added directly to the neutrophils in Step 1 but it does appear to have direct antioxidant effects as a ROS scavenger via its thiol group. Optimum in vitro hypochlorous acid scavenging activity might however require higher concentrations of up to 48 μM of N-acetylcysteine (Aruoma et al. 1989).

Both PP1 and dasatinib impair extracellular superoxide release from neutrophils in response to PAF+fMLP (Chapter 3). ROS production negatively controls efferocytosis via RhoA activation, as explained above. This potential mechanism is therefore worthy of further study in these experiments, using a dose range of 1-100 μM N-acetylcysteine added directly to the transferred supernatant or pre-incubated with the neutrophils.

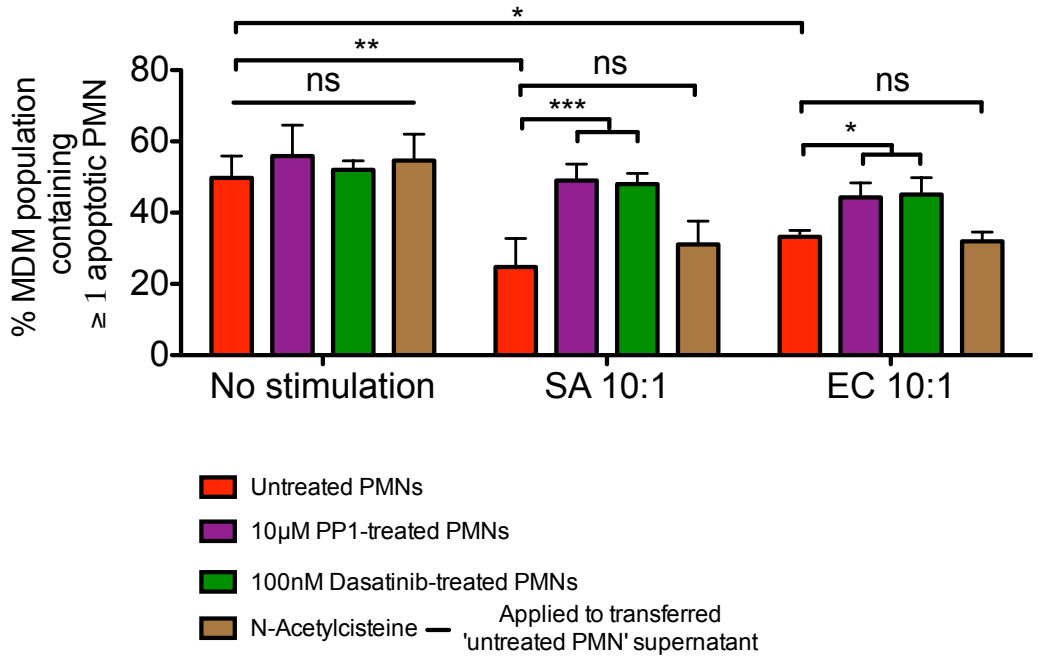

Figure 5-25 Reactive oxygen species are not responsible for impaired efferocytosis by MDMs

Rates of phagocytosis of apoptotic neutrophils by MDMs incubated for 24 hours in filter-sterilised, 10% autologous serum-supplemented supernatants from healthy neutrophils exposed to live SA or EC. In an additional condition, 10 μM N-acetylcysteine, a potent antioxidant (brown), was added to the supernatant prior to transfer to MDM plate. Data show mean and SE values of samples from 1 experiment, each using MDMs from 3 volunteers and a single donor of non-autologous apoptotic neutrophils (total n=3). ***p<0.001 by repeated measures ANOVA; *p<0.05 and **p<0.01 by Dunn's post-hoc test comparing SA and EC-exposed neutrophils with control unstimulated neutrophils. p=0.752 (Unstimulated), **p=0.0019 (SA) and ***p=0.0008 (EC) by repeated measures ANOVA; *p<0.05, ***p<0.001 by Dunn's post-hoc test comparing treated neutrophils or supernatant with control untreated neutrophils.

5.6 Summary of Key Findings

My key findings are summarised as follows:

1. Src kinase inhibition of neutrophils stimulated by *S. aureus*, but not *E. coli,* attenuates secondary alveolar epithelial cell inflammation (with reduced IL-8 release) and damage (with reduced LDH release) in vitro. An associated increase in MCP-1 release may theoretically be part of an autoregulated epithelial cell repair mechanism.

2. Neutrophils from critically ill patients are dysfunctional, with impaired phagocytosis and killing ability, as is described in the literature. They are also more inflammatory than healthy neutrophils, inducing direct and indirect inflammation and damage in alveolar epithelial cells, as seen in ARDS. Src kinase inhibition of neutrophils from critically ill patients has no effect on secondary epithelial inflammation, suggesting that the causative factor is not a product of neutrophil degranulation.

3. Src kinase inhibition of neutrophils promotes resolution in a simple in vitro model of apoptotic cell efferocytosis by macrophages. Neutrophil:bacteria interaction releases a factor or factors that impair efferocytosis, either by a direct effect on macrophage polarity or function, or by inhibiting “Eat me” signals on the apoptotic cells themselves. Src kinase inhibitors prevent this effect, though the mechanism is not clear from the experiments carried out.

In these experiments, I have tested my original hypothesis, which stated:

“In vitro src kinase inhibition of human neutrophils attenuates neutrophil-mediated epithelial cell damage whilst promoting a pro-resolutionary environment, allowing efficient apoptotic cell clearance”.

My hypothesis has therefore been satisfied in an in vitro model of secondary epithelial cell inflammation and damage induced by the secreted products of healthy neutrophil:*S. aureus* interactions. Src kinase inhibition also promotes the generation of a more pro-resolutionary milieu, specifically permitting more efficient clearance of apoptotic neutrophils by macrophages. However, in a

similar ex vivo model, my hypothesis was not fully satisfied. Src kinase inhibition is unable to attenuate the inflammatory effect exerted on epithelial cells by ex vivo neutrophils retrieved from critically ill patients.

The relevance of these findings, and those of Chapters 3 and 4, will be now be further discussed in the next chapter (Chapter 6; General Discussion), together with an acknowledgement of the limitations of my work and suggested future directions of work.

Chapter 6. General Discussion

6.1 Chapter Overview

In this chapter, I will further discuss the main findings of the work contained within this thesis, relating it to past and recently published data where relevant, acknowledging the limitations of my work, before concluding with my thoughts on future directions of work.

6.2 Introduction

The acute respiratory distress syndrome is an extreme pulmonary manifestation of a highly complex interplay between invading pathogens, innate immune cells and their mediators of acute inflammation. It remains associated with unacceptably high levels of mortality and morbidity. Clinical studies are challenging to perform well due to the heterogeneity of the syndrome, but standardising its definition in 2012 has helped in this regard (Ranieri et al. 2012). To date, all randomised-controlled trials of pharmacological therapy have shown no effect on mortality. In fact, lung-protective ventilation is the only supportive measure to show a mortality benefit. Other clinical studies have helped to shape consensus view of current “best practice”.

Post mortem studies, in vitro and in vivo models have identified some of the key features of acute inflammation that lead to ARDS. A central mechanism is the rapid recruitment and degranulation of neutrophils, cells once considered to be simple “suicide killers”. It is now clear that neutrophils not only kill pathogens in various different ways, but can also regulate inflammation and coordinate the innate and adaptive immune systems (Mócsai 2013). The src family of tyrosine kinases occupy a “gateway” position in controlling the signalling pathways that regulate the inflammatory response to a range of stimuli and are strongly implicated in the pathogenesis of ARDS. The src kinases therefore represent attractive therapeutic targets for studying acute inflammation, potentially leading to treatments for conditions such as ARDS.

6.3 Src Kinase Inhibition Impairs Neutrophil Degranulation in Response to Bacteria without Affecting Killing

The in vitro results in Chapter 3 are consistent with previous studies showing that pharmacological src kinase inhibition of neutrophils with PP1 and dasatinib attenuates GPCR-mediated and TLR4-mediated degranulation of primary and secondary granules (Mócsai et al. 2000; Futosi et al. 2012). My experiments also replicate this finding in whole blood using a novel flow cytometric method of measuring membrane expression of the specific granule markers CD63 and CD66b. In addition, CR3-mediated degranulation in response to phagocytosis of live serum-opsonised Gram +ve and –ve bacteria is added to the list of mechanisms controlled by src kinases. Crucially, src kinase inhibition with PP1 or dasatinib does not significantly impair in vitro intracellular bacterial killing in suspension (and in adherent conditions for PP1), supporting my first hypothesis. These observations clearly raise the tantalising possibility that under these conditions, granule fusion with phagosomes is preferentially maintained to permit pathogen killing, perhaps through activation of alternative tyrosine phosphorylation pathways.

6.4 Src Kinase Inhibition Affects In Vitro Neutrophil Motility But Does Not Impair In Vivo Neutrophil Influx

My data also support the well-described effects of src kinase inhibition on adhesion-dependent neutrophil function: adhesion to plastic, chemotaxis along glass and adherent phagocytosis/superoxide release are all inhibited by both PP1 and dasatinib, but phagocytosis in whole blood was not affected. The theory that src kinase inhibition does not affect motility and migration of neutrophils in vivo is supported by Futosi's data. Although dasatinib strongly inhibits migration towards fMLP and IL-8 along a fibrinogen-coated surface, it affects neither two-dimensional mechanotactic migration over integrin ligand surfaces under flow conditions (although sustained adhesion is impaired), nor transmigration through polycarbonate Transwell membranes towards fMLP or IL-8 (Futosi et al. 2012). In a more physiologically representative model of transmigration across an extracellular matrix (Matrigel) suspended above a Transwell membrane, dasatinib also has no effect. In $Hck^{-/-}$ $Fgr^{-/-}$ knockout models, Giagulli et al. may have explained this finding (Giagulli et al. 2006). They addressed the role of src kinases in "inside-out" and "outside-in" integrin signalling and found that Hck and Fgr were dispensable for integrin affinity and upregulation in response to chemoattractant-induced activation (inside-out signalling) but were necessary for sustained adhesion (outside-in signalling) (Shattil et al. 2010; Herter & Zarbock 2013). Another possible explanation for my findings is the non-specificity of PP1 and dasatinib: both chemicals are dual src and Abl kinase inhibitors. Tong et al. showed that c-abl kinase was critical for β_2 integrin-dependent neutrophil migration in vitro and in vivo using both PP2 and a specific c-abl inhibitor ST1571 (Tong et al. 2013). Similar to Futosi et al., the group used identical transmigration assays across fibrinogen-coated Transwell filters.

As there are different schools of thought regarding the precise role of src kinases in neutrophil recruitment in vitro, the actual situation in vivo becomes more complicated. As detailed in Chapter 4, in response to *E.coli*-induced acute lung inflammation, low dose dasatinib (1 mg/kg) reduces neutrophil content in the lung interstitium with no effect in the alveoli, whilst reducing alveolar MPO and TNFα release. There is a slight increase in bacterial survival in the lung interstitium, but all other parameters are unchanged. At high dose (10 mg/kg)

there is an obvious detrimental effect with increased bacterial survival and evidence of extrapulmonary toxicity. It is difficult to conclude whether this marked effect is due to impaired bacterial killing or inadequate neutrophil recruitment, or both. In $Hck^{-/-}$ $Fgr^{-/-}$ $Lyn^{-/-}$ triple knockout models of blistering skin diseases and autoantibody-induced arthritis, mediated by both Fcγ recognition of immune complexes and β_2 integrin-mediated neutrophil recruitment, the authors found that although the neutrophil, monocytes and macrophages all exhibited normal in vivo and in vitro migratory capacity, recruitment was impaired due to inadequate generation of a pro-inflammatory environment (Kovács et al. 2014).

6.5 Src Kinase Inhibitors Act on All Inflammatory Cells, Not Just Neutrophils

Targetting src kinases with systemic administration of dasatinib should theoretically block all forms of src signalling in every living cell, not simply neutrophils. We know something of the role of src kinases in endothelial cells, epithelial cells (Severgnini et al. 2005; Chang et al. 2008; Han et al. 2013) and alveolar macrophages (Byeon et al. 2012). Alveolar macrophages have been shown to promote src-dependent neutrophil transmigration in a septic model by releasing ROS through NADPH oxidase (Wang et al. 2008) and induce protein leak through iNOS (Farley et al. 2006). The recent discovery by Cohen's group in Dundee that salt-inducible kinase (SIK) signalling in macrophages controls the interconversion between classically activated (M1) and regulatory (M2) macrophages may also explain our findings (Clark et al. 2012). Both dasatinib and bosutinib (at high concentrations = 300 nM and 3 μM respectively) polarised murine bone marrow derived macrophages (BMDMs) towards a regulatory-like phenotype with high IL-10 and low TNFα, IL-6 and IL-12 production, through SIK inhibition (Ozanne et al. 2014). It therefore seems likely that dasatinib affects the ability of both neutrophils and alveolar macrophages to generate a pro-inflammatory environment in the context of infection and may explain our finding of reduced neutrophil recruitment to the lung interstitium at low doses of dasatinib.

6.6 Src Kinase Inhibition is Anti-inflammatory in Acid-induced Inflammation

In a sterile model of lung inflammation free from the unpredictability of bacterial survival and stimulus size, such as acid-induced lung inflammation, any effect on neutrophil recruitment should theoretically be easier to detect. In the LPS model, both PP1 and PP2 reduced neutrophil influx amongst other markers of lung inflammation (Severgnini et al. 2005; Lee et al. 2007). Acid-induced lung inflammation is initiated by the generation of danger-associated molecular patterns (DAMPs) from cell necrosis, which modulate TLR and nod-like receptor (NLR) activity (Tolle & Standiford 2013). IL-8 production recruits neutrophils (Folkesson et al. 1995) which degranulate and interact with activated platelets to form aggregates capable of further damaging endothelial cells through thromboxane A_2 (TXA_2) production (Zarbock et al. 2006). In our model of acid-induced lung inflammation, we observe a surprisingly mild anti-inflammatory effect at a moderate dose of 5 mg/kg dasatinib with reduced alveolar neutrophil content, reduced alveolar degranulation of LTF, reduced interstitial CD11b expression on sequestered neutrophils. At 10 mg/kg there is a detrimental effect, with increased alveolar and interstitial neutrophil influx and degranulation, and marked alveolar haemorrhage. Why dasatinib appears pro-inflammatory in this model at high dose is more difficult to explain. It does not appear to be due to impaired neutrophil recruitment. The increased alveolar haemorrhage might relate to endothelial injury from inhibition of Lyn kinase, known to have an opposing function to other src kinases in strengthening endothelial integrity and barrier function (Han et al. 2013).

Taking the results of both in vivo models together, there appears insufficient evidence to conclude that dasatinib impairs neutrophil recruitment in either model. As expected, it does exert an anti-inflammatory effect by inhibiting some markers of degranulation and inflammation. There is no convincing evidence of reduced endothelial cell injury and leak in either model, so my second hypothesis is not supported.

6.7 The Paradox of Impaired Phagocytosis with Normal Bacterial Killing

Do src kinase inhibitors therefore truly inhibit bacterial killing by neutrophils? Although Mocsai's group concluded that dasatinib does not have a major effect in vitro, there was in fact a ~25% increase in the relative counts of both *S. aureus* and *E. coli* with 1 μM dasatinib (Futosi et al. 2012). Only at a PP1 dose of 100 μM did I observe an in vitro inhibitory effect, using almost precisely the same experimental conditions as Futosi: in suspension with serum-opsonised pathogens at an MOI of 10 bacteria: 1 neutrophil.

We have already discussed the possibility that src inhibition may affect NETs production by neutrophils in response to bacterial stimulation. In the short 30 min bacterial killing assay I used, there is insufficient time for NETs to be produced, which typically peak at 3-4 h after PMA stimulation. By contrast, in my 24 h in vivo murine models, NETs formation is likely to be a significant factor in the effective control and clearance of bacteria. As the degranulation product MPO is a key extracellular component of NETs also required to generate the primary ROS in NETs, namely hypochlorite (Akong-Moore et al. 2012), and as I have shown, src kinases themselves are crucial in MPO degranulation and NADPH oxidase function, it would be expected that src kinase inhibition also impairs NETs formation. This has recently been demonstrated in human neutrophils in response to yeasts, where both src and Syk kinase inhibitors switched off NETs production to a similar level seen with the NADPH oxidase inhibitor, DPI (Nanì et al. 2015). We made no direct measure of neutrophil viability in the interstitium or alveoli of the mice exposed to both *E. coli* and acid. Flow cytometric analysis of neutrophil apoptosis and necrosis, together with quantification of NETs production using fluorescent microscopy, would have given some insight into the relative importance of these processes in bacterial clearance.

It therefore still remains difficult to fully explain my apparently paradoxical findings that src kinase inhibition does not affect in vitro bacterial killing, but that both adherent neutrophil phagocytosis and NADPH oxidase function is src-dependent. This may well be an assay-dependent "in vitro phenomenon" and the findings should therefore be repeated using alternative phagocytosis and bacterial killing assay techniques. However, I found that both PP1 and dasatinib

also inhibited phagocytosis of serum-opsonised zymosan particles (data not shown), contradicting the findings of Futosi et al., who showed no effect of up to 1 μM dasatinib on phagocytosis of serum-opsonised GFP-expressing bacteria (Futosi et al. 2012).

The various theories explaining the relative contributions of NADPH oxidase, ROS production, pH and proteases to effective bacterial killing in the phagosome therefore come into focus. The events within the phagosome are dynamic and as such, investigating individual processes is extremely challenging. One might expect some redundancy in the system, such that a defect in one component may only result in a minor effect on bacterial degradation within the phagosome. Patients with chronic granulomatous disease (CGD) have neutrophils defective of NADPH oxidase activity and are highly susceptible to infection. However, their neutrophils exhibit normal bacteriocidal activity towards certain bacteria in vitro, including *Streptococci* (Kaplan et al. 1968), *Pseudomonas aeruginosa* (Speert et al. 1994) and *E. coli* (Rosen & Michel 1997). Similarly, neutrophils from patients with MPO deficiency are unable to kill *Candida* and have a reduced activity against *S. aureus* in vitro (Parry et al. 1981), with little overall clinical effect.

Current consensus opinion would favour the theory that NADPH oxidase creates a membrane potential across both the phagosomal and plasma membranes of the stimulated neutrophil by providing electrons to generate ROS and its downstream metabolites. Granule proteins are then modified and activated by changes in pH, ROS and halogen derivatives to act collaboratively with oxidants to degrade ingested microbes (Nauseef 2007). The absence of an individual component therefore unpredictably alters the balance of the anti-microbial milieu of the host phagosome, without even taking into account of the effect of specific pathogen adaptations to its interaction with the host.

6.8 Src Family Kinases: a Role in Controlling Individual Granule Subsets?

It is beyond the remit of this thesis to draw conclusions on the effects of src kinase inhibition on the anti-microbial activity within the phagosome. It is interesting to speculate on the possibility that some of my observations (and those of others) may be explained by preferential translocation and targeting of individual granules to specific locations within the neutrophil, under the control of individual src kinases. There is evidence to suggest that specific granule populations are associated with individual src kinases. In human neutrophils stimulated by fMLP, the src kinase Fgr is localised and expressed in the membrane of secondary granules, whereas a 61kDa form of Hck translocates to primary granules upon activation (Gutkind & Robbins 1989; Möhn et al. 1995). It is technically possible to measure subcellular localisation of individual neutrophil granules using immunofluorescence and confocal microscopy (Quinn et al. 2007), but studies to test these theories are currently limited to knockout murine models of individual src kinases. siRNA ('small interfering' ribonucleic acid) "knock-in" models are technically extremely challenging in human neutrophils, but may prove effective in cell lines resembling human neutrophils, such as the HL-60 cell line. Due to the similar structure of the countless receptor and non-receptor tyrosine kinases, specificity of kinase inhibition remains a challenge, particularly within the family of 9 src kinases. As pharmaceutical companies continue to develop more and more specific individual src kinase inhibitors for use in chronic myeloid leukaemia and other malignancies, these may be used experimentally in the future to test these theories (Tintori et al. 2013).

6.9 Limitations of In Vitro and In Vivo Studies

There are certain limitations to consider when interpreting my in vitro and in vivo data:

The most important consideration is that although both PP1 and dasatinib are known to be potent src kinase inhibitors and I have shown that they inhibit src kinase phosphorylation in vitro, there is a significant possibility of numerous 'off-target' effects due to the lack of specificity of most tyrosine kinase inhibitors. Although manipulation of src kinase pathways is highly likely to be involved in the in vitro and in vivo observations I have made, it is impossible to directly attribute any effect to src kinase inhibition alone.

As discussed earlier, the number of experimental replicates was limited to between 3-6 in vitro studies, due to a limited availability of healthy blood donors and the logistics of conducting numerous assays within the short lifespan of neutrophils. This is an unavoidable issue when conducting neutrophil research. Some researchers attempt to circumvent the issue by using the HL-60 cell line to study neutrophil biology, but our group believes that research involving primary human cells is considerably more applicable. Although it was a valid approach to carry out statistical comparison tests assuming a normally distributed population where appropriate, there is a risk that I have overestimated any underlying statistical difference between individual conditions. Planning fewer experiments, with fewer individual conditions, may have allowed me to increase my experimental numbers.

Similarly, with the in vivo experiments, although there was a clear dose-response effect of dasatinib in both *E. coli* and acid models, I was surprised that there was no difference in a majority of the markers tested between control and treated mice. We believe that the decision to administer dasatinib at 0 and 12 h was correct, to coincide with the peak neutrophil influx at these timepoints, but that the choice of a 24 h timepoint to end the experiment may have been too late to observe more significant changes in markers of neutrophil influx, activation and degranulation during the earlier stages of acute inflammation. Additional timepoints of 3 h, 6 h, 12 h and 48 h may have helped to clarify this issue.

As previously discussed, our i.p. doses of 1 mg/kg, 5 mg/kg and 10 mg/kg dasatinib were extrapolated from pharmacokinetic data in rats (Seferian et al. 2013). These doses resulted in broadly similar plasma dasatinib levels in rats as measured in human patients taking a daily dose of 70 mg (the daily dose in CML is 100 mg). In reality, the limited number of experiments we carried out were dose-finding in nature, after initial experiments established that doses of 1 mg/kg and 10 mg/kg dasatinib were not toxic to mice unexposed to lung injury. We were therefore reassured to read a recently published paper from Mocsai's group where they used the same doses of 1 mg/kg and 10 mg/kg dasatinib or control 1% DMSO administered by oral gavage to pre-treat C57/BL6 mice exposed to either 1% DMSO control, i.t. LPS or i.p. LPS. The mice were retreated with dasatinib at 6 h and 24 h before the experiment was terminated at 48 h. Interestingly, mortality in the 10 mg/kg group exposed to i.t. LPS was 24% compared to 0% in the 1 mg/kg and DMSO control groups. 1 mg/kg dasatinib favourably affected lung dynamics and function and led to a significant reduction in neutrophil (and mononuclear cell) influx into the BALF. Lung interstitium levels of IL-6, IL-10 and TGFβ were all reduced, with a slight reduction in BALF IL-6. 10 mg/kg dasatinib resulted in further adverse outcomes, including increased BALF neutrophil influx and a considerable increase in Fas receptor positive lung tissue, indicating cell death. Of note, the authors measured no specific markers of neutrophil degranulation such as CD11b/CD63 expression or release of MPO/LTF (Oliveira et al. 2015).

These results complement our data well, indicating that at high doses, dasatinib administered via the oral route has broadly similar effects to our own observations using i.p. administration, irrespective of the aetiology of lung injury. In contrast, the anti-inflammatory effects of dasatinib at lower doses appear to be dependent on the underlying aetiology.

6.10 A Soluble Neutrophil Factor is Responsible for Epithelial Cell Damage and Inflammation

My data in Chapter 5 have also revealed novel indicators of the anti-inflammatory and pro-resolutionary roles of src kinase inhibition in acute inflammation. The data were discussed in detail throughout Chapter 5, and generated more questions than they have answered.

Firstly, what is the nature of the soluble factor released from the interaction of neutrophils with *S. aureus* NCTC 8325, but not *E. coli* K-12, that induces disruption of epithelial cell monolayer integrity? I have postulated that this factor may be related to the release of lipotechoic acid or virulence factors specific to *S. aureus*, such as leukotoxins. It may also be an extracellular product of degranulation, since pre-treatment of neutrophils with both PP1 and dasatinib reduces subsequent release of IL-8 and LDH from A549 epithelial cells, but does not prevent monolayer disruption. This finding was not observed in identical experiments involving *E. coli* K-12. The reader will recall that in Chapter 3, my original experiments to inhibit degranulation were carried out using SA NCTC 8325 **and** *P. aeruginosa* PA01 and not *E. coli* K-12. The reason for changing from PA01 to *E. coli* was to avoid the excessive contamination of A549 culture plates with PA01 that I observed, despite using 0.4μm diameter filter sterilisation and the addition of gentamicin. Future in vitro experiments would therefore need to establish a similar effect of in vitro src inhibition on neutrophil phagocytosis, killing and degranulation functions in response to *E. coli* K-12.

6.11 Neutrophils from Critically Ill Patients are Pro-inflammatory and Unaffected by Src Kinase Inhibition

It is clear from my data that neutrophils derived from critically ill patients, irrespective of underlying disease type, exhibit dysfunctional phagocytosis and bacterial killing, whilst inducing inflammation and cytotoxicity in A549 cells when in direct contact or when separated by a filter membrane. Unsurprisingly src inhibition has no effect on neutrophil dysfunction, nor does it attenuate downstream epithelial cell damage and inflammation. This may be a result of the excessive levels of inflammation inducing neutrophil activation and degranulation via other src-independent signalling pathways in critically ill patients. Indeed, the levels of inflammatory mediators, such as C5a anaphylatoxin, (indirectly associated with neutrophil dysfunction) present in the blood of critically ill patients can reach over 1000 fold higher than those of a healthy individual (Ward 2010). In these experiments, I only used a modest dose of both PP1 and dasatinib (10 μM and 100 nM respectively). Repeating the experiments using higher doses may be required to observe an effect.

6.12 Src Kinase Inhibition Prevents the Release of a Neutrophil-derived Factor that Impairs Repair and Efferocytosis

Resolution of acute inflammation is a highly complex and tightly regulated process believed to occur alongside acute inflammation, even before the clearance of a perpetuating inflammatory stimulus. In resolving lung inflammation, alternatively activated M2 alveolar macrophages (and to a lesser extent, neutrophils) are capable of ingesting debris and apoptotic cells and producing anti-inflammatory cytokines. My experiments showed that a soluble factor released from the interaction of healthy neutrophils with both *S. aureus* and *E. coli* impairs efficient MDM efferocytosis, suggesting that this factor exerts a negative effect on MDMs, or acts on the “Find me” and “Eat me” signals on apoptotic neutrophils to prevent their recognition and uptake.

It is very important to consider that the relatively low rates of apoptosis observed (~50%) may have influenced the results here. Around 25% of ‘apoptotic neutrophils’ were actually alive when co-cultured with healthy MDMs. This can be appreciated in the control experiments, which show a small but significant release of IL-8 and MCP-1 from ‘apoptotic cells’ cultured in media alone. The presence of live neutrophils is likely to have influenced MDM and apoptotic cell signalling and behaviour. Ultraviolet light irradiation would have proved a much more reliable method to induce neutrophil apoptosis and avoid this potential effect.

Initial attempts to elucidate the individual factor(s) involved were unsuccessful. Low experiment numbers (n=3) and highly complex assay steps may have contributed to this. Future work should target serine proteases and ROS using different inhibitors in simplified assays.

Further limitations of my A549 and MDM experiments include the use of a cell line to study the effects on alveolar epithelial cells. It is possible to culture primary alveolar epithelial cells obtained from the healthy tissue margins around lung cancers at wedge resection or lobectomy, or they can be bought in. Additionally, experiments using alveolar macrophages obtained at bronchoscopy in healthy volunteers are far more representative than using MDMs matured in culture for 7 days, but a regular supply of both of these primary human cells is limited.

By separating out each co-culture (neutrophil:bacteria, supernatant:A549s, supernatant:MDMs/apoptotic neutrophils) into different assay steps, these experiments became progressively more complex, requiring numerous control conditions. My experimental approach did have the advantage of working with live bacteria instead of chemical stimuli, making my findings more clinically relevant. In reality it is impossible to recreate the inflammatory cell milieu of an inflamed lung in any model except an in vivo model, but such in vitro experimental systems are important in studying individual components.

6.13 Future Directions and Concluding Remarks

This thesis has investigated the role of src kinases in controlling acute inflammation and its resolution in vitro, as well as their role in in vivo models of experimental lung inflammation. There is still a considerable difference between these models and the situation in ARDS, but the work has nonetheless provided further insights into the mechanisms of neutrophil activation, degranulation, extracellular signalling and repair that are central to the pathogenesis of this and many other serious conditions. Progressing towards the ultimate goal of testing potential ARDS treatments in randomised-controlled trials, I believe there is sufficient evidence to test the role of src inhibition in EVLP models of acid, bacteria and LPS-induced acute lung inflammation. In addition, there are two other potential lines of future investigation relevant to the mechanisms of ARDS that particularly interest and excite me: firstly, the accurate identification of the neutrophil factor(s) responsible for epithelial cell inflammation and damage in vitro and impaired macrophage efferocytosis. Secondly, the possibility of understanding and ultimately controlling the processing and targeting of individual granule subsets to phagosomal and plasma membranes by modulating the function of individual src kinases.

In time, I believe we will discover the “holy grail” of acute lung inflammation, by identifying highly specific therapeutic strategies designed to attenuate acute lung inflammation and promote repair, whilst maintaining a functional immune response to pathogens.

Appendix 1. Presentations of work contained within this thesis

Spoken presentations

Macfarlane JG, Dorward DA, Lucas CD, Scott JA, Ruchaud-Sparagano MH, Khan CMA, Rossi AG, Simpson AJ. In vitro and in vivo studies of the Src/Bcr-abl inhibitor Dasatinib in sterile and non-sterile acute lung inflammation. *British Thoracic Society Winter Conference, London, Dec 2014*

Macfarlane JG, Ruchaud-Sparagano MH, Scott JA, Bulmer DA, Khan CMA, Simpson AJ. Src kinase inhibition attenuates neutrophil degranulation without impairing bacterial killing: a possible therapeutic strategy for acute lung injury. *Newcastle University Institute of Cellular Medicine Research Day, Newcastle, Jun 2013*

Gertig H, Ruchaud-Sparagano MH, Hester KLM, **Macfarlane JG**, Corris PA, Simpson AJ, De Soyza A. Are neutrophils dysfunctional in idiopathic bronchiectasis? ***Spoken presentation*** *by first author at American Thoracic Society International Conference, San Francisco, May 2012*

Poster presentations

Macfarlane JG, Ruchaud-Sparagano MH, Scott JA, Bulmer DA, Khan CMA, Simpson AJ. Dasatinib inhibits neutrophil degranulation in response to sterile and non-sterile stimuli without impairing bacterial killing. ***Poster discussion*** *at American Thoracic Society International Conference, San Diego, May 2014*

Macfarlane JG, Ruchaud-Sparagano MH, Scott JA, Bulmer DA, Khan CMA, Simpson AJ. Src kinase inhibition attenuates neutrophil degranulation without impairing bacterial killing: a possible therapeutic strategy for acute lung injury. ***Poster presentation*** *at British Thoracic Society Winter Conference, London, Dec 2013*

Macfarlane JG, Ruchaud-Sparagano MH, Scott JA, Bulmer DA, Khan CMA, Simpson AJ. Neutrophil dysfunction in respiratory infection: impaired killing efficiency after successive phagocytic stimuli? ***Poster discussion*** *at European Respiratory Society Annual Congress, Barcelona, Sep 2013*

Appendix 2. Publications arising from work contained within this thesis

Scott J, Harris GJ, Pinder EM, **Macfarlane JG**, Hellyer TP, Rostron AJ, Conway Morris A, Thickett DR, Perkins GD, McAuley DF, Widdrington JD, Wiscombe S, Baudouin SV, Roy AI, Linnett VC, Wright SE, Ruchaud-Sparagano MH, Simpson AJ. Exchange protein directly activated by cyclic AMP (EPAC) activation reverses neutrophil dysfunction induced by β_2-agonists, corticosteroids, and critical illness. *J Allergy Clin Immunology 2015 Sep [Epub ahead of print]*

Ruchaud-Sparagano MH, Gertig H, Hester KL, **Macfarlane JG**, Corris PA, Simpson AJ, De Soyza A. Effect of GM-CSF on neutrophil function in idiopathic bronchiectasis. *Respirology. 2013 Nov;18(8):1230-5*

Macfarlane JG et al. The effects of dasatinib in experimental acute lung inflammation. ***Manuscript in preparation for submission, Oct 2015.***

References

Abraham, E. et al., 1999. Liposomal prostaglandin E1 (TLC C-53) in acute respiratory distress syndrome: a controlled, randomized, double-blind, multicenter clinical trial. TLC C-53 ARDS Study Group. *Critical Care Medicine*, 27(8), pp.1478–85.

Abraham, E. et al., 2000. Neutrophils as early immunologic effectors in hemorrhage- or endotoxemia-induced acute lung injury. *American Journal of Physiology. Lung Cellular and Molecular Physiology*, 279(6), pp.L1137–45.

ACCP/SCCM Consensus, 1992. American College of Chest Physicians/Society of Critical Care Medicine Consensus Conference. *Critical Care Medicine*, 20(6), pp.864–874.

Adamson, I.Y. & Bowden, D.H., 1974. The type 2 cell as progenitor of alveolar epithelial regeneration. A cytodynamic study in mice after exposure to oxygen. *Laboratory Investigation; a Journal of Technical Methods and Pathology*, 30(1), pp.35–42.

Akong-Moore, K. et al., 2012. Influences of chloride and hypochlorite on neutrophil extracellular trap formation. *PloS One*, 7(8), p.e42984.

Allport, J.R. et al., 1997. L-selectin shedding does not regulate human neutrophil attachment, rolling, or transmigration across human vascular endothelium in vitro. *Journal of Immunology*, 158(9), pp.4365–72.

ARDSNet, 2000a. Ketoconazole for Early Treatment of Acute Lung Injury and Acute Respiratory Distress Syndrome. *JAMA*, 283(15), p.1995.

ARDSNet, 2002. Randomized, placebo-controlled trial of lisofylline for early treatment of acute lung injury and acute respiratory distress syndrome. *Critical Care Medicine*, 30(1), pp.1–6.

ARDSNet, 2000b. Ventilation with lower tidal volumes as compared with traditional tidal volumes for acute lung injury and the acute respiratory distress syndrome. The Acute Respiratory Distress Syndrome Network. *The New England Journal of Medicine*, 342(18), pp.1301–8.

Aruoma, O.I. et al., 1989. The antioxidant action of N-acetylcysteine: Its reaction with hydrogen peroxide, hydroxyl radical, superoxide, and hypochlorous acid. *Free Radical Biology and Medicine*, 6(6), pp.593–597.

Bainton, D.F. & Farquhar, M.G., 1966. Origin of granules in polymorphonuclear leukocytes. Two types derived from opposite faces of the Golgi complex in developing granulocytes. *Journal of Cell Biology*, 28(2), pp.277–301.

Barletta, K.E. et al., 2012. Leukocyte compartments in the mouse lung: distinguishing between marginated, interstitial, and alveolar cells in response to injury. *Journal of Immunological Methods*, 375(1-2), pp.100–10.

Barr, L.C. et al., 2013. A randomized controlled trial of peripheral blood mononuclear cell depletion in experimental human lung inflammation. *American Journal of Respiratory and Critical Care Medicine*, 188(4), pp.449–55.

Bentwood, B.J. & Henson, P.M., 1980. The sequential release of granule

constitutents from human neutrophils. *Journal of Immunology*, 124(2), pp.855–62.

Bernard, G.R. et al., 1994. The American-European Consensus Conference on ARDS. Definitions, mechanisms, relevant outcomes, and clinical trial coordination. *American Journal of Respiratory and Critical Care Medicine*, 149(3 Pt 1), pp.818–24.

Bonifacino, J.S. & Weissman, A.M., 1998. Ubiquitin and the control of protein fate in the secretory and endocytic pathways. *Annual Review of Cell and Developmental Biology*, 14, pp.19–57.

Boschelli, D.H. et al., 2001. Optimization of 4-phenylamino-3-quinolinecarbonitriles as potent inhibitors of Src kinase activity. *Journal of Medicinal Chemistry*, 44(23), pp.3965–77.

Bournazou, I. et al., 2009. Apoptotic human cells inhibit migration of granulocytes via release of lactoferrin. *The Journal of Clinical Investigation*, 119(1), pp.20–32.

Boyle, A.J. et al., 2015. Aspirin therapy in patients with acute respiratory distress syndrome (ARDS) is associated with reduced intensive care unit mortality: a prospective analysis. *Critical Care (London, England)*, 19(1), p.846.

Bozza, F.A. et al., 2009. Amicus or adversary: platelets in lung biology, acute injury, and inflammation. *American Journal of Respiratory Cell and Molecular Biology*, 40(2), pp.123–34.

Brinkmann, V. et al., 2004. Neutrophil extracellular traps kill bacteria. *Science (New York, N.Y.)*, 303(5663), pp.1532–5.

Brock, J.H. et al., 1976. The effect of trypsin on bovine transferrin and lactoferrin. *Biochimica et Biophysica Acta*, 446(1), pp.214–25.

Brower, R.G. et al., 2004. Higher versus lower positive end-expiratory pressures in patients with the acute respiratory distress syndrome. *The New England Journal of Medicine*, 351(4), pp.327–36.

Brown, L.M. et al., 2011. A simple classification model for hospital mortality in patients with acute lung injury managed with lung protective ventilation. *Critical Care Medicine*, 39(12), pp.2645–51.

Burbelo, P.D. et al., 2010. Rapid induction of autoantibodies during ARDS and septic shock. *Journal of Translational Medicine*, 8(1), p.97.

Buttenschoen, K. et al., 2008. Endotoxemia and endotoxin tolerance in patients with ARDS. *Langenbeck's Archives of Surgery*, 393(4), pp.473–478.

Byeon, S.E. et al., 2012. The role of Src kinase in macrophage-mediated inflammatory responses. *Mediators of Inflammation*, 2012, p.512926.

Calfee, C.S. et al., 2011. Active and passive cigarette smoking and acute lung injury after severe blunt trauma. *American Journal of Respiratory and Critical Care Medicine*, 183(12), pp.1660–5.

Caron, E. & Hall, A., 1998. Identification of Two Distinct Mechanisms of Phagocytosis Controlled by Different Rho GTPases. *Science*, 282(5394), pp.1717–1721.

Casella, J.F., Flanagan, M.D. & Lin, S., 1981. Cytochalasin D inhibits actin polymerization and induces depolymerization of actin filaments formed

during platelet shape change. *Nature*, 293(5830), pp.302–305.

Cham, B.P., Gerrard, J.M. & Bainton, D.F., 1994. Granulophysin is located in the membrane of azurophilic granules in human neutrophils and mobilizes to the plasma membrane following cell stimulation. *American Journal of Pathology*, 144(6), pp.1369–1380.

Chang, R. et al., 2008. Cytokine-induced arginase activity in pulmonary endothelial cells is dependent on Src family tyrosine kinase activity. *American Journal of Physiology. Lung Cellular and Molecular Physiology*, 295(4), pp.L688–97.

Chastre, J. & Fagon, J.-Y., 2002. Ventilator-associated pneumonia. *American Journal of Respiratory and Critical Care Medicine*, 165(7), pp.867–903.

Chollet-Martin, S. et al., 1996. Interactions between neutrophils and cytokines in blood and alveolar spaces during ARDS. *American Journal of Respiratory and Critical Care Medicine*, 154(3), pp.594–601.

Chopra, M., Reuben, J.S. & Sharma, A.C., 2009. Acute lung injury:apoptosis and signaling mechanisms. *Experimental Biology and Medicine (Maywood, N.J.)*, 234(4), pp.361–71.

Christie, J.D. et al., 2012. Genome wide association identifies PPFIA1 as a candidate gene for acute lung injury risk following major trauma. *PloS One*, 7(1), p.e28268.

Clark, K. et al., 2012. Phosphorylation of CRTC3 by the salt-inducible kinases controls the interconversion of classically activated and regulatory macrophages. *Proceedings of the National Academy of Sciences of the United States of America*, 109(42), pp.16986–91.

Clark, S.C., Dark, J.H. & Kirby, J.A., 1997. An assay of neutrophil adhesion to fibronectin and its attenuation by pentoxifylline and nitric oxide. *Biochemical Society Transactions*, 25(2), p.199S.

Conway Morris, A. et al., 2009. C5a Mediates Peripheral Blood Neutrophil Dysfunction in Critically Ill Patients. *Am. J. Respir. Crit. Care Med.*, 180(1), pp.19–28.

Cooke, C.R. et al., 2008. Predictors of hospital mortality in a population-based cohort of patients with acute lung injury. *Critical Care Medicine*, 36(5), pp.1412–20.

Cooper, J. et al., 1986. Tyr527 is phosphorylated in pp60c-src: implications for regulation. *Science*, 231(4744), pp.1431–1434.

Cross, L.J.M. et al., 2013. Keratinocyte growth factor in acute lung injury to reduce pulmonary dysfunction--a randomised placebo-controlled trial (KARE): study protocol. *Trials*, 14, p.51.

Dada, L.A. et al., 2007. Phosphorylation and ubiquitination are necessary for Na,K-ATPase endocytosis during hypoxia. *Cellular Signalling*, 19(9), pp.1893–8.

Dehm, S.M. & Bonham, K., 2004. SRC gene expression in human cancer: the role of transcriptional activation. *Biochemistry and Cell Biology = Biochimie et Biologie Cellulaire*, 82(2), pp.263–74.

Dellinger, R.P. et al., 1998. Effects of inhaled nitric oxide in patients with acute respiratory distress syndrome: results of a randomized phase II trial. Inhaled Nitric Oxide in ARDS Study Group. *Critical Care Medicine*, 26(1),

pp.15–23.

Demetri, G.D. et al., 2009. Phase I dose-escalation and pharmacokinetic study of dasatinib in patients with advanced solid tumors. *Clinical Cancer Research : An Official Journal of the American Association for Cancer Research*, 15(19), pp.6232–40.

Deshmane, S.L. et al., 2009. Monocyte chemoattractant protein-1 (MCP-1): an overview. *Journal of Interferon & Cytokine Research : The Official Journal of the International Society for Interferon and Cytokine Research*, 29(6), pp.313–26.

Devaney, J. et al., 2015. Human mesenchymal stromal cells decrease the severity of acute lung injury induced by E. coli in the rat. *Thorax*, 70(7), pp.625–35.

Dhaliwal, K. et al., 2012. Monocytes control second-phase neutrophil emigration in established lipopolysaccharide-induced murine lung injury. *American Journal of Respiratory and Critical Care Medicine*, 186(6), pp.514–24.

Doeing, D.C., Borowicz, J.L. & Crockett, E.T., 2003. Gender dimorphism in differential peripheral blood leukocyte counts in mice using cardiac, tail, foot, and saphenous vein puncture methods. *BMC Clinical Pathology*, 3(1), p.3.

Donnelly, S.C. et al., 1993. Interleukin-8 and development of adult respiratory distress syndrome in at-risk patient groups. *Lancet (London, England)*, 341(8846), pp.643–7.

Dorward, D.A. et al., 2014. Assessment of neutrophil apoptosis. *Methods in Molecular Biology (Clifton, N.J.)*, 1124, pp.159–80.

Eligini, S. et al., 2013. Human monocyte-derived macrophages spontaneously differentiated in vitro show distinct phenotypes. *Journal of Cellular Physiology*, 228(7), pp.1464–72.

EMEA, 2015. Europeans Medicine Agency Product Information: Dasatinib. *Available from http://www.ema.europa.eu/docs/en_GB/document_library/EPAR_-_Scientific_Discussion/human/000709/WC500056995.pdf*, p.Last accessed 18.5.15.

Ernst, M. et al., 2002. Constitutive activation of the SRC family kinase Hck results in spontaneous pulmonary inflammation and an enhanced innate immune response. *The Journal of Experimental Medicine*, 196(5), pp.589–604.

Farley, K.S. et al., 2006. Effects of macrophage inducible nitric oxide synthase in murine septic lung injury. *American Journal of Physiology. Lung Cellular and Molecular Physiology*, 290(6), pp.L1164–72.

Faurschou, M. & Borregaard, N., 2003. Neutrophil granules and secretory vesicles in inflammation. *Microbes and Infection*, 5(14), pp.1317–1327.

Folkesson, H.G. et al., 1995. Acid aspiration-induced lung injury in rabbits is mediated by interleukin-8-dependent mechanisms. *The Journal of Clinical Investigation*, 96(1), pp.107–16.

Frame, M.C., 2002. Src in cancer: deregulation and consequences for cell behaviour. *Biochimica et Biophysica Acta (BBA) - Reviews on Cancer*, 1602(2), pp.114–130.

Fraser, C.K. et al., 2009. Dasatinib inhibits the secretion of TNF-alpha following TLR stimulation in vitro and in vivo. *Experimental Hematology*, 37(12), pp.1435–44.

Frutos-Vivar, F., Nin, N. & Esteban, A., 2004. Epidemiology of acute lung injury and acute respiratory distress syndrome. *Current Opinion in Critical Care*, 10(1), pp.1–6.

Fumagalli, L. et al., 2007. The Src family kinases Hck and Fgr regulate neutrophil responses to N-formyl-methionyl-leucyl-phenylalanine. *Journal of Immunology*, 178(6), pp.3874–85.

Futosi, K. et al., 2012. Dasatinib inhibits proinflammatory functions of mature human neutrophils. *Blood*, 119(21), pp.4981–91.

Futosi, K., Fodor, S. & Mócsai, A., 2013. Neutrophil cell surface receptors and their intracellular signal transduction pathways. *International Immunopharmacology*, 17(3), pp.638–50.

Gane, J. & Stockley, R., 2012. Mechanisms of neutrophil transmigration across the vascular endothelium in COPD. *Thorax*, 67(6), pp.553–61.

Gao, L. & Barnes, K.C., 2009. Recent advances in genetic predisposition to clinical acute lung injury. *American Journal of Physiology. Lung Cellular and Molecular Physiology*, 296(5), pp.L713–25.

Gates, S. et al., 2013. Beta-Agonist Lung injury TrIal-2 (BALTI-2): a multicentre, randomised, double-blind, placebo-controlled trial and economic evaluation of intravenous infusion of salbutamol versus placebo in patients with acute respiratory distress syndrome. *Health Technology Assessment (Winchester, England)*, 17(38), pp.v–vi, 1–87.

Giagulli, C. et al., 2006. The Src family kinases Hck and Fgr are dispensable for inside-out, chemoattractant-induced signaling regulating beta 2 integrin affinity and valency in neutrophils, but are required for beta 2 integrin-mediated outside-in signaling involved in sustained a. *Journal of Immunology*, 177(1), pp.604–11.

Giard, D.J. et al., 1973. In vitro cultivation of human tumors: establishment of cell lines derived from a series of solid tumors. *Journal of the National Cancer Institute*, 51(5), pp.1417–23.

Golas, J.M. et al., 2003. SKI-606, a 4-anilino-3-quinolinecarbonitrile dual inhibitor of Src and Abl kinases, is a potent antiproliferative agent against chronic myelogenous leukemia cells in culture and causes regression of K562 xenografts in nude mice. *Cancer Research*, 63(2), pp.375–81.

Gray, R.D. et al., 2013. Activation of conventional protein kinase C (PKC) is critical in the generation of human neutrophil extracellular traps. *Journal of Inflammation*, 10(1), p.12.

Greenberger, M.J. et al., 1995. Neutralization of IL-10 increases survival in a murine model of Klebsiella pneumonia. *Journal of Immunology (Baltimore, Md. : 1950)*, 155(2), pp.722–9.

Grommes, J. & Soehnlein, O., 2011. Contribution of neutrophils to acute lung injury. *Molecular Medicine (Cambridge, Mass.)*, 17(3-4), pp.293–307.

Guérin, C. et al., 2013. Prone positioning in severe acute respiratory distress syndrome. *The New England Journal of Medicine*, 368(23), pp.2159–68.

Gullberg, U. et al., 1997. Biosynthesis, processing and sorting of neutrophil

proteins: insight into neutrophil granule development. *European Journal of Haematology*, 58(3), pp.137–53.

Gutkind, J.S. & Robbins, K.C., 1989. Translocation of the FGR protein-tyrosine kinase as a consequence of neutrophil activation. *Proceedings of the National Academy of Sciences of the United States of America*, 86(22), pp.8783–7.

Hampton, M.B., Vissers, M.C. & Winterbourn, C.C., 1994. A single assay for measuring the rates of phagocytosis and bacterial killing by neutrophils. *Journal of Leukocyte Biology*, 55(2), pp.147–52.

Hampton, M.B. & Winterbourn, C.C., 1999. Methods for quantifying phagocytosis and bacterial killing by human neutrophils. *Journal of Immunological Methods*, 232(1-2), pp.15–22.

Han, J. et al., 2013. A critical role for Lyn kinase in strengthening endothelial integrity and barrier function. *Blood*, 122(25), pp.4140–9.

Han, S. & Mallampalli, R.K., 2015. The Acute Respiratory Distress Syndrome: From Mechanism to Translation. *Journal of Immunology*, 194(3), pp.855–860.

Hart, S.P., Dransfield, I. & Rossi, A.G., 2008. Phagocytosis of apoptotic cells. *Methods (San Diego, Calif.)*, 44(3), pp.280–5.

Hashiguchi, N. et al., 2005. Whole-blood assay to measure oxidative burst and degranulation of neutrophils for monitoring trauma patients. *European Journal of Trauma and Emergency Surgery*, 31(4), pp.379–388.

Haslett, C. et al., 1985. Modulation of multiple neutrophil functions by preparative methods or trace concentrations of bacterial lipopolysaccharide. *The American Journal of Pathology*, 119(1), pp.101–10.

Hayashi, F., Means, T.K. & Luster, A.D., 2003. Toll-like receptors stimulate human neutrophil function. *Blood*, 102(7), pp.2660–9.

Herter, J. & Zarbock, A., 2013. Integrin Regulation during Leukocyte Recruitment. *Journal of Immunology*, 190(9), pp.4451–7.

Hirsch, J. et al., 2014. Double impact of cigarette smoke and mechanical ventilation on the alveolar epithelial type II cell. *Critical Care (London, England)*, 18(2), p.R50.

Hogg, J.C., 1994. Felix Fleischner Lecture. The traffic of polymorphonuclear leukocytes through pulmonary microvessels in health and disease. *AJR. American Journal of Roentgenology*, 163(4), pp.769–75.

Huang, S. et al., 2003. Defective activation of c-Src in cystic fibrosis airway epithelial cells results in loss of tumor necrosis factor-alpha-induced gap junction regulation. *The Journal of Biological Chemistry*, 278(10), pp.8326–32.

Huber-Lang, M.S. et al., 2002. Complement-induced impairment of innate immunity during sepsis. *Journal of Immunology*, 169(6), pp.3223–31.

Hunter, T., 1987. A thousand and one protein kinases. *Cell*, 50(6), pp.823–829.

Islam, M.N. et al., 2012. Mitochondrial transfer from bone-marrow–derived stromal cells to pulmonary alveoli protects against acute lung injury. *Nature Medicine*, advance on.

Iwata, K. et al., 2010. Effect of neutrophil elastase inhibitor (sivelestat sodium)

in the treatment of acute lung injury (ALI) and acute respiratory distress syndrome (ARDS): a systematic review and meta-analysis. *Internal Medicine (Tokyo, Japan)*, 49(22), pp.2423–32.

Kamen, L.A., Schlessinger, J. & Lowell, C.A., 2011. Pyk2 is required for neutrophil degranulation and host defense responses to bacterial infection. *Journal of Immunology*, 186(3), pp.1656–65.

Kaplan, E.L., Laxdal, T. & Quie, P.G., 1968. Studies of polymorphonuclear leukocytes from patients with chronic granulomatous disease of childhood: bactericidal capacity for streptococci. *Pediatrics*, 41(3), pp.591–9.

Karlsson, A., Nixon, J.B. & McPhail, L.C., 2000. Phorbol myristate acetate induces neutrophil NADPH-oxidase activity by two separate signal transduction pathways: dependent or independent of phosphatidylinositol 3-kinase. *Journal of Leukocyte Biology*, 67(3), pp.396–404.

Khadaroo, R.G. et al., 2004. The role of the Src family of tyrosine kinases after oxidant-induced lung injury in vivo. *Surgery*, 136(2), pp.483–8.

Kiefer, F. et al., 1998. The Syk protein tyrosine kinase is essential for Fcgamma receptor signaling in macrophages and neutrophils. *Molecular and Cellular Biology*, 18(7), pp.4209–20.

Kitchen, E. et al., 1996. Demonstration of reversible priming of human neutrophils using platelet-activating factor. *Blood*, 88(11), pp.4330–7.

Kitchens, R.L., 2000. Role of CD14 in cellular recognition of bacterial lipopolysaccharides. *Chemical Immunology*, 74, pp.61–82.

Knaus, W.A. et al., 1985. APACHE II: a severity of disease classification system. *Critical Care Medicine*, 13(10), pp.818–29.

Kor, D.J. et al., 2012. Lung Injury Prevention with Aspirin (LIPS-A): a protocol for a multicentre randomised clinical trial in medical patients at high risk of acute lung injury. *BMJ Open*, 2(5), pp.e001606–e001606.

Kovács, M. et al., 2014. The Src family kinases Hck, Fgr, and Lyn are critical for the generation of the in vivo inflammatory environment without a direct role in leukocyte recruitment. *The Journal of Experimental Medicine*, 211(10), pp.1993–2011.

Lacy, P., 2006. Mechanisms of degranulation in neutrophils. *Allergy, Asthma, and Clinical Immunology : Official Journal of the Canadian Society of Allergy and Clinical Immunology*, 2(3), pp.98–108.

Lacy, P. & Eitzen, G., 2008. Control of granule exocytosis in neutrophils. *Frontiers in Bioscience : A Journal and Virtual Library*, 13, pp.5559–70.

Lee, H.S. et al., 2007. Src tyrosine kinases mediate activations of NF-kappaB and integrin signal during lipopolysaccharide-induced acute lung injury. *Journal of Immunology*, 179(10), pp.7001–11.

Lee, J.W. et al., 2009. Allogeneic human mesenchymal stem cells for treatment of E. coli endotoxin-induced acute lung injury in the ex vivo perfused human lung. *Proceedings of the National Academy of Sciences of the United States of America*, 106(38), pp.16357–62.

Li, G. et al., 2011. Eight-year trend of acute respiratory distress syndrome: a population-based study in Olmsted County, Minnesota. *American Journal of Respiratory and Critical Care Medicine*, 183(1), pp.59–66.

Li, J.D. et al., 1998. Activation of NF-kappaB via a Src-dependent Ras-MAPK-pp90rsk pathway is required for Pseudomonas aeruginosa-induced mucin overproduction in epithelial cells. *Proceedings of the National Academy of Sciences of the United States of America*, 95(10), pp.5718–23.

Li, Y. et al., 2002. A critical concentration of neutrophils is required for effective bacterial killing in suspension. *Proceedings of the National Academy of Sciences of the United States of America*, 99(12), pp.8289–94.

Li, Y. et al., 2006. ADAM17 deficiency by mature neutrophils has differential effects on L-selectin shedding. *Blood*, 108(7), pp.2275–9.

Li, Y. et al., 2004. Determination of the Critical Concentration of Neutrophils Required to Block Bacterial Growth in Tissues. *The Journal of Experimental Medicine*, 200(5), pp.613–622.

Liau, D.F. et al., 1996. Effects of human polymorphonuclear leukocyte elastase upon surfactant proteins in vitro. *Biochimica et Biophysica Acta*, 1302(2), pp.117–28.

Lin, C.H. et al., 2001. Induction of cyclooxygenase-2 protein by lipoteichoic acid from Staphylococcus aureus in human pulmonary epithelial cells: involvement of a nuclear factor-kappa B-dependent pathway. *British Journal of Pharmacology*, 134(3), pp.543–52.

Liu, F.-L. et al., 2012. Lipoteichoic acid induces surfactant protein-A biosynthesis in human alveolar type II epithelial cells through activating the MEK1/2-ERK1/2-NF-κB pathway. *Respiratory Research*, 13, p.88.

Liu, K.D. et al., 2014. Design and implementation of the START (STem cells for ARDS Treatment) trial, a phase 1/2 trial of human mesenchymal stem/stromal cells for the treatment of moderate-severe acute respiratory distress syndrome. *Annals of Intensive Care*, 4, p.22.

Liu, M. et al., 1996. Mechanical strain induces pp60src activation and translocation to cytoskeleton in fetal rat lung cells. *The Journal of Biological Chemistry*, 271(12), pp.7066–71.

Looney, M.R. et al., 2009. Platelet depletion and aspirin treatment protect mice in a two-event model of transfusion-related acute lung injury. *Journal of Clinical Investigation*, 119(11), pp.3450–61.

Lowell, C.A. & Berton, G., 1998. Resistance to endotoxic shock and reduced neutrophil migration in mice deficient for the Src-family kinases Hck and Fgr. *Proceedings of the National Academy of Sciences of the United States of America*, 95(13), pp.7580–4.

Lu, Y.-C., Yeh, W.-C. & Ohashi, P.S., 2008. LPS/TLR4 signal transduction pathway. *Cytokine*, 42(2), pp.145–51.

Lundien, M.C. et al., 2002. Induction of MCP-1 expression in airway epithelial cells: role of CCR2 receptor in airway epithelial injury. *Journal of Clinical Immunology*, 22(3), pp.144–52.

Lundin, S. et al., 1999. Inhalation of nitric oxide in acute lung injury: results of a European multicentre study. The European Study Group of Inhaled Nitric Oxide. *Intensive Care Medicine*, 25(9), pp.911–9.

Malachowa, N. et al., 2013. Staphylococcus aureus leukotoxin GH promotes formation of neutrophil extracellular traps. *Journal of Immunology*, 191(12), pp.6022–9.

Mallampalli, R.K. et al., 2013. Targeting F box protein Fbxo3 to control cytokine-driven inflammation. *Journal of Immunology (Baltimore, Md.: 1950)*, 191(10), pp.5247–55.

Maniatis, N.A. et al., 2012. Acid-induced acute lung injury in mice is associated with P44/42 and c-Jun N-terminal kinase activation and requires the function of tumor necrosis factor α receptor I. *Shock (Augusta, Ga.)*, 38(4), pp.381–6.

Maniatis, N.A. et al., 2008. Endothelial pathomechanisms in acute lung injury. *Vascular Pharmacology*, 49(4-6), pp.119–33.

Mansfield, P.J. et al., 2002. Regulation of polymorphonuclear leukocyte degranulation and oxidant production by ceramide through inhibition of phospholipase D. *Blood*, 99(4), pp.1434–41.

Mantovani, A., 2006. Macrophage diversity and polarization: in vivo veritas. *Blood*, 108(2), pp.408–409.

Matthay, M.A. et al., 2011. Randomized, Placebo-controlled Clinical Trial of an Aerosolized β 2 -Agonist for Treatment of Acute Lung Injury. *American Journal of Respiratory and Critical Care Medicine*, 184(5), pp.561–568.

Matthay, M.A., Ware, L.B. & Zimmerman, G.A., 2012. The acute respiratory distress syndrome. *The Journal of Clinical Investigation*, 122(8), pp.2731–40.

McPhillips, K. et al., 2007. TNF-alpha inhibits macrophage clearance of apoptotic cells via cytosolic phospholipase A2 and oxidant-dependent mechanisms. *Journal of Immunology (Baltimore, Md.: 1950)*, 178(12), pp.8117–26.

McQualter, J.L. et al., 2010. Evidence of an epithelial stem/progenitor cell hierarchy in the adult mouse lung. *Proceedings of the National Academy of Sciences of the United States of America*, 107(4), pp.1414–9.

Meade, M.O. et al., 2008. Ventilation strategy using low tidal volumes, recruitment maneuvers, and high positive end-expiratory pressure for acute lung injury and acute respiratory distress syndrome: a randomized controlled trial. *JAMA*, 299(6), pp.637–45.

Meduri, G.U. et al., 2009. Activation and regulation of systemic inflammation in ARDS: rationale for prolonged glucocorticoid therapy. *Chest*, 136(6), pp.1631–43.

Mege, J.L. et al., 1988. Phagocytic cell function in aged subjects. *Neurobiology of Aging*, 9(2), pp.217–20.

Mercat, A. et al., 2008. Positive end-expiratory pressure setting in adults with acute lung injury and acute respiratory distress syndrome: a randomized controlled trial. *JAMA*, 299(6), pp.646–55.

Mócsai, A. et al., 1999. Adhesion-dependent degranulation of neutrophils requires the Src family kinases Fgr and Hck. *Journal of Immunology*, 162(2), pp.1120–6.

Mócsai, A., 2013. Diverse novel functions of neutrophils in immunity, inflammation, and beyond. *The Journal of Experimental Medicine*, 210(7), pp.1283–99.

Mócsai, A. et al., 2000. Kinase pathways in chemoattractant-induced degranulation of neutrophils: the role of p38 mitogen-activated protein

kinase activated by Src family kinases. *Journal of Immunology*, 164(8), pp.4321–31.

Mócsai, A. et al., 2002. Syk is required for integrin signaling in neutrophils. *Immunity*, 16(4), pp.547–58.

Möhn, H. et al., 1995. The src-family protein-tyrosine kinase p59hck is located on the secretory granules in human neutrophils and translocates towards the phagosome during cell activation. *The Biochemical Journal*, 309 (Pt 2, pp.657–65.

Moon, C. et al., 2010. N-acetylcysteine inhibits RhoA and promotes apoptotic cell clearance during intense lung inflammation. *American Journal of Respiratory and Critical Care Medicine*, 181(4), pp.374–87.

Morris, A.C. et al., 2011. C5a-mediated neutrophil dysfunction is RhoA-dependent and predicts infection in critically ill patients. *Blood*, 117(19), pp.5178–88.

Moser, B. et al., 1990. Neutrophil-activating properties of the melanoma growth-stimulatory activity. *The Journal of Experimental Medicine*, 171(5), pp.1797–802.

Moss, M. et al., 1996. The role of chronic alcohol abuse in the development of acute respiratory distress syndrome in adults. *JAMA*, 275(1), pp.50–4.

Mosser, D.M. & Zhang, X., 2008. Interleukin-10: new perspectives on an old cytokine. *Immunological Reviews*, 226, pp.205–18.

Mullmann, T. et al., 1993. Phospholipase C and phospholipase D are activated independently of each other in chemotactic peptide-stimulated human neutrophils. *J. Leukoc. Biol.*, 53(6), pp.630–635.

Nakaya, M. et al., 2006. Opposite effects of rho family GTPases on engulfment of apoptotic cells by macrophages. *The Journal of Biological Chemistry*, 281(13), pp.8836–42.

Nanì, S. et al., 2015. Src family kinases and Syk are required for neutrophil extracellular trap formation in response to β-glucan particles. *Journal of Innate Immunity*, 7(1), pp.59–73.

Nathan, C.F., 1987. Neutrophil activation on biological surfaces. Massive secretion of hydrogen peroxide in response to products of macrophages and lymphocytes. *The Journal of Clinical Investigation*, 80(6), pp.1550–60.

Nauseef, W.M., 2007. How human neutrophils kill and degrade microbes: an integrated view. *Immunological Reviews*, 219, pp.88–102.

Nelson, R.D., Quie, P.G. & Simmons, R.L., 1975. Chemotaxis under agarose: a new and simple method for measuring chemotaxis and spontaneous migration of human polymorphonuclear leukocytes and monocytes. *Journal of Immunology*, 115(6), pp.1650–6.

O'Hare, T., 2005. In vitro Activity of Bcr-Abl Inhibitors AMN107 and BMS-354825 against Clinically Relevant Imatinib-Resistant Abl Kinase Domain Mutants. *Cancer Research*, 65(11), pp.4500–4505.

Okutani, D. et al., 2006. Src protein tyrosine kinase family and acute inflammatory responses. *American Journal of Physiology. Lung Cellular and Molecular Physiology*, 291(2), pp.L129–41.

Oliveira, G.P. et al., 2015. The Effects of Dasatinib in Experimental Acute

Respiratory Distress Syndrome Depend on Dose and Etiology. *Cellular Physiology and Biochemistry*, 36(4), pp.1644–1658.

Oppermann, H. et al., 1979. Uninfected vertebrate cells contain a protein that is closely related to the product of the avian sarcoma virus transforming gene (src). *Proceedings of the National Academy of Sciences of the United States of America*, 76(4), pp.1804–8.

Ozanne, J., Prescott, A.R. & Clark, K., 2014. The clinically-approved drugs Dasatinib and Bosutinib induce anti-inflammatory macrophages by inhibiting the Salt-Inducible Kinases. *The Biochemical Journal*.

Pai, A.B. et al., 2012. Lipoteichoic acid from Staphylococcus aureus induces lung endothelial cell barrier dysfunction: role of reactive oxygen and nitrogen species. *PloS One*, 7(11), p.e49209.

Palić, D. et al., 2005. A rapid, direct assay to measure degranulation of primary granules in neutrophils from kidney of fathead minnow (Pimephales promelas Rafinesque, 1820). *Fish & Shellfish Immunology*, 19(3), pp.217–27.

Papazian, L. et al., 2010. Neuromuscular blockers in early acute respiratory distress syndrome. *The New England Journal of Medicine*, 363(12), pp.1107–16.

Park, Y.-J. et al., 2008. PAI-1 inhibits neutrophil efferocytosis. *Proceedings of the National Academy of Sciences of the United States of America*, 105(33), pp.11784–9.

Parker, J.C., Ivey, C.L. & Tucker, A., 1998. Phosphotyrosine phosphatase and tyrosine kinase inhibition modulate airway pressure-induced lung injury. *Journal of Applied Physiology (Bethesda, Md. : 1985)*, 85(5), pp.1753–61.

Parry, M.F. et al., 1981. Myeloperoxidase deficiency: prevalence and clinical significance. *Annals of Internal Medicine*, 95(3), pp.293–301.

Parsons, P.E. et al., 1985. Chemotactic activity in bronchoalveolar lavage fluid from patients with adult respiratory distress syndrome. *The American Review of Respiratory Disease*, 132(3), pp.490–3.

van Pelt, L.J. et al., 1996. Limitations on the use of dihydrorhodamine 123 for flow cytometric analysis of the neutrophil respiratory burst. *Journal of Immunological Methods*, 191(2), pp.187–96.

Pepe, P.E. et al., 1982. Clinical predictors of the adult respiratory distress syndrome. *American Journal of Surgery*, 144(1), pp.124–30.

Peter, J. V. et al., 2008. Corticosteroids in the prevention and treatment of acute respiratory distress syndrome (ARDS) in adults: meta-analysis. *BMJ*, 336(7651), pp.1006–1009.

Pham, C.T.N., 2006. Neutrophil serine proteases: specific regulators of inflammation. *Nature Reviews. Immunology*, 6(7), pp.541–50.

Piegeler, T. et al., 2014. Ropivacaine attenuates endotoxin plus hyperinflation-mediated acute lung injury via inhibition of early-onset Src-dependent signaling. *BMC Anesthesiology*, 14, p.57.

Poon, I.K.H. et al., 2014. Apoptotic cell clearance: basic biology and therapeutic potential. *Nature Reviews. Immunology*, 14(3), pp.166–80.

Proudfoot, A.G. et al., 2011. Human models of acute lung injury. *Disease*

Models & Mechanisms, 4(2), pp.145–53.

Pugin, J. et al., 1996. Proinflammatory activity in bronchoalveolar lavage fluids from patients with ARDS, a prominent role for interleukin-1. *American Journal of Respiratory and Critical Care Medicine*, 153(6 Pt 1), pp.1850–6.

Pulli, B. et al., 2013. Measuring myeloperoxidase activity in biological samples. *PloS One*, 8(7), p.e67976.

Quinn, M.T., DeLeo, F.R. & Bokoch, G.M., 2007. Neutrophil methods and protocols. Preface. *Methods in Molecular Biology (Clifton, N.J.)*, 412, pp.vii–viii.

Ranieri, V.M. et al., 2012. Acute respiratory distress syndrome: the Berlin Definition. *JAMA : The Journal of the American Medical Association*, 307(23), pp.2526–33.

Remsing Rix, L.L. et al., 2009. Global target profile of the kinase inhibitor bosutinib in primary chronic myeloid leukemia cells. *Leukemia*, 23(3), pp.477–85.

Rice, T.W. et al., 2011. Enteral omega-3 fatty acid, gamma-linolenic acid, and antioxidant supplementation in acute lung injury. *JAMA*, 306(14), pp.1574–81.

Rorvig, S. et al., 2009. Ficolin-1 is present in a highly mobilizable subset of human neutrophil granules and associates with the cell surface after stimulation with fMLP. *Journal of Leukocyte Biology*, 86(6), pp.1439–1449.

Rosen, H. & Michel, B.R., 1997. Redundant contribution of myeloperoxidase-dependent systems to neutrophil-mediated killing of Escherichia coli. *Infection and Immunity*, 65(10), pp.4173–8.

Rubenfeld, G.D. et al., 2005. Incidence and outcomes of acute lung injury. *The New England Journal of Medicine*, 353(16), pp.1685–93.

Sabroe, I., Dower, S.K. & Whyte, M.K.B., 2005. The role of Toll-like receptors in the regulation of neutrophil migration, activation, and apoptosis. *Clinical Infectious Diseases : An Official Publication of the Infectious Diseases Society of America*, 41 Suppl 7(Supplement_7), pp.S421–6.

Sadowska, A.M. et al., 2006. Effect of N-acetylcysteine on neutrophil activation markers in healthy volunteers: in vivo and in vitro study. *Pharmacological Research : The Official Journal of the Italian Pharmacological Society*, 53(3), pp.216–25.

Sakuma, T. et al., 1998. ONO-5046 is a potent inhibitor of neutrophil elastase in human pleural effusion after lobectomy. *European Journal of Pharmacology*, 353(2-3), pp.273–9.

Seferian, A. et al., 2013. Effects Of Broad Spectrum Tyrosin Kinase Inhibitor On Pulmonary Circulation Homeostasis. In *A52. MECHANISMS OF PULMONARY VASCULAR DISEASE*. American Thoracic Society International Conference Abstracts. American Thoracic Society, pp. A1738–A1738.

Segal, A.W., 2005. How neutrophils kill microbes. *Annual Review of Immunology*, 23, pp.197–223.

Sengeløv, H. et al., 1995. Mobilization of granules and secretory vesicles during in vivo exudation of human neutrophils. *Journal of Immunology (Baltimore, Md. : 1950)*, 154(8), pp.4157–65.

Sengeløv, H., Kjeldsen, L. & Borregaard, N., 1993. Control of exocytosis in early neutrophil activation. *Journal of Immunology (Baltimore, Md. : 1950)*, 150(4), pp.1535–43.

Severgnini, M. et al., 2004. Activation of the STAT pathway in acute lung injury. *American Journal of Physiology. Lung Cellular and Molecular Physiology*, 286(6), pp.L1282–92.

Severgnini, M. et al., 2005. Inhibition of the Src and Jak kinases protects against lipopolysaccharide-induced acute lung injury. *American Journal of Respiratory and Critical Care Medicine*, 171(8), pp.858–67.

Shah, N.P. et al., 2006. Dasatinib (BMS-354825) inhibits KITD816V, an imatinib-resistant activating mutation that triggers neoplastic growth in most patients with systemic mastocytosis. *Blood*, 108(1), pp.286–91.

Shalaby, S.M. et al., 2014. Mesenchymal stromal cell injection protects against oxidative stress in Escherichia coli-induced acute lung injury in mice. *Cytotherapy*, 16(6), pp.764–75.

Shattil, S.J., Kim, C. & Ginsberg, M.H., 2010. The final steps of integrin activation: the end game. *Nature Reviews. Molecular Cell Biology*, 11(4), pp.288–300.

Sheshachalam, A. et al., 2014. Granule protein processing and regulated secretion in neutrophils. *Frontiers in Immunology*, 5, p.448.

Shyamsundar, M. et al., 2014. Keratinocyte growth factor promotes epithelial survival and resolution in a human model of lung injury. *American Journal of Respiratory and Critical Care Medicine*, 189(12), pp.1520–9.

Solomkin, J.S. et al., 1981. Neutrophil dysfunction in sepsis. II. Evidence for the role of complement activation products in cellular deactivation. *Surgery*, 90(2), pp.319–27.

Speert, D.P. et al., 1994. Infection with Pseudomonas cepacia in chronic granulomatous disease: role of nonoxidative killing by neutrophils in host defense. *The Journal of Infectious Diseases*, 170(6), pp.1524–31.

Spragg, R.G. et al., 2004. Effect of recombinant surfactant protein C-based surfactant on the acute respiratory distress syndrome. *The New England Journal of Medicine*, 351(9), pp.884–92.

Steinberg, K.P. et al., 1994. Evolution of bronchoalveolar cell populations in the adult respiratory distress syndrome. *American Journal of Respiratory and Critical Care Medicine*, 150(1), pp.113–22.

Summers, C. et al., 2010. Neutrophil kinetics in health and disease. *Trends in Immunology*, 31(8), pp.318–24.

Tandon, S. et al., 2001. Peri-operative risk factors for acute lung injury after elective oesophagectomy. *British Journal of Anaesthesia*, 86(5), pp.633–8.

Thammavongsa, V., Missiakas, D.M. & Schneewind, O., 2013. Staphylococcus aureus degrades neutrophil extracellular traps to promote immune cell death. *Science (New York, N.Y.)*, 342(6160), pp.863–6.

Thomas, S.M. & Brugge, J.S., 1997. Cellular functions regulated by Src family kinases. *Annual Review of Cell and Developmental Biology*, 13, pp.513–609.

Tintori, C. et al., 2013. Identification of Hck inhibitors as hits for the development

of antileukemia and anti-HIV agents. *ChemMedChem*, 8(8), pp.1353–60.

Tolle, L.B. & Standiford, T.J., 2013. Danger-associated molecular patterns (DAMPs) in acute lung injury. *The Journal of Pathology*, 229(2), pp.145–56.

Tong, H. et al., 2013. C-Abl tyrosine kinase plays a critical role in β2 integrin-dependent neutrophil migration by regulating Vav1 activity. *Journal of Leukocyte Biology*, 93(4), pp.611–22.

Toonen, R.F.G. & Verhage, M., 2003. Vesicle trafficking: pleasure and pain from SM genes. *Trends in Cell Biology*, 13(4), pp.177–86.

Truwit, J.D. et al., 2014. Rosuvastatin for sepsis-associated acute respiratory distress syndrome. *The New England Journal of Medicine*, 370(23), pp.2191–200.

Tsai, W.C. et al., 2000. CXC chemokine receptor CXCR2 is essential for protective innate host response in murine Pseudomonas aeruginosa pneumonia. *Infection and Immunity*, 68(7), pp.4289–96.

Vadász, I., Weiss, C.H. & Sznajder, J.I., 2012. Ubiquitination and proteolysis in acute lung injury. *Chest*, 141(3), pp.763–71.

Vincent, J.L., Sakr, Y. & Ranieri, V.M., 2003. Epidemiology and outcome of acute respiratory failure in intensive care unit patients. *Critical Care Medicine*, 31(4 Suppl), pp.S296–9.

Walsh, L.J. et al., 1991. Human dermal mast cells contain and release tumor necrosis factor alpha, which induces endothelial leukocyte adhesion molecule 1. *Proceedings of the National Academy of Sciences of the United States of America*, 88(10), pp.4220–4.

Wang, H. et al., 2014. Combined effects of sivelestat and resveratrol on severe acute pancreatitis-associated lung injury in rats. *Experimental Lung Research*, 40(6), pp.288–97.

Wang, Z. et al., 2008. Alveolar macrophages from septic mice promote polymorphonuclear leukocyte transendothelial migration via an endothelial cell Src kinase/NADPH oxidase pathway. *Journal of Immunology (Baltimore, Md. : 1950)*, 181(12), pp.8735–44.

Ward, P.A., 2010. The harmful role of c5a on innate immunity in sepsis. *Journal of Innate Immunity*, 2(5), pp.439–45.

Ware, L.B., 2014. Acute respiratory distress syndrome. *BMJ Online*.

Ware, L.B. & Matthay, M.A., 2000. The acute respiratory distress syndrome. *The New England Journal of Medicine*, 342(18), pp.1334–49.

Weiland, J.E. et al., 1986. Lung neutrophils in the adult respiratory distress syndrome. Clinical and pathophysiologic significance. *The American Review of Respiratory Disease*, 133(2), pp.218–25.

Wenisch, C. et al., 2000. Effect of age on human neutrophil function. *Journal of Leukocyte Biology*, 67(1), pp.40–5.

Wheeler, A.P. et al., 2006. Pulmonary-artery versus central venous catheter to guide treatment of acute lung injury. *The New England Journal of Medicine*, 354(21), pp.2213–24.

Wiedemann, H.P. et al., 2006. Comparison of Two Fluid-Management Strategies in Acute Lung Injury. *New England Journal of Medicine*, 354(24), pp.2564–2575.

Wurfel, M.M. et al., 2014. Validation Of Genome-Wide Association Study Of Acute Respiratory Distress Syndrome Risk Loci In The iSPAAR Consortium. In *C107. INFORMING LUNG DISEASE WITH BIOINFORMATICS*. American Thoracic Society International Conference Abstracts. American Thoracic Society, pp. A6716–A6716.

Yamashiro, S., Kamohara, H. & Yoshimura, T., 1999. MCP-1 is selectively expressed in the late phase by cytokine-stimulated human neutrophils: TNF-alpha plays a role in maximal MCP-1 mRNA expression. *Journal of Leukocyte Biology*, 65(5), pp.671–9.

Zarbock, A., 2012. The shady side of dasatinib. *Blood*, 119(21), pp.4817–8.

Zarbock, A. & Ley, K., 2008. Mechanisms and consequences of neutrophil interaction with the endothelium. *The American Journal of Pathology*, 172(1), pp.1–7.

Zarbock, A., Singbartl, K. & Ley, K., 2006. Complete reversal of acid-induced acute lung injury by blocking of platelet-neutrophil aggregation. *The Journal of Clinical Investigation*, 116(12), pp.3211–9.

Zemans, R.L., Colgan, S.P. & Downey, G.P., 2009. Transepithelial migration of neutrophils: mechanisms and implications for acute lung injury. *American Journal of Respiratory Cell and Molecular Biology*, 40(5), pp.519–35.

Zheng, G. et al., 2014. Treatment of acute respiratory distress syndrome with allogeneic adipose-derived mesenchymal stem cells: a randomized, placebo-controlled pilot study. *Respiratory Research*, 15, p.39.

Zingg, U. et al., 2011. Factors associated with postoperative pulmonary morbidity after esophagectomy for cancer. *Annals of Surgical Oncology*, 18(5), pp.1460–8.

Word count 55,784